REPORT UAG-12
PART II

WORLD DATA CENTER A

Upper Atmosphere Geophysics

DATA ON SOLAR-GEOPHYSICAL ACTIVITY ASSOCIATED WITH THE MAJOR GEOMAGNETIC STORM OF MARCH 8, 1970

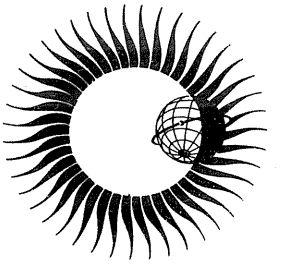

April 1971

WORLD DATA CENTER A

National Academy of Sciences

2101 Constitution Avenue, N. W. Washington, D. C. U.S.A., 20418

World Data Center A consists of the Coordination Office

and nine subcenters:

World Data Center A
Coordination Office
National Academy of Sciences
2101 Constitution Avenue, N.W.
Washington, D. C., U.S.A. 20418
Telephone (202) 961-1478

Solar and Interplanetary Phenomena, Ionospheric Phenomena, Flare-Associated Events, Aurora, Cosmic Rays, Airglow:
World Data Center A:
Upper Atmosphere Geophysics
National Oceanic and Atmospheric Administration
Boulder, Colorado, U.S.A. 80302
Telephone (303) 447-1000 Ext. 3381

Geomagnetism, Seismology and Gravity:
World Data Center A:
Geomagnetism, Seismology and Gravity
Environmental Data Service, NOAA
Rockville, Maryland, U.S.A. 20852
Telephone (301) 496-8160

Glaciology:
World Data Center A:
Glaciology
American Geographical Society
Broadway at 156th Street
New York, New York, U.S.A. 10032
Telephone (212) 234-8100

Longitude and Latitude:
World Data Center A:
Longitude and Latitude
U. S. Naval Observatory
Washington, D. C., U.S.A. 20390
Telephone (202) 698-8422

Meteorology (and Nuclear Radiation):
World Data Center A:
Meteorology
National Climatic Center
Federal Building
Asheville, North Carolina, U.S.A. 28801
Telephone (704) 254-0961

Oceanography:
World Data Center A:
Oceanography
Building 160
Second and N Streets, S.E.
Washington, D. C., U.S.A. 20390
Telephone (202) 698-3753

Rockets and Satellites:
World Data Center A:
Rockets and Satellites
Goddard Space Flight Center
Code 601
Greenbelt, Maryland, U.S.A. 20771
Telephone (301) 982-6695

Tsunami:
World Data Center A:
Tsunami
National Oceanic and Atmospheric Administration
P. O. Box 3887
Honolulu, Hawaii, U.S.A. 96812
Telephone (808) 546-5698

Upper Mantle Project:
World Data Center A:
Upper Mantle Project
Lamont-Doherty Geological Observatory
Palisades, New York, U.S.A. 10964
Telephone (914) 359-2900 Ext. 209

Notes:

(1) World Data Centers conduct international exchange of geophysical observations in accordance with the principles set forth by the International Council of Scientific Unions. WDC-A is established in the United States under the auspices of the National Academy of Sciences.
(2) Communications regarding data interchange matters in general and World Data Center A as a whole should be addressed to: World Data Center A, Coordination Office (see address above).
(3) Inquiries and communications concerning data in specific disciplines should be addressed to the appropriate subcenter listed above.

WORLD DATA CENTER A

Upper Atmosphere Geophysics

REPORT UAG-12 PART II

DATA ON SOLAR-GEOPHYSICAL ACTIVITY ASSOCIATED WITH THE MAJOR GEOMAGNETIC STORM OF MARCH 8, 1970

compiled by

J. Virginia Lincoln and Dale B. Bucknam

WDC-A, Upper Atmosphere Geophysics

Boulder, Colorado

Prepared by Research Laboratories, NOAA, Boulder, Colorado
and published by

U.S. DEPARTMENT OF COMMERCE
NATIONAL OCEANIC AND ATMOSPHERIC ADMINISTRATION

ENVIRONMENTAL DATA SERVICE
Asheville, North Carolina, USA 28801

April 1971

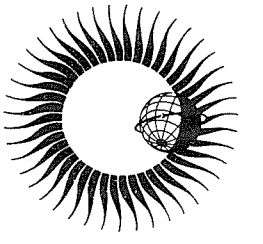

SUBSCRIPTION PRICE: $9.00 a year; $2.50 additional for foreign mailing; single issue price varies.* Order from the Superintendent of Documents, Government Printing Office, specifying the Catalog order number, C52.16/2:12. Checks and money orders should be made payable to the Superintendent of Documents. Remittance and correspondence regarding subscriptions should be sent to the Superintendent of Documents, Government Printing Office, Washington, D. C. 20402.

*Price of this issue $3.00

TABLE OF CONTENTS

		Page
PART I		
	FOREWORD	i
1.	INTRODUCTION AND SUMMARY OF GENERAL ACTIVITY	1
2.	SOLAR DISK AND LIMB PHENOMENA	8
3.	SOLAR RADIO PHENOMENA	43
4.	SOLAR X-RAYS	98
5.	SUDDEN IONOSPHERIC DISTURBANCES	109
6.	SOLAR WIND	122
7.	SOLAR ENERGETIC PARTICLES	130
PART II		
8.	IONOSPHERIC PHENOMENA	179
9.	AIRGLOW	272
10.	AURORA	298
PART III		
11.	COSMIC RAYS	312
12.	INTERDISCIPLINARY STUDIES	325
13.	GEOMAGNETIC DATA	359
14.	INTERPLANETARY MAGNETIC FIELD	408
	APPENDIX: ECLIPSE	413
	ACKNOWLEDGEMENTS	461
	ALPHABETICAL INDEX	461
	AUTHOR INDEX	464

TABLE OF CONTENTS

PART II

		Page
8.	IONOSPHERIC PHENOMENA	
	Total Electron Content, Amplitude Scintillations, Slab Thickness, and True Height of Plasma Frequencies from Fort Monmouth and Wallops Island Data for 6-9 March 1970 (P. R. Arendt, F. Gorman, Jr. and H. Soicher)	179
	Total Electron Content Measurements during the March 7-11, 1970 Period (Michael Mendillo and M. D. Papagiannis and John A. Klobuchar)	185
	Quasi-periodic Fluctuations in the Scintillation Index obtained on March 8, 1970 from Four Synchronous Satellites (Henry Mullaney, Michael D. Papagiannis and Jules Aarons)	188
	Incoherent Scatter Observations of an Overhead Aurora (J. V. Evans)	191
	Jicamarca Incoherent Scatter Observations during the March 1970 Storm (Ronald F. Woodman)	194
	Slough Ionospheric f-plots March 6-10, 1970 (D. E. Mortimer)	201
	Ionosonde and Riometer Data from Narssarssuaq, Godhavn and Thule (J. Taagholt)	207
	Ionospheric Disturbance during the Night of March 8-9, 1970 (P. Triska and J. Lastovicka)	211
	Ionospheric Structure during the Storm of March 8, 1970 (Richard B. Fritz)	213
	Ionospheric Effects Observed at Kiruna March 5-10, 1970 (G. Gustafsson, B. Aparicio, C. Jurén and J. Svennesson)	216
	Midlatitude Ionospheric Effects in March 1970 (R. Knuth, W. Lippert and J. Weiss)	222
	On HF Propagation Disturbances from March 6-10, 1970 (Yugoro Takenoshita)	227
	HF Doppler Observation Associated with Magnetic Storm of March 8, 1970 (M. Tsutsui and T. Ogawa)	231
	Riometer Observations during the Period 6-9 March, 1970 (Warner L. Ecklund and Herbert H. Sauer)	233
	Mid-latitude Radio Absorption by A1 and A3 Techniques - A1 Data for Lancaster (53°52'N, 2°45'W) (J. K. Hargreaves)	236
	Measurements of Phase and Amplitude at VLF and LF over Short and Medium Paths for the Period March 5-18, 1970 (E. Hammond and M. D. Harrison)	237
	Summary of VLF Activity at Chilbolton, England; South Uist, Outer Hebrides, Scotland; and St. John's STADAN Station, Newfoundland for the Period March 6-10, 1970 (S. K. Adjepong, A. Mathur, C. D. Reeve and M. J. Rycroft)	240
	VLF Effects as Observed at the Station Panska Ves on 8-10 March 1970 (Frantisek Jiricek)	244
	VLF Radiowave Observations of Ionospheric Disturbances during the Period 4-18 March 1970 (T. B. Jones)	247
	VLF Phase and Amplitude Measurements during the PCA Event 6-10 March, 1970 (Trygve Røed Larsen)	258
	VLF Observations at College, Alaska during the Great Magnetic Substorm of March 8, 1970 (R. N. Srivastava and D. W. Swift)	260
	Ionospheric Absorption Data (Kevo and Sodankylä)	265
	Magnetic Storm Effects at Arecibo (L. L. Cogger and G. J. Nelson)	268
9.	AIRGLOW	
	Optical Observations at the AFCRL Geopole Observatory Thule A.B., Greeland from 6-10 March 1970 (S. M. Silverman and J. G. Moore)	272
	Zenith Airglow Intensity at Dodaira Station, Tokyo Astronomical Observatory	284
	Minor Emissions in the SAR arc of March 8/9, 1970 (R. J. Hoch, L. L. Smith and K. C. Clark)	286
	Airglow Variations, Mid-latitude Red Arc around March 8, 1970 (J. Christophe and G. Weill)	292

PART II (continued)

		Page
10.	AURORA	
	Polar Aurora Observation at Mt. Lomnický Štít (M. Rybanský)	298
	Middle-latitude Aurora of March 8-9, 1970 at Zvenigorod (V. G. Sobolev, A. A. Kozlova, E. P. Kropotkina, L. V. Simakova, Yu. L. Truttse, N. N. Shefov, and O. T. Yurchenko)	299
	Visual Auroral Observations in Canada, February - March, 1970 (Peter M. Millman)	307
	Auroral Infrasonic Wave Activity at College, Alaska during the March 8, 1970 Magnetic Storm (Charles R. Wilson)	309

"Total Electron Content, Amplitude Scintillations, Slab Thickness, and True Height of Plasma Frequencies from Fort Monmouth and Wallops Island Data for 6 - 9 March 1970"

by

P. R. Arendt, F. Gorman, Jr., and H. Soicher
Institute for Exploratory Research
U. S. Army Electronics Command
Fort Monmouth, New Jersey

Data for this report have been obtained by courtesy of ESSA (now NOAA) and from our own measurements. We used ATS-3 beacon observations from our Diana test site and bottomside ionograms taken by ESSA at Wallops Island. These ionograms are of specific value for our ATS-3 observations because the subionospheric point of the slant range (from our test site at W 74.056°, N 40.185°) toward ATS-3 was very close to the Wallops Island position. We have used the Wallops Island ionograms for calculation of the slab thickness. For the eclipse period, we have converted these ionograms to curves of true height versus time for fixed plasma frequencies 2 to 9 MHz.

Figures 1 and 2 show the total electron content variation for 6-9 March; the variation during the eclipse is clearly seen, as are the changes of content value during the storm. The related slab

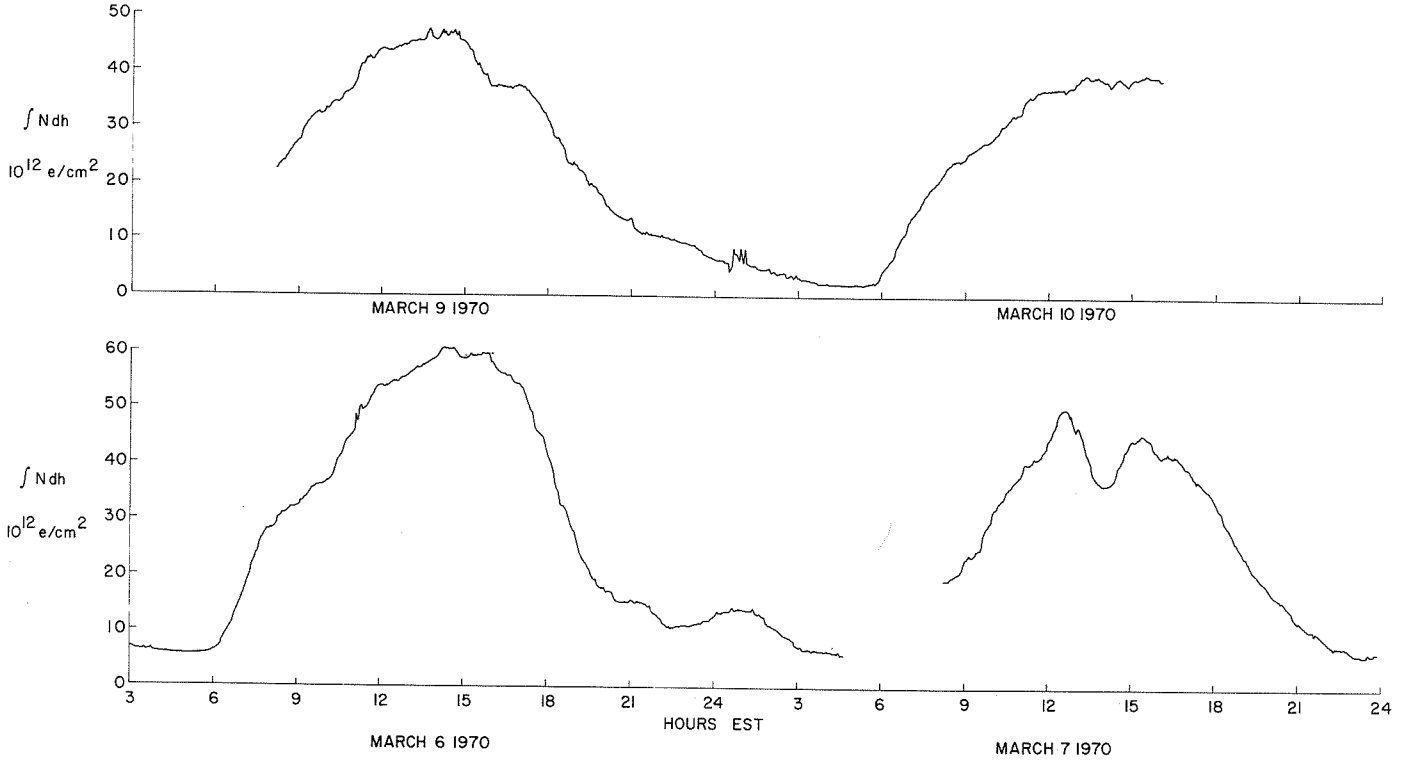

Fig. 1. Total electron content variation for March 6-7, 1970.

thickness is given in Figures 3 and 4 (note the different scaling in Figure 4). For 6 and 9 March, the slab thickness has a rather normal appearance (see Figure 3) when compared with mean values published by AFCRL [Klobuchar and Allen, 1970]. The slab thickness on the eclipse day (see Figure 3) also follows the normal trend. The apparent jitter during the eclipse observations is due to the narrow sequence of data (ionograms) taken during that period. The slab thickness on the day of the severe storm (8 March, Figure 4) reflects the unusual conditions. The fast variations indicate quick changes of the electron-density vs. altitude profiles. The greatest change between 1600 and 1700 hours EST corresponds to a sharp drop in critical-F (from about 13 to about 4 MHz) indicating substantial depletion. From topside sounding it is known that enhancement and depletion of ionization occurs during storms, but no enhancement [Arendt, 1969] with storms smoothly reaching maximum activity (no sc). The variations of the slab thickness on 8 March as well as the content data (see Figure 2) reflect enhancement and depletion.

Figure 5 shows the amplitude scintillations measured with signals on 137.35 MHz from ATS-3. The scintillation index was obtained using the AFCRL method described in literature [Whitney and Malik, 1968]. It is of special interest to note in detail the changes of the scintillation index during the eclipse day. The index was zero from 0900 to 1100 EST and seven from 1100 to 1200 EST. With the start of the eclipse it reached 34, but then fell below 20 where it remained until 1130 EST.

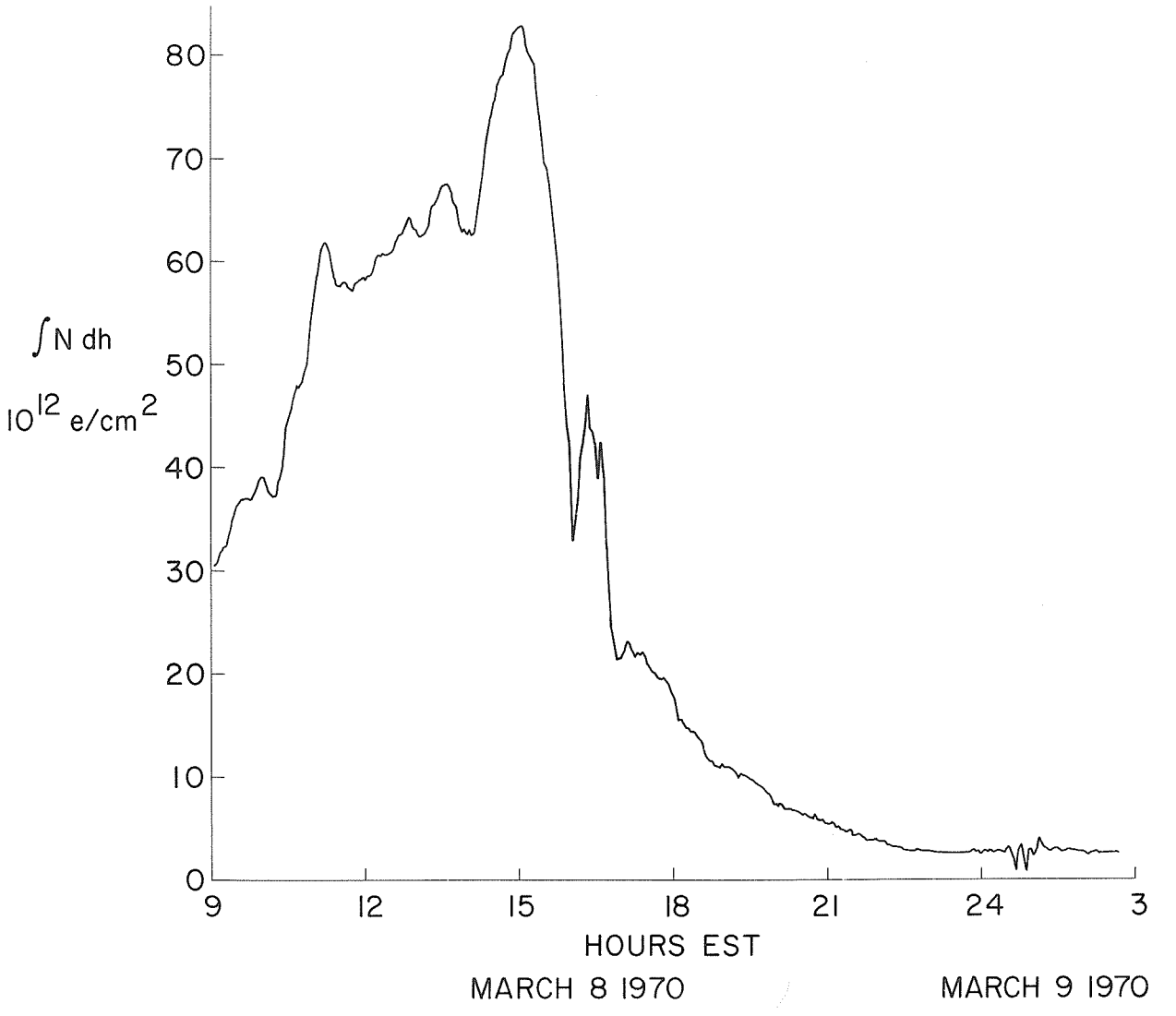

Fig. 2. Total electron content variation for March 8-9, 1970.

Peak values of up to 75 were observed in the interval 1430 to 1515 EST when the eclipse effects were already diminishing. After that interval, the index remained below 20 until 2300 EST. From the relatively small variations, it can be concluded that ionospheric observations during the actual eclipse period were not largely affected by the magnetic activity. Together with the scintillation index, the variations of the Kp-index are given in Figure 5. A direct correlation of the scintillation index with the Kp-index does not appear to be possible for the data in Figure 5. However, the data indicate that fast changes of Kp are more likely to produce scintillations than smooth variations of Kp.

Figure 6 shows the evaluation of the Wallops Island ionograms of the eclipse day. Curves of true height vs time for the plasma frequencies 2 to 9 MHz display the typical variations produced by an eclipse. The apparent jitter which is shown during the actual eclipse interval can be ignored because it is mainly related to the fast sequence of data taken during that period. Some undulating altitude variations in the time interval before the eclipse are seen at the plasma frequencies 4 to 8 MHz. The 2 MHz reflection disappears before the eclipse started. The maximum altitude for the 3 MHz plasma frequency coincides with maximum coverage at 100 km. The upward motion of the F-region is delayed with reference to that time (compare the curves for 3 and 9 MHz in Figure 6).

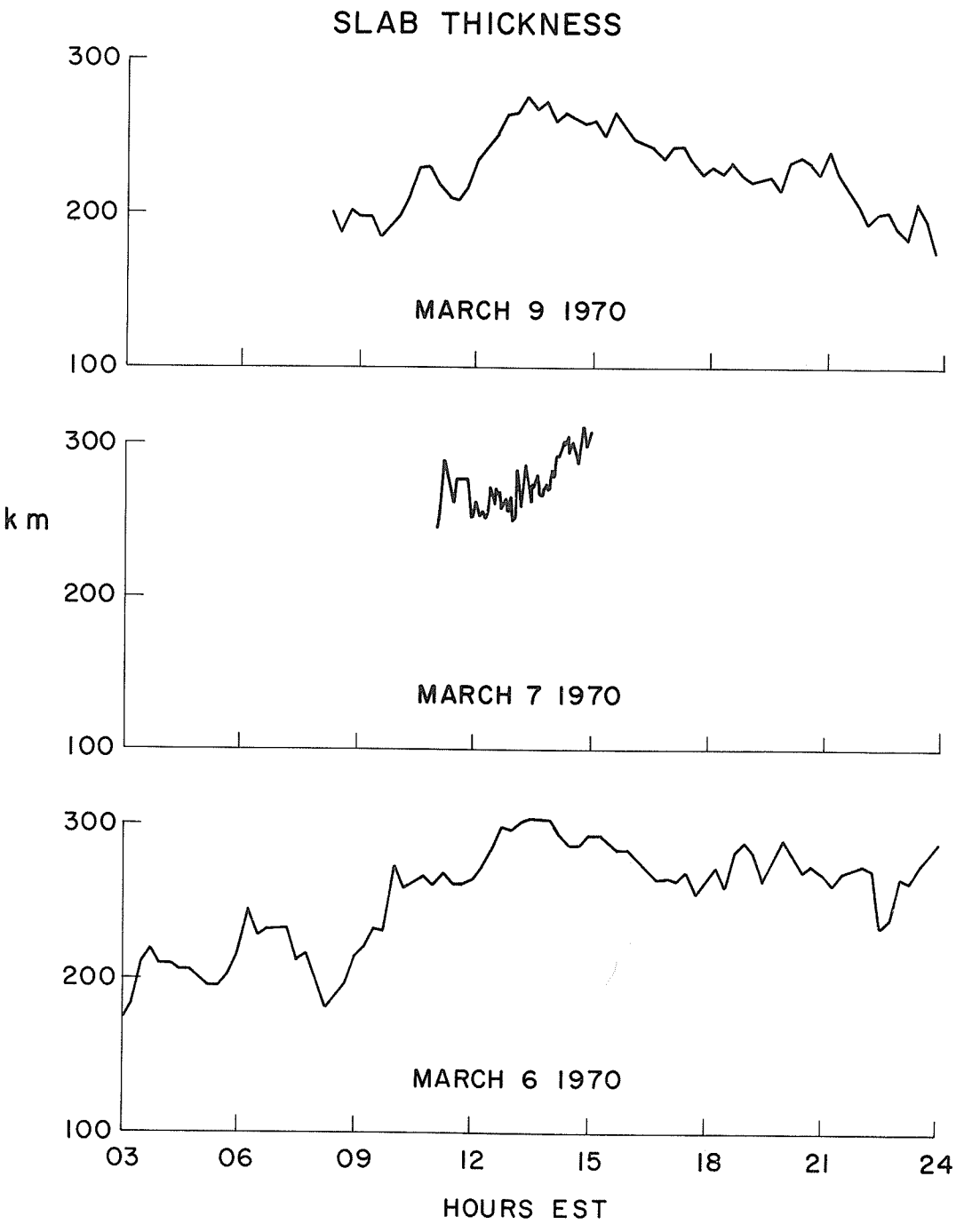

Fig. 3. Slab thickness for March 6, 7 and 9, 1970.

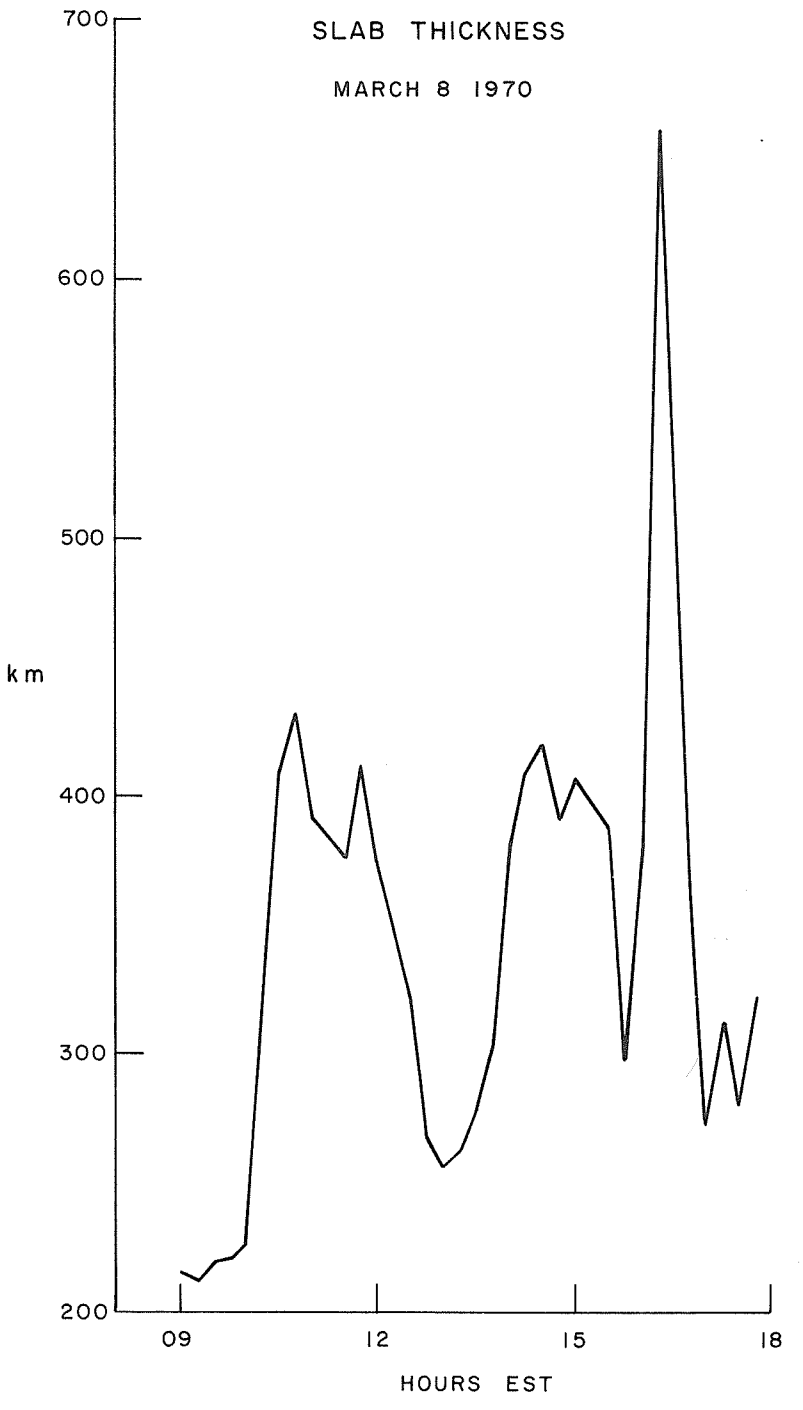

Fig. 4. Slab thickness for March 8, 1970.

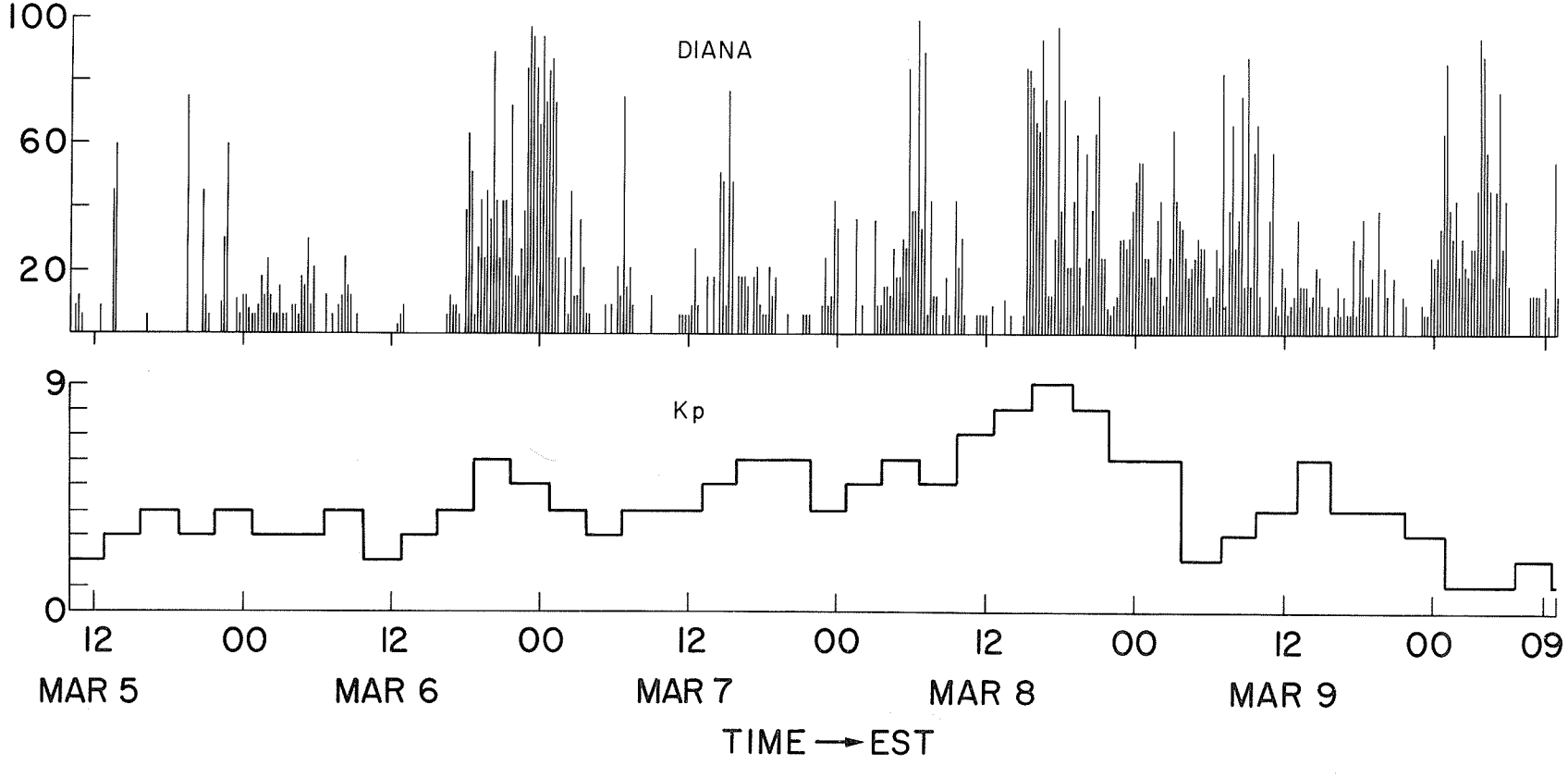

Fig. 5. Amplitude scintillations measured with signals on 137.35 MHz (ATS-3) for March 5-9, 1970.

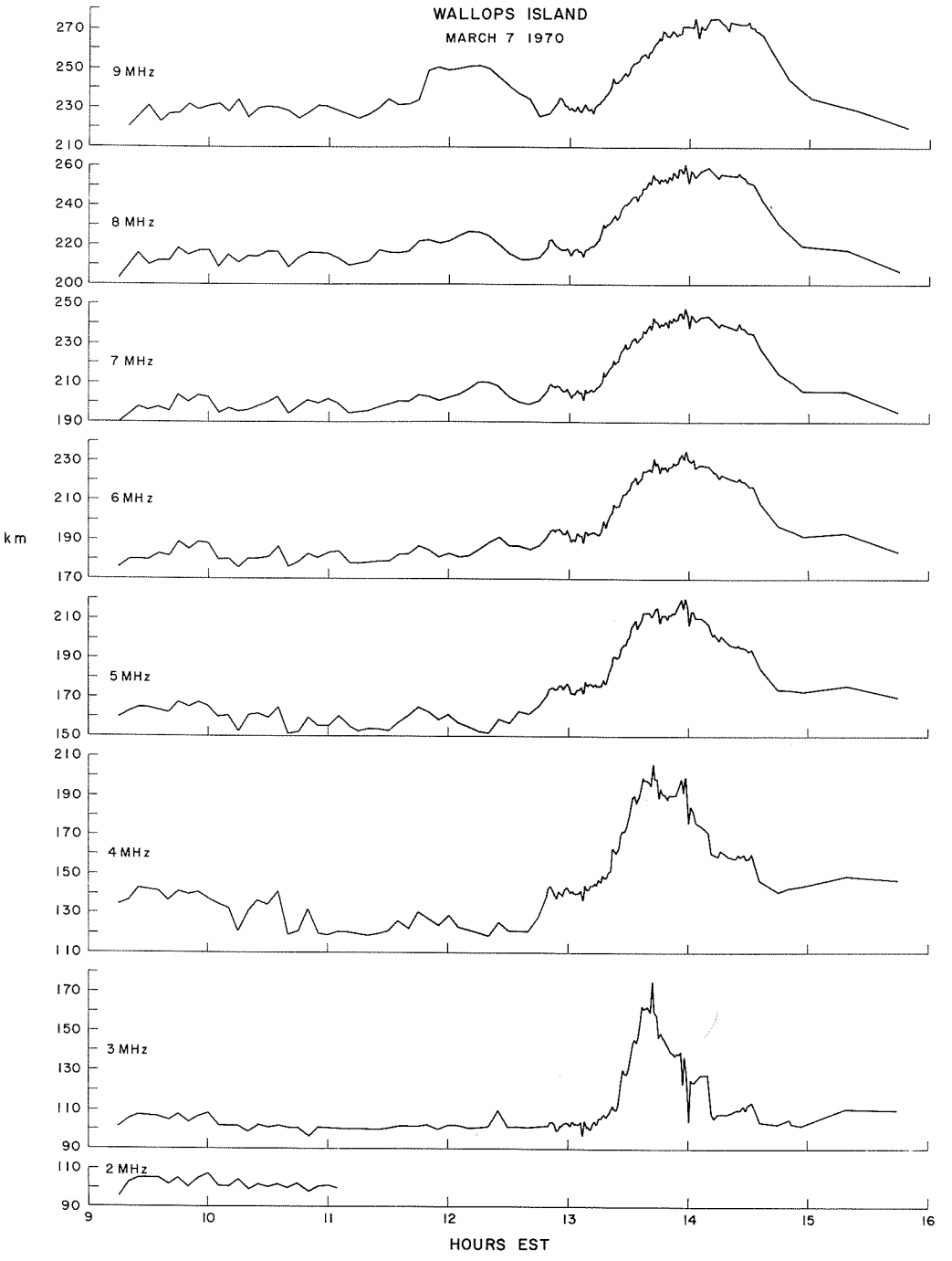

Fig. 6. True height vs. time curves (Wallops Is., Va. data) for plasma frequencies 2-9 MHz for March 7, 1970.

REFERENCES

ARENDT, P. R. 1969 Comparison of the topside ionosphere during magnetic storms of various types; Planet. Space Sci. 17, 1993-1995.

KLOBUCHAR, JOHN A. and RICHARD S. ALLEN 1970 A first-order prediction model of Total-Electron-Content group path delay for a midlatitude ionosphere, AFCRL Report 70 - 0403, 8 July 1970.

WHITNEY, H. E. and CHESTER MALIK 1968 A proposed index for measuring ionospheric scintillation, AFCRL Report 68-0138, March 1968.

"Total Electron Content Measurements during the March 7-11, 1970 Period"

by

Michael Mendillo and M. D. Papagiannis
Department of Physics and Astronomy
Boston University
Boston, Massachusetts

and

John A. Klobuchar
Air Force Cambridge Research Laboratories
Bedford, Massachusetts

Introduction

By continuously monitoring the VHF signal from the geostationary satellite ATS-3, measurements of the amount of Faraday rotation of the plane of polarization can be related to the integral with height of the electron density profile of the earth's ionosphere. This quantity is called the total electron content (TEC) and is usually expressed in the units 10^{16} el/m^2. The major contribution to this integral occurs in the vicinity of the F-region and thus TEC data mainly describe the electron content of the topside ionosphere. The integrated density along the ray path from the satellite is converted to an "equivalent vertical columnar content" relevant to a height at 350 km. The geographic coordinates of this point at 350 km are N39 and W73 for TEC measurements taken at the AFCRL Sagamore Hill Radio Observatory in Hamilton, Massachusetts. When converted to geomagnetic coordinates, the present set of data refers to a geomagnetic latitude of N53.

Results

Measurements of ionospheric TEC taken during the first two weeks in March 1970, included a period during which a near total solar eclipse and a great geomagnetic storm occurred. This brief report concentrates on the TEC variations which occurred during the geomagnetic storm period commencing at 1418 UT on 8 March. The effects of the total eclipse which occurred on 7 March have already been presented by Klobuchar and Malik [1970] and will not be further discussed here. In analyzing geomagnetic storm effects, we have found it useful to augment the TEC data with measurements of the geomagnetic field taken at the nearby Weston Observatory (N42 W71), foF2 data from the Wallops Island ionosonde (N37 W75), as well as the Kp and Ap magnetic indices obtained from the Solar-Geophysical Data. All of these parameters are presented in the accompanying figure.

At the top of the figure is the 3-hr world-wide magnetic index Kp. Next, magnetic field measurements of the horizontal component (H) and the total field (F) are presented in the form of hourly values averaged from 5 readings per hour. The horizontal dashed lines give the monthly mean values of H and F. The total electron content data were read at 5-minute intervals and are displayed in the next row. The dashed curve represented the median hourly TEC values for the first 12 days in March. The Wallops Island foF2 values were converted to electron density values at the peak of the F-region (N_{max}) and are plotted in comparison to their monthly median values (dashed curve). In the final entry, we examine a parameter called Slab Thickness (τ) which is defined as the ratio of TEC to N_{max}. Variations in slab thickness (τ) describe the relative changes in the gross shape of the F-region. We computed hourly values of τ and plotted the deviation ($\Delta\tau$) from median values obtained during the period 1-12 March.

In examining this figure, we first note that the eclipse effects on the 7th are imbedded in a significant amount of geomagnetic activity (Ap=42). Nevertheless, quite a pronounced dip is found in both total content and peak density during the time of maximum obscuration (95%). The event of prime concern, the severe geomagnetic storm of 8 March, began with a storm commencement (SC) at approximately 0930 LT. The beginning of the storm period was peculiar in that the magnetic field showed a rapid decrease rather than the usual increase during the initial phase. During the afternoon hours there was a remarkable increase in the geomagnetic field with a peak enhancement at 1700 LT. The total field (F) increased by 500 gammas which is nearly 1% and Kp also reached its maximum possible value of 9 during this period. While the TEC data show that after the SC the daytime total content was enhanced, the major increase in TEC occurred during the period when the total field was increasing. The phenomenon of substantial simultaneous enhancements in the total magnetic field and the total electron content during the early phase of a geomagnetic storm has been discussed by Mendillo, Papagiannis and Klobuchar [1970a]. The fact that the total field and horizontal component are both greatly increased suggests strong compressive effects. Such a compression implies a contraction of F-region plasma as well as a protonospheric flux into the topside ionosphere. The reason why the effect is localized to the afternoon hours probably lies in the fact that the dawn-dusk electric field associated with magnetospheric convection partially cancels the co-rotational motion of the ionospheric plasma near the sunset region. This stress hindering co-rotation causes both plasma and magnetic field to pile up along the entire sunset meridian. This "Dusk Effect" is discussed in detail by Papagiannis, Mendillo and Klobuchar [1971].

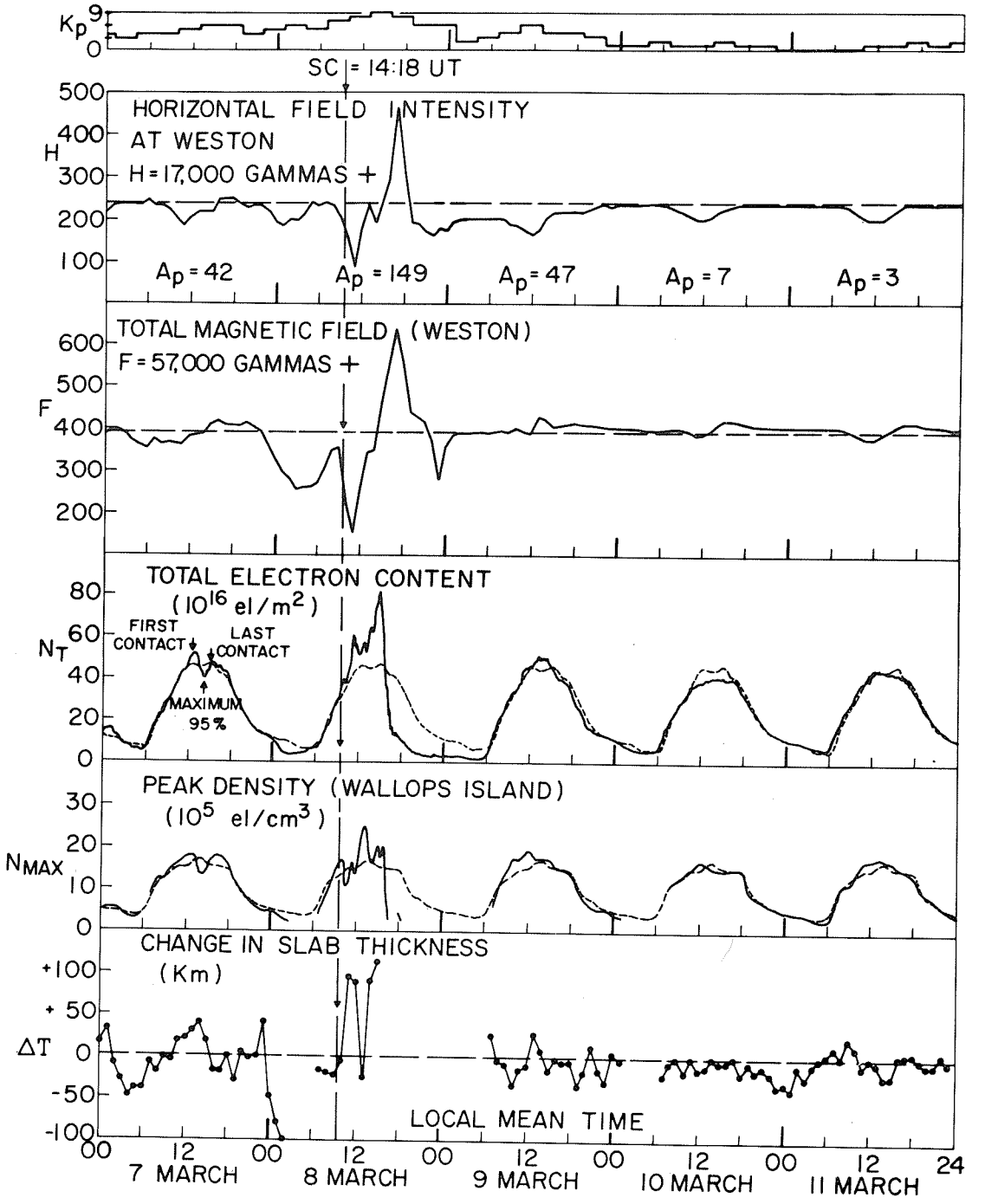

Fig. 1. Total electron content from geostationary satellite ATS-3 as observed at Sagamore Hill Radio Observatory March 7-11, 1970, compared with magnetic indices and measurements, Wallops Island electron density values and change in slab thickness.

While TEC and N_{max} usually respond in similar ways to perturbations, the irregular nature of N_{max} on the 8th indicates that strong motions may have severely distorted the $N_e(h)$ profile. This is also shown in the slab thickness results. The high τ values on the 8th are due to the enhancements in electron density above the peak (i.e., in TEC) being greater than those at the peak (i.e., in N_{max}).

After the maximum total content value is reached at about 1500 LT, there is a rapid decrease in TEC at several times the normal decay rate. This is a common feature also evident in our earlier study of geomagnetic storm effects. Following this large decrease in TEC, the nighttime values remained severely depressed until sunrise on the following day. These TEC depletions give evidence for strong heating of the neutral atmosphere enhancing the N_2 and O_2 concentrations at F-region heights and therefore the electron loss rate. Considering that the depressions in TEC are so severe early on the 9th, it is somewhat surprising that the subsequent daytime values are not similarly depressed. On March 10 and 11, the TEC is only slightly depressed while N_{max} is basically unchanged. This leads to slab thickness values somewhat lower than usual.

The reason why the durations of both the magnetic and ionospheric effects are abnormally short is an interesting question which deserves further attention. We have recently completed an analysis of over 2 years of TEC, N_{max}, and τ data for geomagnetic activity effects by studying 28 individual storm periods. Our results show that the average period of TEC depletions (i.e., the negative phase) lasts for at least 60 hours, except during equinox storms when this period is reduced to 48 hours, and in particular for Spring storms when the negative phase lasts only 12-24 hours. A detailed discussion of these results is in preparation [Mendillo, Papagiannis and Klobuchar, 1970b].

REFERENCES

KLOBUCHAR, J. A. and C. MALIK 1970 Comparison of Changes in Total Electron Content Along Three Paths, Nature, 226, 1113-1114.

MENDILLO, M., M. D. PAPAGIANNIS and J. A. KLOBUCHAR 1970 Ionospheric Storms at Midlatitudes, Radio Science, 5, 895-898.

PAPAGIANNIS, M. D., M. MENDILLO and J. A. KLOBUCHAR 1971 Simultaneous Storm-time Increases of the Ionospheric Total Electron Content and the Geomagnetic Field in the Dusk Sector, Planetary and Space Science, in press.

MENDILLO, M., M. D. PAPAGIANNIS and J. A. KLOBUCHAR 1970b The Morphology of Mid-Latitude Total Electron Content Variations during Geomagnetic Storms, presented at the AGU National Fall Meeting (San Francisco), 7-10 December 1970.

"Quasi-Periodic Fluctuations in the Scintillation Index obtained on March 8, 1970, from Four Synchronous Satellites"

by

Henry Mullaney and Michael D. Papagiannis
Department of Physics and Astronomy
Boston University
Boston, Massachusetts 02215

and

Jules Aarons
Air Force Cambridge Research Laboratories
Bedford, Massachusetts 01730

Scintillations in the amplitude of the signals from ATS-3, ATS-5, Early Bird, and LES-6, received at the Sagamore Hill Radio Observatory of the AFCRL in Hamilton, Massachusetts, have been analyzed for the March 6-10, 1970, period. During these days, the longitude of the satellites (the latitude of all these geostationary satellites is nearly 0) and their respective sub-ionospheric points (the latitude and longitude of the point where the signals cross a height of 350 km) are given in Table I.

Table I

Satellite	Frequency	Longitude	Sub-Ionospheric Longitude	Latitude
ATS-5	136 MHz	104 W	74.7 W	39.2 N
ATS-3	136 MHz	85 W	72.4 W	39.3 N
Early Bird	136 MHz	54 W	68.9 W	39.3 N
LES-6	254 MHz	43.5 W	67.5 W	39.2 N

On March 8, the scintillation indices were unusually high (see Figure 1). At 0200 UT a sharp increase occurred in the scintillation of the signals from LES-6 and Early Bird, the two eastern satellites. Commencing at about 0700 UT, scintillations from all four satellites displayed a quasi-periodic structure with a period of about 90 minutes. The maximum of the scintillation activity seems to occur in the 0900 - 1000 UT interval.

During this period of high scintillation activity, strong magnetic fluctuation was observed at the Weston Observatory in Weston, Massachusetts. As seen from Figure 2, the decreases in the total field strength during this period correspond extremely well to the increases in the scintillation index from ATS-3. This strong correlation is indeed impressive in light of the facts that the scintillation index is determined every 15 minutes (and hence some fine structure may be lost), and that Weston Observatory is at 42.4 N, while the sub-ionospheric point of ATS-3 is 39.3 N. It should be pointed out, however, that the longitude of the ATS-3 was approximately the same as that of Weston Observatory, which might be the reason why the magnetic fluctuations are best correlated with the scintillation index from the ATS-3.

Since the period of the oscillations in scintillation index is suggestive of gravity waves, the total electron content from ATS-3 was examined and is plotted in Figure 2. Near the times of the second and third peaks in the scintillation index, the total electron content dropped by about 5×10^{15} el/m^2 between 1000 and 1015 UT (a drop of 8%) and by about 9×10^{15} el/m^2 between 1100 and 1120 UT (a drop of 9%). It should be noted that, except for these two decreases, the total electron content increased continually after 0705 UT, despite the fact that dawn at the F-layer did not occur until about 0940 UT. This could have been the result of an external source of ionization such as particle precipitation, or the movement of the minimum of the trough out of the sub-ionospheric region. The invariant latitude Λ of the trough was given by Rycroft and Burnell [1970]

$$\Lambda = 60.4 - 1.4Kp - 0.7t \pm 3.5$$

When the increase in the total content started, the local time t was t=2 and the Kp index was Kp=6. This places the trough at an invariant latitude $\Lambda = 50.6 \pm 3.5$, and therefore our sub-ionospheric point with Λ=52.5 would very easily be in the trough. The onset of high scintillations at this time suggests that the trough was moving to lower latitudes, and that the increase in total content would be the result of the sub-ionospheric point moving out of the trough. It has been observed [Aarons and Allen, 1971] that the scintillation boundary also moves toward the equator with increasing geomagnetic activity. During the magnetically disturbed period, the sub-ionospheric points of the paths to the four satellites were within the irregularity region north of the scintillation boundary.

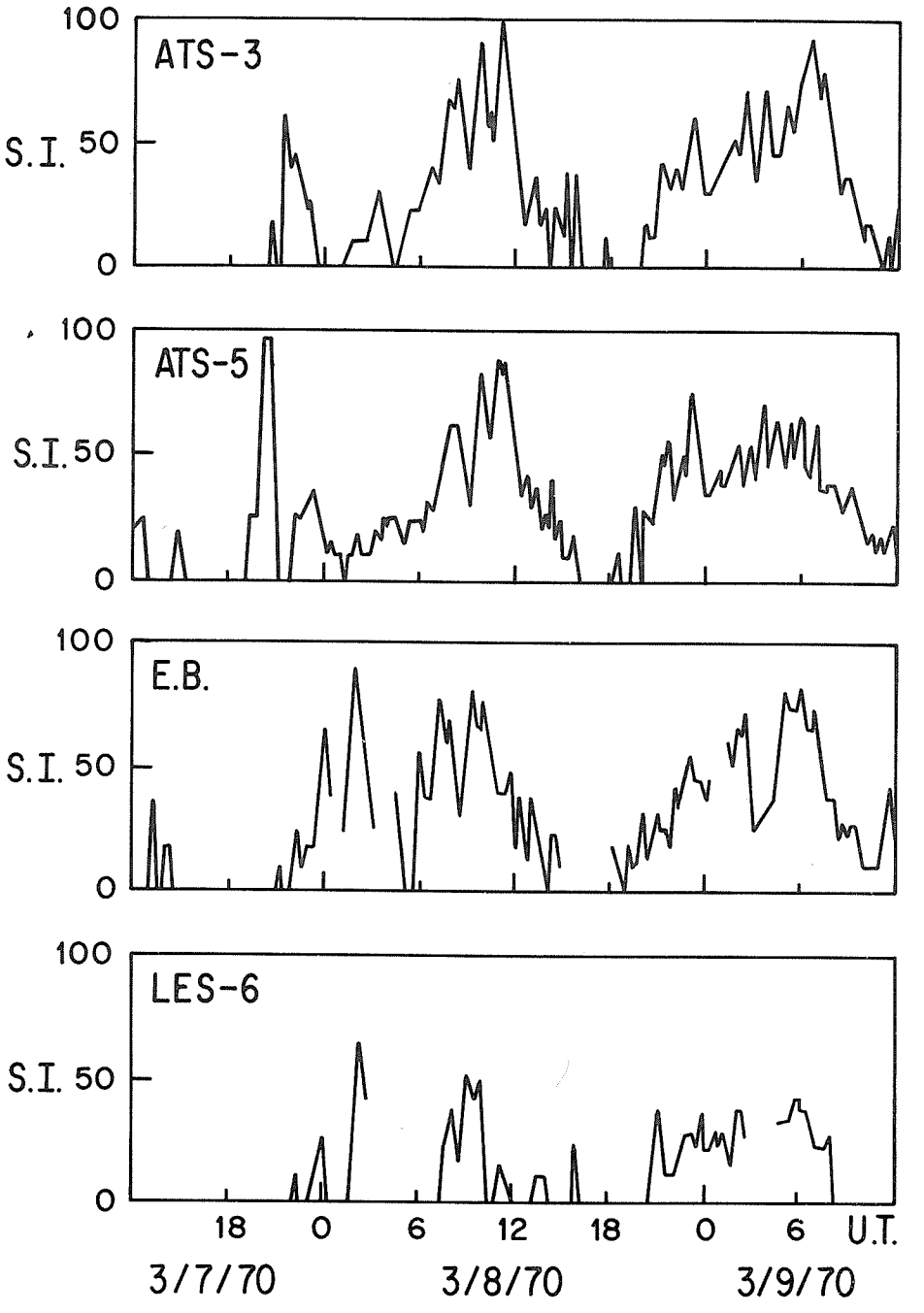

Fig. 1. Scintillation indices from ATS-3, ATS-5, Early Bird and LES-6 as observed at Sagamore Hill Radio Observatory March 7-9, 1970.

In summary, it seems possible that on March 8, 1970, enhanced geomagnetic activity pushed the scintillation boundary and the ionospheric trough to lower latitudes, so that our sub-ionospheric points moved out of the trough and were located in a region of high scintillation activity. It is interesting that under these conditions points along the same meridian show a very high correspondence between the peaks on the scintillation index and the valleys of the total magnetic field as well as the peaks of the total magnetic field and the valleys of the scintillation index.

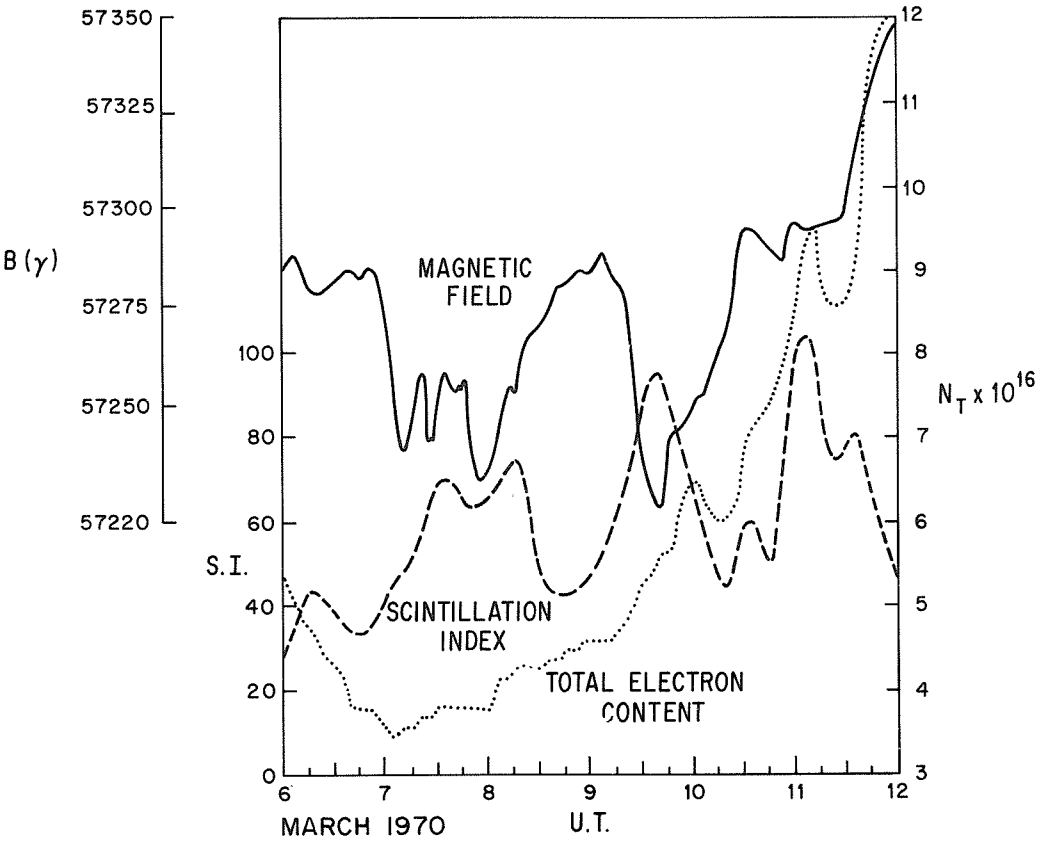

Fig. 2. Scintillation index and total electron content from ATS-3 compared with magnetic field measurements observed at Weston, Massachusetts.

Acknowledgement

We would like to thank J. A. Klobuchar of AFCRL for providing the total electron content data, and Weston Observatory for providing the magnetograms.

REFERENCES

AARONS, J. and R. S. ALLEN 1971 The Scintillation Boundary During Quiet and Disturbed Magnetic Conditions, J. Geophys. Res., 76, 170.

AARONS, J., J. P. MULLEN and H. E. WHITNEY 1969 The Scintillation Boundary, J. Geophys. Res., 74, 884.

RYCROFT, M. J. and S. J. BURNELL 1970 Statistical Analysis of Movements of the Ionospheric Trough and the Plasmapause, J. Geophys. Res., 75, 5600.

WHITNEY, H. E., J. AARONS and C. MALIK 1969 A Proposed Index for Measuring Ionospheric Scintillations, Planet. Space Sci., 17, 1069.

"Incoherent Scatter Observations of an Overhead Aurora"

by

J. V. Evans
Lincoln Laboratory M.I.T.
Lexington, Massachusetts 02173

The Millstone Hill incoherent scatter radar (N42.5 W71.6) was operated during the magnetic storm in March 1970 on the night of March 8-9 for 10 hours. These observations were carried out following notice kindly provided by Dr. John Noxon, Blue Hill Observatory, (Harvard University) that a visual aurora was in progress. The auroral luminosity was chiefly evident to the north of the station and persisted until about 2300 EST.

Measurements were made of the electron density, electron and ion temperatures over the altitude range 200-800 km using procedures described by Evans et al. [1970]. The time resolution in the measurements was 30 minutes. The vertical profiles obtained have been converted to contour diagrams (Figures 1-3). Considerable difficulty was encountered in reading the Millstone Hill ionosonde during the observing period to obtain the value of foF2 (used to provide an absolute calibration of the electron density profiles produced by the radar). Prior to midnight strong returns from the E-region were visible; probably these were reflections from the ionization produced in the E-region by the auroral precipitation. During this period foF2 appeared to be varying rapidly in an irregular manner. Following midnight foF2 fell below the lowest value (∿ 2.5 MHz) observable with the Millstone Hill ionosonde. Thus, in order to obtain the variation of foF2 with time we were obliged to supplement the ionosonde measurements with values derived from the variation of the echo power observed with the incoherent scatter radar.

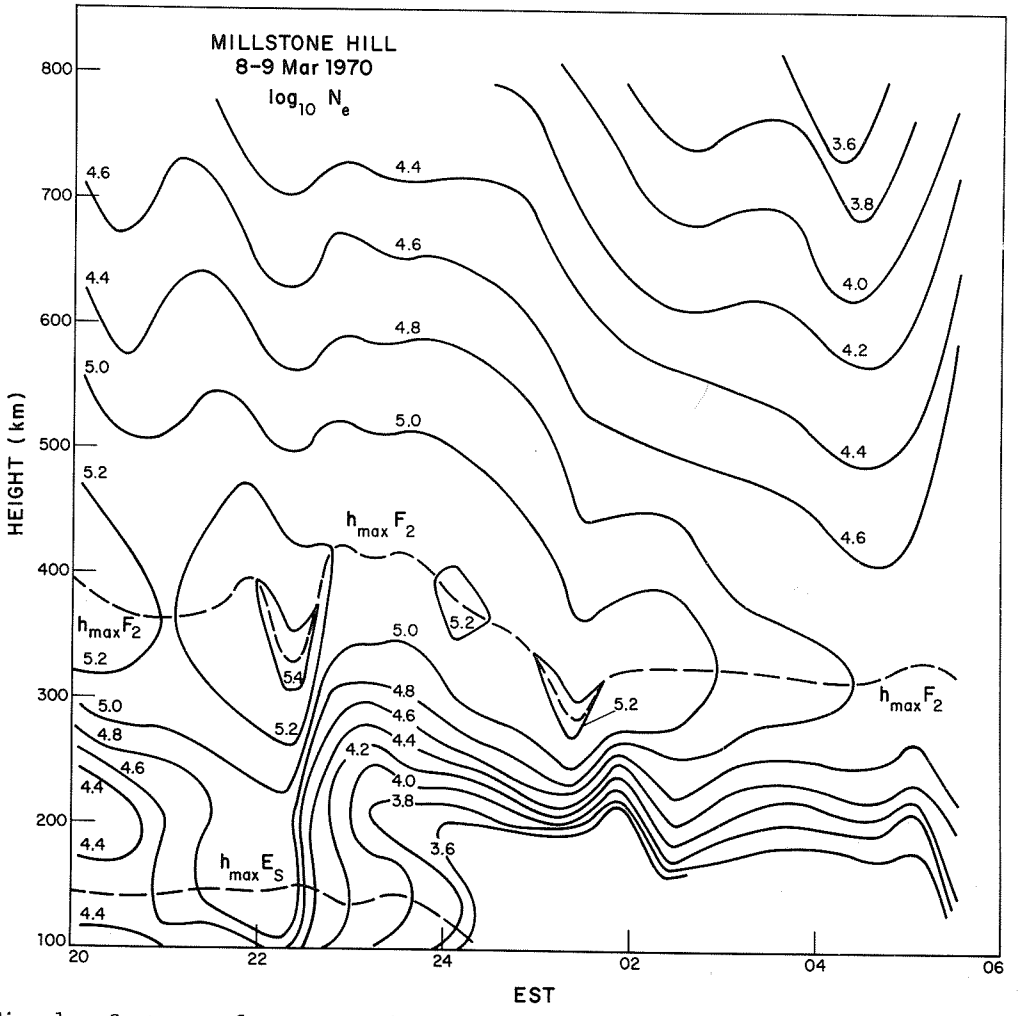

Fig. 1. Contours of constant electron density vs. height and time during the period 20-06 EST, March 8-9, 1970. A visual aurora was present during the evening.

Figure 1 presents the electron density contours obtained. The presence of the aurora seems to have given rise to a layer below the normal nighttime F layer with a height of maximum density of 130-140 km. In Figure 1 this layer is indicated by the symbol Es. The largest density in this layer occurred a little before 2200 EST and was then somewhat less than 10^5 el/cm^3. This is considerably lower than the electron density ($\sim 10^6$) deduced for intense aurorae from observations of the luminosity [Walker and Rees, 1968] suggesting that Millstone lay only on the fringe of the precipitation region. The Es layer disappeared rapidly around midnight. The F-layer peak appears to have been much higher than normal during the period prior to midnight and the series of maxima and minima (Figure 1) suggests that a large travelling ionospheric disturbance was present. These maxima could have been produced by successive increases in the precipitation of very soft electrons, but this interpretation seems to be ruled out by the electron temperature variation (Figure 2) which shows no increases during these times.

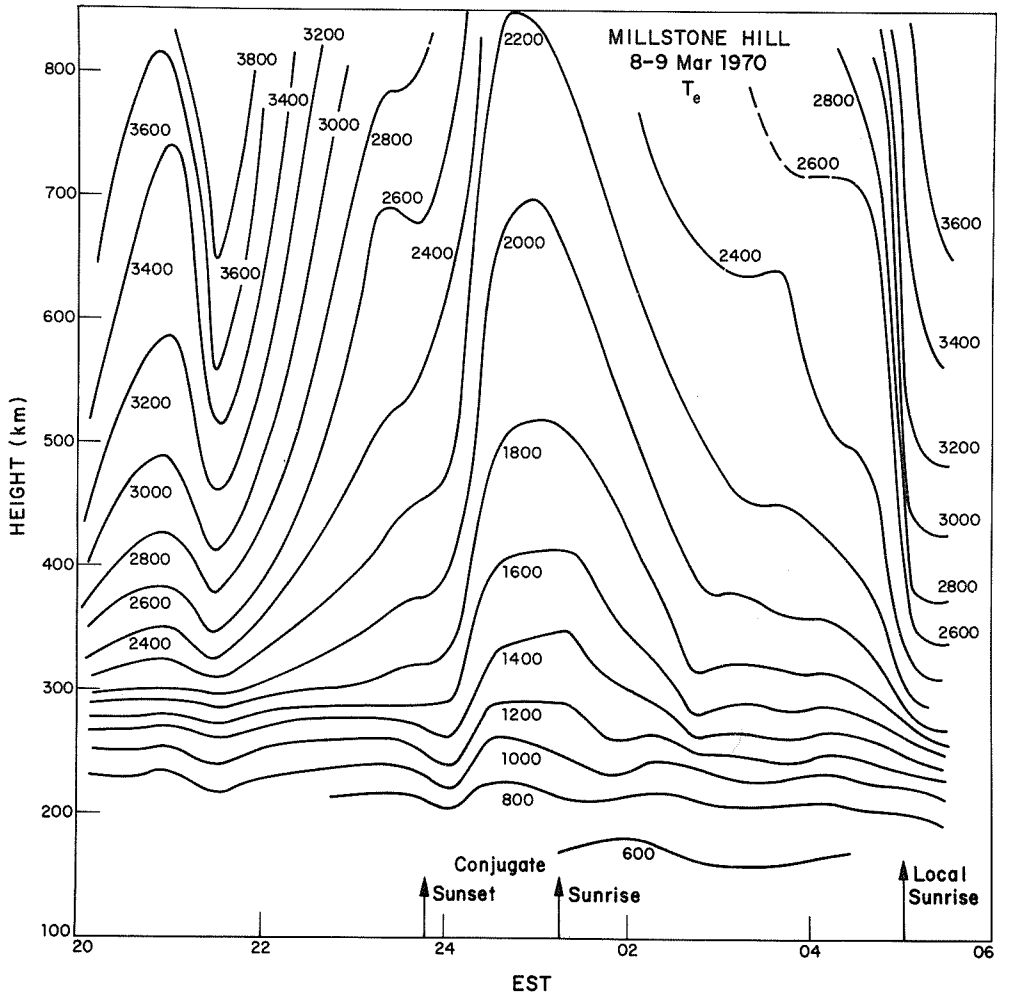

Fig. 2. Contours of constant electron temperature during the period 20-06 EST March 8-9, 1970.

The electron temperature behavior (Figure 2) observed on this night is complicated by the variations introduced by conjugate sunset and sunrise. The conjugate point to Millstone lies to the south of the Antarctic circle [Evans, 1968] and thus, experienced only a brief period of sunset (defined here as $\chi \geq 105°$); during this period the local electron temperature declined considerably. It is possible, however, that conjugate sunset coincided with the cessation of the auroral precipitation and that this accounts for the rapid drop in Te at midnight. Prior to midnight the electron temperature was anomalously high though not as high as has been reported in a number of red arcs [Norton and Findlay, 1969]. A peak in the temperature just prior to 2200 EST appears to be associated with a peak in the Es layer density.

The ion temperature values (Figure 3) follow the general trend of the electron temperature but do not exhibit the same rapid variations; this is to be expected in view of the coupling between the

ion and neutral temperatures. The values shown in Figure 3 suggest that the exospheric temperature was quite high before 2200 EST but did not exceed about 1300°K.

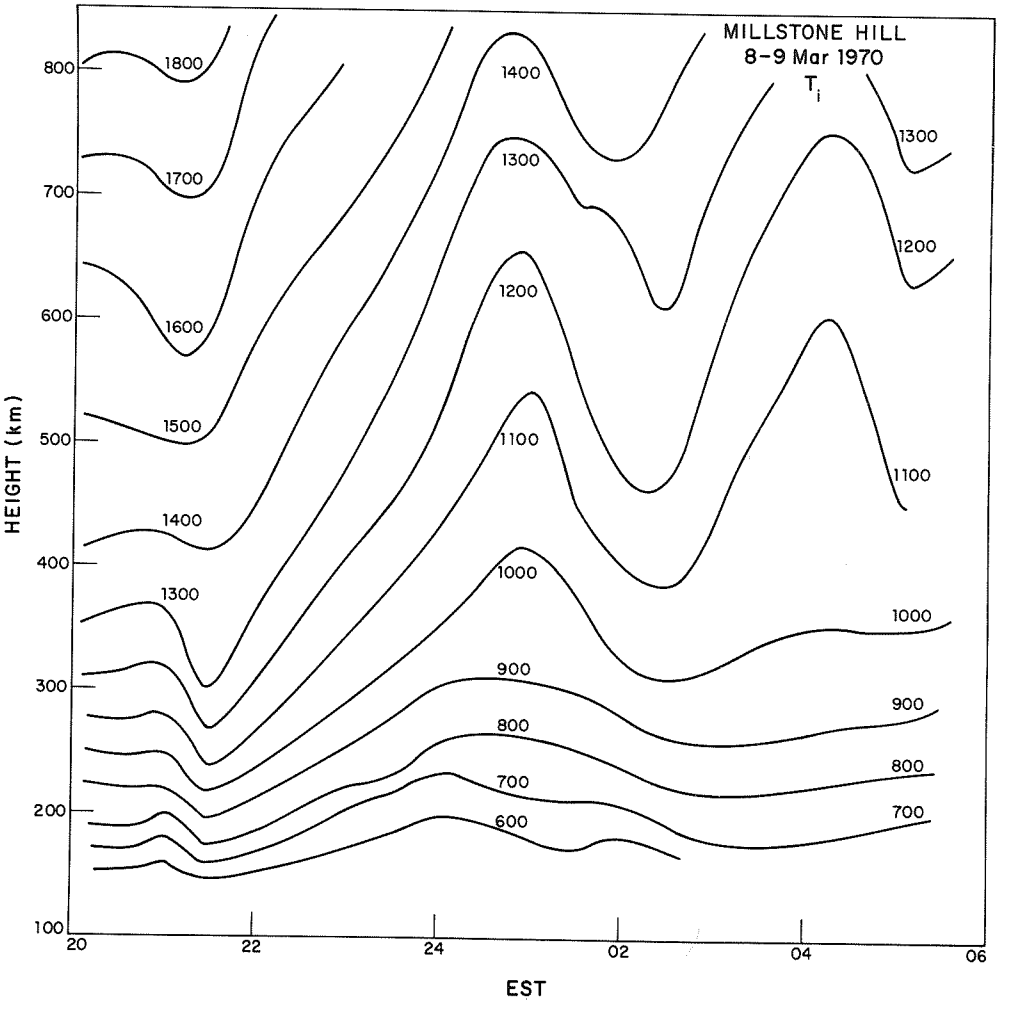

Fig. 3. Contours of constant ion temperature during the period 20-06 EST March 8-9, 1970.

The measurements reported here are consistent with the following over-all picture. Prior to midnight Millstone lay at the equatorward edge of the region of auroral precipitation. If any red arc were present it lay considerably to the south of Millstone. Following midnight the boundary of the precipitation moved northward leaving Millstone lying under the trough of low ionization density.

REFERENCES

EVANS, J. V. 1968 Sunrise Behavior of the F-layer at Midlatitudes, J. Geophys. Res., 73, 3489.

EVANS, J. V., R. F. JULIAN and W. A. REID 1970 Incoherent Scatter Measurements of F-Region Density, Temperatures and Vertical Velocity at Millstone Hill, Lincoln Laboratory M.I.T., Lexington, Mass. T.R. 477.

NORTON, R. B. and J. A. FINDLAY 1969 Electron Density and Temperature in the Vicinity of the 29 September 1967 Middle Latitude Red Arc, Planet. Space. Sci., 17, 1867.

WALKER, J. C. G. and M. H. REES 1968 Ionospheric Electron Densities and Temperatures in Aurora, Planet. Space. Sci., 16, 459.

"Jicamarca Incoherent Scatter Observations during the March 1970 Storm"

by

Ronald F. Woodman
Jicamarca Radar Observatory
Instituto Geofisico del Peru
Apartado 3747, Lima, Peru

The purpose of this note is to report on ionospheric observations taken at Jicamarca (1° N Magnetic Latitude) during the March 8, 1970 magnetic storm. This report includes measurements of the electron density, electron temperature and vertical drift (or E-W electric field) for the 7, 8 and 9 of March 1970. These measurements are complemented by C-4 ionograms and magnetic field measurements taken at the Huancayo Observatory which is located at the same magnetic latitude 100 km east from the Jicamarca Observatory. We are including Huancayo ΔH magnetograms to illustrate our discussion.

The data reported here are still under study and it is being reported in response to the request of the World Data Center A, Upper Atmosphere Geophysics, in its effort to gather world-wide data taken during the magnetic storm in a single publication. Therefore, we shall present the experimental facts limiting our discussion and conclusions to those which can be derived from simple inspection of the records.

The techniques used to gather the data have been reported previously. The electron densities have been obtained using the Faraday rotation method and the electron temperatures using the cross correlation technique, both systems have been described by Farley [1969a,b]. The technique to obtain the vertical drift (E-W electric field) is described by Woodman and Hagfors [1969]. The three parameters were measured almost simultaneously.

We do not have quiet day measurements of density and temperature sufficiently close to the day of the storm to be taken as a control day. The reader will have to refer to the statistical behavior of these parameters as measured at Jicamarca and reported by J. P. McClure, D. T. Farley and R. Cohen [1970] and J. P. McClure [1970]. We have included here the statistical behavior of vertical drifts for the same season taken from Woodman [1970].

Results and Discussion

Figures 1a) and 1b) show the electron temperature, electron density and vertical drift (E-W electric field) for March 7, 1970. The conversion factor between velocity to electric field is 40 m/sec equal 1 millivolt/meter March 7 was already disturbed with three hour Kp's as high as 6-. The behavior of the electron density shows nothing very unusual, and the electron temperature agrees well with what one would expect from previous experience for the corresponding density profile. The vertical drifts did show some disturbance which can be better appreciated in Figure 4 (curve 7) in comparison with the typical behavior for the season. The fluctuations with low values at 1100 and 1500 hours LT* can be attributed to the storm.

There were two passes of OGO-6 close to the station which could be used to take a reference value for the electron temperature as measured by the satellite. The passes are shown by a satellite looking symbol in Figure 1a) (disregard the satellite height, it corresponds to the satellite range from the station).

On March 7 there was a solar eclipse but it was not seen at Jicamarca. The line of totality crossed our longitude at 1330 LT and 46° to the north of us. We did not see any effects which could be attributed to the eclipse, as could be expected being so far away from the affected zone.

Figures 2a) and b) show the electron temperature, electron density and vertical drift (E-W electric field) for March 8, 1970, the most disturbed day. Sudden commencement occurred at 0918 LT. We do not have any data from 0830 to 1130 LT; the transmitter was turned off to make some adjustments. We were not aware of the storm and were running a control day for the eclipse of the previous day.

The effects on the density contours are very dramatic. There was a very rapid uprising of the F layer starting at 1300 hours LT reaching a height for the maximum density, H_{max}, of 800 km at least! The sensitivity of the system at these heights went down as a new layer appeared at 1500 LT, increasing the Faraday dispersion effects [McClure, 1967] as a consequence of the increase in total electron content, and it is possible that the top peak went even higher at later times. The rapid uprising of the F layer was due to a very high upward vertical velocity as shown in the same Figure 2a) and in Figure 4, curve 8. The slope in the contour lines agrees well with the measured velocities. The appearance of a second peak can be attributed, in part, to new production in a re-

* All local times refer to 75° W.

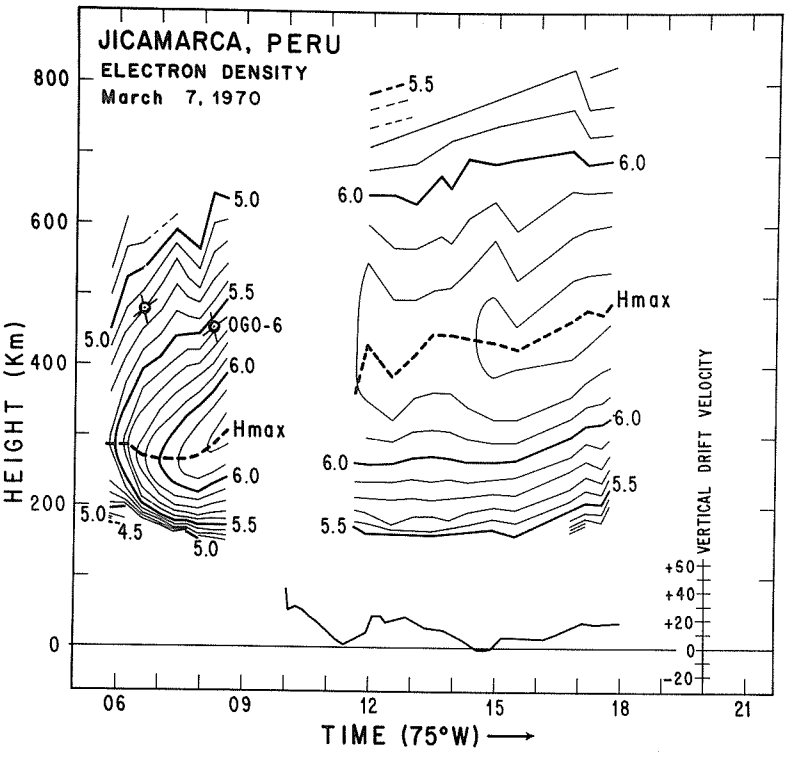

Fig. 1a. Contour line plot of the logarithm of electron density and F region vertical drift taken at the Jicamarca Radar Observatory on March 7, 1970.

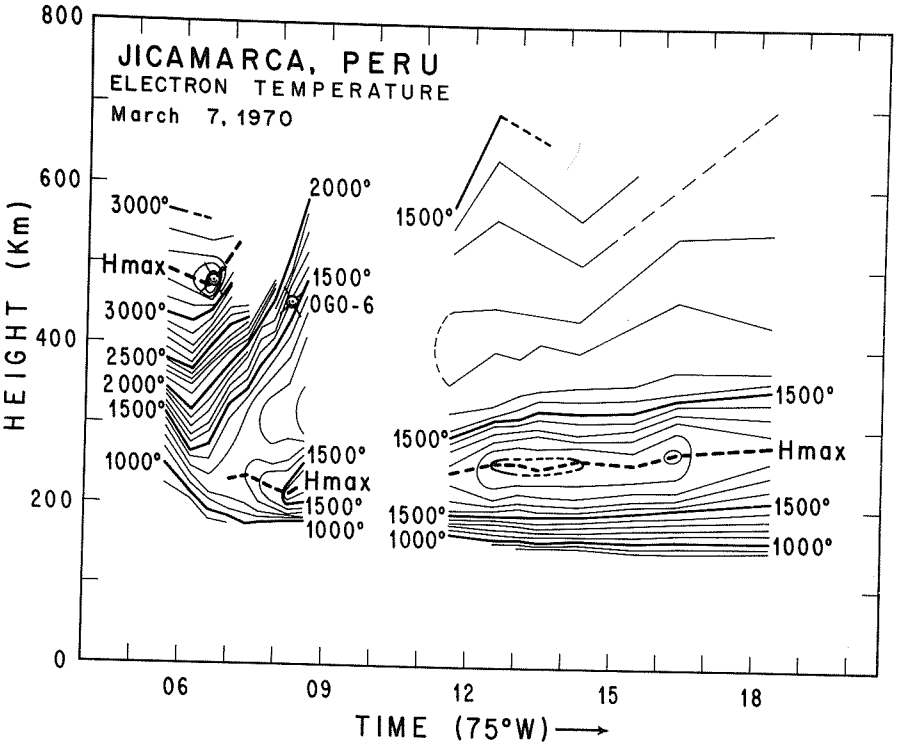

Fig. 1b. Electron temperature contour plot for March 7, 1970.

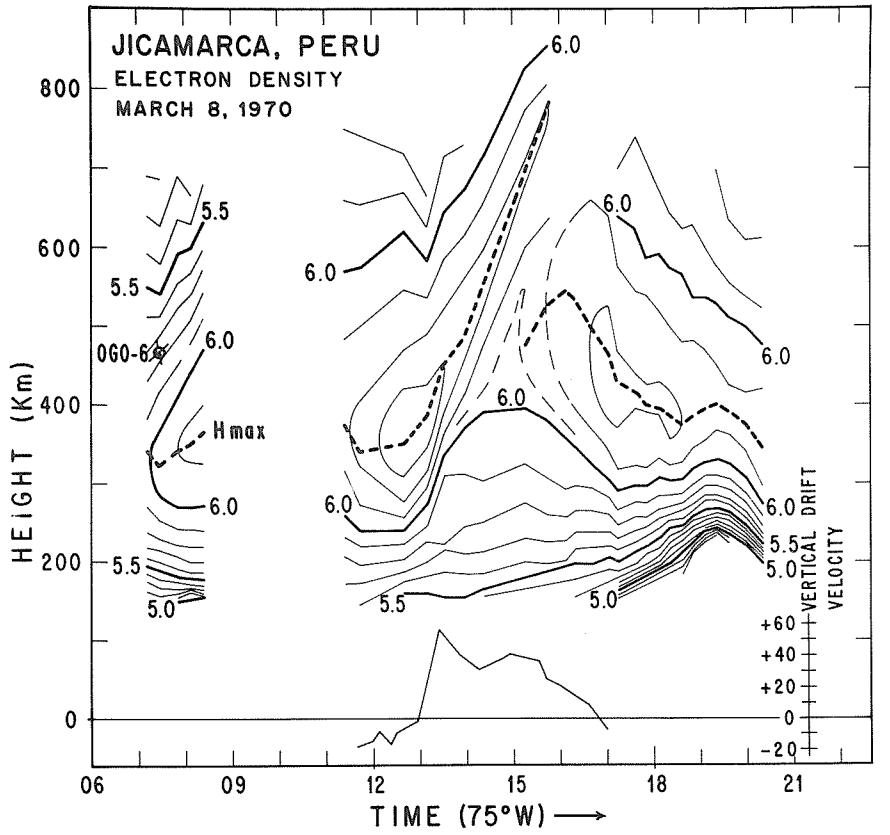

Fig. 2a. Contour line plot of the logarithm of electron density and F region vertical drift taken at the Jicamarca Radar Observatory on March 8, 1970.

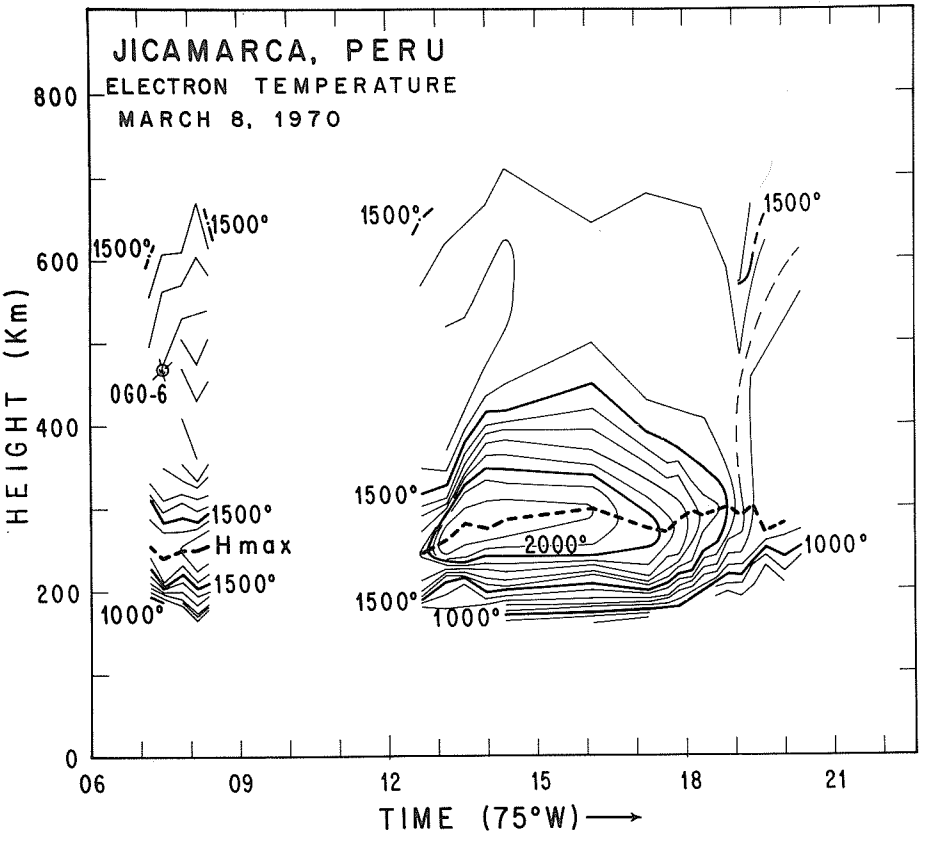

Fig. 2b. Electron temperature contour plot for March 8, 1970.

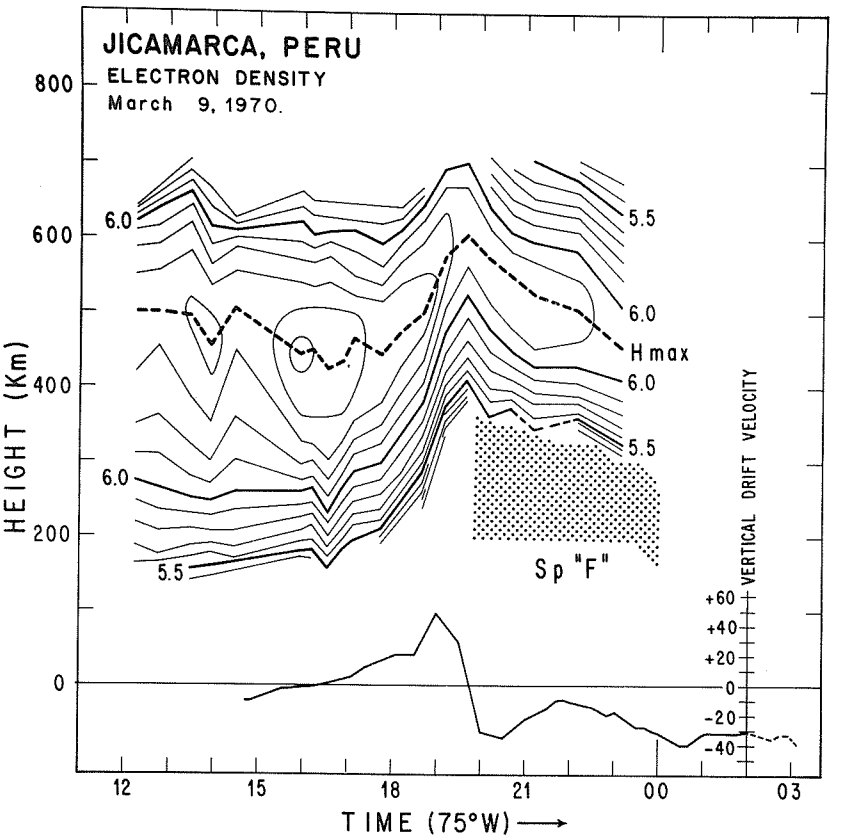

Fig. 3a. Contour line plot of the logarithm of electron density and F region vertical drift taken at the Jicamarca Radar Observatory on March 9, 1970.

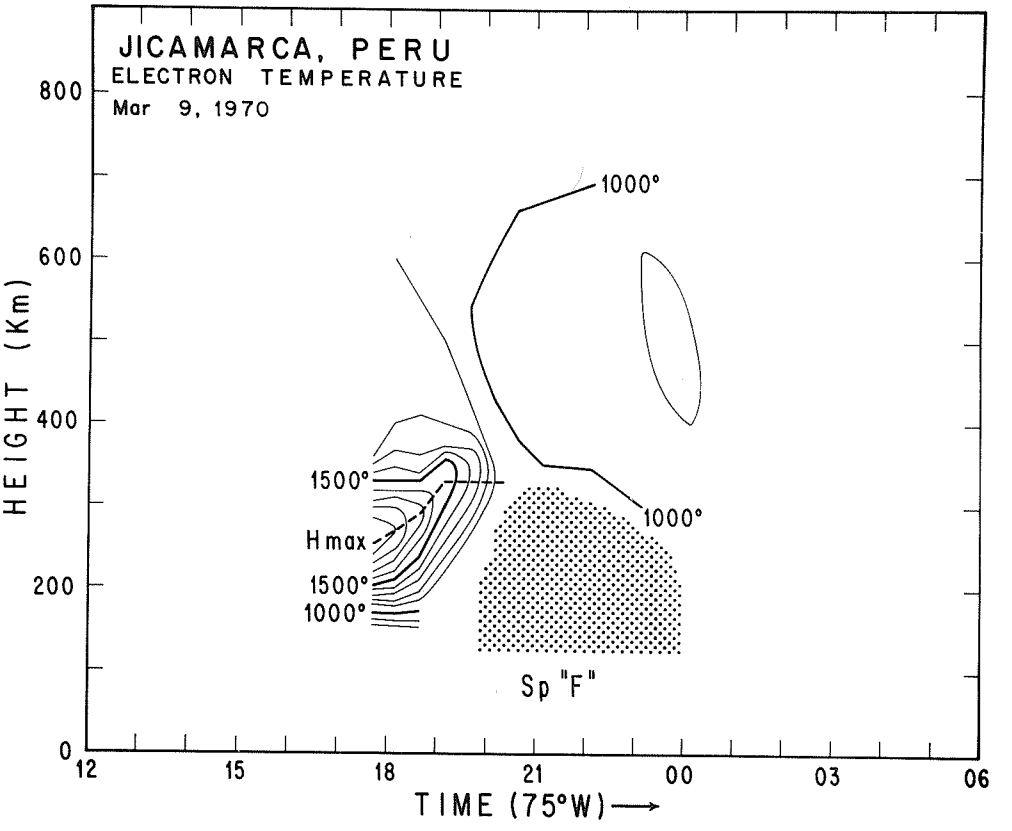

Fig. 3b. Electron temperature contour plot for March 9, 1970.

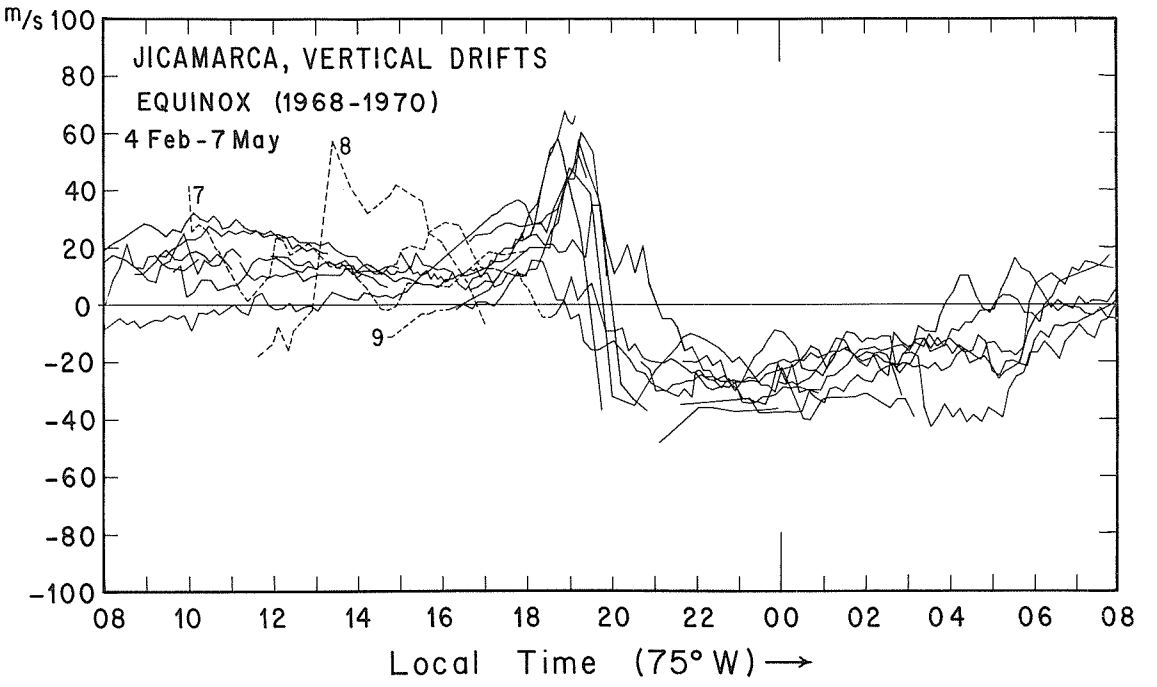

Fig. 4. Composite of vertical drifts taken at Jicamarca centered about March equinox. Curves 7, 8, 9 correspond to March 7, 8, 9, respectively. [After Woodman, 1970]

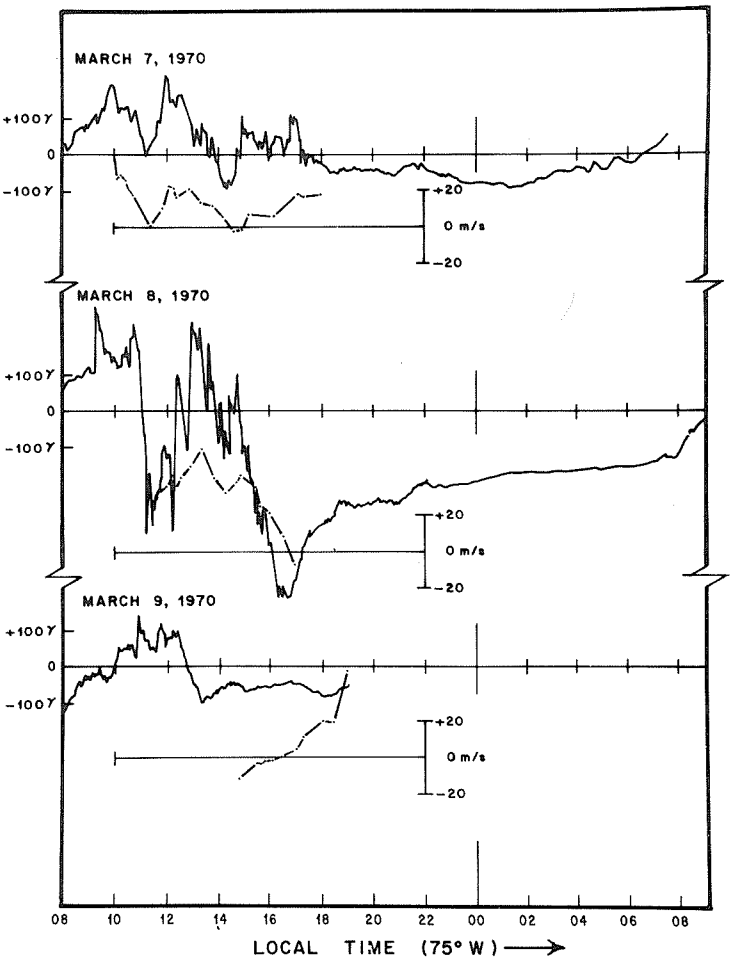

Fig. 5. Huancayo ΔH magnetograms and Jicamarca vertical drifts during the storm.

gion depleted of ionization due to the rapid up-lift, but the peak is too high in altitude to be attributed to production alone. The vertical velocity as a function of height is fairly constant, therefore, the divergence term in the direction of the magnetic field lines must be large to explain this behavior. This must also be true to explain the downward motion of H_{max} and of the top electron density contour lines, even though the measured velocities indicated an upward motion.

The electron temperature is also unusual. A typical quiet day behavior is more like the one shown for March 7, 1970. There is usually a nose shaped temperature profile with a maximum about 250 km with temperatures as high as 2100°K and fairly constant temperature in the order of 1200°K from 350 km and up. The most conspicuous feature of the March 8 temperature profile is the broad "nose", the 1500°K contour being as high as 450 km at 1600 LT rather than a usual 320 to 350 km. The maximum temperature is also higher than usual; in any case 200° higher than on March 7. Both features could be explained by the fact that the densities were lower at the heights in question, due to the rapid uplift of the layer. At lower density, there is less thermal contact between electron and ions and T_e is higher than T_i (and T_n) for a given solar energy input.

The electron density, vertical drift and electron temperature for March 9 are shown in Figures 3a) and b). The only obvious feature which could be attributed to the storm is the unusual negative velocity shown between 1430 and 1630 LT. There is a downward motion of H_{max} at this time in agreement with the measured negative velocity.

We are showing on Figure 5 the ΔH variations taken from Huancayo magnetograms as well as the vertical drift measured at Jicamarca for the same days reported above. Note the correlation between ΔH fluctuations, with time scales of the order of one to two hours, and the fluctuations on the vertical velocity at F region heights. Balsley and Woodman [1969] have shown the high correlation that exists between the electrojet current at E region heights and the E-W electric field associated with the vertical electromagnetic drift at F region heights. So we can take the vertical drifts as a measure of the electric field that drive the current at E region heights which in turn is responsible for the ΔH variations shown in the magnetograms; at least those fluctuations that correlate. There is a bias with a larger time constant which does not correlate. This is more conspicuous on March 8 and can be attributed to the ring current.

We cannot say much about the smaller time scale fluctuations, for this we would have had to take vertical drifts more often and with shorter integration times. We used a 5 to 10 minute integration with sample points at the straight line breaks.

Conclusions

We have presented simultaneous measurements of electron density, electron temperature and vertical drifts taken during one of the largest magnetic storms of the present solar cycle. From simple inspection of the data we can arrive at the following qualitative conclusions: There is a close relationship between magnetic activity and the behavior of the vertical drift at ionospheric heights. The electron density variations are mainly due to changes in the vertical drift although not in a simple manner. Diffusion along magnetic field lines is important and has to be considered in modeling the behavior of the ionosphere in a magnetic storm. There are electron temperature variations at F region heights but these can be explained, partially at least, by the changes in thermal contact due to changes in electron density. The one to two hour features of ΔH variations in a magnetic field at equatorial latitudes were an indication of what the vertical drift, or E-W electric field, was doing at F region heights. The electric field responsible for the changes in current in the electrojet is mapped at F region heights and drives the vertical motion of the ionosphere.

REFERENCES

BASLEY, B. B. and R. WOODMAN	1969	On the control of the F-region drift velocity by the E-region electric field: experimental evidence, J. Atmos. Terr. Phys., 31, 865-867.
FARLEY, D. T., JR.	1969a	Faraday rotation measurements using incoherent scatter, Radio Sci., 4, 143-152.
FARLEY, D. T.	1969b	Incoherent scatter correlation function measurements, Radio Sci., 4, 935-953.
McCLURE, J. P.	1967	Faraday dispersion loss at Jicamarca, In: Thomson Scatter Studies on the Ionosphere-An Informal Conference Record, edited by J. V. Evans. University of Illinois, Department of Electrical Engineering, Aeronomy Report No. 19, May 15, 1967, p. 192-194.
McCLURE, J. P.	In press	Thermospheric temperature variations inferred from incoherent scatter observations. Submitted to J. Geophys. Res., 1970.
McCLURE, J. P., D. T. FARLEY and R. COHEN	1970	Ionospheric electron concentration measurements at the magnetic equator, 1964-1966. Personal communication.
WOODMAN, R. F. and T. HAGFORS	1969	Methods for the measurements of vertical ionospheric motions near the magnetic equator by incoherent scattering, J. Geophys. Res., 74, 1205-1212.
WOODMAN, R. F.	1970	Vertical drift velocities and East-West electric fields at the magnetic equator, J. Geophys. Res., 75, 6249.

"Slough Ionospheric f-plots March 6-10, 1970"

by

D. E. Mortimer
Radio and Space Research Station
Slough, U.K.

These f-plots presented for March 6-10, 1970 are those as published in the Slough "Ionospheric Data" for March, 1970. The interval between observations on the four days March 6-9 is hourly except for the period 1600 to 2400 UT on March 8 when observations were made at 10 minute intervals in support of a solar eclipse - gravity wave experiment. March 10 was a Regular World Day so that the interval between observations was 15 minutes. Large ionospheric storm effects are indicated the night of 8-9 March, 1970 at Slough (N51.50° geographic latitude, or N54.35° geomagnetic latitude with L-value 2.43).

IONOSPHERIC DATA

f - PLOT

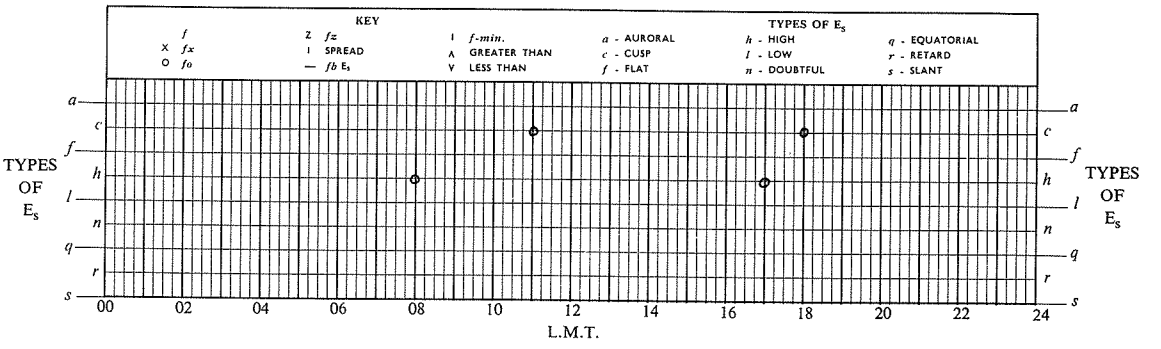

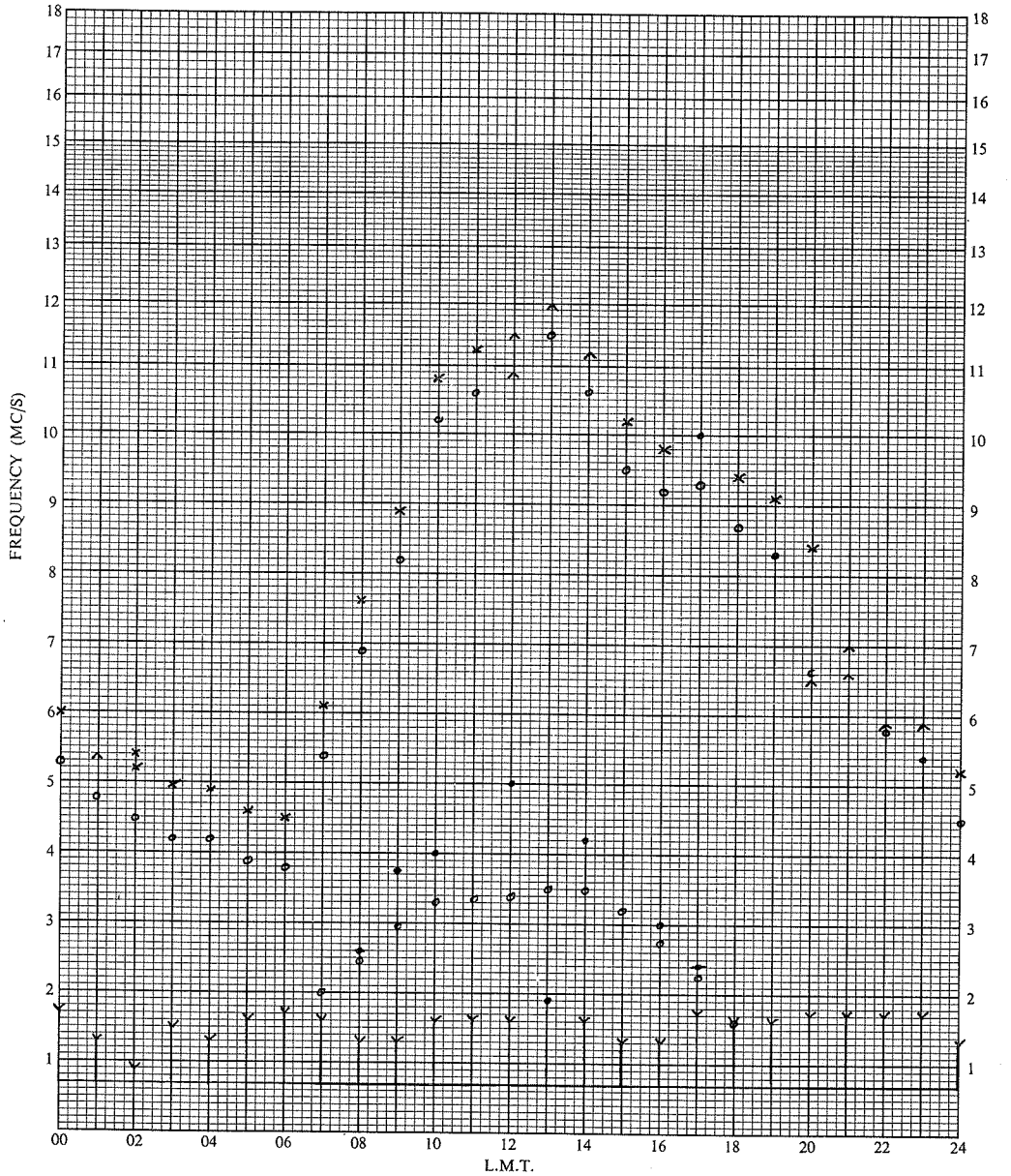

STATION: SLOUGH 113

TIME MERIDIAN: 0°

DATE: 6 MARCH 1970

IONOSPHERIC DATA

f - PLOT

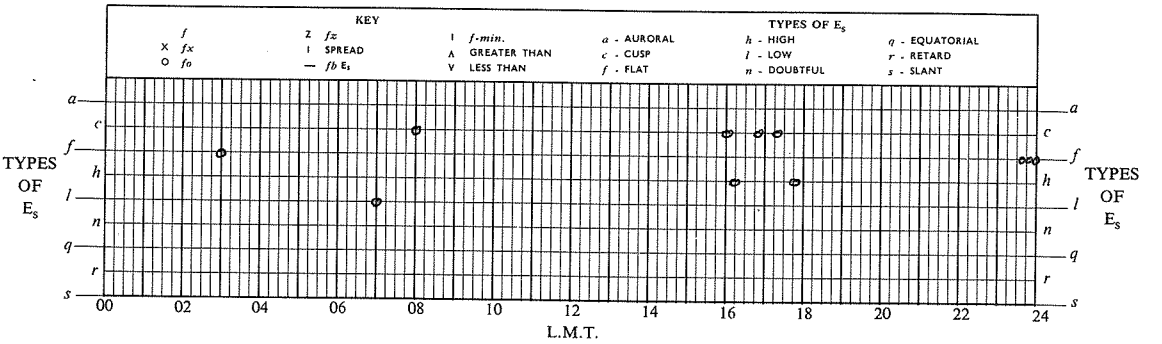

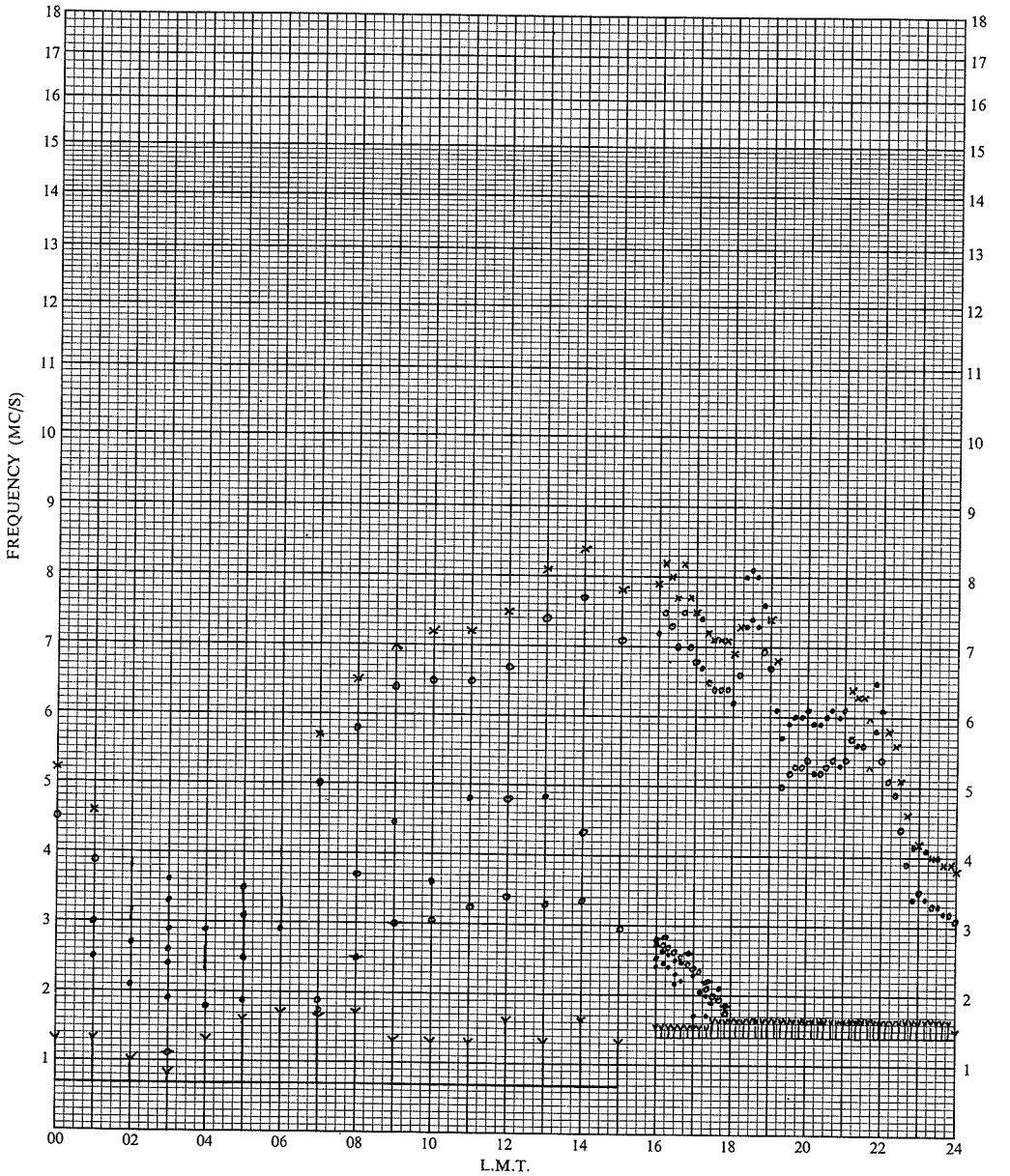

STATION: SLOUGH 113

TIME MERIDIAN: 0°

DATE: 7 MARCH 1970

IONOSPHERIC DATA

f - PLOT

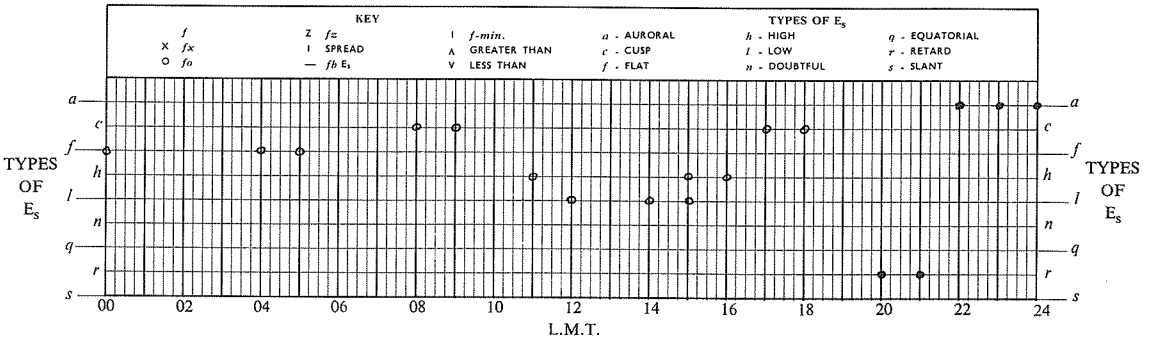

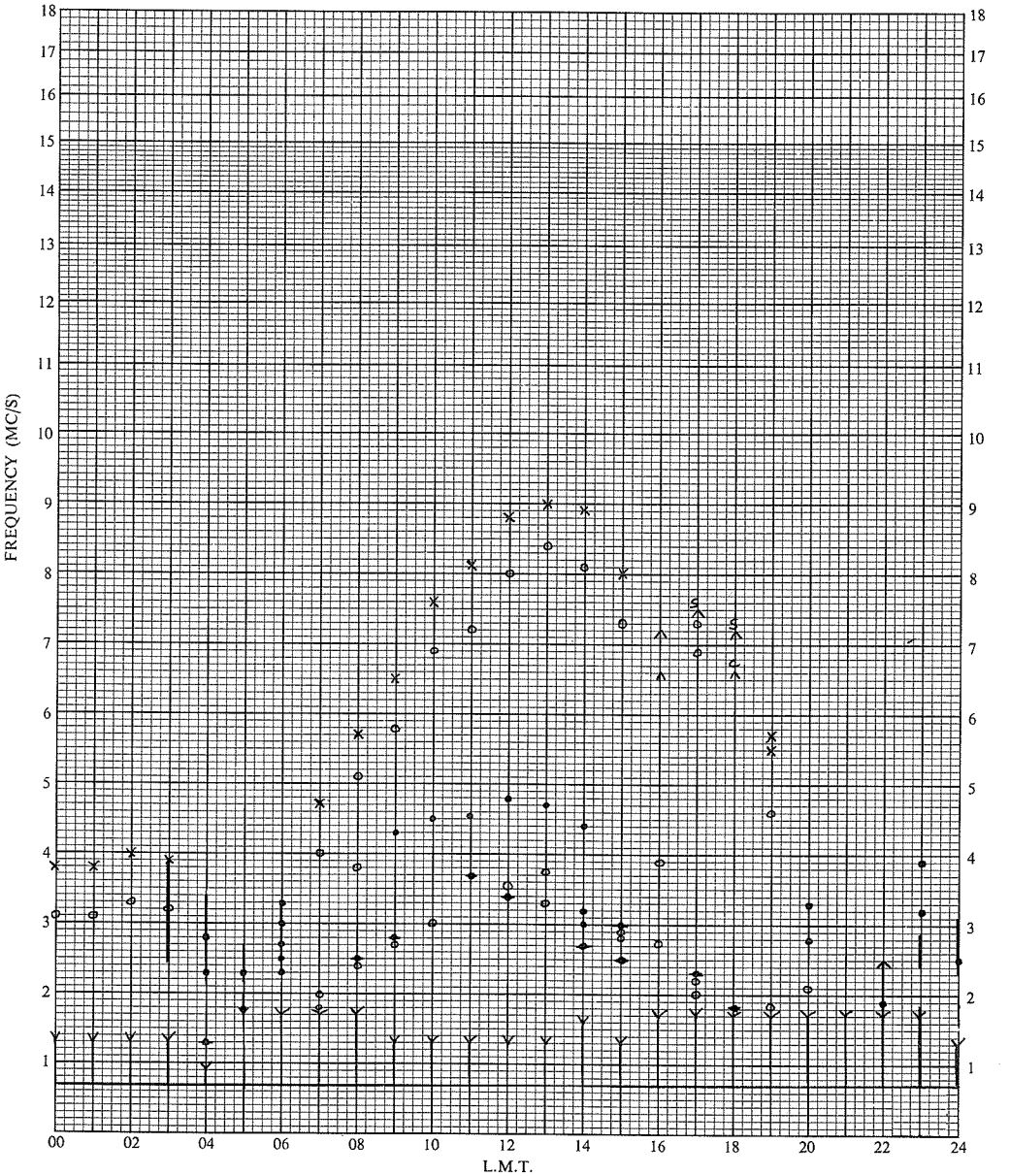

STATION: SLOUGH 113

TIME MERIDIAN: 0°

DATE: 8 MARCH 1970

IONOSPHERIC DATA

f - PLOT

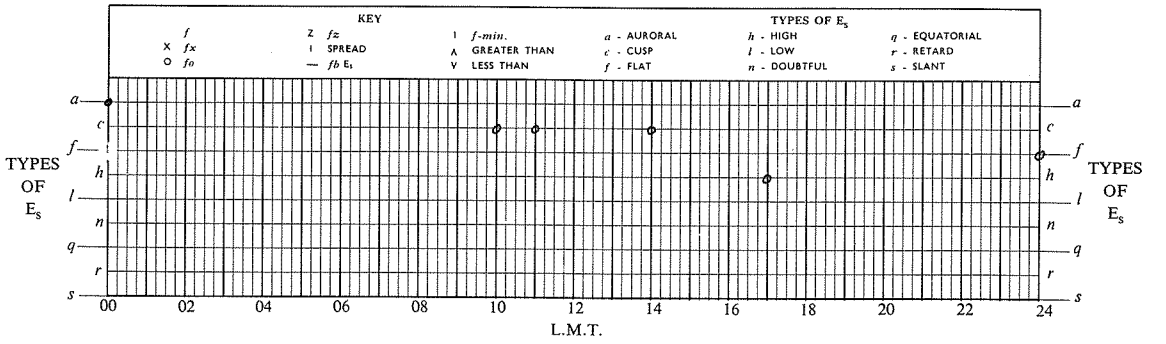

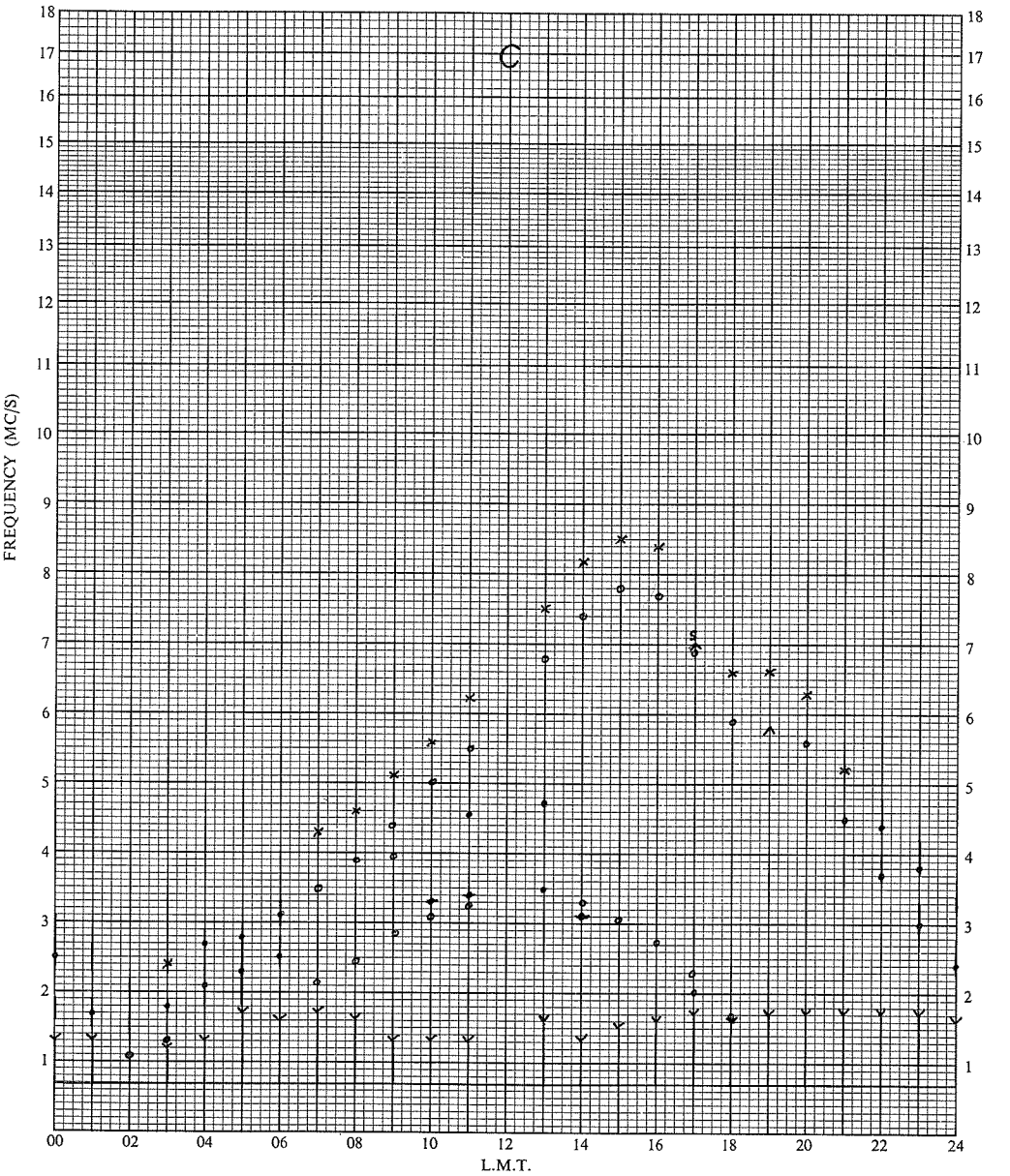

STATION: SLOUGH 113 TIME MERIDIAN: 0°

DATE: 9 MARCH 1970

IONOSPHERIC DATA

f - PLOT

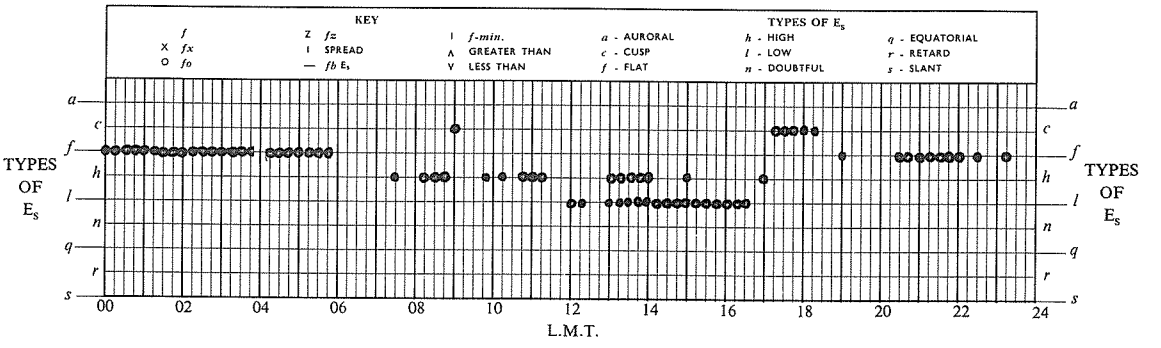

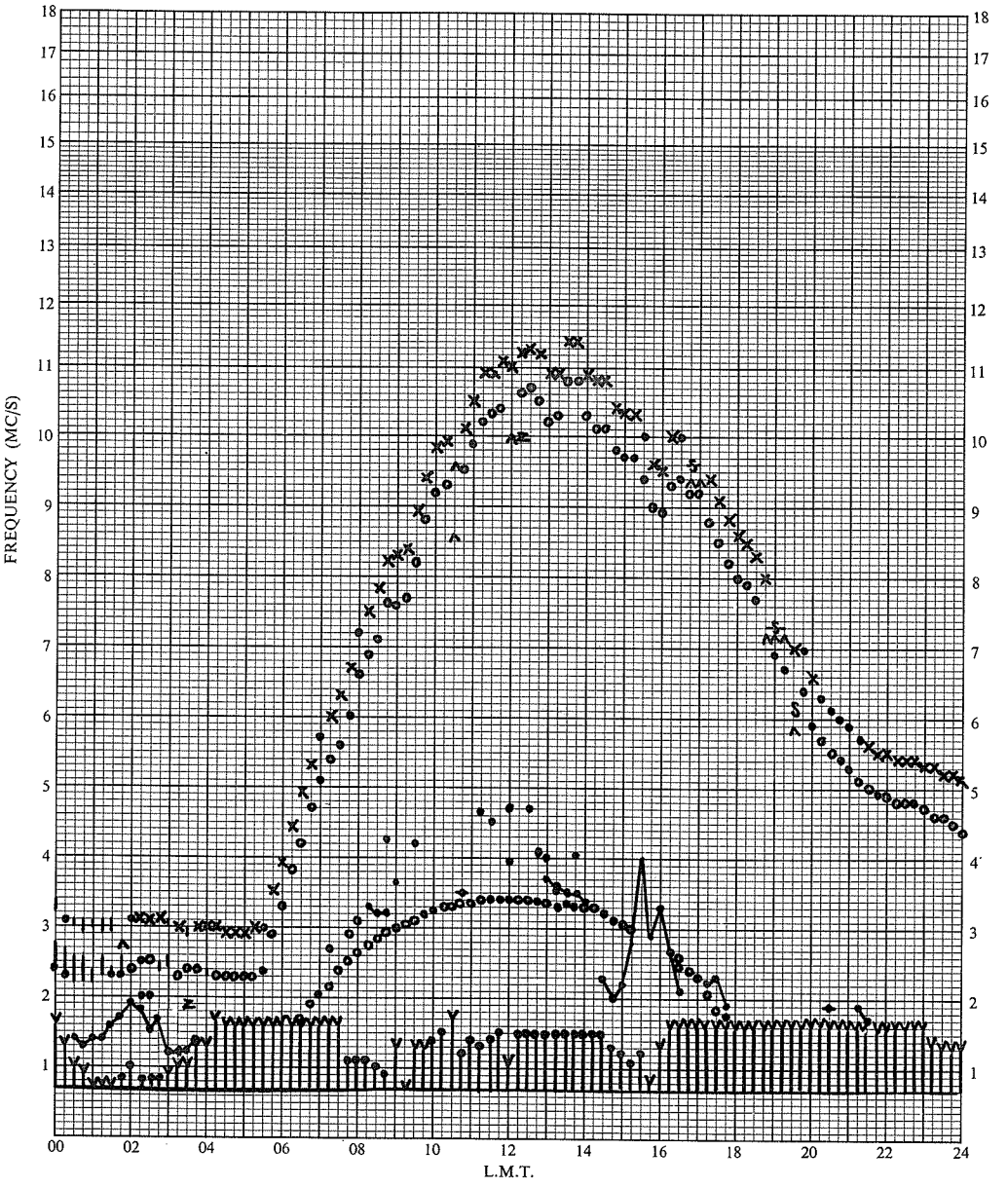

STATION: SLOUGH 113 TIME MERIDIAN: 0°

DATE: 10 MARCH 1970

"Ionosonde and Riometer Data from Narssarssuaq, Godhavn and Thule"

by

J. Taagholt
Ionosphere Laboratory
Technical University of Denmark
Lyngby, Denmark

The data published below are reduced data based on routine measurements made on the field sites Narssarssuaq (geomagnetic coordinates: N71.2° E36.8°), Godhavn (geomagnetic coordinates N80.0° E32.5°) and Thule (geomagnetic coordinates N89.0° E358.0°). All three stations situated on the west coast of Greenland are run by the Ionosphere Laboratory, Technical University of Denmark, Bldg. 348, 2800 Lyngby, Denmark.

The sequence of ionograms from the three stations shows the normal features of an ionospheric storm: a depression of foF2, and increased spreadiness, both connected with slant Es condition (see Narssarssuaq March 5, 1500 UT). An increase of fmin and complete black out during parts of March 6, 7 and 8. Also, possibly a decrease in Es occurrences has taken place within this period.

The vertical sounders used are at Narssarssuaq a modified C-3/4, at Godhavn a J-5 and at Thule a C-4.

The cosmic noise absorption data show the absorption in dB (below the daily curve). The data below 0 dB indicates periods where interference caused the actual minimum curve to lie above the level of the computed daily curve.

The instruments used are at Narssarssuaq an IGY riometer (now replaced by a 30.5 MHz riometer designed and built by the Ionosphere Laboratory) and at Godhavn an ARI riometer.

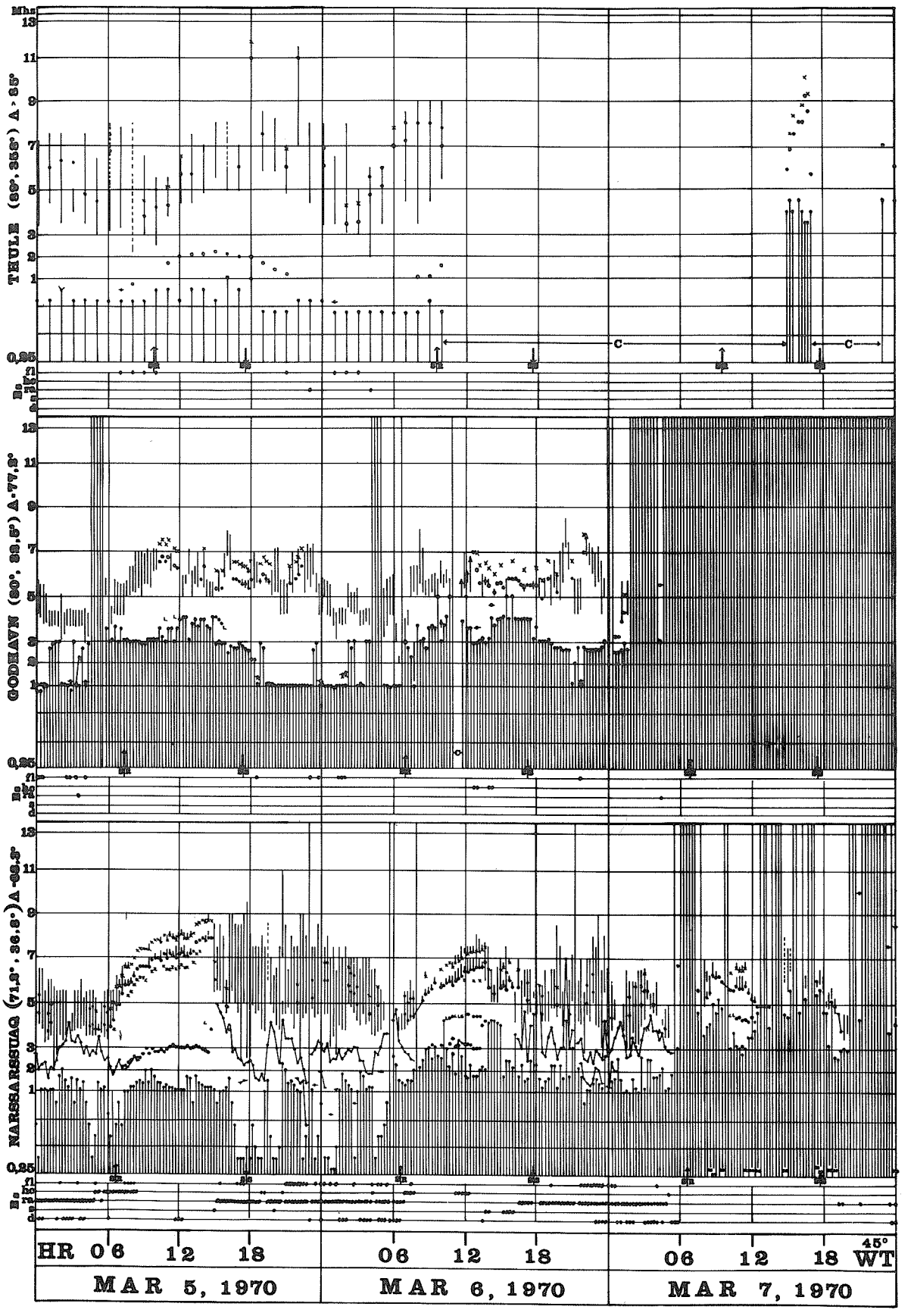

Fig. 1. f-plots March 5-7, 1970 at Thule, Godhavn and Narssarssuaq.

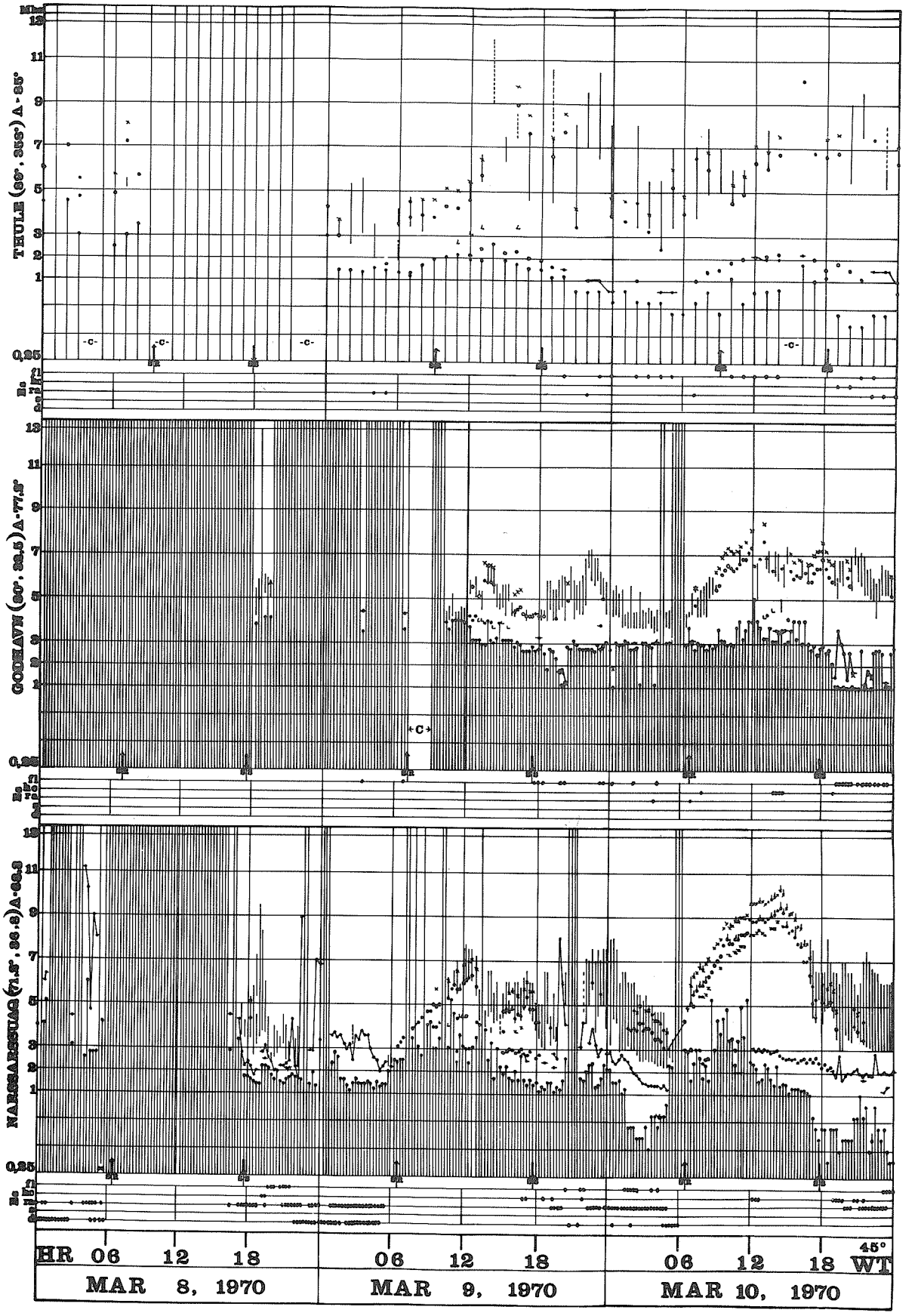

Fig. 2. f-plots March 8-10, 1970 at Thule, Godhavn and Narssarssuaq.

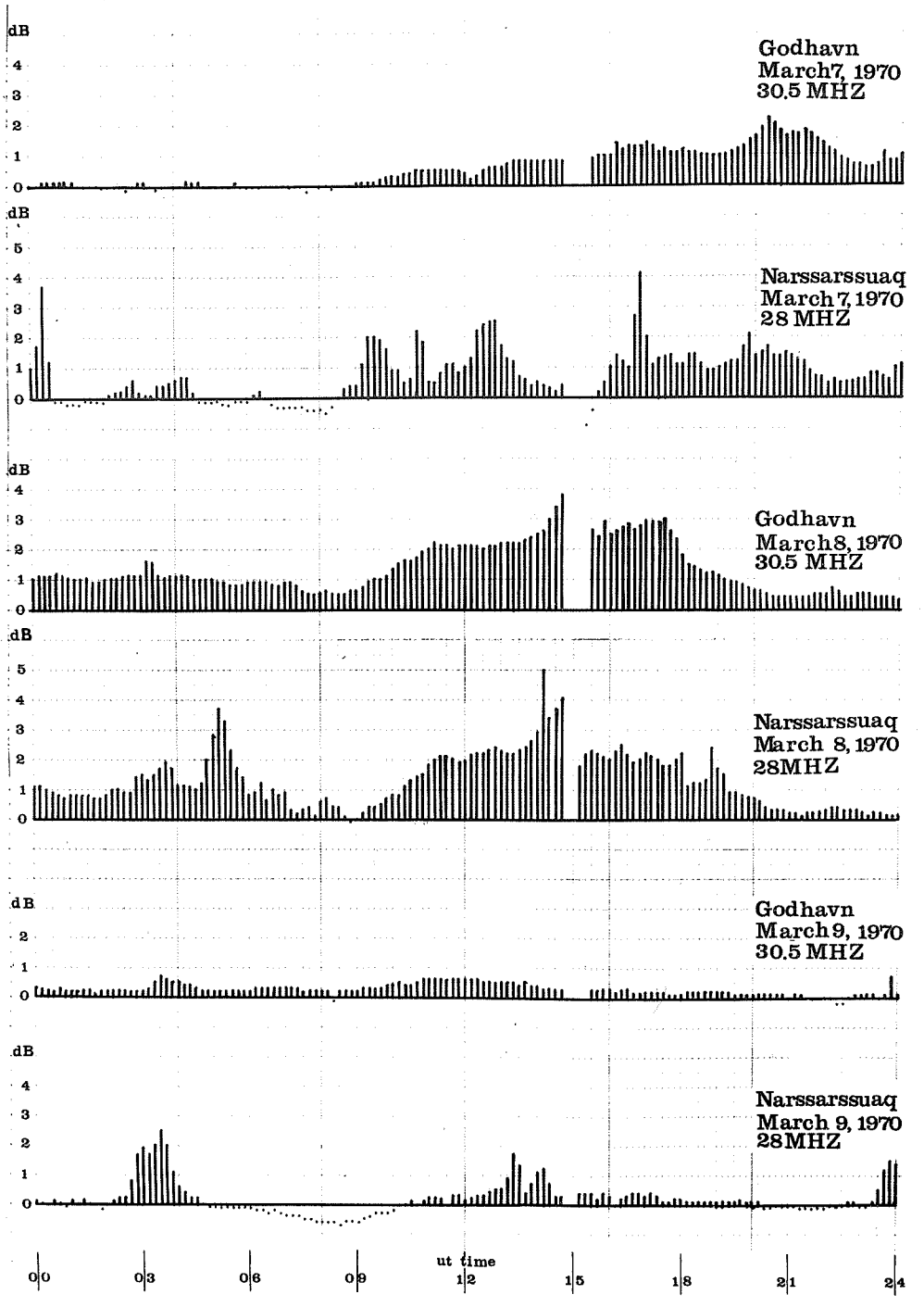

Fig. 3. Riometer absorption March 7-9, 1970 at Godhavn and Narssarssuaq.

"Ionospheric Disturbance during the Night of March 8-9, 1970"

by

P. Tříska and J. Laštovička
Geophysical Institute
Czechoslovak Academy of Sciences
Prague, Czechoslovakia

The strong magnetic storm which started on 8 March 1970 at 1418 UT (SSC) with maximum intensity during the following evening and night hours, caused large disturbances in the upper ionosphere, the lower ionosphere disturbances being considerably smaller; both can be seen from the measurements made at the observatories Pruhonice (Geographic coordinates 49°59'N, 14°33'E) and Panska Ves (Geographic coordinates 50°32'N, 14°34'E).

The behavior of the lower ionosphere around sunset and during the night can be derived from LF absorption measurements (A3 method; 272 kHz and 185 kHz received at Pruhonice). At 272 kHz (reflection point 49°34'N, 16°03'E, assumed reflection height h' = 95 km), the absorption value was for the solar zenith angle $\chi \leq 85°$ several decibels lower than in several preceding and following days. Afterwards it was enhanced between about 1625 - 1825 UT so that for $\chi = 90°$ (1650 UT), the absorption was 4 - 4.5 dB higher than in the days before and after the event, and it was even higher by 6.5 - 7 dB for $\chi = 95° - 100°$ (1715 - 1745 UT). The absorption values during the night, however, were roughly equal to the preceding and following days. The time development of the absorption on 8 March is shown in Table 1 and Figure 1.

Table 1

Development of ionospheric absorption at 272 kHz on March 8, afternoon and night.
χ - solar zenith angle, L - absorption

χ	70° - 75°	75° - 80°	80° - 85°	90°	95° - 100°	night
L(dB)	38.5	29.8	24.4	26.0	27.2	18.5

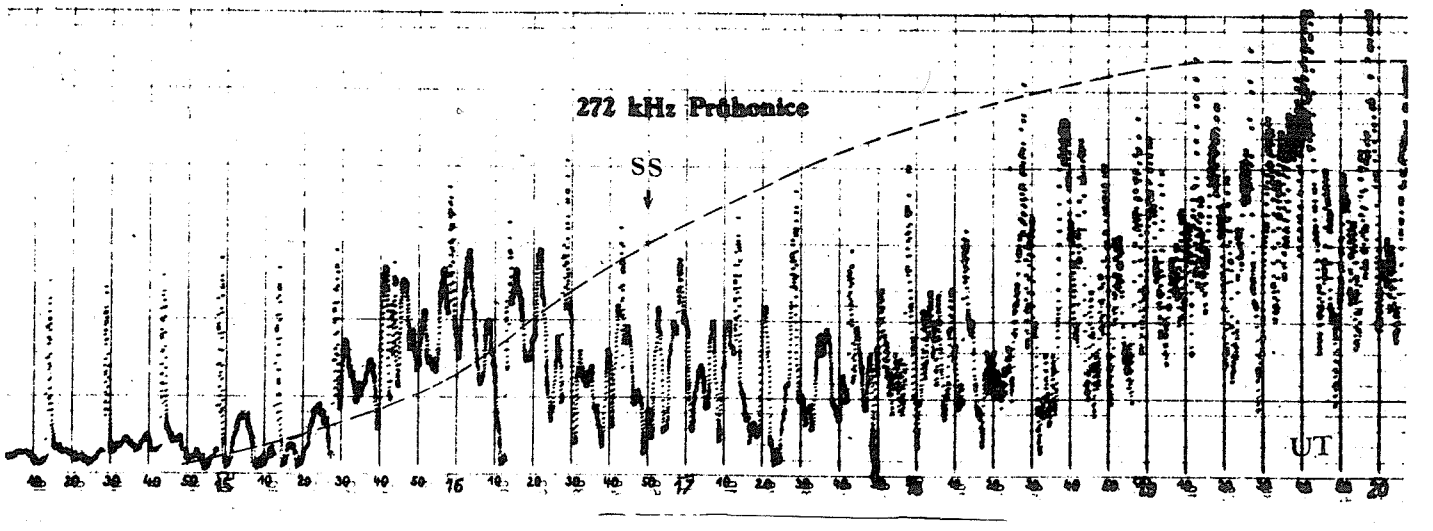

Fig. 1. The field-strength record of one-hop sky wave at 272 kHz (d = 236 km) around the sunset on March 8, 1970. Dotted curve gives the average values derived from several preceding and following days. (Peaks every 15 minutes - interference caused by the near-by ionosonde.)

The absorption measured at 185 kHz (reflection point 51°09'N, 14°06'E) exhibited an increase between about 1630 - 1930 UT. According to the A3-records of Pruhonice, a large enhancement of LF absorption did not occur as observed at the more northerly located observatory of Kühlungsborn, 54° N, GDR (large sudden increase in absorption at 1850 UT, which indicates enhanced corpuscular ionization in the lower ionosphere).

Changes in the upper ionosphere, mainly during the night, can be found from foF2 values, and partly also from field-strength measurements at 6.09 MHz (A3 method). The foF2 values at Pruhonice on 8 March showed the usual diurnal pattern up to 1900 UT, then began to decrease below the expected values, and after 2030 UT the echoes practically disappeared as a result of a considerable increase of absorption (B-type). This disappearance of echoes lasted until 0500 UT March 9. The measurements at 6.09 MHz (reflection point 50°04'N, 10°20'E) showed a decrease of the MUF-value for the distance of 610 km as early as between 1900 - 1930 UT whereas on the following and preceding days this decrease did not start before 2230 UT.

During the remaining days of the period of March 6-10, only the 185 kHz measurements showed enhanced absorption values for the night of 9-10 March, and nearly normal values were recorded for all other days at 272 kHz and 185 kHz as well. On the other hand, a disturbance of the upper ionosphere was observed from March 6 (about 2330 UT) to March 12 (about 0500 UT) as indicated by the unusually low night time foF2-values (Table 2).

Table 2

foF2 values (in 0.1 MHz) at 0000 UT, observatory Pruhonice, March 1 - 15, 1970

Date	1	2	3	4	5	6	7	8	9	10	11	12	13	14	15
foF2	50	47	48	53	51	50	38	37	B	30	36	33	48	58	50

"Ionospheric Structure during the Storm of March 8, 1970"

by

Richard B. Fritz
Space Disturbances Laboratory
NOAA Environmental Research Laboratories
Boulder, Colorado 80302

The ionospheric storm on 8 March 1970 exhibited both depletion and enhancement in the total electron content measured at Boulder. Content was recorded by monitoring Faraday Rotation of the 137.35 MHz signal from ATS-3, which at the time was geostationary at longitude W75. Seen from the Boulder Table Mountain field site (N41.13 W105.24), ATS-3 appeared at azimuth 150°, elevation 39°.

The geomagnetic storm sudden commencement occurred at 0717 MST, which was approximately one hour after ground sunrise at Boulder. The vertical ionospheric electron content (N_t) had indicated the occurrence of a storm at sunrise when normal ionization production did not occur. Figure 1 compares the behavior on March 8 with that on two quiet days in the same month. The linear post-sunrise buildup of ionization on the quiet days is typical [Garriott and Smith, 1965].

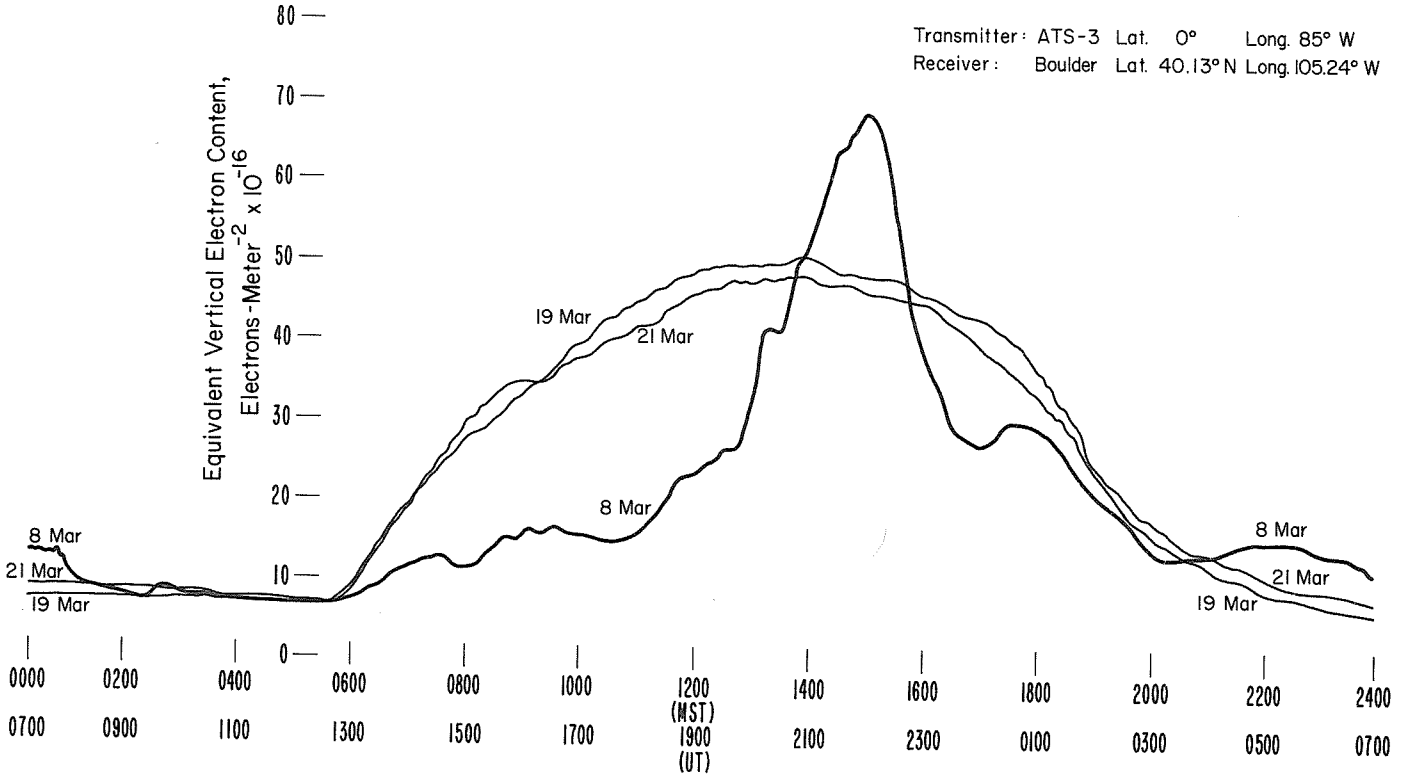

Fig. 1. Total Electron Content Records, March 1970.

It can be seen that the electron content was depressed throughout most of the day, with the exception of the midafternoon peak. During the morning hours of March 9, the content declined to an unusually low value of about 2 x 10^{16} electrons-meter^{-2} before dawn. Content values recovered to normal levels by the 10th of March.

The Boulder ionosonde data were complicated by the existence of a G-condition, i.e. the F2 layer was masked by the underlying F1 layer which had a higher maximum electron density, during much of the day. There is evidence that the profile of electron density did not show the expected single F region peak. The height of maximum density (Hmax) is usually observed to drop from about 380 km to 280 km over sunrise and then rise slowly throughout the day. On March 8, though, Hmax continued to drop after sunrise to a low of about 170 km at 1100 MST (MST is local mean time at 105°W long.) under the "G-condition". In midafternoon, Hmax was suddenly discovered to be near 500 km. Hmax went through several less dramatic reversals during the remainder of the day, as can be seen by Figure 2.

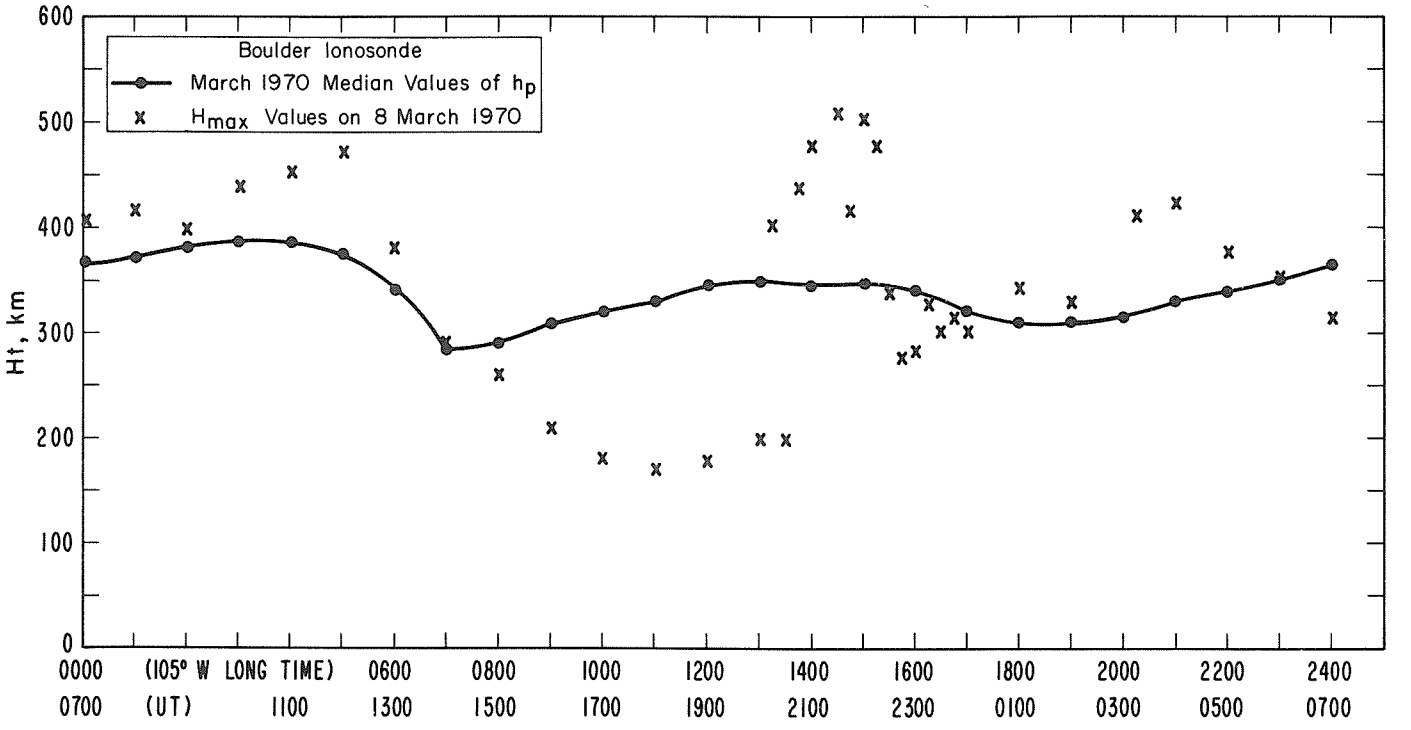

Fig. 2. Heights of Maximum Electron Density, March Medians and 8 March 1970.

Significantly, the value of Nmax, the maximum electron density noted by the ionosonde, was below normal throughout the day, rising to the monthly median only at 1500 MST and falling again after that time. Figure 3 compares Nmax on March 8 with the Boulder monthly median values.

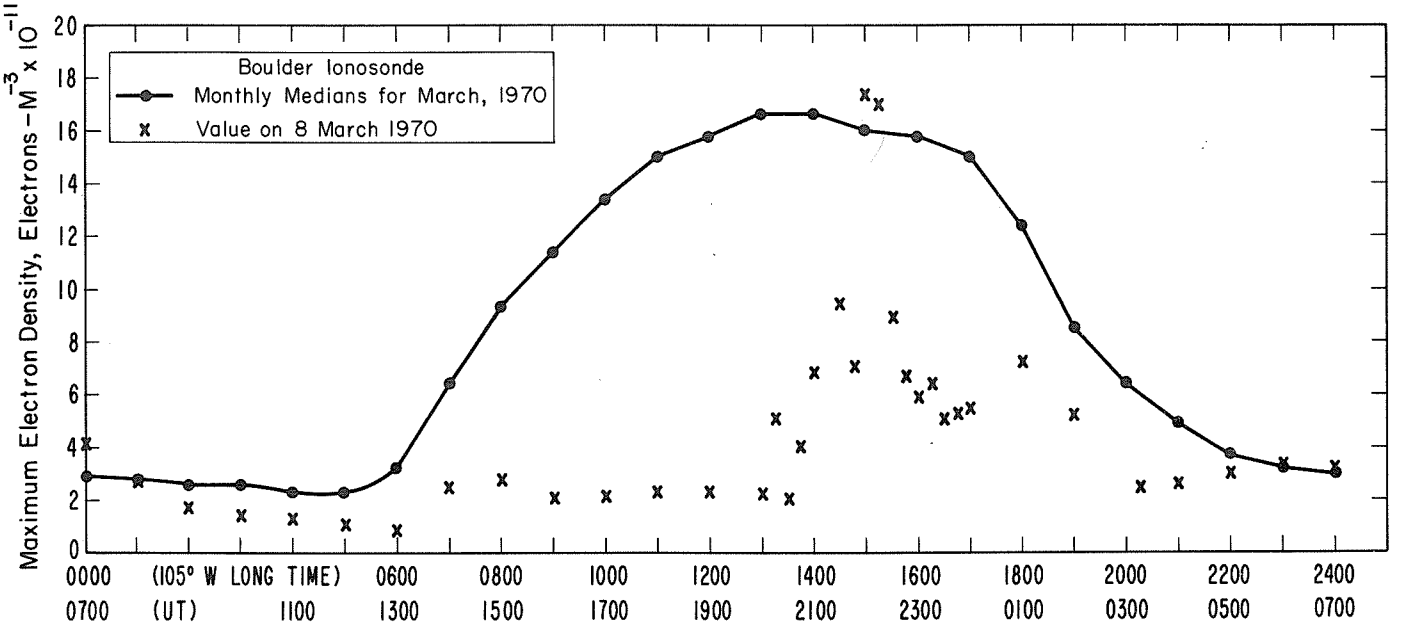

Fig. 3. Maximum Electron Densities (Nmax), March Medians and 8 March 1970.

Combining the observations of Nmax, Hmax, and N_t, it is possible to estimate the development of the ionospheric structure during the storm. In the morning, ionization production in the F2 layer was almost completely inhibited, while the F1 layer seemed to develop normally. At about 1100, the F2 layer began to develop, as shown by the upturn of N_t, but this was masked from the ionosonde by the F1 layer. The F2 layer peak developed at high altitude, probably creating a valley between the F1

and F2 peaks. A similar wide separation of F1 and F2 was hypothesized by Norton [1969] to explain topside and bottomside ionograms during a 1965 storm. At 1315 MST the F2 peak became visible, only to recede at 1330 MST, finally re-emerging at 1345 MST. During the afternoon, the F region consolidated, with the F1-F2 valley diminishing and the region peak descending to lower altitude. The evening plateau of content at about 2200 MST is accompanied by another rise of Hmax, implying that ionization loss processes were greatest in the lower F region, as expected, but substantial ionization remained at high elevation. As mentioned earlier, the content decreased all evening and reached a very low level before dawn on the 9th.

The variability of the electron content response to ionospheric storms is well recognized [Hibberd and Ross, 1967; Titheridge and Andrews, 1967; Taylor and Earnshaw, 1969]. The March 8 event exhibited both positive and negative phases within half a day of the sudden commencement. The ionospheric content usually does not respond this quickly. The time scale of the event, with its rapid changes, implies that explanation based on changes of the photochemical processes alone would require very high values of integrated production rate and loss rate. Transport of ionization is assumed to have been a major contributor to the electron content behavior. During the positive phase of the storm, the greatest changes occurred in the topside ionosphere where the loss rate is lower, but downward drift later in the day and storm depleted the ionization.

The source of ionization could be compression of the dayside magnetosphere [Bauer and Krishnamurthy, 1968] but such an effect should be evident over a wide geographical area. In fact, observations by F. L. Smith at Ft. Collins, Colorado, monitoring Faraday Rotation of signals from ATS-1 toward the southwest showed no increase in content in contrast to the Boulder observations, which were of ATS-3 toward southeast. The implications of this difference are now under study.

The assistance of Miss Irene Brophy in analysis of the ionosonde records and of Dr. K. Davies and Mrs. Margo Leftin for discussions on interpretation of results is acknowledged with thanks.

REFERENCES

BAUER, S. J. and B. V. KRISHNAMURTHY 1968 Behavior of the topside ionosphere during a great magnetic storm, Planet. Space Sci., 16, 653.

GARRIOTT, O. K. and F. L. SMITH 1965 The rate of production of electrons in the ionosphere, Planet. Space Sci., 13, 839.

HIBBERD, F. H. and W. J. ROSS 1967 Variations in total electron content and other ionospheric parameters associated with magnetic storms", J. Geophys. Res., 72, 5331.

NORTON, R. B. 1969 The middle-latitude F Region during some severe ionospheric storms, Proc. IEEE, 57, 1147.

TAYLOR, G. N. and R.D.S. EARNSHAW 1969 Changes in the total electron content and slab thickness of the ionosphere during a magnetic storm in June 1965, J. Atmosph. Terr. Phys., 31, 211.

TITHERIDGE, J. E. and M. K. ANDREWS 1967 Changes in the topside ionosphere during a large magnetic storm, Planet. Space Sci., 15, 1157.

"Ionospheric Effects Observed at Kiruna March 5-10, 1970"

by

G. Gustafsson, B. Aparicio, C. Juren and J. Svennesson
Kiruna Geophysical Observatory

Introduction

A magnetic storm with a sudden commencement at 0805 UT, March 5, started a geomagnetically active period which remained until March 10, with an additional sudden commencement at 1418 UT, March 8 [Solar-Geophysical Data]. A 2B flare was reported in an URSIGRAM at 0926 UT, March 6 with the coordinates N12 W90. It was associated with an X-ray event with onset at 0934 UT [Solar-Geophysical Data], and it was seen as an SPA on the VLF record of the GBR - Kiruna signal. A weak PCA event with a slow onset started at 1047 UT, March 6 (as reported in an URSIGRAM). An associated increase in the proton flux from the sun was measured by Explorer 41 [Solar-Geophysical Data] from March 6 to March 10 with a maximum on March 8.

Data which may be related to the magnetic storms and the PCA have been collected and demonstrated in Figure 1, and reproductions of magnetometer and riometer recordings are given in Figures 2 and 3, respectively. Ionosounder recordings and K-indices from other observing stations than Kiruna have been included to show the latitudinal variation. The geographic coordinates of the stations are:

Tromsö	N69.7 E18.9	Uppsala	N59.8 E17.6
Kiruna	N67.8 E20.4	Lovö	N59.3 E17.8
Lycksele	N64.7 E18.8		

Geomagnetic activity

The magnetic storm which started on March 8 was somewhat unusual because a large bay occurred immediately after the sudden commencement and later there was a negative bay of a magnitude of 1870γ.

The magnetogram at Kiruna showed the following deflections from the Sq-curve at 1417 UT, March 8, X = +390γ, Y ≈ 0γ and Z = +100γ. Then suddenly at $14^h17^m50 \pm 5^s$ UT a positive deflection started on the X-component which reached a maximum of 550γ and changed rapidly into a negative deflection at 1424 UT. During the corresponding time interval the Y-component made a negative excursion of 272γ, while the Z-component remained almost unchanged until 1422 UT. This indicates a line current almost overhead or a sheet current during this first phase of the disturbance. At 1436 UT the X-component had reached a value of -795γ relative the value at 1417 UT, the Y-component +288γ and the Z-component -570γ which corresponds to a current to the north of Kiruna. The horizontal components recovered within one hour while the vertical component stayed at a large negative value for more than three hours. There was a small negative bay at about 1600 UT. The largest bay during March 8 was observed between 1830 UT and 2400 UT, with a short recovery at about 2050 UT. During the maximum phase of the negative bay at 1839 UT, March 8 a short (5 min duration) peak of -795γ was superimposed on the general negative excursion of the X-component giving a total deflection of -1870γ from the Sq-curve.

Comparing the K-indices in Figure 1b it may be noted that the magnetic activity was more pronounced during March 8 at Lovö than at the other two stations at higher latitude. (The magnetic data from Tromsö has been provided by the Auroral Observatory, Tromsö, Norway, and from Lovö by the Geological Survey, Stockholm, Sweden.)

Radio wave absorption

The absorption of cosmic radio noise at 27.6 MHz showed the common effect of a PCA, i.e. strong absorption during day and lower absorption during night. This was most pronounced on March 8, when the minimum value of absorption during the day was 2.4 dB, but as the magnetic activity was rather high during the whole period March 5-10, the records also show large variations due to what is usually called auroral absorption. Therefore, it is very difficult to separate one effect from the other. However, it may be seen (Figure 1a) that an absorption peak coincided with the sudden commencement of the storm. A rapid increase in absorption began at 1418 UT, March 8 from a level of 3.5 dB to greater than 20 dB. The maximum was reached at 1420 UT and it recovered to the value it had before the sudden commencement at about 1428 UT. There was also an increase in the absorption which began at 1845 UT, March 8 coinciding with the negative bay, and it reached a maximum in magnitude of 6.3 dB.

The latitude distribution of the absorption can be seen from the plots of the critical frequency of the F2-layer (see Figure 1a) in the form of black-out. (The ionosounder data used in Figure 1 are from the bulletins published by Norwegian Research Establishment and the Research Institute of National Defence, Stockholm, Sweden.) Black-out appeared at Tromsö at 17 UT, March 6 (recordings are only made each integral hour at all the stations) and continued until March 10. The ionosonde at Kiruna showed black-out from 18 UT and Lycksele from 23 UT which reflects the progression of the PCA in latitude. The ionosounder at Uppsala did not show black-out until the commencement of the magnetic storm at 15 UT, March 8.

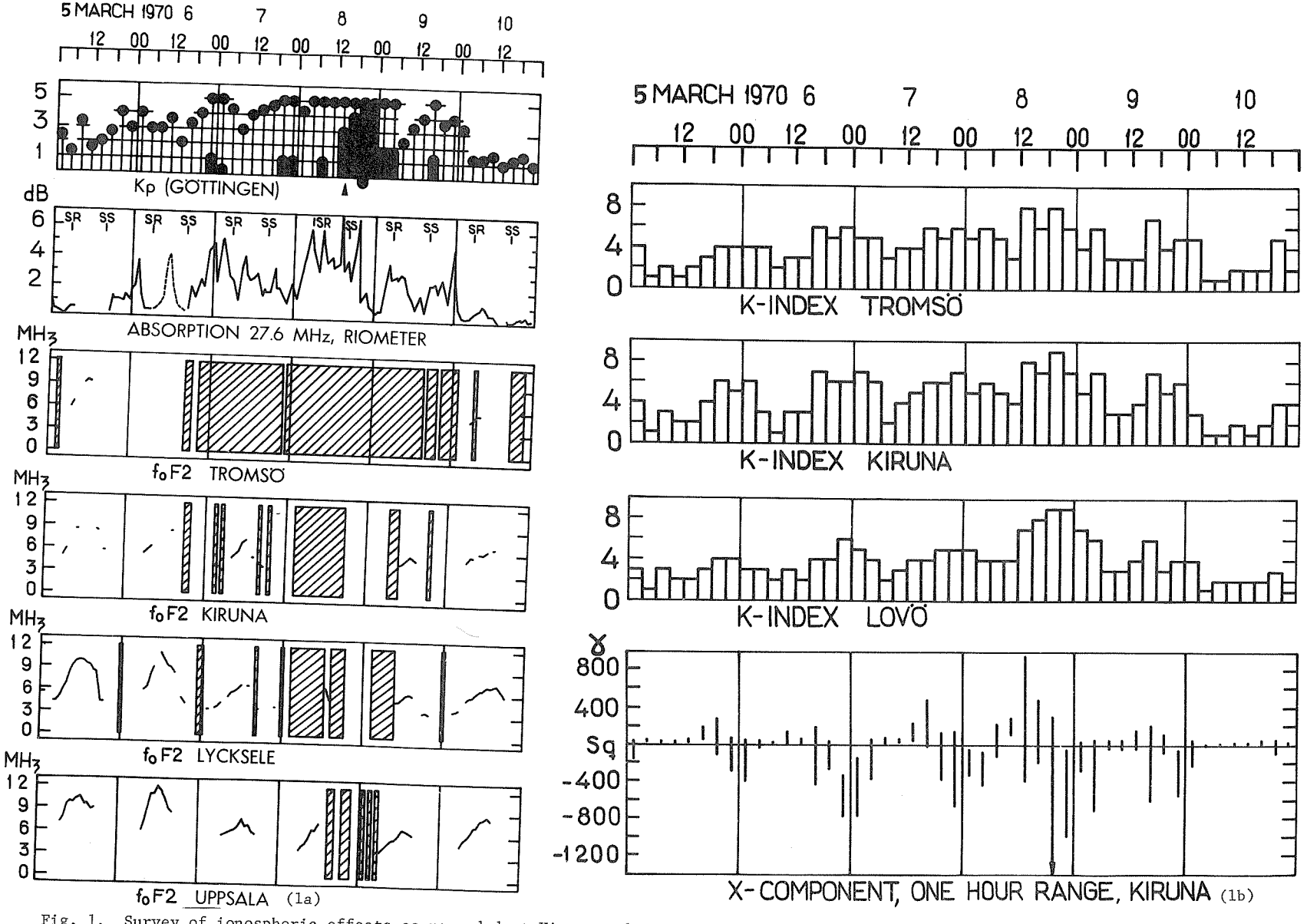

Fig. 1. Survey of ionospheric effects as recorded at Kiruna and nearby observatories. The foF2 plots and the K-indices are presented in order of decreasing latitude. The arrow below the Kp plot indicates the sudden commencement. The riometer absorption curve showing the maximum absorption during each hour, has been dashed on March 6 indicating the increased uncertainty due to interference. One-hour values of the critical frequency foF2 have been plotted. The hatched areas indicate periods when the critical frequency was not measured due to black-out and empty areas correspond to periods when foF2 could not be measured for other reasons.

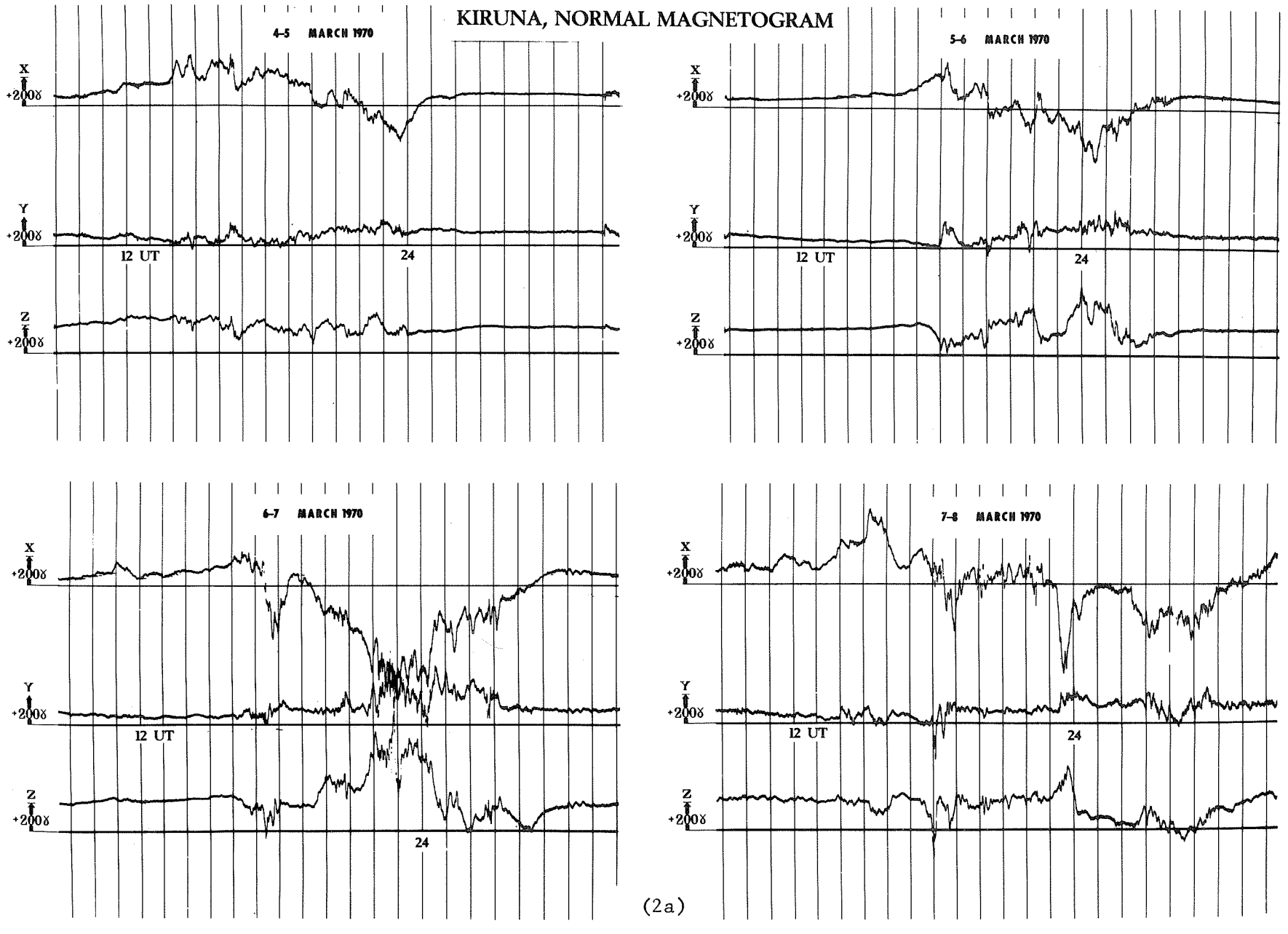
KIRUNA, NORMAL MAGNETOGRAM
4-5 MARCH 1970
5-6 MARCH 1970
6-7 MARCH 1970
7-8 MARCH 1970
X
Y
Z
+200γ
12 UT
24

(2a)

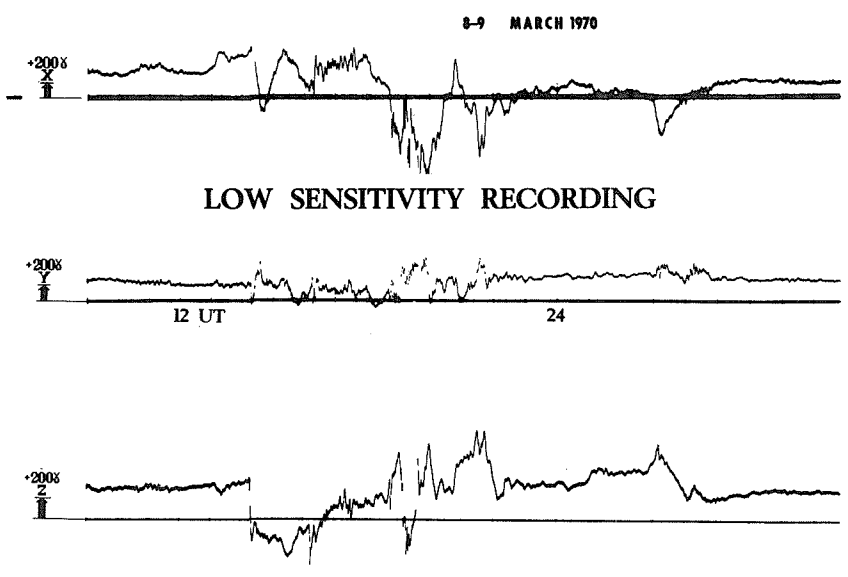

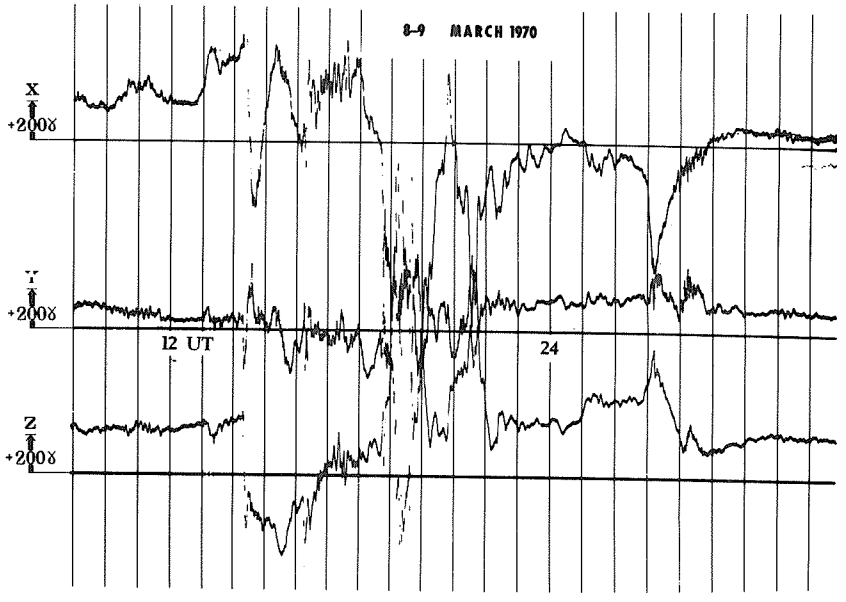

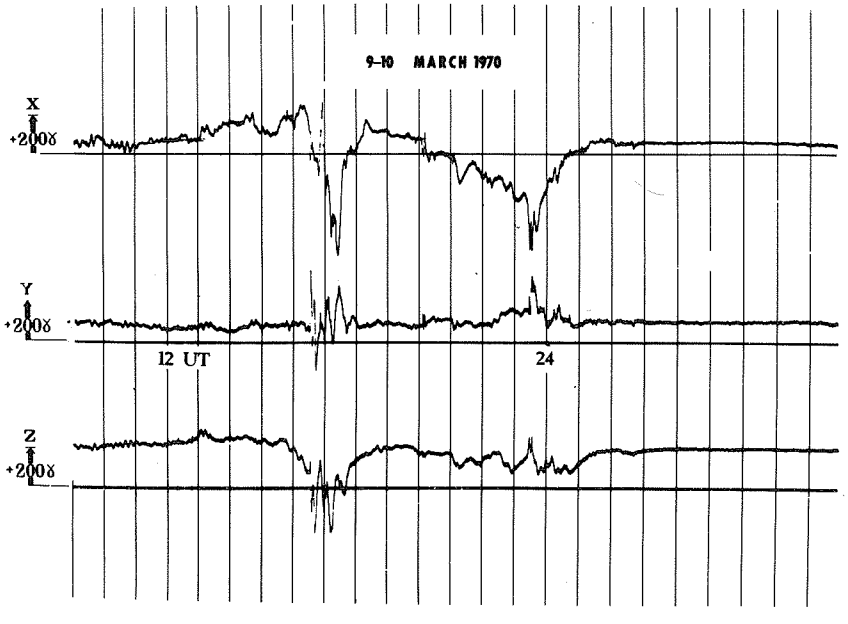

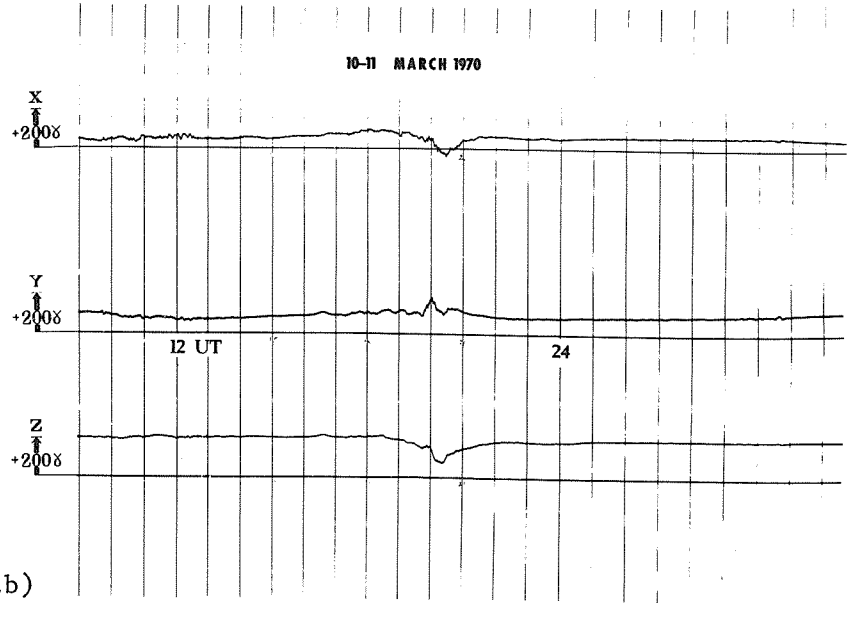

(2b)

Fig. 2. Kiruna normal magnetograms. For the most disturbed period, 8-9 March, the record of a low sensitive magnetometer is added to the normal magnetograms.

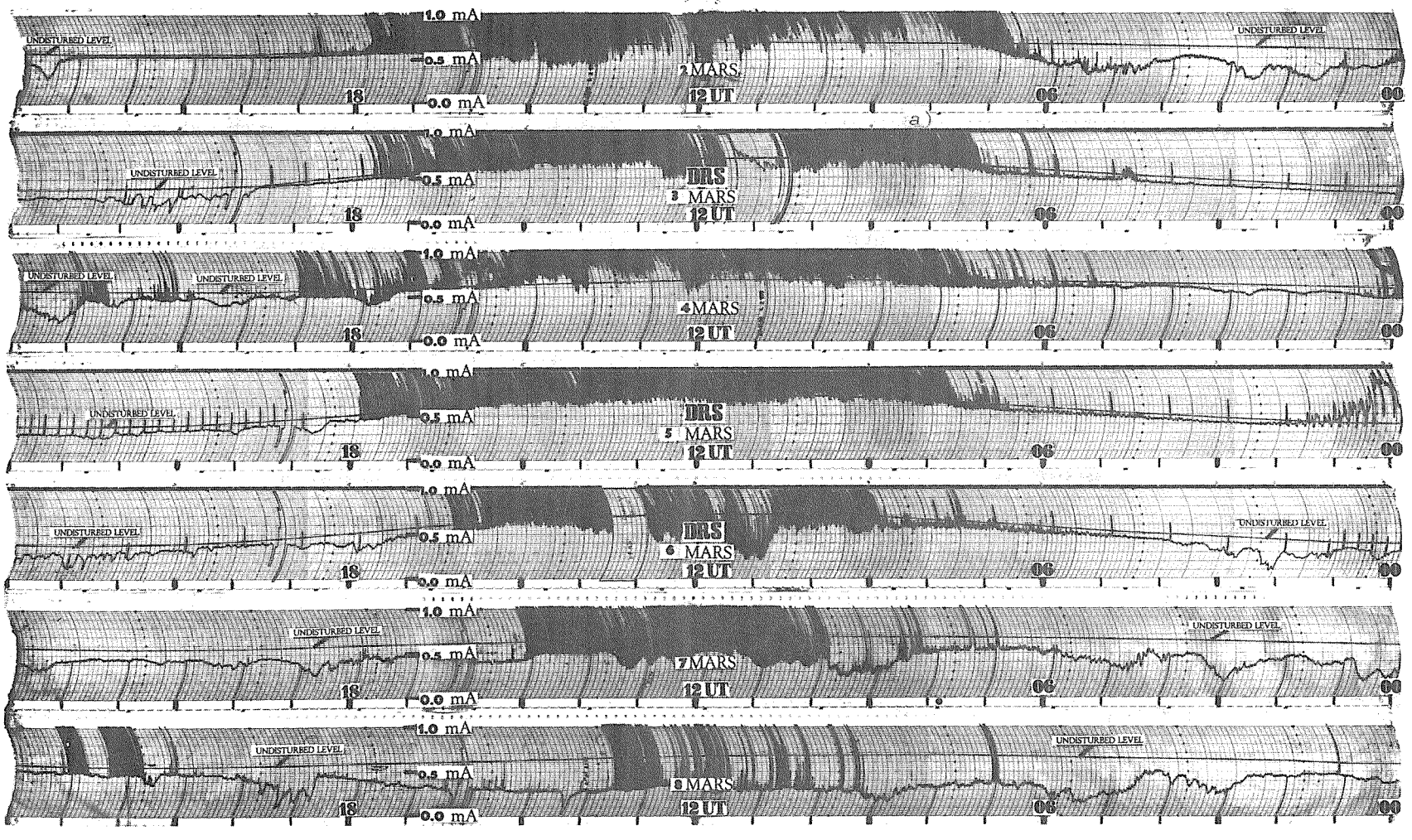

Fig. 3a.

Fig. 3. Riometer records from Kiruna 27.6 MHz receiver. In case of severe interference in Kiruna, the less disturbed records of the Down Range Station (DRS) at ESRANGE, (27.6 MHz), have replaced the Kiruna records. The reproductions are extracted from "Kiruna Geophysical Data".

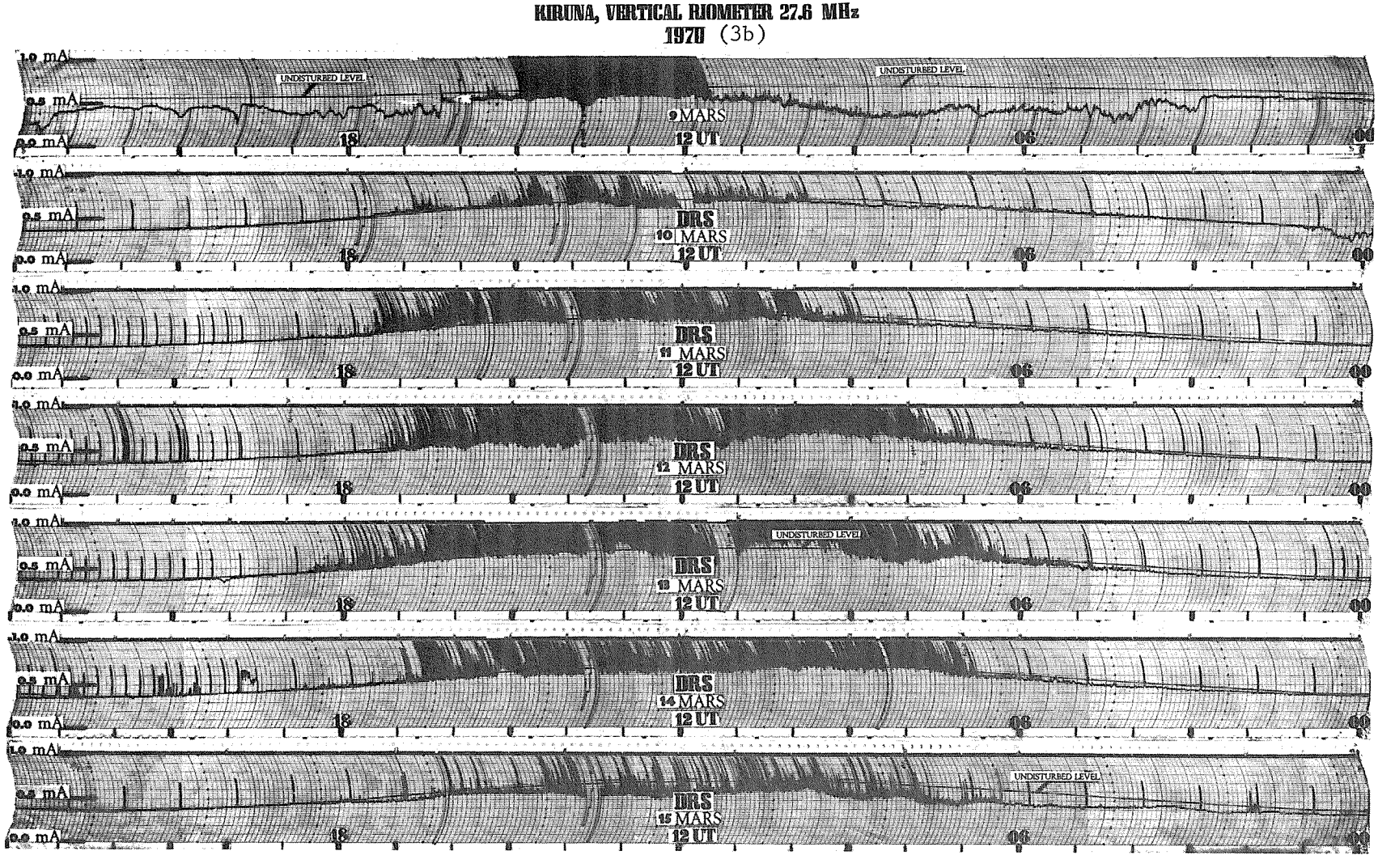
KIRUNA, VERTICAL RIOMETER 27.6 MHz
1970 (3b)
1.0 mA
0.5 mA
0.0 mA
UNDISTURBED LEVEL
9 MARS
12 UT
18
06
00
DRS
10 MARS
11 MARS
12 MARS
13 MARS
14 MARS
15 MARS

Fig. 3b.

"Midlatitude Ionospheric Effects in March 1970"

by

R. Knuth, W. Lippert and J. Weiss
Zentralinstitut für Solar-Terrestrische Physik (HHI)
der Deutschen Akademie der Wissenschaften zu Berlin,
G.D.R.
Observatory Neustrelitz

According to ionospheric observations in northern geomagnetic latitudes between about 50° and 60° N the event of March 1970 can be divided in two different phases: first the probable equatorward propagation of auroral zone ionization during the main phase of the geomagnetic storm for some hours during the night March 8/9 as the primary disturbance; secondly, the after-effect in LF-propagation indicating a more or less steady precipitation of quasitrapped magnetospheric particles into the lower ionosphere.

Ionospheric Disturbances during the Geomagnetic Storm of March 8/9, 1970

It is well known from many investigations, that during the main phase of strong geomagnetic storms the cutoff-latitudes for invading high energy particles are shifted towards the equator. This normally leads to the occurrence of distinct excessive ionization anomalies in geomagnetic latitudes of 55° or less for some hours. Figure 1 is a very complex survey of what happens during such a disturbance in different types of ionospheric observations.

Roughly coinciding with the first strong variations in geomagnetic H-component Niemegk (apart from the ssc at 1417 UT) the Kiruna Riometer shows a pronounced absorption increase at 1900 UT during a period of steady declining absorption. This short-term outbreak is followed by a period of very low absorption, indeed the most quiet interval in the Kiruna recordings between about March 6 at 1700 UT, and March 9 at 2400 UT.

The variation in geomagnetic H-component in Niemegk is indicative of intensity variations in the auroral electrojet above 60°N geomagnetic, therefore this recording is placed on (Figure 1) directly below Kiruna (b). In striking contrast the effects of excessive ionization in latitudes below 60°N also start with the onset of high geomagnetic activity but reach their maxima during or after the main phase of the storm, i.e. after 2048 UT. This can be concluded from (Figure 1) by five very different observations (c - g). Radar-aurora recorded by a 33 MHz-backscatter in Kuhlungsborn during the first minutes of each hour reaches its maximum intensity in the observation period at 2100 UT. This coincides very well with the highest excessive absorption in LF-A3-propagation and in Cosmic Noise Absorption in geomagnetic latitudes of 55° and 53.8°N.

Under normal conditions, the night time whistler activity in Neustrelitz is about 1-3 whistlers per 2 minutes observation interval. As is obvious from Figure 1 (f) this activity is very much higher during the night 8/9 March. But in good correlation with the above mentioned period of excessive ionospheric absorption the whistler activity has a minimum at 2050 UT, followed again not only by the continuation of the whistler storm but also by the frequent occurrence of VLF-emissions (indicated by the letter E). This leads to the conclusion, that during this phase of the March-event the magnetospheric conditions for the propagation of whistlers and for the generation of VLF-emissions are extremely favorable, but the excessive ionization of the lower ionosphere during the main phase of geomagnetic storm causes a temporary interruption due to increased ionospheric absorption. It is well known, that during daytime and for solar flares it is possible to deduce the height variations of the lower ionospheric border from records of the so-called phase height of LF-transmitters over distances of about 1000 km [for instance Lauter et al., 1960]. During the night the recordings are very irregular. But during the night of March 8/9 there occurred such distinct field-strength variations, that for the first time the resulting ionospheric height variations were deduced. The results for two different paths and frequencies are given in Figure 1 (g). Very cautiously interpreted they show a decrease of reflection level (about 500 electrons/cm^3) by about 20 km down to 73 - 78 km at 2204 UT and 2209 UT. The path with reflection point at 48.6°N shows the smaller height decrease and the later maximum. A downward movement of the lower ionosphere by such an amount should cause considerable excessive absorption in the low frequency propagation also in these latitudes around 50°N. But a careful check of many LF-A3-observations with reflection points in this region indicated almost no absorption anomalies, but the occurrence of strong unusual fading with maximum rate around 2200 UT. This normally means, that the additional ionization below the reflection level (about 95 - 100 km during the night) is low and probably only the reflection level itself is disturbed. The reasons for this apparent difference in the conclusions from LF-phase height and LF-A3-observations are not known.

In summary, Figure 1 gives the following time history: Starting with the strong geomagnetic storm at about 1900 UT a belt of invading high energy particles shifted equatorward and reached latitudes below 55°N during the main phase due to the cutoff reduction. Effects of these ionizing particles can be found in a lot of different ionospheric observations. According to absorption-recordings the south-

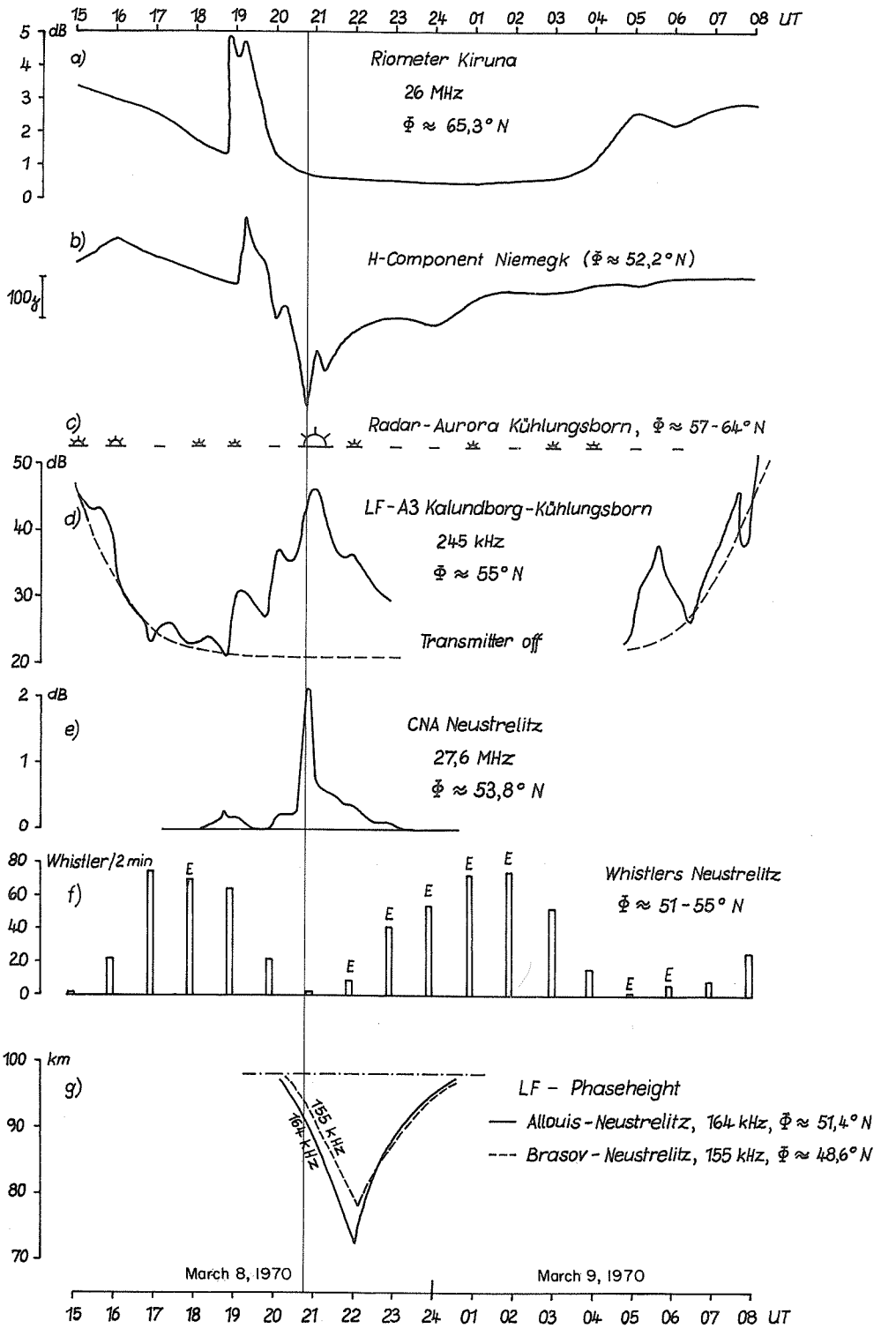

Fig. 1. Ionospheric disturbances during the geomagnetic storm of March 8/9, 1970
(a) Cosmic Noise Absorption Kiruna, hourly values
(b) Magnetic H-Component Niemegk, hourly values, from 1845 - 2200 UT 15 min - values
(c) 33 MHz backscatter aurora-radar Kühlungsborn; dashes mark observations without aurora-echoes
(d) LF-A3-absorption in Kühlungsborn, dashed line indicates normal values
(e) Cosmic Noise Absorption Neustrelitz
(f) Number of whistlers per 2 min observation interval each hour. The letter E denotes additional occurrence of VLF-emissions
(g) Height variation of lower ionospheric border ($n_e \approx 500$ el/cm^3) after LF-Phase height observations -·-·-·-·-·- : assumed nighttime reflection level
All indicated latitudes are geomagnetic conventional, the geomagnetic corrected latitudes after Hakura are about 3 degrees lower.

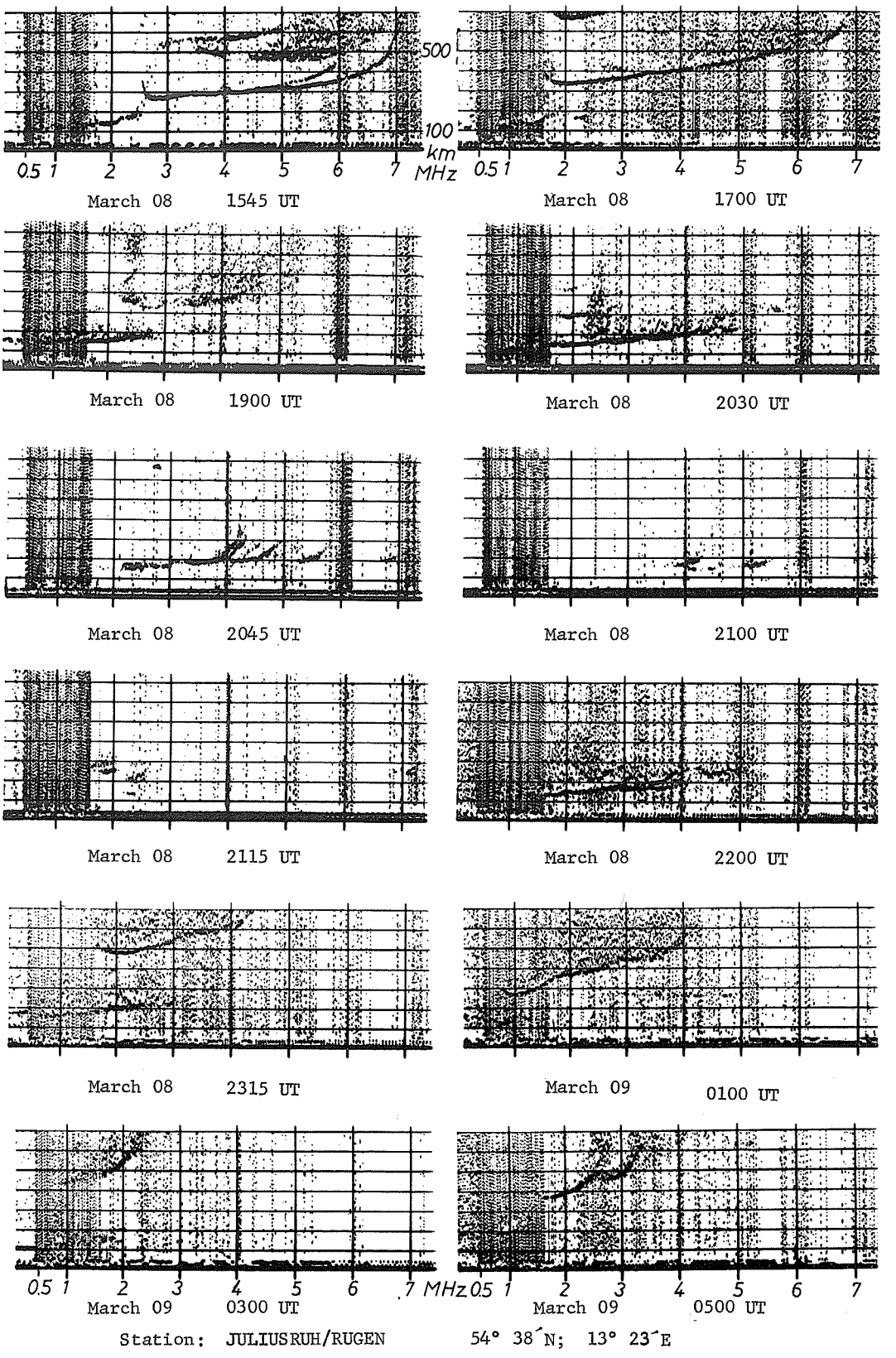

Fig. 2. Ionosonde recordings in Juliusruh/Rugen

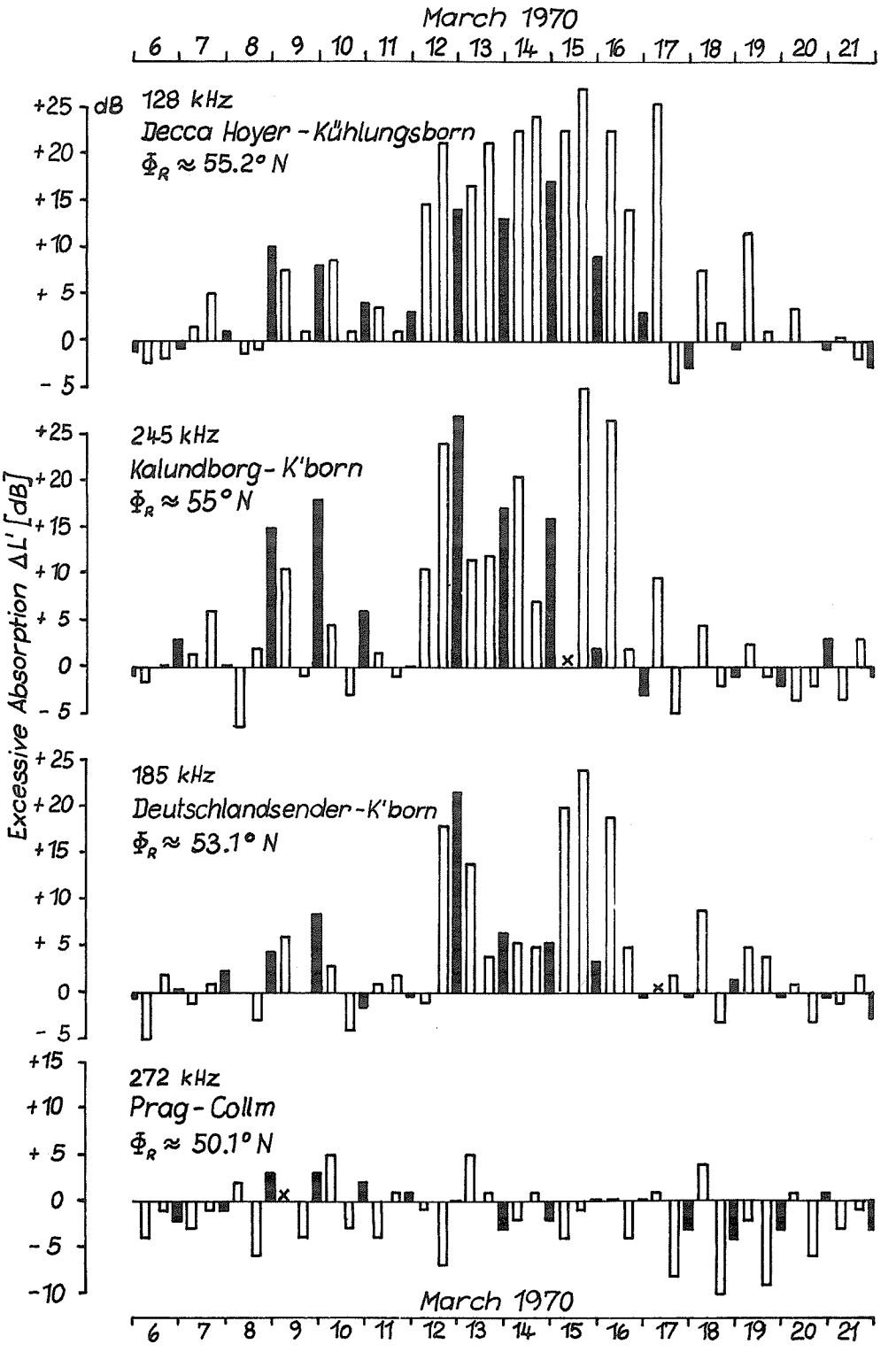

Fig. 3. The after-effect in LF-propagation. Indicated are the differences of absorption in comparison to the undisturbed normal values as excessive absorption

■ : excessive nighttime absorption

□ : excessive absorption during sunset and sunrise

X : no observation

Indicated are the geomagnetic conventional latitudes of the respective reflection points.

ern border of this temporary movement was situated at about 51°N, according to phase height-measurements it probably reached geomagnetic latitudes around 45°N. If the interpretation in terms of a southward movement is correct, then we get mean travel times of 10 minutes per degree in latitude between 65° and 54°N and of 15 minutes per degree in latitude between 54° and 50°N.

Also observations of the ionosphere by an ionosonde in Juliusruh/Rugen (54.5°N geomagnetic) indicated strong disturbances, which are represented in Figure 2 and may be interpreted in the following manner:

1545 UT: First indications of an ionospheric disturbance by the occurrence of scattered oblique reflections from the F-region up to 6.5 MHz (probably caused by the approach of a front with horizontal electron gradient from North).
1700 UT: Scattered oblique echoes. The sky wave reception of terrestrial broadcasting transmitters between 1.5 and 7 MHz is normal.
1900 UT: Development of an auroral-type Es-layer. The F-region disappeared, only scattered echoes appear. The sky wave propagation in HF-range is highly disturbed.
2030 UT: The F2-region vanished completely only the auroral Es-layer can be seen. f min is $\lesssim$ 0.8 MHz, that means that the absorption in the lower ionosphere is not remarkably increased until this time.
2045 UT: Strong increase of absorption. f min reaches 2.2 MHz about the same value as during strong SID-effects. No sky wave reception of broadcast transmitters.
2100 UT: f min increases further to 3.8 MHz, indicating extremely high excessive ionization in the lower ionosphere.
2115 UT: f min $\lesssim$1.6 MHz, but only faint and unclear ionospheric echoes can be seen. The sky wave blackout continues.
2200 UT: f min is again about normal ($\lesssim$ 0.9 MHz). Only echoes from the Es-layer are identified, but they indicate a sharp lower border of this region which permits sky wave propagation in HF-range.
2315 UT: The Es-layer diminishes, F-region echoes occur. The broadcast reception is about normal.
0100 UT and
0300 UT: The F-region has formed again, the Es-layer gradually disappears.
0500 UT: The view of F-region is about normal, the critical frequency is 1 MHz low.

With some variations the foF2 remains 1 - 2 MHz below the normal value until March 10, 0200 UT.

The After-Effect Period

As usual after strong geomagnetic storms the LF-propagation via the lower ionosphere in medium latitudes was disturbed for many days. This after-effect by a more or less steady precipitation of quasitrapped magnetospheric particles can best be seen during sunset and sunrise, but also during the night. It is thought to be due to excessive ionization in heights between 60 and 90 km, which has its relative intensity maxima due to photodetachment processes at solar zenith angles $\chi \approx 90°$. Figure 3 indicates, that such an after-effect period in geomagnetic latitudes above 53°N lasted until March 20. The latitudinal dependence is obvious, in 50°N no indications for any long lasting after-effect can be found.

Acknowledgements

The authors are kindly indebted to Professor Hultqvist, Kiruna Observatory (Sweden), Dr. Triskova, Geophysical Institute Prague (Czechoslovakia), Professor Sprenger, Ionospheric Observatory Kuhlungsborn (GDR) and Dr. Schminder, Geophysical Observatory Collm (GDR) for use of their unpublished observational material.

REFERENCES

1970 — Geophysikalische Beobachtungsergebnisse (Geophysical Data), Zentralinstitut für solar-terrestrische Physik (Heinrich-Hertz-Institut), 21, No. 3

LAUTER, E. A., G. ENTZIAN and R. KNUTH, 1960 — Die Formen der Störungen in der tiefen Ionosphäre und ihre Deutung, dargestellt am Beispiel des November-Event 1960 Zschr. f. Met., 14 Heft 11/12, 275-286

"On HF Propagation Disturbances from March 6 - 10, 1970"

by

Yugoro Takenoshita
Hiraiso Branch, Radio Research Laboratories
Nakaminato-Shi Ibaraki-Ken, Japan

This short note summarizes HF propagation disturbances during the geomagnetic storms which occurred in early March, 1970. Two geomagnetic storms occurred, beginning suddenly at 0805 UT on March 5, and 1418 UT on March 8. The latter storm as recorded at Kakioka Magnetic Observatory (36°14'N, 140°11'E) was especially outstanding with an enhancement of the geomagnetic horizontal component as large as 93 gammas, and also with the total range of horizontal component as large as 323 gammas.

During these geomagnetic storms, the ionosphere and hence HF wave propagation conditions were severely disturbed. Figure 1 shows disturbed features of WWV (15 MHz) and WWVH (15 MHz) waves observed at Hiraiso (36°22.0'N, 140°37.5'E). In this figure the day-to-day variation of deviations of hourly field intensities from the monthly median is indicated for March 6 through 10, 1970. WWV-Hiraiso (solid line) and WWVH-Hiraiso (dotted line) may be regarded as typical mid-latitude and low latitude circuits, respectively.

As seen in Figure 1, field intensities on both circuits were lower than the monthly median value for almost all hours considered. Concerning these lower field intensities, the following four characteristic features should be pointed out:

1) Temporal variations of absorption for the two circuits were almost similar one to each other in form and values early in the morning at the receiving point (Hiraiso) for this period except March 8. The propagation distance of WWV-circuit is 9150 km, and that of WWVH is 6270 km as given in Table 1. The fact that absorption is similar, in spite of the wide separation between the two transmitting points of more than 6000 km (about three hours in local time), would more likely be due to lowered MUF early in the morning over the common receiving region of both circuits than due to other reasons.

Table 1

Particulars of the transmitter and receiver

Transmitter

	WWV	WWVH
Location	Fort Collins, Colorado Long. 105°02'W Lat. 40°41'N	Puunene, Maui, Hawaii Long. 156°28'W Lat. 20°46'N
Power	3 kW for the upper side-band	0.5 kW* for the upper side-band
Antenna	half wave length, vertical	half wave length, vertical
Distance	9150 km	6270 km

* Reduced from the carrier power of 2 kW with amplitude modulation of 100%.

Receiver

Antenna	4.5 metre, vertical rod
Bandwidth	± 40 Hz for the upper side-band
Calibration	every hour

2) From the later half of March 8 to earlier half of March 9, field intensities of both circuits were remarkably low. Especially, WWV could not be received for six hours from 15 through 21 UT on March 8. WWVH also could not be received from 16 to 18 UT on March 8. Moreover WWV showed attenuation of more than 20 dB from 00 to 05 UT and WWVH showed attenuation from 08 to 11 UT on March 9. This attenuation is considered to be caused by the lowered MUF accompanying the geomagnetic storm which suddenly occurred at 1418 UT on March 8. The geomagnetic storm was most severe from 14 hours on March 8 to 05 hours on March 9. WWV reception passing through a mid-latitudinal region was more affected by the storm than WWVH reception passing through a low latitude region.

3) Intensities of WWV were considerably low from 05 to 06 hours and WWVH from 09 to 12 hours almost every day. These periods correspond to the early night or midnight at the transmitting points. Now, the lowest MUF occurs usually early in the morning. Therefore, it appears that the lower intensities are due to unidentified absorption. Lower intensities which are expected to occur early in the morning over the transmitting region did not appear.

4) On account of the diurnal variation on the storm day mentioned above in 1) and 3), storm-time variations of field intensity in both circuits were generally parallel to temporal variation of Kp without any delay time. On the other hand, a deviation of propagation character figures from monthly median over the North Atlantic is shown in Figure 2. It is roughly seen that the propagation condition followed Kp with a delay of 6 hours, in contrast to the variations which occurred over the Pacific.

On HF wave propagation disturbances observed at Hiraiso from March 6 to 10, 1970, it could be concluded that

i) characteristically lowered MUF appeared early in the morning over the receiving region, while it did not appear over the transmitting region,

ii) some absorption was observed during early night or midnight over the transmitting region, and

iii) variation of propagation conditions over the Pacific was simultaneous with geomagnetic activity, while that over the North Atlantic was delayed by almost six hours after the geomagnetic activity.

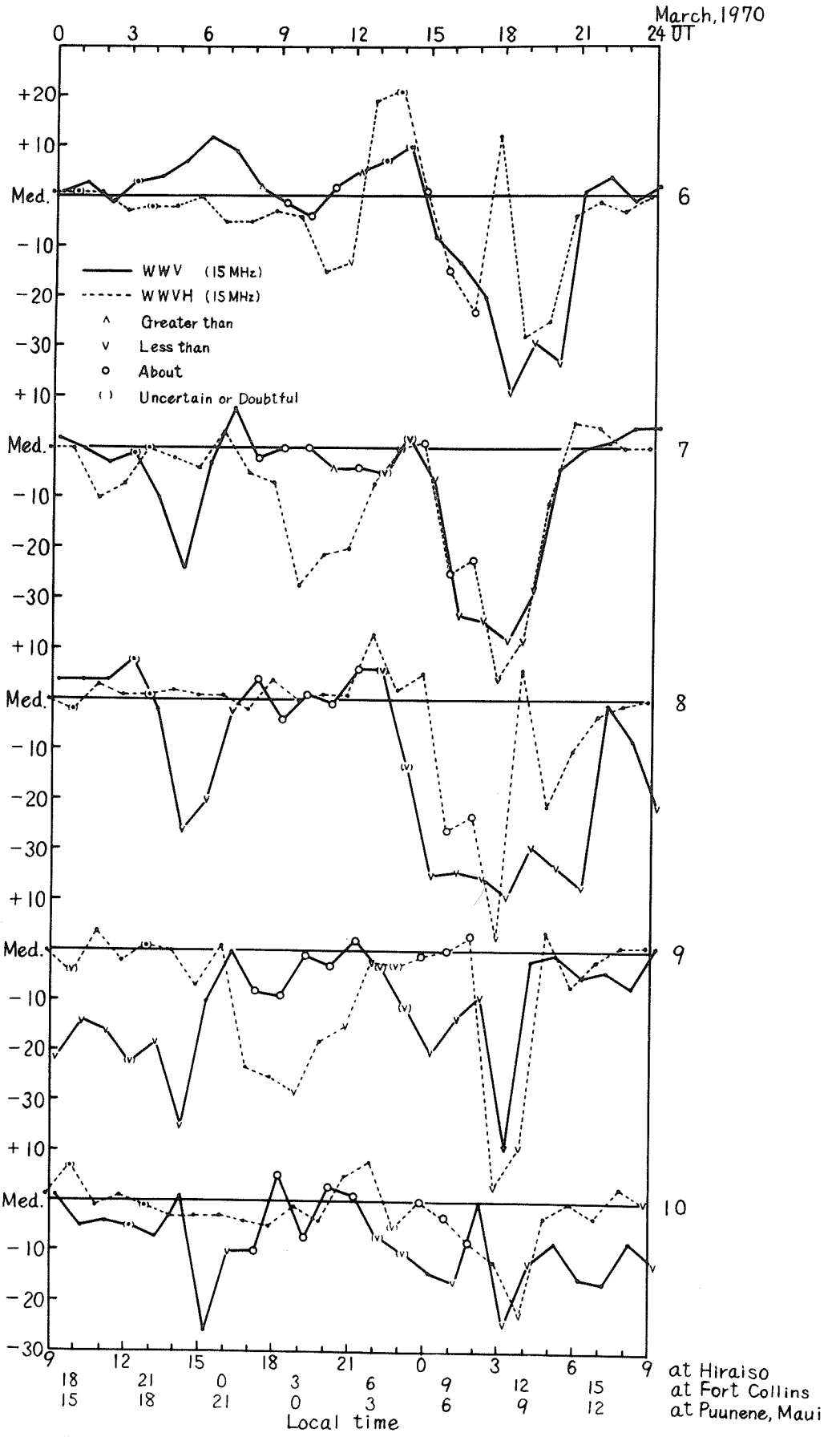

Fig. 1. Deviation from Monthly Median Values of Field Intensity (15MHz) Received at Hiraiso.

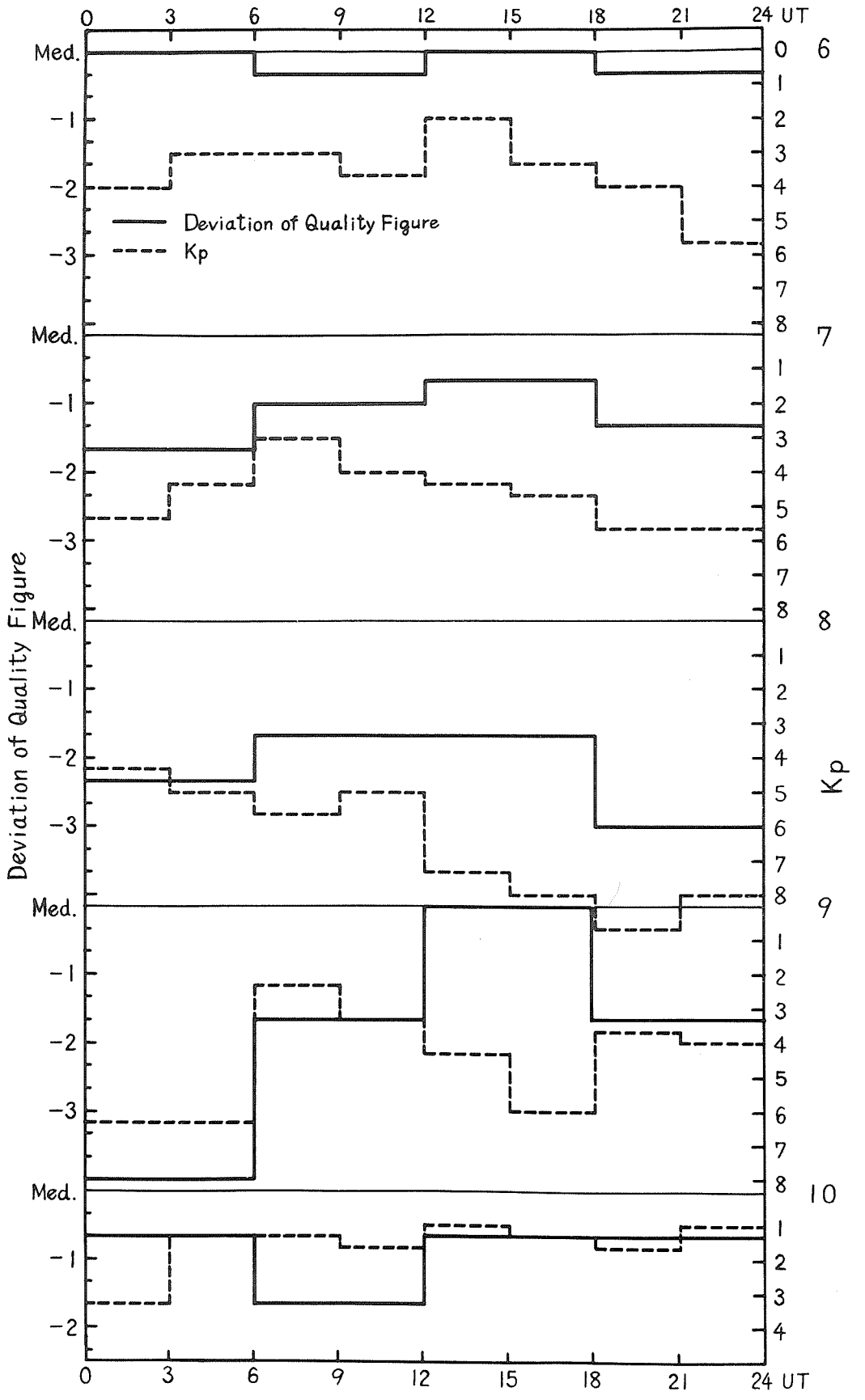

Fig. 2. Deviation from Monthly Median Values of Radio Propagation Quality Figure over North Atlantic and Kp.

"HF Doppler Observation Associated with Magnetic Storm of March 8, 1970"

by

M. Tsutsui and T. Ogawa
Ionosphere Research Laboratory
Kyoto University
Uji, Kyoto, Japan

We observed an HF Doppler effect associated with the geomagnetic storm which started at about 1418 UT (2318 LT), March 8, 1970.

Figure 1(a) shows the HF Doppler records observed at Uji (34°54'N, 135°47'E) on March 8, 1970. The receiving frequency is 5 MHz, the distance between the transmitting site and Uji is about 360 km, and the reflecting region in the ionosphere is the F-layer because it is a midnight observation. There were station breaks from 25 min. to 34 min. past each hour. Figure 1(b) shows the H component of the geomagnetic field observed at Kakioka Magnetic Observatory (36°14'N, 140°11'E).

The HF Doppler shift shows a good correlation with the geomagnetic rapid increase. The sudden commencement occurred at about 1418 UT. The receiving frequency had negative Doppler shift from around 1535 UT which showed the decrease of electron density due to the negative storm [King, 1970]. The radio-wave penetrated the ionosphere at 1548 UT and recovered at 1721 UT.

Several rapid increases of geomagnetic field which began after 1720 UT brought about positive Doppler shifts as shown with arrows. It might be thought that these frequency shifts were caused by the change in the value of the refracting index due to the change in the intensity of geomagnetic field [Jacobs and Watanabe, 1966]. At 1915 UT the radio-wave penetrated again due to the decrease of magnetic field.

REFERENCES

KING, G. A. M. 1970 (in press) The Ionosphere F-Region Storm, J. Atmos. Terr. Phys.,

JACOBS, J. A. and T. WATANABE 1966 Doppler Frequency Changes in Radio Waves Propagating Through a Moving Ionosphere, Radio Science, Vol. 1, No. 3, 257-264.

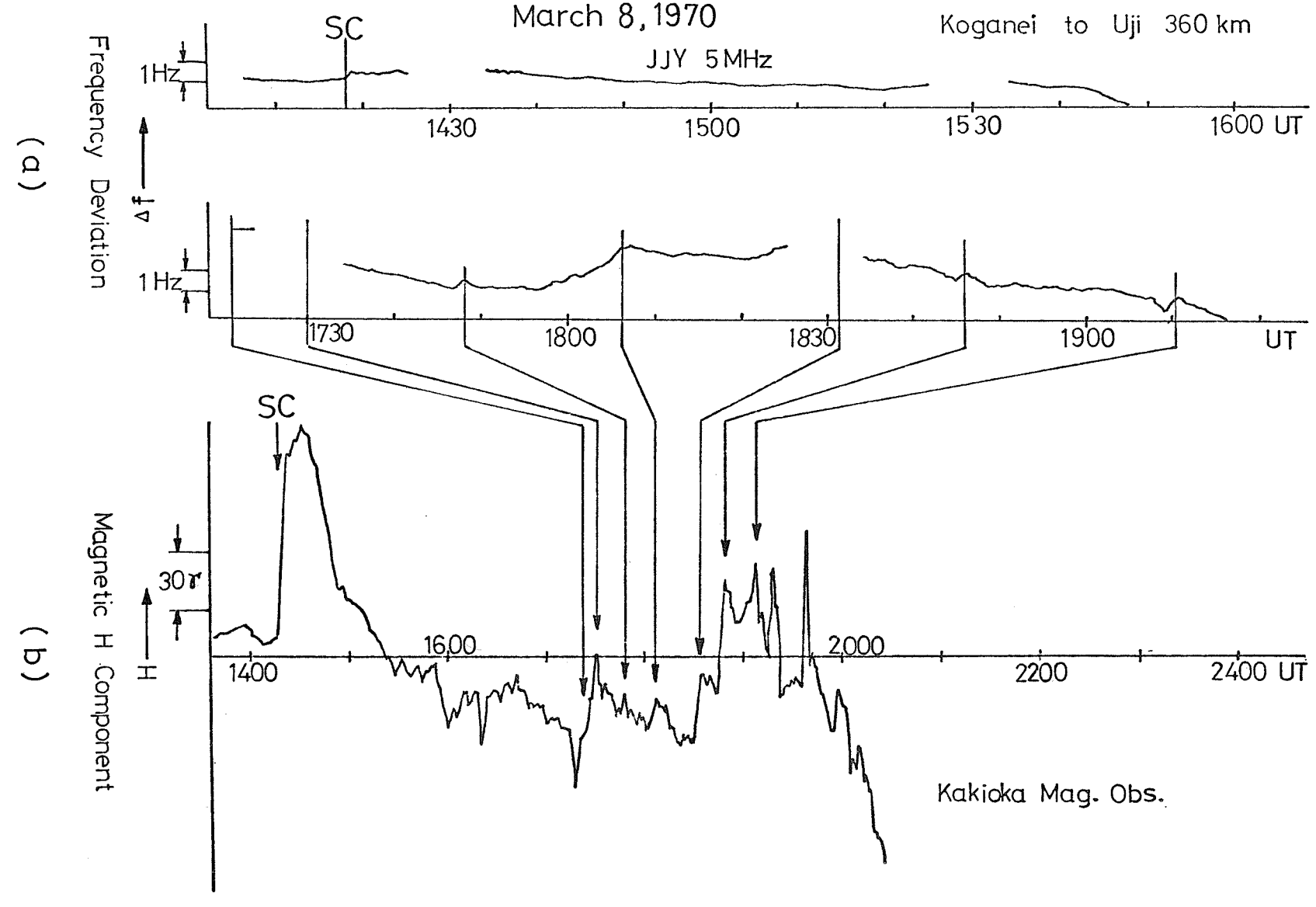

Fig. 1. Correlated frequency and geomagnetic field fluctuation during magnetic storm (The geomagnetic record is supplied by Kakioka Magnetic Observatory).

Riometer Observations During the Period 6 - 9 March, 1970

by

Warner L. Ecklund and Herbert H. Sauer
NOAA-Environmental Research Laboratories

This laboratory operates a network of riometers observing sites in both the northern hemisphere and on the Antarctic continent. The principal data are obtained from the Alaskan riometer chain operated in cooperation with the Geophysical Institute of the University of Alaska, while the data from Thule were obtained through the cooperation of the Air Force Cambridge Research Laboratories. The names, geographic coordinates and approximate L-values of the observing sites are tabulated below.

TABLE I

Station name	Geographic Coordinates		L
	Latitude	Longitude West	
Wildwood	60.4	151.2	3.75
Anchorage	61.2	149.85	4.2
Sheep Mountain	61.8	147.6	4.5
Paxson	63.0	145.7	5.05
College	64.9	147.8	5.5
Fort Yukon	66.6	145.3	6.5
Bar I	70.0	142.5	8.0
Thule	76.5	68.8	50.
Byrd	-80.02	119.53	7.23
South Pole	-90.0	-	14.02

The period covered by this communication includes the most geomagnetically active of this solar cycle, the riometer observations for this period are shown in Figures 1 and 2. The shaded bars in these figures indicate nighttime conditions for the respective sites. During this period as well, solar protons were observed by several satellites (as reported in "Solar-Geophysical Data") to arrive in the vicinity of the earth and were detected by several ground-based sensors. Details of these observations will undoubtedly be reported elsewhere in this publication, and will, therefore, not be repeated here.

As will be seen from the figures, the period was generally characterized by the occurrence of substantial auroral absorption (typified by the College record). Particular activity may be noted following the indicated time of the sudden commencement of the great storm at 1417 UT on March 8. This activity severely compromised the ability of the Alaskan stations to unequivocally yield the concurrent PCA (Polar Cap Absorption), although drawing a lower envelope through the indicated absorption would yield a reasonable estimate of that contribution.

The data from the high latitude stations of Byrd, South Pole and Thule indicate the first measureable PCA to have occurred at about 0900 on March 6, however, ATS-1 did not indicate an enhancement of proton flux until about 1530. The low level of absorption observed in this interim may possibly have been due in fact to some auroral contamination at these latitudes, since the lower latitude stations show a large peak of auroral absorption at that time. Considering the polar stations only, the peak of the PCA seems to have occurred in the early hours of March 8, reaching an absorption of about 3.5db.

REFERENCES

Solar-Geophysical Data, IER-FB 318, Part I, April 1970, U.S. Department of Commerce, (Boulder, Colo., U.S.A. 80302)

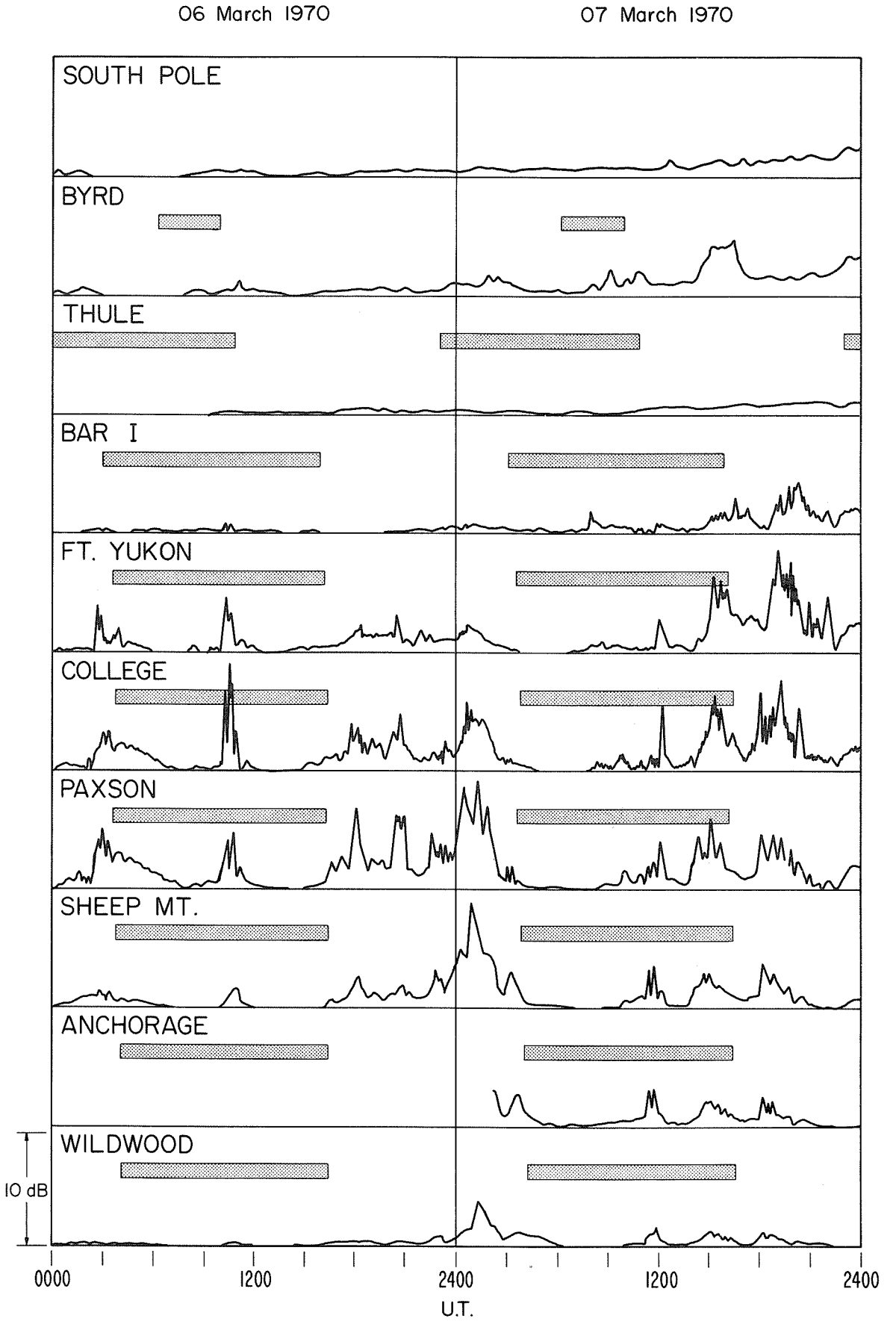

Fig. 1. Riometer observations March 6-7, 1970.

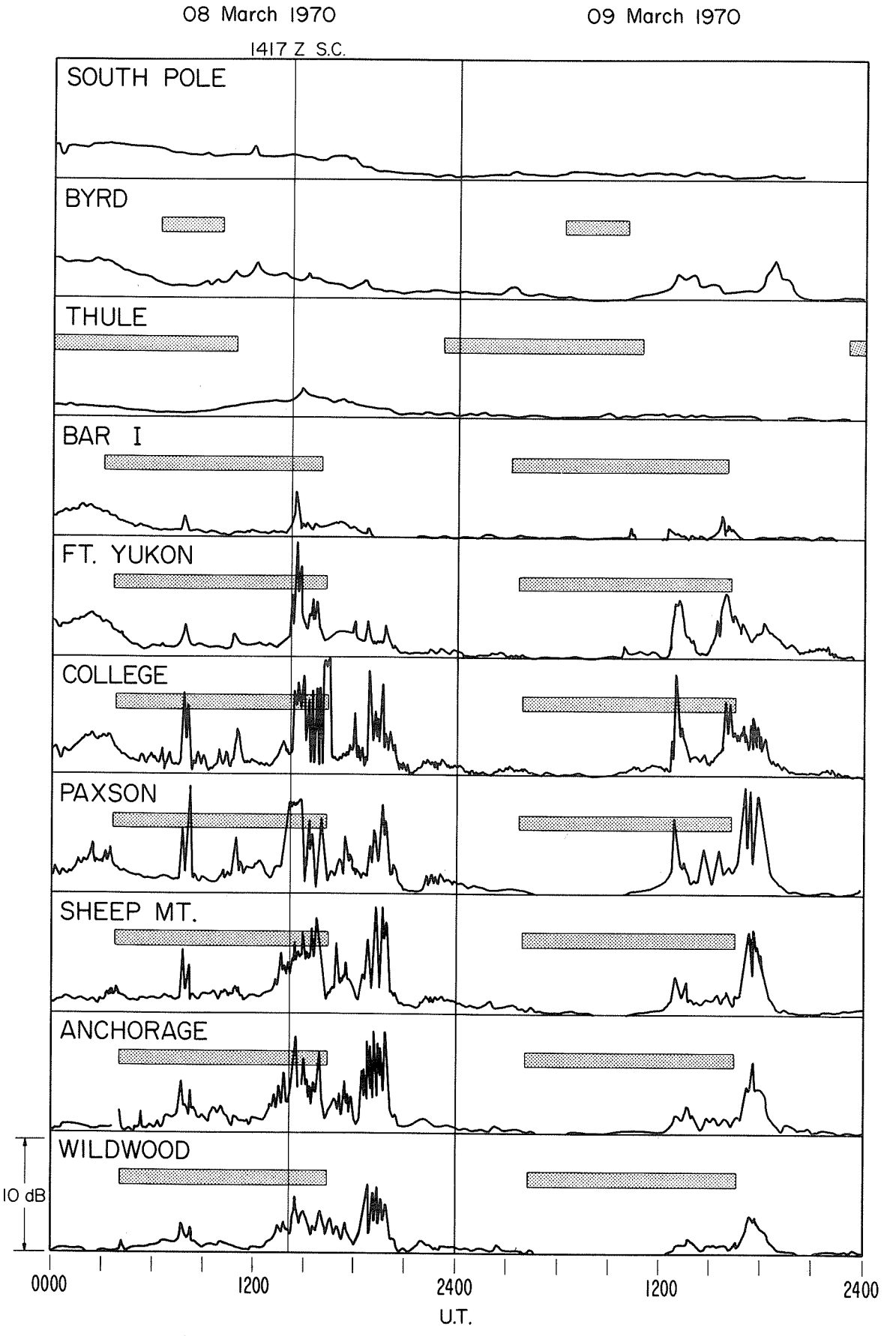

Fig. 2. Riometer observations March 8-9, 1970.

"Mid-latitude Radio Absorption by A1 and A3 Techniques - A1 data for Lancaster (53°52'N, 2°45'W)"

by

J. K. Hargreaves
Environmental Sciences Department
University
Lancaster, England

The cause (or causes) of the day-to-day variability of mid-latitude ionospheric absorption ("the winter anomaly") is not yet fully known. On one hand there is good evidence that on at least some occasions the phenomenon is a meteorological one, related to stratospheric temperatures and circulation patterns. However, this correlation is not always maintained, and it may be that the effect occurs only with the more intense stratospheric events. On the other hand, there is observational evidence that anomalous absorption is due to the precipitation of energetic particles, and related to variations of Kp, possibly with a time lag of several days.

It would therefore be interesting to collect and compare mid-latitude A1 and A3 data for periods containing major storms. A1 data for Lancaster are given in the table. These are the values for 1200 and 1300 UT on the days during March 1-20, 1970 when measurements were made, each value being an average of 20 spot readings taken at one-minute intervals. The values are corrected to 100 km reflection level. The radio frequency was 2.14 MHz.

1970	Absorption in dB at 1200 UT	1300 UT
March 2	36	34
4	41	38
6	36	SID
9	35	33
11	38	39
13	46	34
16	38	35
20	40	38

"Measurements of Phase and Amplitude at VLF and LF over Short and Medium Paths for the Period March 5-18, 1970"

by

E. Hammond and M. D. Harrison
S.R.C., Radio and Space Research Station
Ditton Park, Slough, Bucks., England

Introduction

This report presents and discusses recordings of radio wave transmissions at 16 kHz over paths of 106 and 537 km, and at 60 kHz over the 106 km path, which show effects associated with the magnetic storm of March 8, 1970. The solar eclipse of March 7 occurred before sunrise on these paths, and will not be considered.

Transmission paths and receiving equipment

The transmission paths and the field components monitored are summarized in Table 1.

Table 1

TRANSMITTER			RECEIVER		PATH	
Location	Call Sign	Frequency	Location	Field components monitored	Length	Latitude of mid-point
		kHz			km	
Rugby 52°22'N 01°11'W	GBR	16.0	Aberdeen 57°10'N 02°06'W	Resultant of vertically polarized sky-wave plus ground-wave	537	54°46'N
ditto	GBR	16.0	Slough 51°30'N 0°34'W	Horizontally polarized sky-wave	106	51°56'N
	MSF	60.0				

The recordings at Aberdeen were made using a loop aerial in the plane of propagation and the recorded amplitude is, therefore, a function of both the phase and amplitude of the sky-wave.

The Slough recordings were obtained with the transverse loop technique described by Best, Ratcliffe and Wilkes [1936], with a vertical wire aerial to provide a phase reference signal at 16 kHz.

Observations

Figure 1 shows the variations in signal strength of the 16 and 60 kHz transmissions received at Slough and of the 16 kHz transmissions at Aberdeen during the period March 5-18, 1970, together with the phase lag of the 16 kHz waves relative to the ground wave at Slough. The planetary magnetic disturbance index ap, and the start times of sudden ionospheric disturbances are also shown. The amplitude scales are based on signal generator calibrations of the receivers, and the phase zero for the 16 kHz recordings at Slough was obtained by rotating the loop aerial 90° anti-clockwise into the ground-wave plane.

The values shown in Figure 1 are hourly samples in each case and, therefore, the nighttime amplitude variations do not accurately represent the depth and periodicity of fading.

The quiet-day variations of the propagation parameters are represented by the dotted curves in Figure 1 and have been derived from the period prior to the storm. For the more stable recordings of GBR amplitude received at Aberdeen and phase received at Slough, the mean values based on the days February 24 to March 5 are used. Slightly smoothed median values are used for the more variable

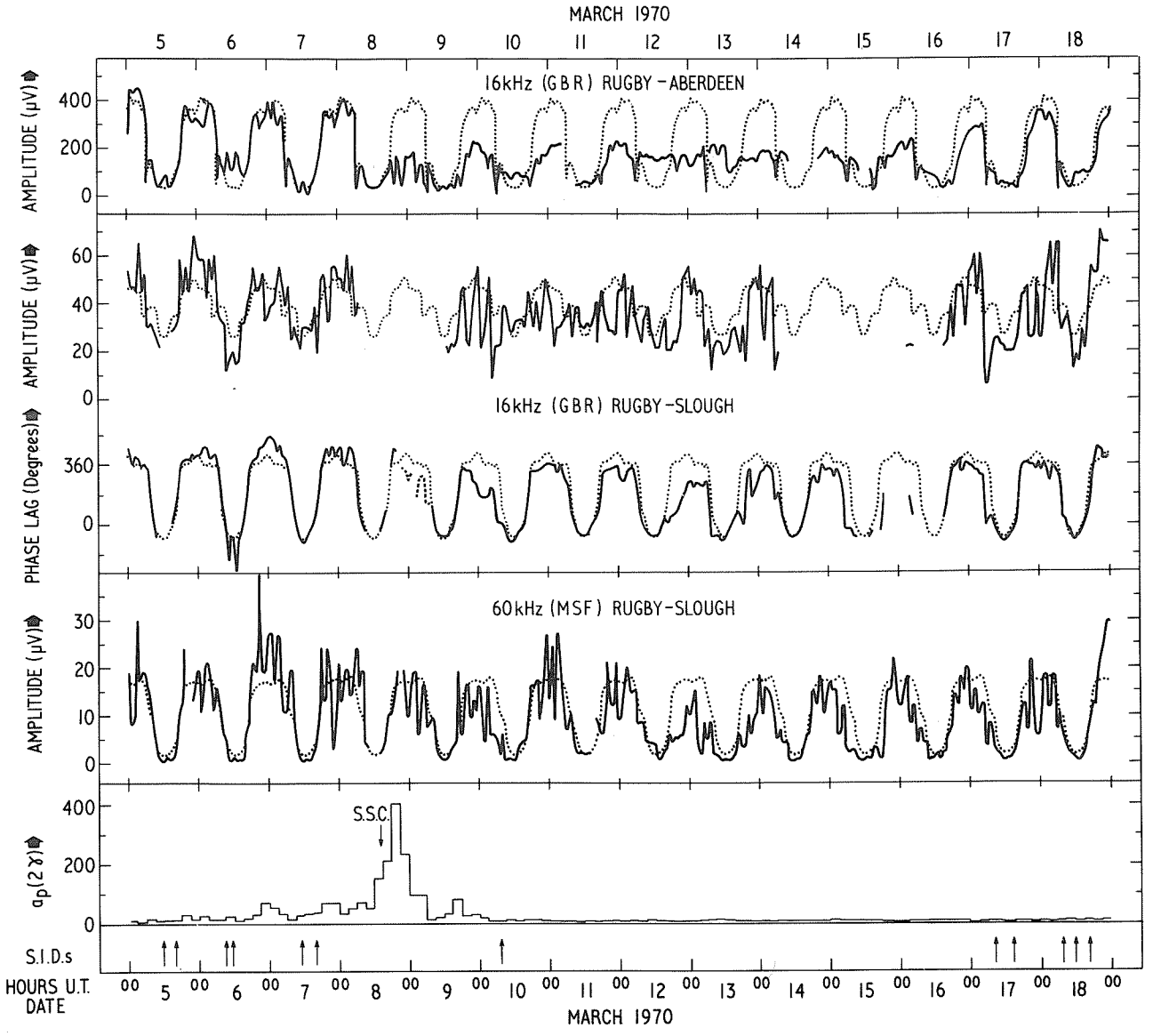

Fig. 1. Phase and amplitude variations during March 5 to 18, 1970.

amplitude records of GBR and MSF received at Slough. For the GBR to Slough path, amplitude data was only available from March 1, so a smaller sampling interval of 0.25 hours was used to obtain a median hourly value.

Although the sudden commencement of the storm occurred at 1418 UT on March 8, the effects on the VLF and LF records are not apparent until 1800 UT, near ground sunset, the effect being most marked on the Aberdeen path at this time. The geomagnetic field has recovered by the evening of March 9 and the quiet conditions persist for the remainder of the period considered.

The rapid fading observed on the GBR signal received at Aberdeen during the night of 8/9th is not reproduced in Figure 1 owing to the hourly sampling rate. This rapid fading disappears at sunrise on the 9th and does not reappear on subsequent nights. The nighttime amplitude is reduced by about 200 μV from the 8th until the 16th. The daytime amplitude is normal until the 12th and 13th, by which time there is little difference between the daytime and nighttime values, that for daytime having increased. However, the pronounced drop in amplitude occurring about an hour before ground sunrise on quiet days is maintained throughout the disturbed period. The daytime amplitude on the 12th and 13th is 150 μV, which is very close to the ground wave value of 130 μV, estimated from a

Hollingworth interference pattern observed in June 1969 [Smeathers, 1970]. It is, therefore, possible that the sky wave is too weak to be detected. The general features of these observations are similar to those reported by Bain et al. [1952], for the same transmission path during magnetic storms in 1940.

The amplitude of GBR received at Slough shows a definite reduction at night and increased variability during the storm period. The corresponding phase during the night of 8/9th is shown as a dashed curve as the pen recorder trace became intermittent. However, it can be seen that a large reduction in phase occurred during this night and that following. The phase on the two subsequent nights exhibits almost normal behaviour, but abnormal effects begin at sunset on 12th. The phase on the night of 12/13th implies a reduction in reflection height of approximately 4.5 km from the quiet-day value. Recordings for the four subsequent nights show anomalous behaviour at either sunrise or sunset, or possibly both on 15/16th for which all the data is not available. During these four nights the nighttime phase gradually returns to its undisturbed state.

The nighttime amplitude at 60 kHz behaves in a similar manner to the 16 kHz phase received at Slough. The amplitude during the nights of the 8/9th and 9/10th is decreased but shows a partial return to the normal value on the nights of 10/11th and 11/12th. A drastic reduction of amplitude is observed on the night of the 12/13th and a gradual return to normal takes place on subsequent nights. As mentioned above, the sampling interval is an hour, and since the fading period of the 60 kHz amplitude is much shorter than this, the fading shown in the Figure is not representative. However, very rapid oscillations occurred in the records between the hours of 2000 and 0300 UT on the night of 8/9th.

Acknowledgements

The authors wish to thank members of the staff at the Natural Philosophy Department of the University of Aberdeen for operating recording equipment at Aberdeen.

The work described was carried out at the Radio and Space Research Station of the Science Research Council and is published with the permission of the Director.

REFERENCES

BEST, J. E., J. A. RATCLIFFE and M. V. WILKES 1936 Experimental Investigation of Very-Long Waves Reflected from the Ionosphere, Proceedings of the Royal Society, A, 156, 614

SMEATHERS, J. R. 1970 The Ground Interference Pattern of 16 kHz Radio Waves during Summer Days, submitted for publication in Proceedings I.E.E.

BAIN, W. C., R. N. BRACEWELL, T. W. STRAKER and C. H. WESTCOTT 1952 The Ionospheric Propagation of Radio Waves of Frequency 16 kc/s over Distances of about 540 km, Proceedings I.E.E., 99, Part IV, 250

"Summary of VLF Activity at Chilbolton, England; South Uist, Outer Hebrides, Scotland; and St. John's STADAN Station, Newfoundland, for the Period March 6 - 10, 1970"

by

S. K. Adjepong, A. Mathur, C. D. Reeve and M. J. Rycroft
Department of Physics, The University
Southampton, England

Introduction

The receivers used at the three stations were of a similar type consisting of a 3m square loop aerial, the normal to which was magnetic N-S, upon which is mounted a preamplifier with an upper cut-off frequency of 30 kHz. The signal from this is amplified by a battery powered, low noise amplifier and then recorded on magnetic tape. Depending on the location of the station the signal is first filtered at certain frequencies to reduce signals from powerful VLF transmitters (e.g. GBR, Rugby, 16 kHz) and mains hum: at all three stations a low pass filter with a cut-off frequency of 18 kHz is also used. The integrated background signal intensities at 2.90 and 5.36 kHz are also recorded on paper chart running at 2.5 cm hr^{-1}; however, these monitors were not in operation at Chilbolton for the period in question. The frequency range of chorus is usually 2 - 4 kHz at these latitudes; hence, when chorus occurs the intensity recorded on the 2.90 kHz channel increases. This is referred to as an event on 2.9 kHz (Figures 1). VLF hiss may show up as an event on either, or both, the 2.90 or 5.36 kHz channels. Fluctuations in the horizontal (N-S) component (H) of the earth's magnetic field were also recorded at South Uist and St. John's but are not referred to in the following summary:

Summary of received VLF phenomena (all times are given in Universal Time)

i) Chilbolton, Winchester, England: L≃2.4

March 6, 1970	0000 - 0445	tape recordings: atmospherics only
	1600 - 1645)	tape recordings: atmospherics, occasional whistlers
	1700 - 1745)	
	1800 - 1845)	
	1856 - 1941)	
	2005 - 2050)	
	2300 - 2359)	
March 7	0000 - 0035	tape recording: atmospherics only
	0100 - 0145	tape recording: risers and whistlers
	0200 - 0245	tape recording: risers and whistlers
	0255 - 0340	tape recording: risers and emissions
	0400 - 0445	tape recording: risers
	1600 - 1645	tape recording: atmospherics only
	1700 - 2205	tape recordings: atmospherics only
March 8	0030 - 0115	tape recording: atmospherics only
	0118 - 0345	tape recordings: a few whistlers
	1600 - 1950	tape recordings: VLF emissions, strong whistlers and knee (plasmapause) whistlers; about 1,100 whistlers received during this period
	2100 -2359	tape recordings: diffuse whistlers
March 9	0000 - 0400	tape recordings: strong, spaced whistlers
	0500 - 0650	tape recordings: risers and chorus
	0650 - 0740	tape recordings: risers, chorus and whistlers
March 10		no recordings

ii) South Uist, Outer Hebrides, Scotland: L≃3.4

March 6, 1970	0415 - 0615:	event on 2.90 kHz
	1345 - 1515:	event on 2.90 kHz
	No records were obtained on 5.36 kHz channel	
March 7	0000 - 0030	tape recording: hiss, weak chorus
	0200 - 0230	tape recording: weak chorus
	0400 - 0545:	event on 2.90 kHz
	0400 - 0430	tape recording: chorus
	0800 - 1300:	event on 2.90 kHz
	1600 - 1630	tape recording: atmospherics only
	1700 - 1730	tape recording: atmospherics only
	1800 - 1830	tape recording: atmospherics only
	1846 - 1935	tape recording: atmospherics only
	1935 - 2024	tape recording: hiss and weak risers
	2027 - 2117	tape recording: chorus and hiss
	2123 - 2213	tape recording: hiss and weak chorus
March 8	0000 - 0030	tape recording: hiss, chorus
	0303 - 0320	tape recording: chorus
	0245 - 1300:	event on 2.90 kHz
	0400 - 0430	tape recording: chorus
	1600 - 1830	tape recording: risers and whistlers
March 9 and 10		no chart or tape recordings

iii) St. John's STADAN station, Newfoundland: L≃3.5

March 6, 1970	0840 - 0955:	event on 2.90 kHz
	1800 - 1845)	tape recordings: atmospherics only
	1900 - 1945)	
	2000 - 2045)	
	2100 - 2145)	
	2200 - 2245)	
	2300 - 2345)	
March 7	0000 - 0045	tape recording: atmospherics
	0215 - 0245:	event on 2.90 kHz
	0200 - 0224	tape recording: chorus
	0230 - 0254	tape recording: chorus
	0325 - 0349	tape recording: chorus
	0400 - 0425	tape recording: chorus
	0830 - 1040:	event on 2.90 kHz
	0900 - 1044:	chart speed increased to 2.5 cm min^{-1}
	0849 - 1120	tape recording: chorus
	1200 - 1224	tape recording: chorus
	1400 - 1424	tape recording: hiss
	1500 - 1705:	event on 2.90 kHz (Figure 1)
	1530 - 1600:	event on 5.36 kHz
	1600 - 1800	tape recordings: emissions and hiss
	1800 - 1848	tape recording: risers between 1845 and 1848

iii) St. John's STADAN station, Newfoundland: L≃3.5 (continued)

	1815:	intensity at 5.36 kHz begins to increase: solar eclipse effect
	1845:	intensity at 2.90 kHz begins to increase: solar eclipse effect
	1900:	intensity at 5.36 kHz reaches a maximum
	1905:	intensity at 2.90 kHz reaches a maximum
	1945:	intensity at 5.36 kHz returns to pre-eclipse value
	2000:	intensity at 2.90 kHz returns to pre-eclipse value
	1848 - 1936	tape recording: risers between 1901 and 1904 (i.e. around eclipse totality at St. John's) (Nature, 226, 1126-1127, 1970)
	1944 - 2032	tape recording: some whistlers around 2020
	2034 - 2122	tape recording: many whistlers, and whistlers with precursors
	2124 - 2212	tape recording: more whistlers and precursors
	2215 - 2303	tape recording: whistlers, risers and hiss
	2230 - 2330:	event on 2.90 kHz
	2305 - 2353	tape recording: hiss and a few whistlers
March 8	0515 - 1145:	event on 2.90 kHz
	1400 - 1600:	event on 2.90 kHz
	1400 - 1449	tape recording: chorus, risers, whistlers and hiss
	1505 - 1544:	event on 5.36 kHz
	1518 - 1532	tape recording: hiss and whistlers
	1600 - 1648	tape recording: hiss, chorus, risers and emissions
	1700 - 1748	tape recording: emissions, hiss and whistlers
	1800 - 1848	tape recording: risers, whistlers and emissions
	1900 - 1948)	tape recordings: atmospherics only
	2000 - 2048)	
	2100 - 2148)	
March 9	0735 - 1045:	event on 2.90 kHz
	1140 - 1230:	event on 2.90 kHz
	No tape recordings made	

March 10

Nothing of note appears on charts. No tape recordings made.

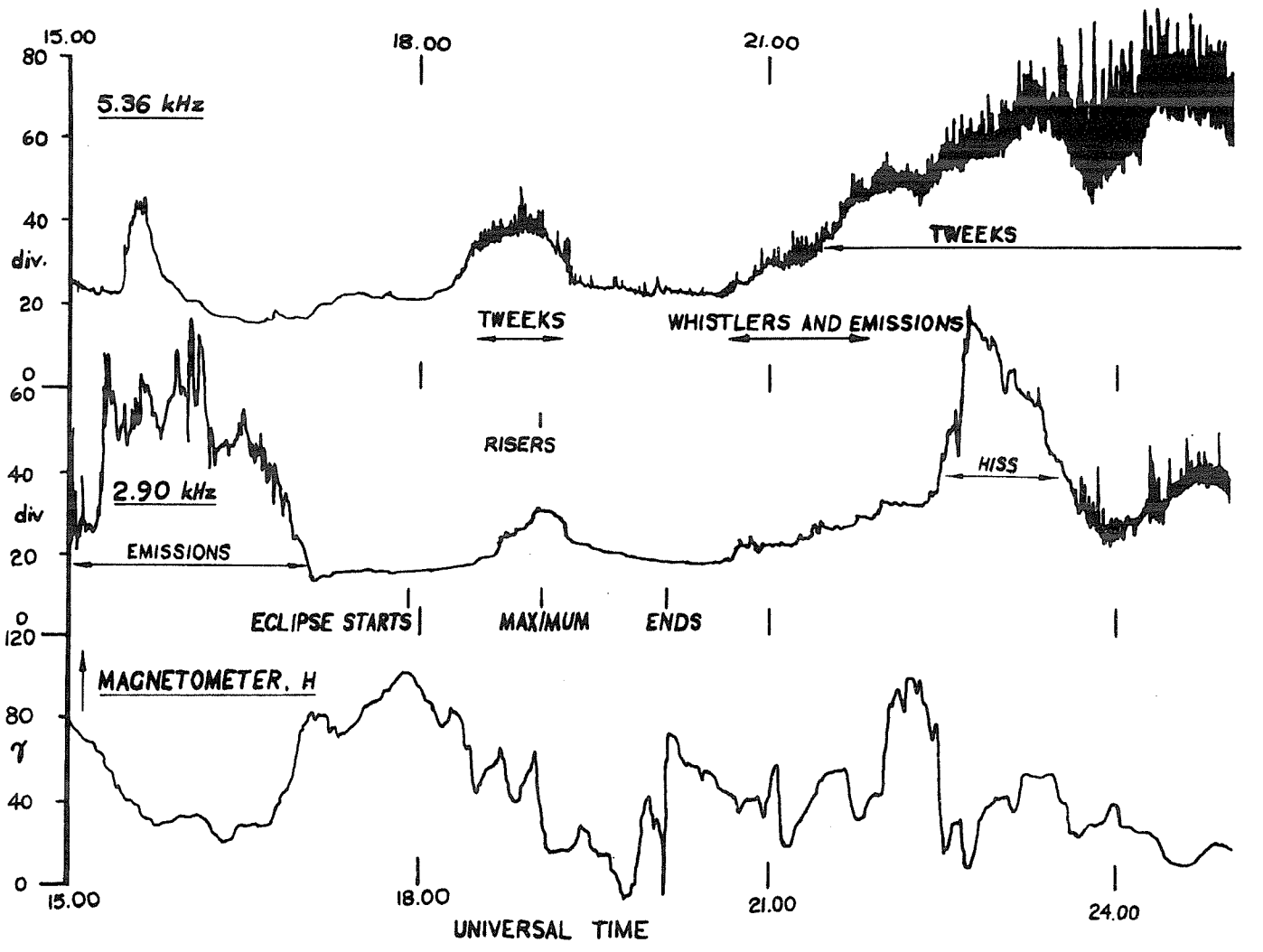

Fig. 1. Variations with time for the eclipse period of:

upper trace) the intensity of the background signal at 5.36 kHz, showing the occurrence of tweeks during the eclipse and during the local night, each vertical trace corresponding to a particularly strong atmospheric,

middle trace) the intensity of the background signal at 2.90 kHz, showing the occurrence of chorus emissions before 1700 UT, of risers between 19h01m31s and 19h03m42s UT, and of hiss between 2230 and 2330 UT, and

lower trace) the north-south horizontal component of the geomagnetic field, 1 γ being 1 nanoTesla.

All quantities are increasing upwards.

"VLF Effects as Observed at the Station Panska Ves on 8-10 March 1970"

by

František Jiříček
Geophysical Institute
Czechoslovak Academy of Sciences
Prague, Czechoslovakia

The station Panska Ves is located in middle geomagnetic latitude (ϕ = 50.5° N, λ = 14.6° E, Φ = 46.9°)*, and under normal conditions it is possible to observe ducted whistlers here, and VLF emissions propagating along paths between L = 1.6 - 3.2 [Jiříček, 1970]. From the preceding, it follows that excepting extraordinary strong disturbances, the paths of all observed VLF phenomena remain within the plasmasphere, and cases can occur where even a geomagnetic storm of medium intensity will not show any influence upon VLF observations. The geomagnetic storm of 8 March 1970, however, showed a marked influence upon VLF phenomena. This can be seen even from the plot of whistler occurrence on 8 - 10 March 1970 (lower part of Figure 1). Ordinates represent the number of whistlers as observed during two-minute intervals between 50 - 52 minutes before each full hour, "x" denotes intervals with VLF emissions.

In the first place, the occurrence of VLF emissions at Panska Ves is an indication of disturbed conditions. In all cases marked on the plot, discrete emissions (chorus) were observed with maximum intensity on 9 March at 0450-0452 UT where also continuous emission (hiss) occurred (see Figure 2). Besides that, whistler-excited emissions were observed in the two following hours (see Figure 3).

Even when taking the dependence of whistler occurrence upon the existence of their sources into account, the high number of observed whistlers (all being one-hop) indicates favorable conditions for the formation of whistler ducts. This is also demonstrated by whistler spectrograms from which dispersion values at 4 kHz were measured as given in the upper part of Figure 1. The whistler rate shows a deep decrease during the evening hours up to zero at 2050 UT. During this time, whistler traces with higher dispersion disappeared and the general arrangement of whistler ducts changed. The increase of ionospheric absorption in higher latitudes is also likely to have contributed to the disappearance of higher-dispersion whistler traces that correspond to paths with a higher value of L than should correspond to the observing station (L = 2.1).

Even though we succeeded to identify initial atmospherics for a number of whistlers, the properties of whistler traces in the night from 8 to 9 March made the determination of the values of L for the paths of individual whistler components impossible. Nevertheless, the shape of low-dispersion whistler traces indicate lower electron density values along the propagation path with L > 2 up to the early morning hours of March 9. One-hop whistlers with initial atmospherics and a marked narrow trace, D(4) = 38.4 $s^{\frac{1}{2}}$, suitable for a more accurate analysis, were not observed until 9 March 2150 UT. In this case, however, it is a whistler component propagating along a low path, L = 1.75. The dispersion value as given for this path yields the electron density value at its top in the equatorial plane of about 2 x $10^9 m^{-3}$ which corresponds to normal values.

REFERENCES

HAKURA, Y. 1965 Tables and maps of geomagnetic coordinates corrected by the higher order spherical harmonic terms. J.Radio Res. Labs. Japan, 12, 121.

JIŘÍČEK, F. 1970 On the determination of propagation paths of mid-latitude whistlers for purposes of estimating the magnetospheric electron density. Studia geoph. et geod., 14, 402.

* Geomagnetic coordinates corrected by the higher order spherical harmonic terms [Hakura, 1965].

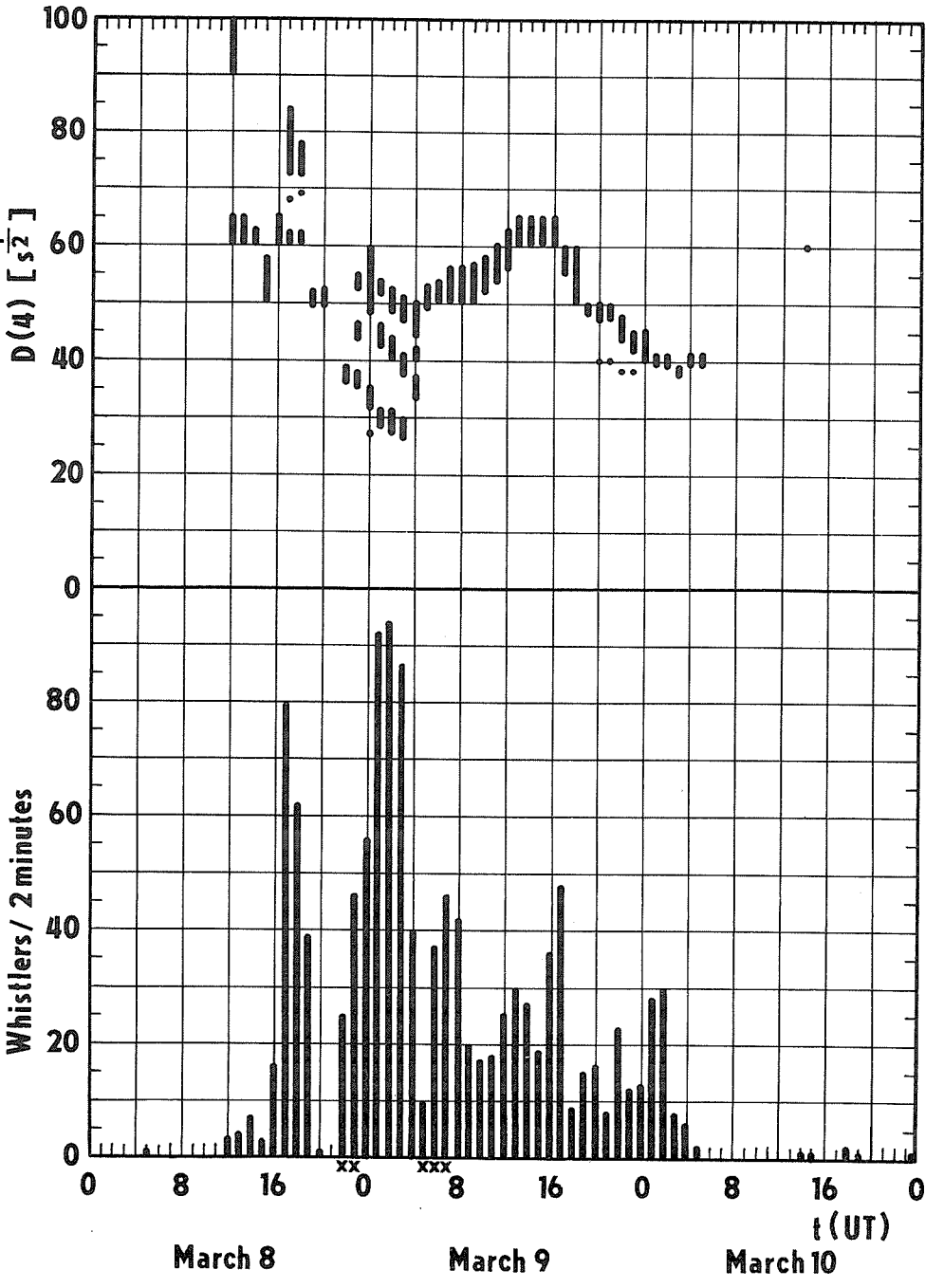

Fig. 1. Lower part-whistler rate as observed at Panska Ves during two-minute intervals between 50 - 52 minutes before each full hour, "x" denotes intervals with VLF emissions. Upper part - dispersion values of observed whistlers measured at 4 kHz.

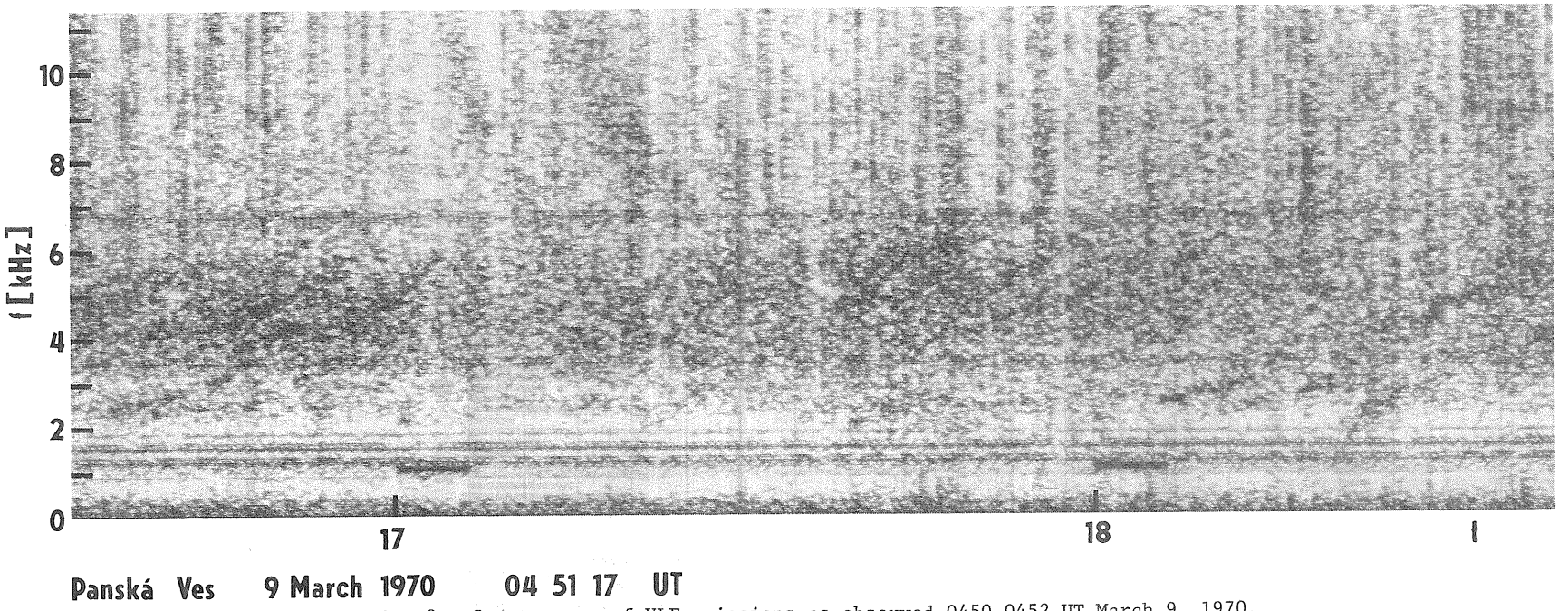

Fig. 2. Spectrogram of VLF emissions as observed 0450-0452 UT March 9, 1970.

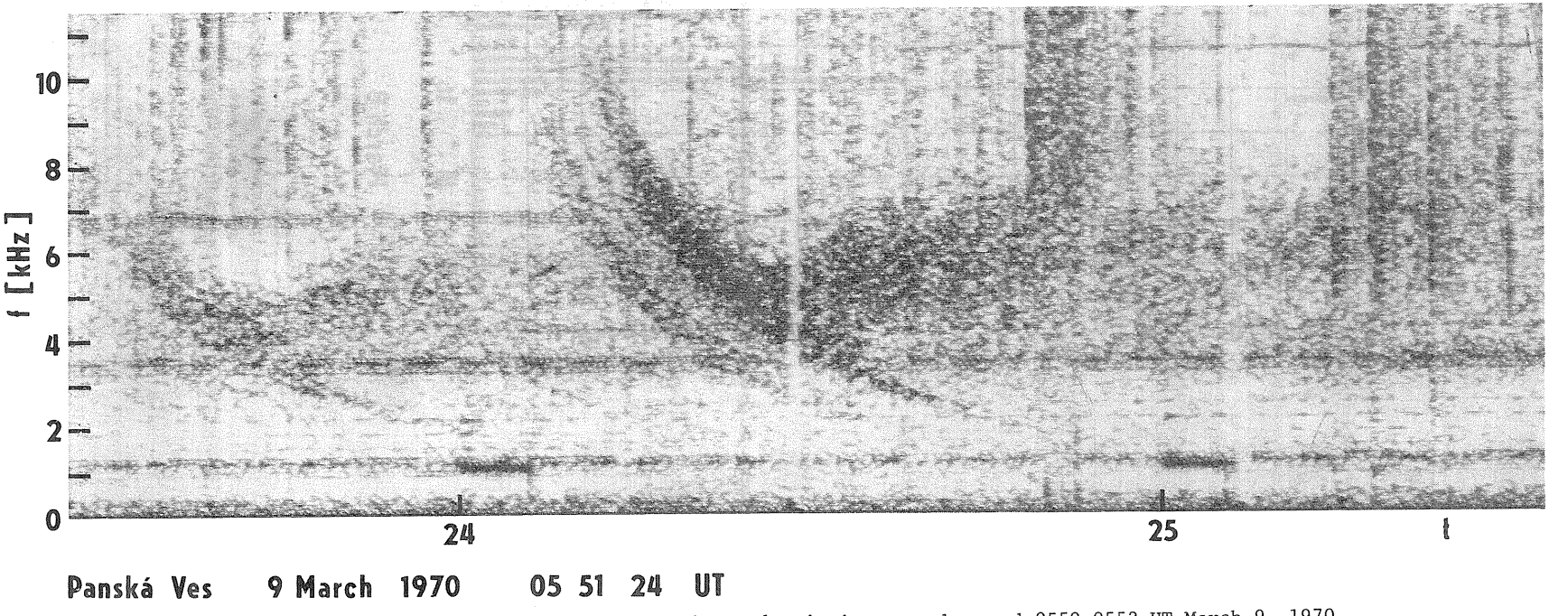

Fig. 3. Spectrogram of whistler-triggered emissions as observed 0550-0552 UT March 9, 1970.

"VLF Radiowave Observations of Ionospheric Disturbances during the Period 4 - 18th March 1970"

by

T. B. Jones
Physics Department
University of Leicester, England

Introduction

Many authors [See references] have reported the effects of solar and magnetic activity on the propagation of very low frequency (VLF) radiowaves. Usually these observations have been confined to long propagation paths, although Belrose [1963] has commented on the sensitivity of VLF propagation at steep incidence to geomagnetic and solar disturbances. The purpose of this paper is to present simultaneous observations of effects of the solar and geomagnetic disturbances of March 1970 on VLF waves propagated over paths ranging from 28 to 7200 km.

Experimental Observations

During the last few years the phase and amplitude of the signals received from the following transmitters have been monitored continuously at Leicester.

Transmitter	Frequency (kHz)	Path Length (km)
GBR	16.0	28
GBZ	19.6	130
Aldra	12.6	1800
NAA	17.8	4900
Trinidad	12.0	7200

Two distinct types of disturbance associated with solar flare activity can be identified from these observations. The first is a sudden disturbance in phase and sometimes in amplitude, due to the enhanced D-region ionization which results from the increased flux of ionizing solar x-radiations produced by some flares. Sudden short lived anomalies (SPA and SES) of this kind were associated with the flares during the first few days of March 1970 and these events are described elsewhere in this report [Jones and Evans, 110]. The second type of event consists of a disruption of the regular day-to-night phase and amplitude changes, and marked fluctuations can occur in both parameters, especially at night. A close correlation exists between these VLF anomalies and the influx of solar cosmic ray particles which can produce large scale changes in the high latitude ionosphere. Disturbances of the geomagnetic field, often associated with these events, also give rise to similar propagation anomalies. This second type of phase and amplitude disturbance is characterized by its relatively long life-time and several days can elapse before the diurnal variations revert to their original configuration.

Marked disruption of the regular day-to-night phase variation occurred during 4 - 18th March, 1970, and smaller, less well defined anomalies were present in the signal amplitude. Changes in the phase fluctuation rates were also observed at night during this period. Hourly values of the phase of the various VLF signals are presented in Figure 1 (a) together with other relevant geophysical data (Figure 1 (b)). The night-time phase recordings for 4 to 14th March are reproduced in Figure 2 in order to illustrate the changes in the phase fluctuation rate.

Discussion

The geophysical disturbances of March 1970 produced marked anomalies in the phase of all the VLF transmissions monitored and the interrelation between the various events is illustrated schematically in Figure 3. In view of the marked differences in the anomalies observed on the long, medium and short propagation paths these are described separately below.

Short Paths

The phases of the GBR and GBZ signals show similar behaviour during the disturbance and the following comments apply equally to the observations on both frequencies. No disturbances were detected before the night of 5th March, indicating that the high level of Kp and the small but significant increase above background level of the 5 - 21 Mev solar proton flux have little effect. Following the sudden commencement geomagnetic storm at 0805 UT on the 5th, the phase does not recover to its normal night-time value and large fluctuations are present during the night. The night-time disturbance is associated with the initial response of the neutron monitor (Figure 1) and also the rise in Ap. The phase is abnormal during the next day and for most of the following

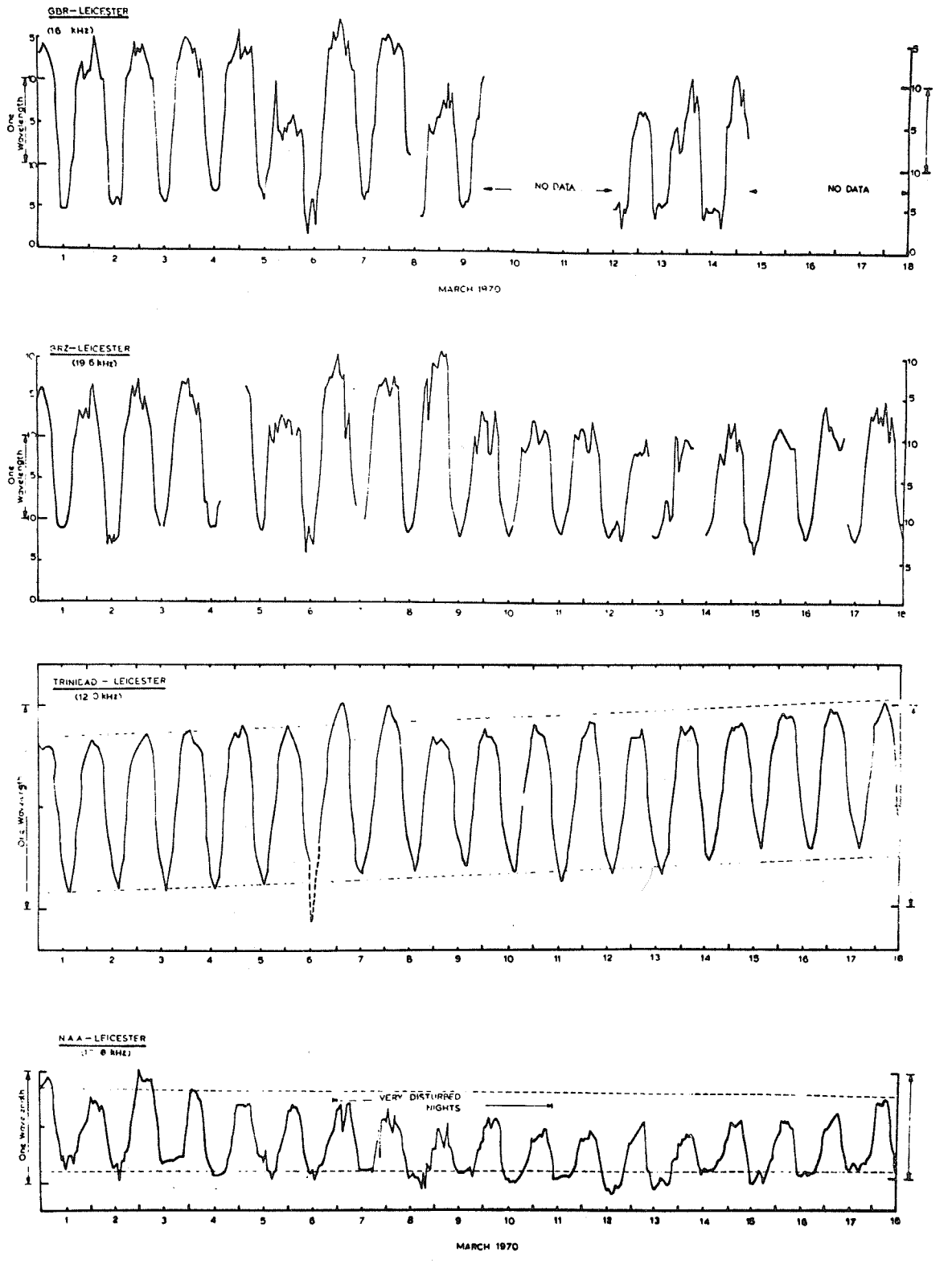

Fig. 1a. Diurnal variation in phase of various VLF transmissions monitored at Leicester. (Oscillator drift indicated by broken lines).

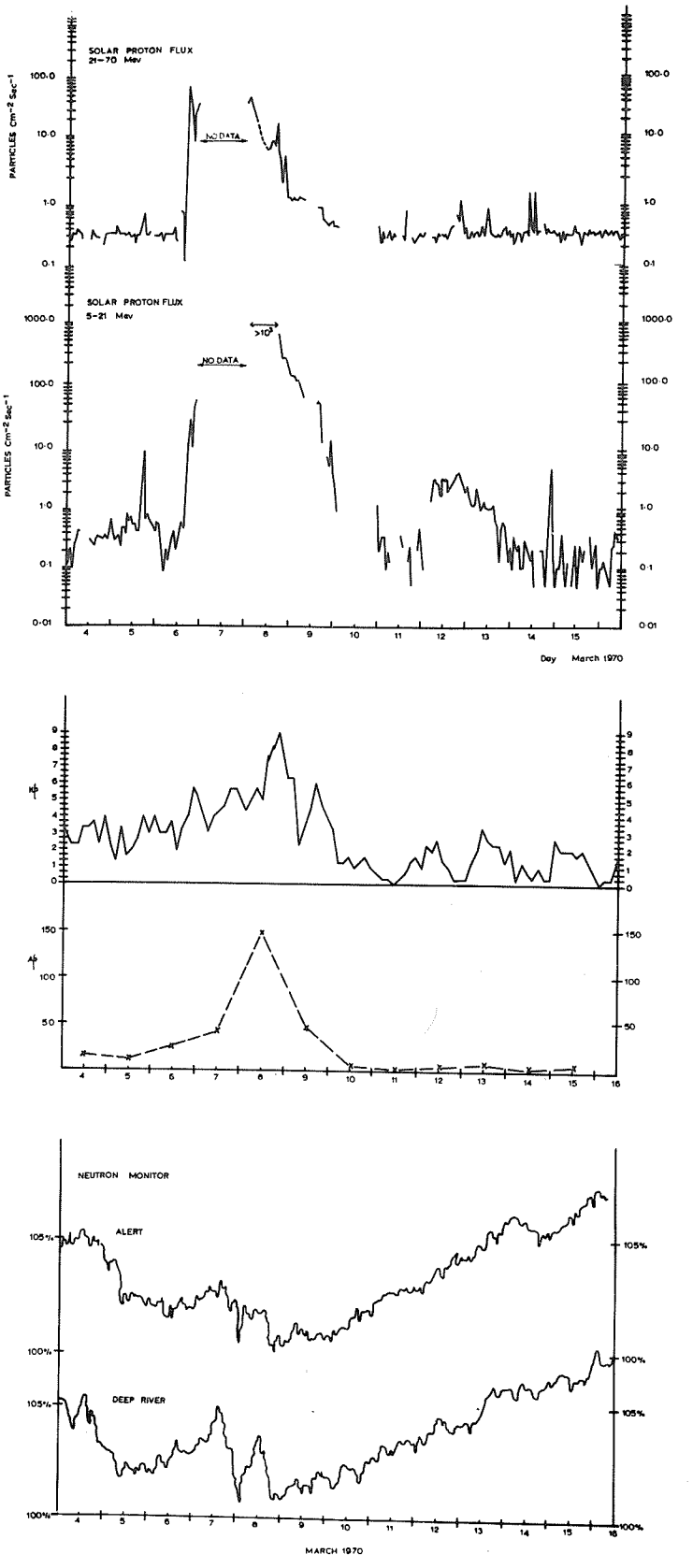

Fig. 1b. Relevant geophysical data for March, 1970 (reproduced from Solar-Geophysical Data - ESSA Bulletin).

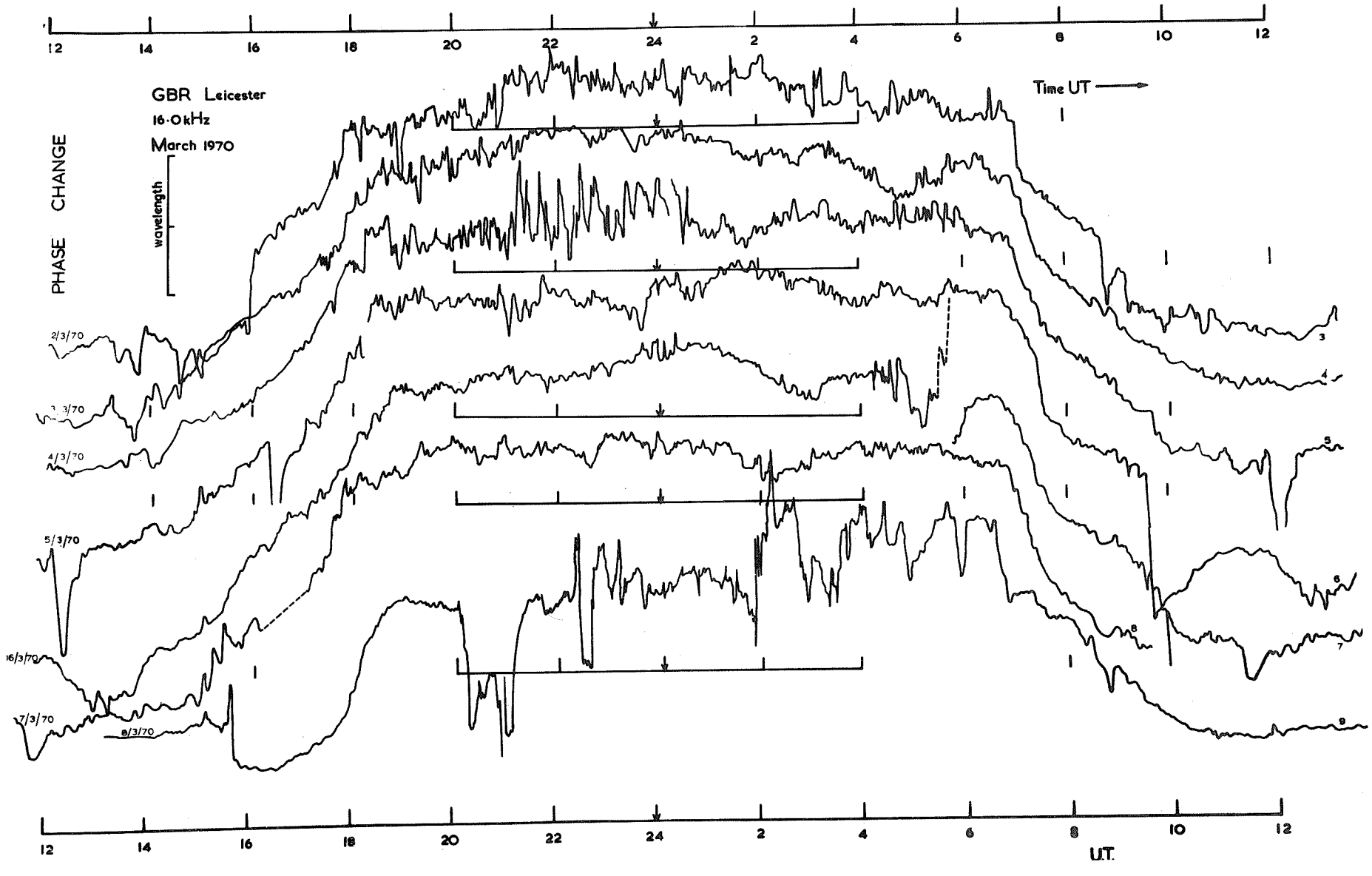

Fig. 2a, Night time fluctuation in VLF phase recorded for 16.0 kHz GBR - Leicester.

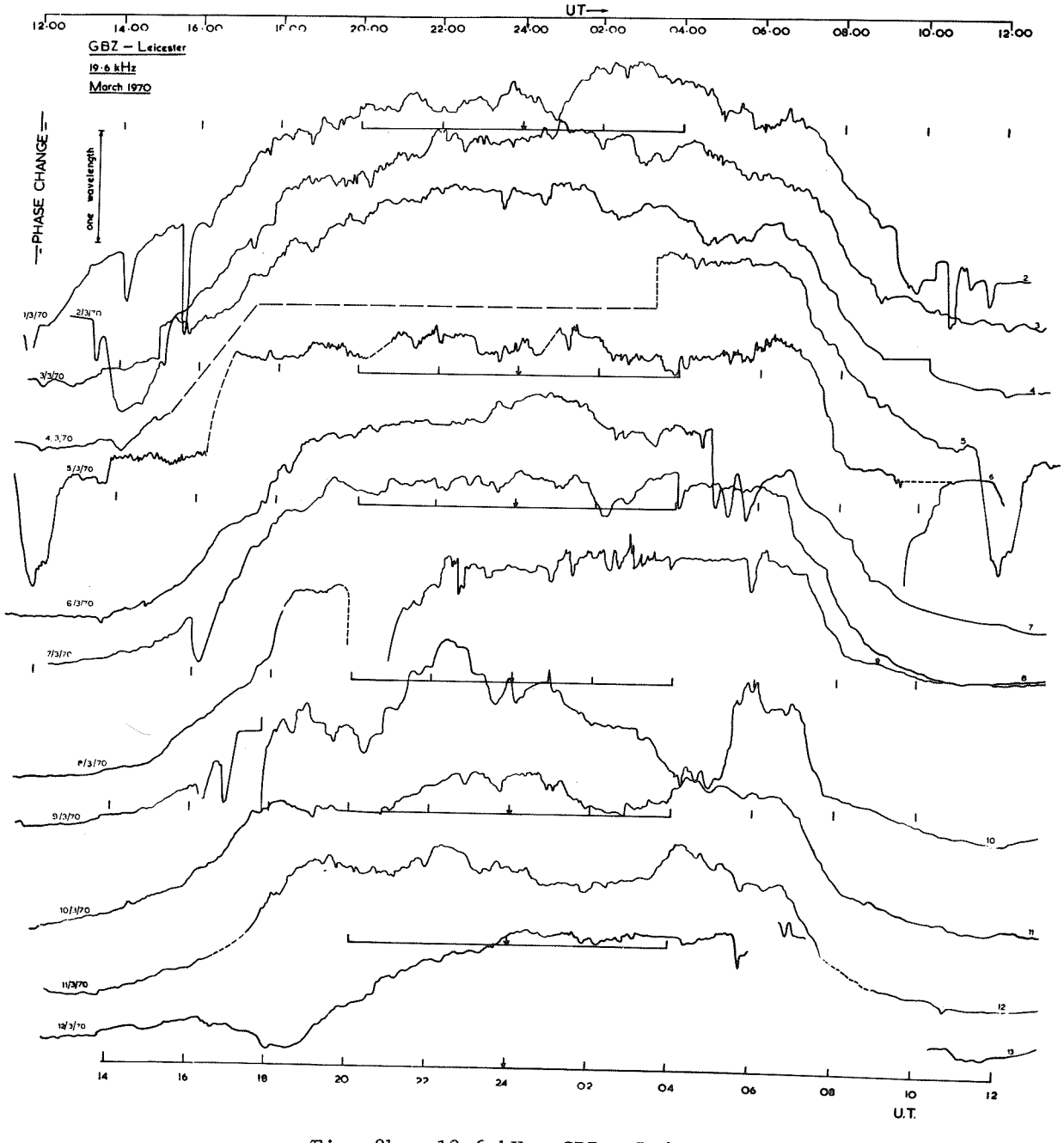

Fig. 2b. 19,6 kHz GBZ - Leicester

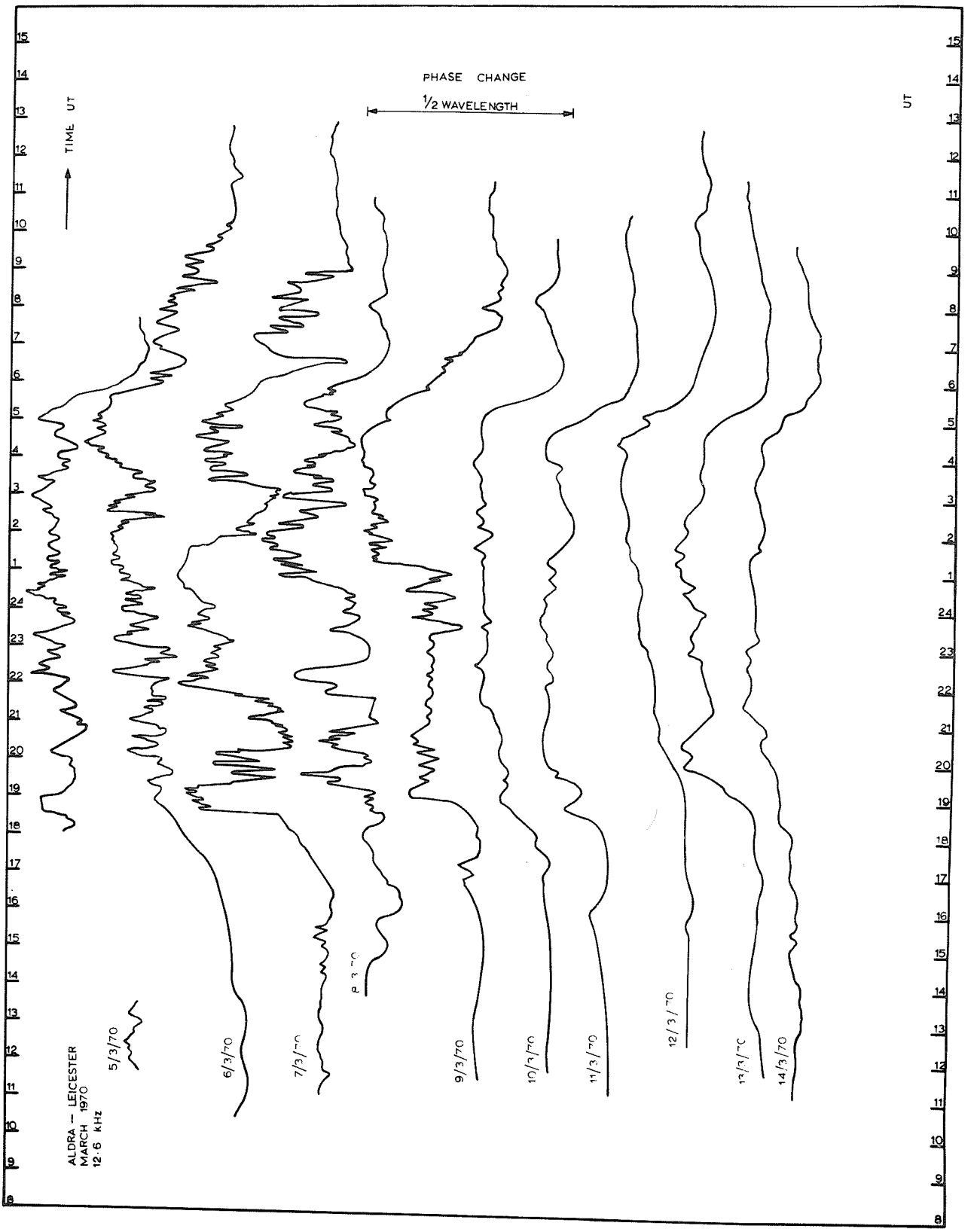

Fig. 2c. 12.6 kHz Aldra - Leicester

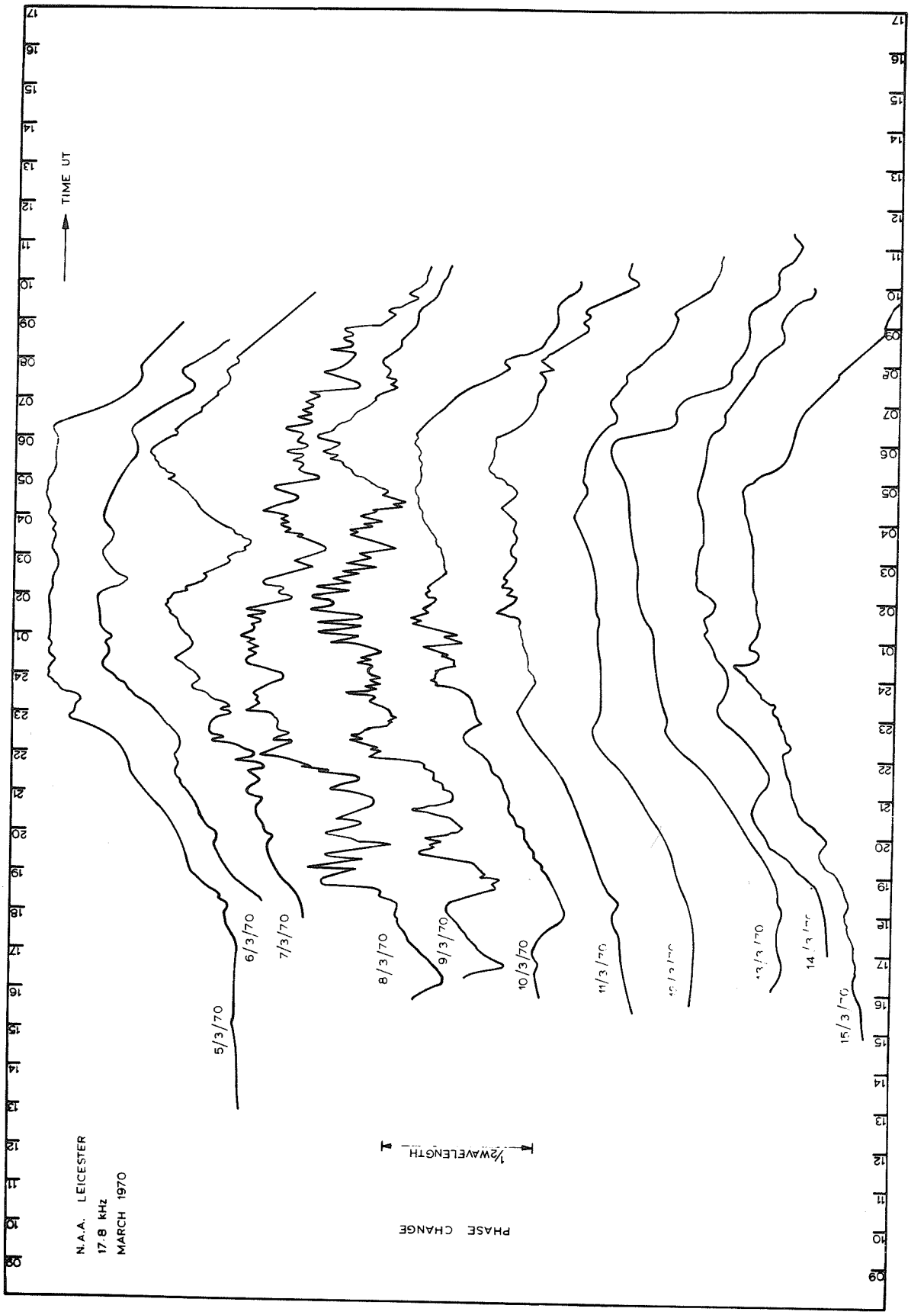

Fig. 2d. 17.8 kHz NAA - Leicester

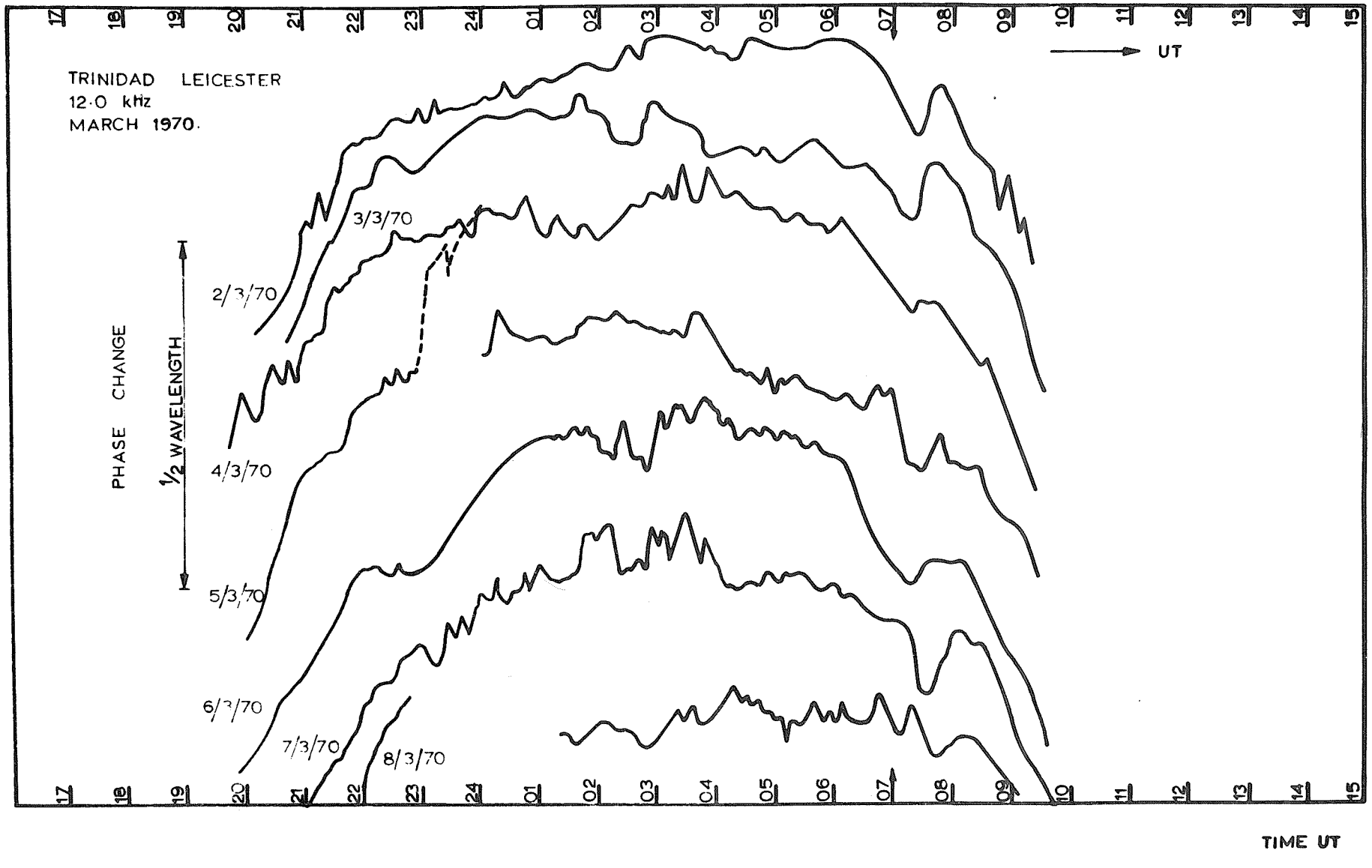

Fig. 2e. 12.0 kHz Trinidad - Leicester

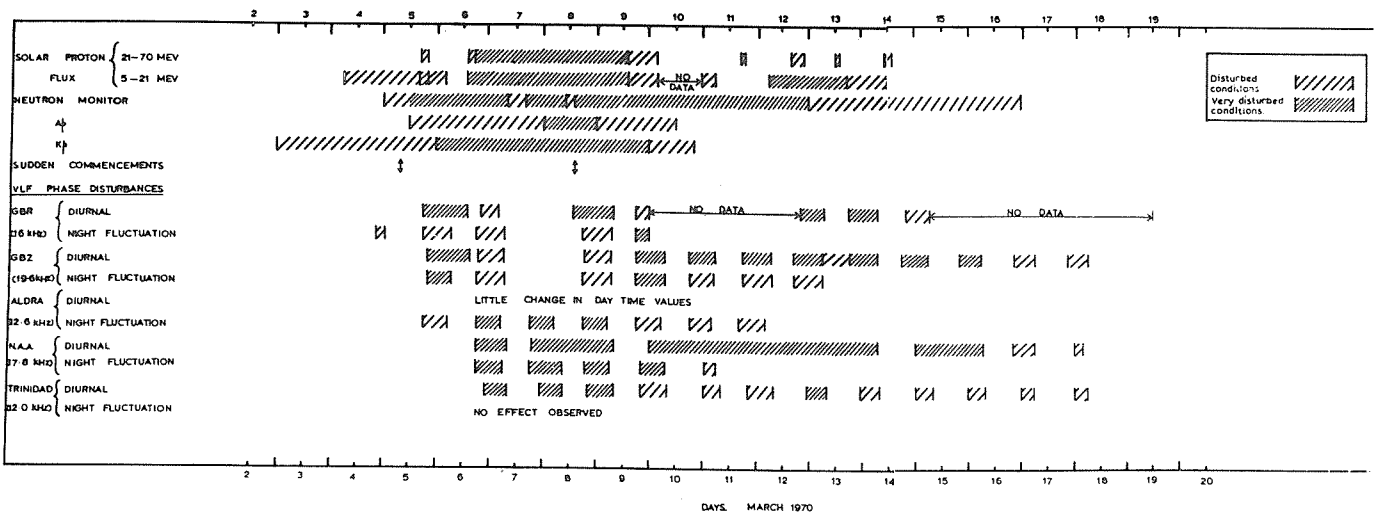

Fig. 3. Schematic presentation of the various related observations during 2 - 20 March, 1970.

night. On the 7th the phase returns to its normal day-time position and no further day-time displacement is observed. The phase is restored to its normal level during the night of the 7th and this "recovery period" is a well known feature of magnetic storm effects on steep incidence VLF propagation [Belrose, 1963; Belrose and Thomas 1968]. The phase disturbance resumes on the night of 8th, probably as a result of the sudden commencement at 1415 UT on this day, although it is possible that the so-called "storm after-effect" following the first sudden commencement contributes to the event. The night time phase levels then gradually recover until the night of 12th, when a small but significant disturbance occurs. This disturbance is less intense than those of the 5th and 9th and is not preceded by a sudden commencement. The magnitude of the night-time phase anomaly gradually becomes smaller and the normal pattern has reappeared by night of 18th.

The very large increases in the solar proton flux at 1700 UT on 6th do not apparently produce marked changes in the phase of the GBR and GBZ signals, although any effects could be masked by disturbances resulting from the first sudden commencement. The small decrease in phase on the night of 12th March could however be due to the increased proton flux recorded from 11th to 12th March.

Medium range paths

The 1800 km path Aldra, Norway, to Leicester, is of particular interest since the transmitter is situated at an auroral latitude. For undisturbed conditions the diurnal phase change is relatively small, amounting to only about 1/4 wavelength. During the disturbances of early March, the night-time phase pattern is severely disrupted but little change occurs during day-time. Although no recordings were available prior to 5th March, it is evident from Figure 2 that some departure from the normal variation occurs during the night of 5th. The magnitude of the phase irregularities increases on subsequent nights becoming a maximum on the night of the 8th. There follows a fairly rapid recovery, normal conditions having returned by the night of March 12th. The maximum phase deviations of the VLF signals for this propagation path appear to occur at the time of the maximum enhancement of the solar proton flux. The geomagnetic sudden commencement of 5th March seems to produce only minor disturbances in the night time phase pattern.

Long paths

The two long propagation paths are of interest since they traverse quite different geomagnetic latitudes. The NAA-Leicester path lies between geomagnetic latitudes (Λ) 55° and 60°, while Λ is less than 40° for about half of the Trinidad-Leicester circuit. Phase disturbances were observed on both transmissions during the event of March 1970, although for the Trinidad transmission they were confined to night-time only. It should be noted that during the solar proton event of October-November, 1968, no phase disturbances were recorded on the Trinidad-Leicester transmission [Jones, 1970].

Phase disturbances were first observed on both NAA and Trinidad transmissions during the night of 6th March, i.e. 24 hours later than on the steep incidence circuits. It appears that the sudden commencement on the 5th does not produce an immediate effect on the long path transmissions and the

phase changes on the night of the 6th probably result from the marked increase in the solar proton flux observed on the preceding day. The intermediate and long propagation paths all show disturbed conditions during the night of 7th March in contrast to the normal undisturbed phase levels recorded on the steep incidence transmissions. On the 6th and 7th March, the day-to-night phase changes of the Trinidad signals are larger than normal resulting in greater retardation of the night-time phase. This is an unusual observation since geophysical events of this kind normally yield depressed phase levels at night, such as those recorded on the Trinidad path for all nights after the 8th, and on the NAA signals throughout the disturbance.

The night time phase levels on both frequencies gradually recover during the nights of 8th - 11th March; however, a small but noticeable phase displacement is observed on the Trinidad transmission during the night of the 12th, which is not evident in the NAA recordings. A similar effect was noted in the steep incidence phase data and is probably associated with the increase in proton flux on the 11th March. For the NAA transmission the day time phase levels have returned to normal by March 16th and the night-time values by the 19th. The night-time phase of the Trinidad transmission is fully recovered by the night of 18th March.

Night-time phase fluctuation rates

An interesting feature of the VLF disturbances was the marked changes in the rate of fluctuation of the phase during night-time, this being particularly noticeable on the long propagation paths. Rapid phase changes occurred on both GBR and GBZ transmissions during the night of 5th March, although there is some indication of phase fluctuation on the GBR records for the previous night. Further disturbances occur on both short paths on the nights of 8th, 9th, 11th and 12th, but these are less rapid than those of the 5th March.

The changes in night-time phase oscillation rates are most easily seen on the 12.6 kHz (Aldra) and 17.8 kHz (NAA) recordings (Figures 2). No marked variations were observed on the 12 kHz (Trinidad) signals. Small fluctuations in the phase of the Aldra and NAA signals were first observed during the night of the 5th March. The amplitude of the irregularities increased on the night of the 6th March and a large "bay-like" feature is present on both phase recordings from about 0200 - 0500 UT. This feature persists during the following night on both frequencies and can still be detected on the NAA records until the night of the 10th March. The night of the 7th is also noteworthy due to the very marked increase in the rate of the phase fluctuation. This continues on both frequencies until the night of the 10th March when slow changes in phase are again observed. Long-period disturbances of small amplitude in the nocturnal phase pattern occur again on the 12th and 13th March and to a lesser extent on the 14th.

The fast fluctuation rates are observed during the large influx of solar cosmic ray particles and are undoubtedly associated with the particle precipitation events. It is unlikely that these particles will penetrate to the lowest ionospheric levels at the geomagnetic latitudes of the Trinidad-Leicester circuit, which would account for the absence of the fast-phase fluctuations in phase recordings of this transmitter.

Conclusion

The geophysical disturbances of March 1970 produced anomalies in the phase of VLF transmissions monitored over a wide range of propagation paths. In general the normal day-to-night phase variation was disrupted and also changes occurred in the phase fluctuation rates at night. The phase disturbances have been qualitatively related to the various geophysical observations available during the disturbed period. The response of the short and long propagation circuits to the disturbances differs greatly, especially during the initial period. A more detailed interpretation of the propagation anomalies in terms of ionospheric changes will be presented in a later paper.

Acknowledgment

The contribution of Mr. G. Woods to the experimental program is gratefully acknowledged.

REFERENCES

BRACEWELL, R. N., K. G. BUDDEN, J. A. RATCLIFFE, T. W. STRAKER and K. WEEKS	1951	The Ionospheric Propagation of Low - and Very-Low - Frequency Radio Waves over Distances Less than 1000 Km., Proc. Instn. Elec. Engrs., 98 III, p. 221.
BELROSE, J. S	1964	The Oblique Reflection of cw Low Frequency Radio Waves from the Ionosphere, AGARDograph 74, Propagation of Radio Waves at Frequencies below 300 kcs, p. 149, (Pergamon Press)
BURGESS, B. and T. B. JONES	1967	Solar Flare Effects and VLF Radio Wave Observations of the Lower Ionosphere, Radio Science, 2, 619.
BELROSE, J. S. and L. Thomas	1968	Ionization Changes in the Middle Latitude D-Region Associated with Geomagnetic Storms, J. Atmosph. Terr. Phys., 30, 1397.
LANGE-HESSE, G. and K. RINNERT	In press	Proc. AGARD Conf. on Frequency and Phase Instabilities in Radio Wave Propagation, ANKARA 1968.
EGELAND, A	1969	Discussions of VLF Records Obtained during Polar Cap Absorption and Auroral Disturbances, Ionospheric Radio Communications, (Ed. K. Folkstad) p. 117.
LARSEN, T. R.	1970	VLF Phase and Amplitude Measurements During the P.C.A. Event October 31 - November 6, 1968, World Data Center A, Upper Atmosphere Geophysics Report UAG-8, 279.
JONES, T. B.	1970	Long Path VLF Observations of the Ionospheric Disturbances Resulting from the Solar Proton Event of October - November 1968, World Data Center A, Upper Atmosphere Geophysics Report UAG-8, 282.

"VLF Phase and Amplitude Measurements during the PCA Event 6-10 March, 1970"

by

Trygve Røed Larsen*
The Auroral Observatory
P.O. Box 387, 9001 Tromsø, Norway

VLF phase and amplitude data from both short and long propagation paths were recorded in Tromsø during the polar cap absorption (PCA) event, which started on 6 March 1970. A brief and qualitative description of our data is given below.

The first indications of PCA phase disturbance were observed at 1400 UT on 6 March on the trans-polar path Hawaii to Tromsø (10.2 kHz). At 1700 UT the phase had advanced about 45 μs from normal value. Maximum phase advance of about 65 μs was observed between 7-8 March. The path Trinidad-Tromsø (10.2 kHz) showed maximum phase disturbance of about 25 μs on 8 March. The amplitude, however, was most reduced at path night conditions during 9-10 March. The recovery to normal conditions was slow, but by 14 March both paths showed approximately normal phase and amplitude.

The phase and amplitude of the abnormal sky wave component for the path Omega Norway to Tromsø (12.3 kHz) were also monitored. This path which is 432 km long is situated between L = 5.1 to 6.3 (McIlwain's L-parameter) and is very sensitive to disturbances connected with the auroral oval. Phase disturbances were seen from about 0800 on 6 March, but these were probably due to auroral events and not PCA effects. Diurnal phase changes of only 10 μs were observed during the PCA event while normal day/night phase change is about 60 μs.

On 0017 UT 8 March an instrumented rocket was flown from Andøya Rocket Range (L = 6.2). This rocket carried among other experiments a VLF Doppler shift experiment. From this experiment (by Dr. A. Egeland, Norwegian Institute of Cosmic Physics) the electron density height profile will be calculated and applied in a full wave analysis of the short VLF path. The rocket range is only about 150 km away from this path mid point.

Awaiting these rocket data, we here present only the amplitude recording from the short path VLF experiment, see Figure 1a. Figure 1b shows the riometer recordings (30 MHz) at Tromsø; the quiet level is indicated as a broken line. Maximum absorption during 8 March was about 3 dB. Figures 1c - 1f show phase and amplitude data for the long VLF paths. For explanation cf. figure caption.

The raw data presented in Figure 1 will be fully analyzed in a separate publication in the near future.

This PCA was accompanied by a strong magnetic storm with an sc at 1420 UT on 8 March 1970. Maximum H-field deviation at Tromsø was - 2000γ at 1917 UT on the same day.

Acknowledgement

The VLF work in Tromsø is carried out in cooperation with the Norwegian Institute of Cosmic Physics. Mr. L. A. Fletcher at the Omega Systems Project Office, Washington, D. C., is thanked for having supplied part of the VLF equipment.

---

* Seconded from Norwegian Defence Research Establishment.

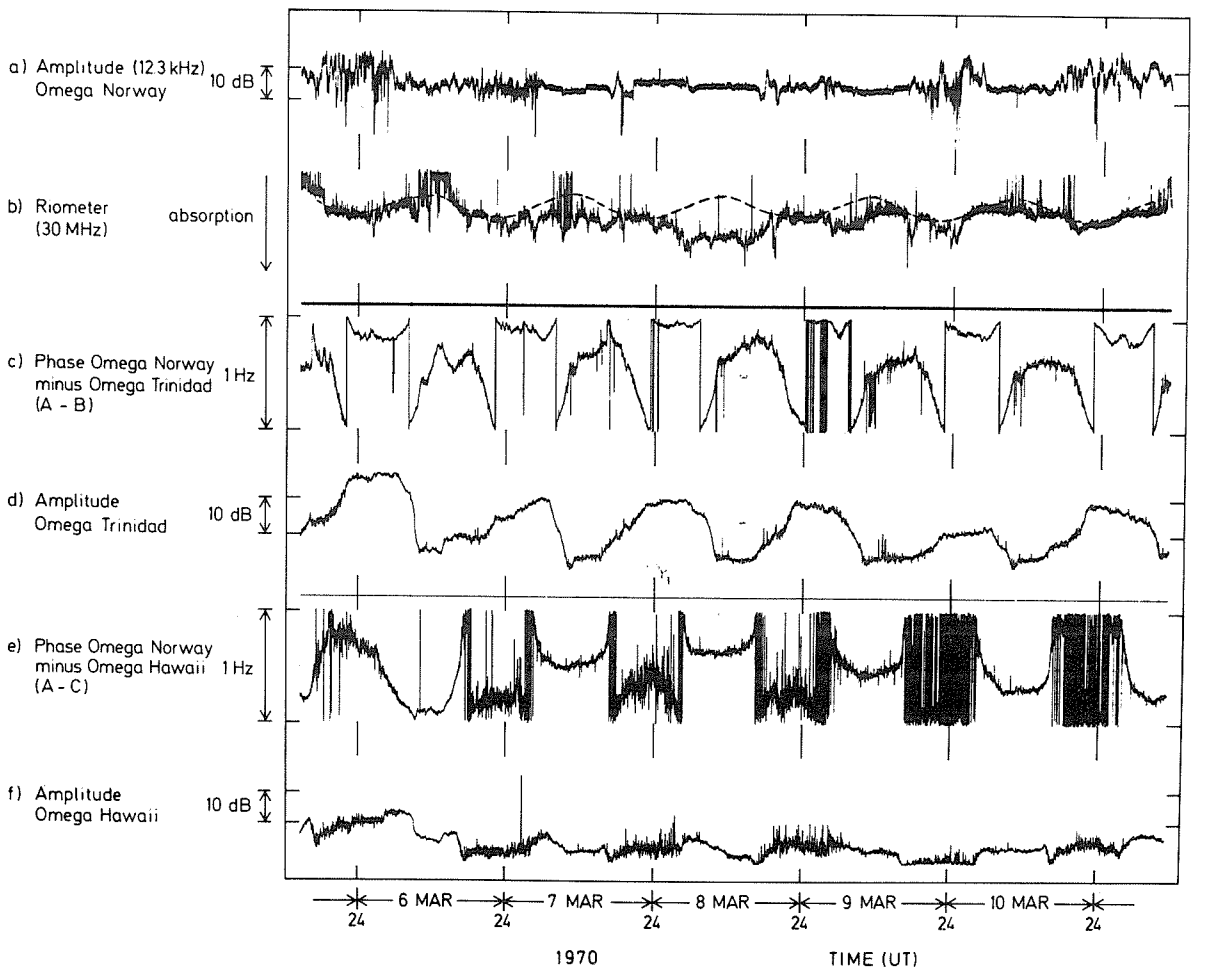

Fig. 1. Collection of raw data for the PCA event 6-10 March, 1970.

Curve a) Amplitude at 12.3 kHz of abnormal sky wave component for the path Omega Norway to Tromsø.

b) Riometer (30 MHz) at Tromsø. The record shows diode current (in mA) as a full line, while normal, undisturbed variation is indicated by a broken line.

c) Phase difference between Omega Norway and Omega Trinidad. For this context the phase of Omega Norway may be regarded as constant during the event and the record shows essentially the phase-variations of the path Trinidad to Tromsø. Phase advance of Omega Trinidad is upwards in the figure.

d) Amplitude of Omega Trinidad, received at Tromsø (path length 8600 km).

e) Phase difference between Omega Norway and Omega Hawaii. The remarks given under c) apply here, and the records show essentially the phase variations of the path Hawaii to Tromsø. Phase advance of Omega Hawaii is upwards in the figure.

f) Amplitude of Omega Hawaii received at Tromsø (path length 9800 km).

"VLF Observations at College, Alaska During the Great Magnetic Substorm of March 8, 1970"

by

R. N. Srivastava and D. W. Swift
Geophysical Institute
University of Alaska
College, Alaska, 99701

ABSTRACT

Very intense VLF emissions were recorded at College, Alaska during a great magnetic substorm that started at 0417 150° WMT (1417 UT) on March 8, 1970 with a negative bay reaching 4900 γ at 0445 150° WMT. The emissions were confined to the region from 400 to 1500 Hz and it is inferred that the ELF hiss had been the predominant feature. It was particularly noteworthy that the VLF signals were observed during a period when there was absorption in excess of 25 dB as obtained from the College 30 MHz riometer data. Accompanying the VLF emissions were relatively high levels of H-β emission as indicated by photometers. It is concluded that the propagation conditions in the upper ionosphere and magnetosphere were affected by the substorm in a manner to have allowed the signals to reach the ground rather than being reflected outward.

The purpose of this communication is to describe in detail the VLF emissions during the most intense magnetic substorm since the IGY. It was observed to start at 0417 150° WMT (1417 UT) at the College observatory (64.7°N) on March 8, 1970 with a negative bay reaching 4900 γ at 0445 150° WMT. The event was also recorded at a number of other polar and non-polar stations at about the same time but with differing intensities. The substorm was unusual in the sense that some of the most intense VLF emissions we have observed to date were recorded during the substorm. It was particularly noteworthy that the VLF signals were observed during a time when there was heavy ionospheric absorption present and also during a part of the day when these emissions are seldom observed.

The VLF emissions were received on a triangular loop (IGY-type) antenna oriented with the normal to the plane of the antenna pointing geomagnetically East-West. Thus, the system has greater sensitivity to signals propagating in the magnetic meridian plane than to signals propagating in an East-West direction. The receiver is essentially a wideband amplifier. The output of the amplifier is passed through filters centered at 400, 800, 1500, 3500 and 8000 Hz. The filter outputs and the broadband signal are then passed through detectors and the DC outputs of the detectors are recorded on a 6 channel chart recorder at 1mm/minute. The relative outputs of the various detectors provide an indication of the spectral content of the incoming VLF signal.

Figure 1 shows the VLF signal amplitudes as detected on the 400, 800 and 1500 Hz channels. The ambient field strengths plotted against time are reduced to the same scale for comparison purposes. Note that most of the energy is concentrated near or below 400 Hz, and the spectral content is typical of the emission that is referred to as ELF hiss. Also, it is likely that VLF chorus was present in the received data. We also recorded the signal amplitudes on the 3500 and 8000 Hz channels, but the signal level was considerably below the level measured on the other three channels.

Several other effects were observed simultaneously during this substorm. In particular, very intense radio wave absorption in the ionosphere and intense H-β emission from the aurora were observed at College. Figures 2, 3 and 4 show the ionospheric absorption as measured on the 30 MHz riometer, the H-component of the magnetic disturbance vector and the H-β photometer record, respectively, all recorded at College. These figures are shown so that the VLF data may be viewed in the context of the total substorm event. The riometer and the photometer data indicate the precipitation intensities of electrons and protons, respectively. It can be seen that the disturbance events shown in Figures 2-4 begin almost simultaneously at 0417 150° WMT. Unfortunately, due to the remote location of the VLF receiver and chronic problems with power outages, we were not able to maintain a realiable time base for the VLF data. In fact, the original records indicated that the VLF event started at 0407 150° WMT. The onset of the VLF event was well defined and the onset of the disturbances shown in Figures 2-4 are also well defined and nearly coincident. This suggests that the most likely time base for the VLF data is that shown in Figure 1. In other words, we have advanced the time base for the VLF data by 10 minutes over that indicated in the original chart record in order to make the VLF event coincident with the other substorm events.

It is useful to compare the riometer data and the VLF data since the ionospheric absorption of VLF signals can be related to absorption of 30 MHz radio waves. Assuming a model for the ionospheric electron density, it is possible to calculate the absorption at 30 MHz

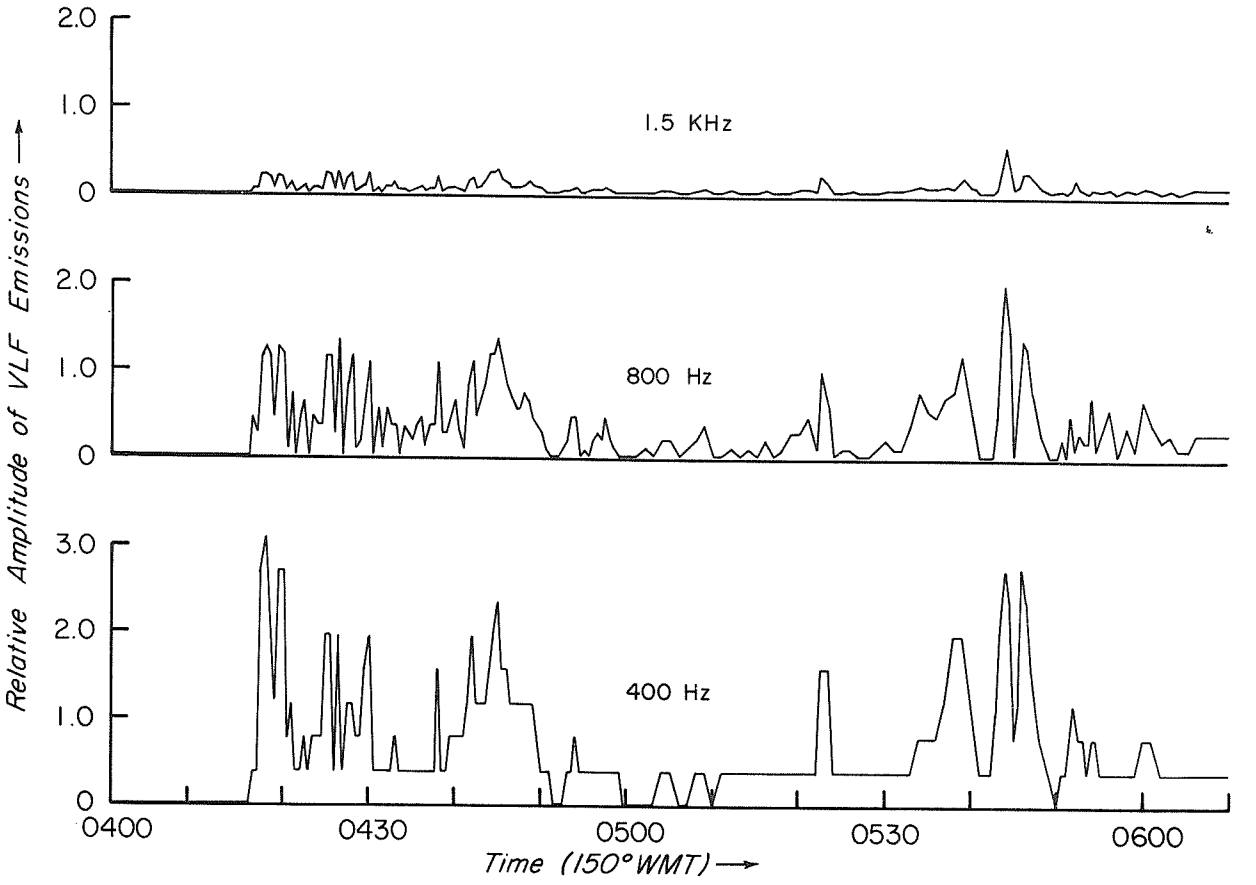

Figure 1. The VLF emissions recorded by the College station at 400, 800 and 1500 Hz during the substorm on March 8, 1970. The emissions observed at 3500, and 8000 Hz were too small to be shown within the ordinate scale.

and at VLF frequencies. From the result it is possible to give a quantitative relationship between absorption at the two frequencies. Calculations carried out by D. Wallis [private communication, 1968] using the auroral model ionosphere of Holt and Lerfald [1967] indicate that the ratio between absorption at 500 Hz and 30 MHz is 0.35. That is, an ionosphere which resulted in 10 dB of absorption at 30 MHz could be expected to result in 3.5 dB of absorption at 500 Hz. However, in interpreting these calculations, it should be kept in mind that the absorption ratio is sensitive to the model used. For example, using the PCA model of Belrose [1963] Wallis calculated an absorption ratio of 9.5. In any event the model calculations indicate that the magnitude of the absorption shown in Figure 2 should have an appreciable effect on the transmission of VLF energy through the ionosphere. The 30 MHz absorption observed at College at 0440 150° WMT was near 30 dB or higher, indicating that the absorption at 500 Hz should have been at least 10 dB. It should be pointed out here that the absolute magnitude of the ionospheric absorption higher than 15 dB is not very meaningful although it has been reported here by making some finer calibration. Examination of other 30 MHz riometer data published by ESSA (now NOAA) from other stations in Alaska indicates that the region of intense absorption extends south of Anchorage (61.2°N) and northward to somewhere between Fort Yukon (66.34°N) and Barter Island (69.35°N). The actual magnitude of the absorption at the stations reported by NOAA is difficult to determine if the absorption was in excess of 9dB since the plots were folded back on themselves. However, the swath of 30 MHz absorption in excess of 9 dB extended from Anchorage (61.2°N) to Fort Yukon (66.34°N).

Examination of Figure 1 indicates that there were measurable VLF signals during most of the substorm and that these signals were certainly present during the peak in absorption centered around 0440 150° WMT. Comparison of Figures 1 and 2 does not indicate a simple relationship between the intensity of VLF emissions and 30 MHz absorption but the period between 0520 and 0555 150° WMT does show a tendency towards positive correlation between the VLF amplitudes and the 30 MHz absorption.

In relating the intensity of the VLF emissions to 30 MHz absorption, it should be kept in mind that both events appear to be the consequence of the substorm and the two events may be re-

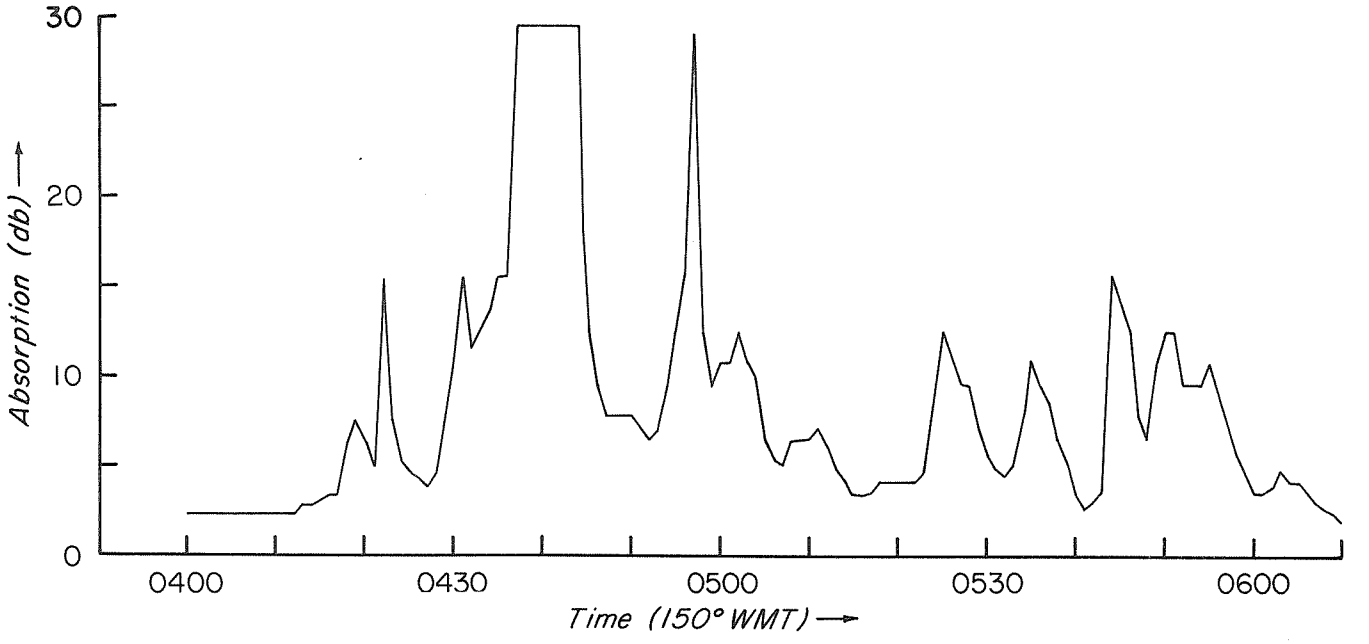

Figure 2. The 30 MHz riometer absorption data during the substorm at College on March 8, 1970.

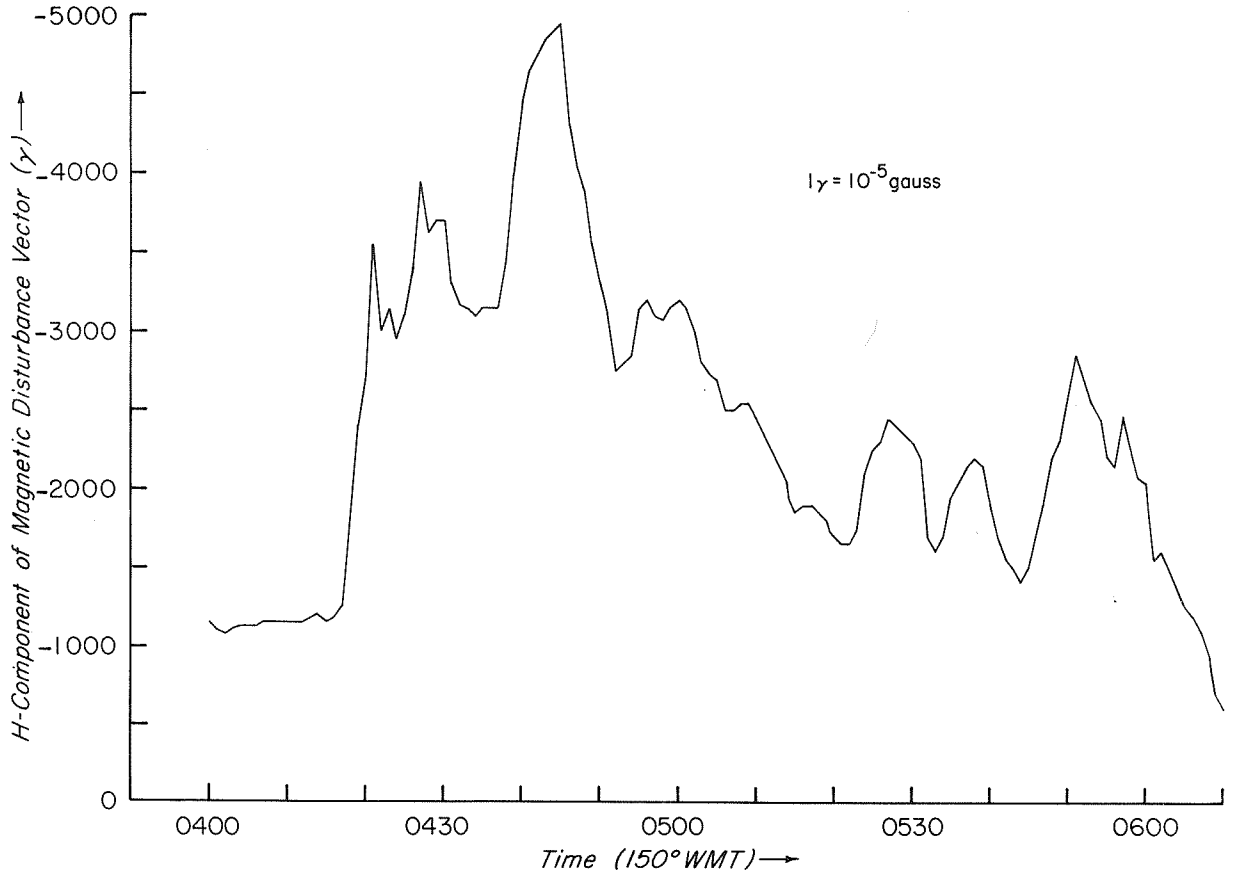

Figure 3. The H-component of the magnetic disturbance vector as recorded by the College observatory during the substorm on March 8, 1970.

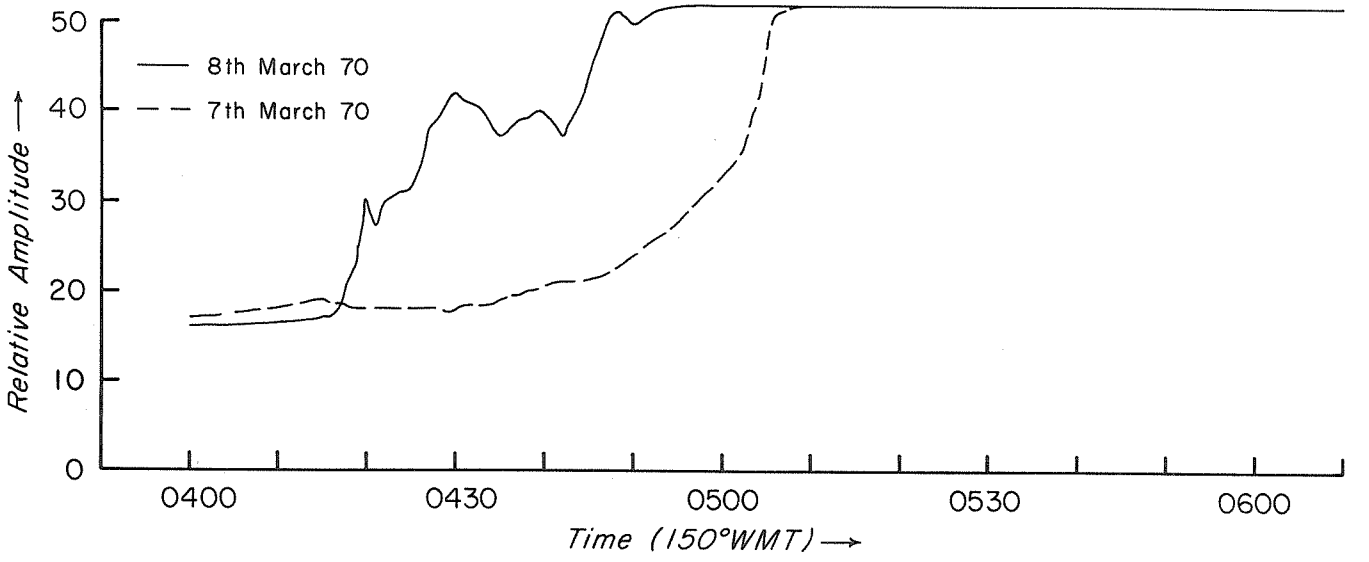

Figure 4. The H-β photometer record during the substorm on March 8, 1970. The dotted line represents the record for March 7, 1970. The two records merge into the twilight zone after 0508 (150° WMT). The strength of the emission could not be exactly determined due to the cloudy sky conditions but it was estimated to be of the order of 600 Rayleighs.

lated to the same source. That is, the agent responsible for the precipitation of electrons may also be responsible for the generation of VLF emissions. A possible mechanism is pitch angle scattering of electrons by electromagnetic waves at VLF frequencies [Kennel and Petschek, 1966]. In support of this idea, Oliven and Gurnett [1968] report simultaneous occurrences of VLF chorus and the electron microbursts, with their instrumentation on the Injun 3 satellite. Moreover, Morozumi and Helliwell [1966] in their analysis of Antarctic VLF data indicate that VLF emissions are positively correlated with 30 MHz absorption for low values of absorption; but under conditions of strong absorption, the intensities of VLF emissions appear to be anti-correlated with 30 MHz absorption. Our data tend to support this conclusion.

As indicated earlier the substorm was unusual simply in that VLF emissions were received during the predaylight morning hours. We think that the fact that VLF emissions were detected during the substorm cannot be entirely attributed to the intensity of the emitting source. Rather, it is likely that the propagation conditions in the upper ionosphere and magnetosphere were affected by the substorm in a manner to have allowed the signals to reach the ground rather than being reflected outward.

Acknowledgements

The authors wish to express their sincere thanks to F. T. Berkey for providing the riometer data and for helpful suggestions. We thank the ESSA (now NOAA) Space Disturbances Laboratory for their cooperation in getting us the absorption data from various stations in Alaska. The H-β record was provided by Bill Stringer of the Geophysical Institute and the magnetogram was supplied by the staff of the Coast and Geodetic Survey, College observatory. Finally, we would like to thank Professor A. E. Belon for going through the manuscript and for helpful comments.

This work was supported by the U. S. Army Research Office, Durham, North Carolina through Contract DAHC-04-69-C-0054.

REFERENCES

BELROSE, J. S. 1964 Electron density measurements in the D-region by the method of partial reflection, in Electron Density Distribution in Ionosphere and Exosphere edited by E. Thrane, North-Holland Publishing Company, Amsterdam

HOLT, O. and G. M. LERFALD 1967 Results from a RF capacity probe experiment in the auroral ionosphere, Radio Science, 2, 1283

KENNEL, C. F. and H. E. PETSCHEK 1966 Limit on Stably Trapped Particle Fluxes, J. Geophys. Res., 71, 1-29

MOROZUMI, H. M. and R. A. HELLIWELL 1966 A correlation study of the diurnal variation of upper atmospheric phenomena in the southern auroral zone, SU-SEL-66-124, Stanford University, Stanford, California

OLIVEN, M. N. and D. A. GURNETT 1968 Microburst phenomena 3. An association between microburst and VLF chorus, J. Geophys. Res., 73, 2355-2362

WALLIS, D. 1968 Private Communication

"Ionospheric Absorption Data"

by

Geophysical Observatory
Sodankylä, Finland

The tables and figure have been prepared from a quarterly report sent to WDC-A Upper Atmosphere Geophysics. The riometer absorption data at 27.6 MHz from Kevo N69°45' E26°29' and Sodankylä N69°21' E26°38' are presented. The equipment type is David Andersen Radio, D-A87, Norway with a vertical three element Yagi antenna. The data are recorded at 6 cm per hour. The absorption in decibels is computed from the formula:

$$A = 10 \log_{10} \frac{Po}{P}$$

where P is the received cosmic noise power and Po the cosmic noise under quiet conditions at the same sidereal time.

The first minute absorption and the maximum absorption values for March 6-10, 1970 are given in the tables. For the maximum the time of occurrence is given in tenths of the hour preceding the absorption value. The entry 0.0 signifies equipment malfunction, and letter S signifies interference.

The Figure shows the monthly values for each hour of mean diurnal absorption, the day-to-day variation during the month (maximum absorption on March 8) and the number of hourly values exceeding 0.3 dB for each hour during the month.

Ionospheric Absorption at the First Minute of Each Hour

Kevo — Frequency 27 MHz — March 1970

Universal Time

Day	0000	0100	0200	0300	0400	0500	0600	0700	0800	0900	1000	1100
	1200	1300	1400	1500	1600	1700	1800	1900	2000	2100	2200	2300
6	0.71	0.12	1.88	0.76	0.79	0.54	0.19	0.0S	0.0S	0.0S	0.0S	0.0S
	0.0S	0.0S	0.0S	0.0S	0.0S	0.0S	0.44	1.25	0.26	0.0	0.42	0.15	2.64
7	0.0S	0.0S	0.0S	1.18	2.18	1.77	1.10	0.62	0.75	3.01	0.95	1.47
	0.69	2.57	1.11	1.58	1.79	0.86	0.63	1.36	0.84	0.99	0.39	0.60
8	1.48	1.18	1.71	2.11	3.39	5.17	3.09	0.0S	2.93	3.74	2.72	3.31
	3.15	3.49	4.06	3.95	2.92	2.39	1.14	3.59	0.66	0.17	0.0S	0.36
9	0.10	0.08	0.25	0.29	0.97	2.23	1.96	1.57	1.81	1.78	0.41	0.52
	0.52	0.54	0.48	0.40	0.66	2.90	0.88	0.46	0.16	0.41	0.82	1.17
10	1.60	1.50	0.20	0.18	0.20	0.24	0.21	0.04	0.05	0.05	0.0S	0.0S
	0.35	0.45	0.0S	0.57	0.76	0.62	0.0S	0.0	0.0S	0.49	0.0	0.0

Sodankylä

Day	0000	0100	0200	0300	0400	0500	0600	0700	0800	0900	1000	1100
	1200	1300	1400	1500	1600	1700	1800	1900	2000	2100	2200	2300
6	1.15	0.57	2.49	0.43	0.34	0.23	0.0	0.0	0.0S	0.0S	0.0S	0.0S
	0.0S	0.0S	0.0S	0.0S	0.0S	0.17	1.41	0.54	0.80	1.19	2.12	4.12
7	3.22	1.49	1.24	3.26	1.50	1.07	0.52	0.36	0.25	2.23	0.57	1.46
	1.14	3.44	1.24	1.27	1.62	0.94	1.61	2.47	1.63	1.62	1.10	0.92
8	1.57	0.76	0.92	2.76	1.34	2.53	3.68	0.0S	2.65	6.45	3.25	3.28
	2.67	2.67	2.67	2.99	2.20	2.22	1.19	4.51	1.09	0.60	0.81	0.40
9	0.29	0.36	0.53	0.62	1.51	3.50	1.81	2.25	2.89	1.86	1.08	0.95
	0.86	0.59	0.77	0.54	0.40	1.03	0.90	0.88	0.79	0.43	0.63	0.66
10	1.58	0.88	0.25	0.21	0.18	0.16	0.16	0.05	0.20	0.38	0.0S	0.0S
	0.09	0.0	0.0S	0.0S	0.01	0.0	0.06	0.17	0.26	0.09	0.12	0.16

Ionospheric Absorption
Maximum Value During Each Hour

Kevo

Frequency 27 MHz
Universal Time

Day	0000	0100	0200	0300	0400	0500	0600	0700	0800	0900	1000	1100
	1200	1300	1400	1500	1600	1700	1800	1900	2000	2100	2200	2300
6	0 0.7	9 0.9	0 1.9	4 0.9	5 1.1	0 0.5	0 0.2	9 0.0	4 0.8	0 0.0S	0 0.0S	0 0.0S
	0 0.0S	0 0.0S	0 0.0S	0 0.0S	7 1.0	3 1.6	0 1.3	0 0.3	8 0.8	0 0.4	9 2.5	0 2.6
7	0 0.0S	0 0.0S	0 0.0S	7 3.2	4 3.1	0 1.8	0 1.1	3 1.4	5 4.1	0 3.0	7 1.9	0 1.5
	7 1.7	0 2.6	0 1.1	2 2.0	0 1.8	2 1.0	6 3.4	0 1.4	2 1.3	0 0.6	9 0.6	5 1.5
8	1 1.8	9 1.5	9 2.1	9 3.5	9 5.4	6 6.4	0 3.1	5 3.5	8 4.8	0 3.7	9 3.5	0 3.3
	0 3.1	9 4.0	3 7.6	0 3.9	3 3.4	0 2.4	8 4.0	3 7.2	2 0.8	0 0.2	0 0.0S	0 0.4
9	0 0.1	2 0.2	0 0.3	9 1.5	4 3.9	2 2.4	5 2.1	9 2.4	2 2.1	0 1.8	1 0.8	0 0.5
	0 0.5	0 0.5	0 0.5	0 0.4	5 7.8	4 3.8	0 0.9	9 0.7	1 4.1	3 1.3	9 1.1	6 2.7
10	4 2.7	0 1.5	0 0.2	0 0.2	0 0.2	0 0.2	9 0.3	9 0.4	8 0.5	9 0.2	8 0.1	9 0.2
	8 0.5	0 0.4	0 0.0S	0 0.6	0 0.8	0 0.6	0 0.0S	0 0.0	0 0.0S	0 0.5	0 0.0	0 0.0

Sodankylä

Day	0000	0100	0200	0300	0400	0500	0600	0700	0800	0900	1000	1100
	1200	1300	1400	1500	1600	1700	1800	1900	2000	2100	2200	2300
6	3 1.7	9 2.8	0 2.5	4 0.8	0 0.3	0 0.2	0 0.0	0 0.0	0 0.0S	0 0.0S	0 0.0S	0 0.0S
	0 0.0S	0 0.0S	0 0.0S	0 0.0S	9 0.1	9 1.4	0 1.4	6 0.9	8 1.1	9 2.9	7 4.6	0 4.1
7	2 5.1	2 2.8	9 3.0	0 3.6	0 1.5	0 1.1	0 0.5	0 0.4	9 2.3	2 3.1	7 2.3	0 1.5
	9 4.2	0 3.4	0 1.2	4 1.7	0 1.6	5 2.1	7 2.9	0 2.5	1 2.5	4 1.9	0 1.1	5 2.0
8	1 2.0	0 0.8	9 2.5	3 4.2	8 2.7	8 3.8	0 3.7	6 2.7	8 7.0	0 6.4	0 3.3	6 4.0
	0 2.7	3 3.0	3 7.5	0 3.0	2 6.9	0 2.2	9 4.4	2 7.5	0 1.1	6 1.6	0 0.8	0 0.4
9	0 0.3	0 0.4	2 0.8	5 2.4	5 4.4	0 3.5	9 2.4	9 3.0	0 2.9	0 1.9	0 1.1	0 0.9
	0 0.9	8 0.9	0 0.8	0 0.5	5 1.4	4 1.8	4 1.3	9 1.7	1 1.9	2 0.9	0 0.6	6 3.6
10	0 1.6	0 0.9	0 0.3	0 0.2	0 0.2	0 0.2	0 0.2	6 0.6	2 0.6	0 0.4	0 0.0S	0 0.0S
	0 0.1	0 0.0	0 0.0S	0 0.0S	0 0.0	0 0.0	0 0.1	0 0.2	0 0.3	0 0.1	0 0.1	0 0.2

COSMIC NOISE ABSORPTION KEVO - MARCH 1970

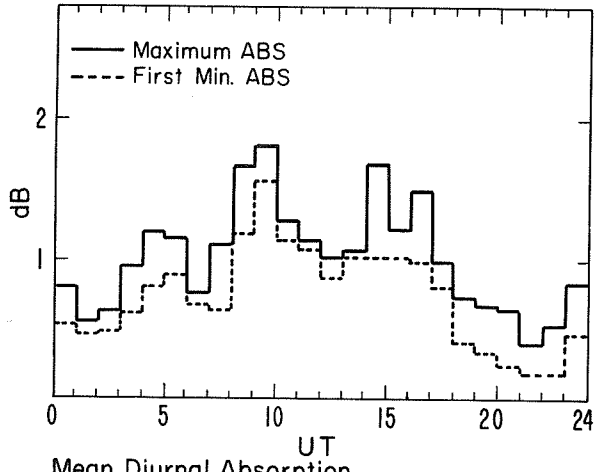

Mean Diurnal Absorption

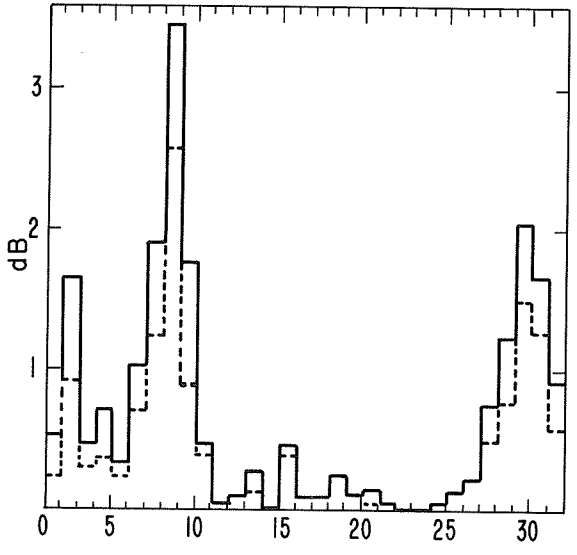

Day to Day Variation

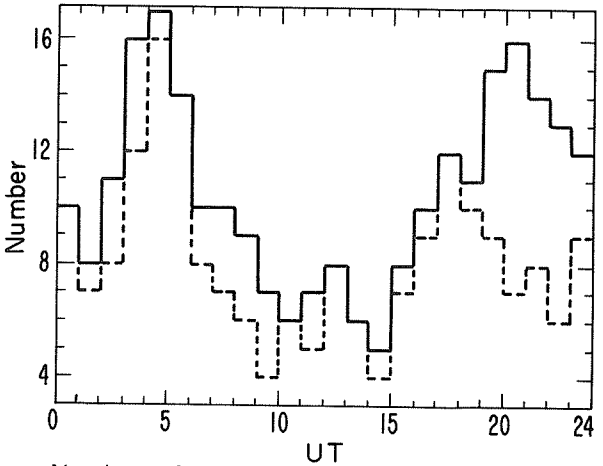

Number of Hourly Values Exceeding 0.3 dB

COSMIC NOISE ABSORPTION SODANKYLA - MARCH 1970

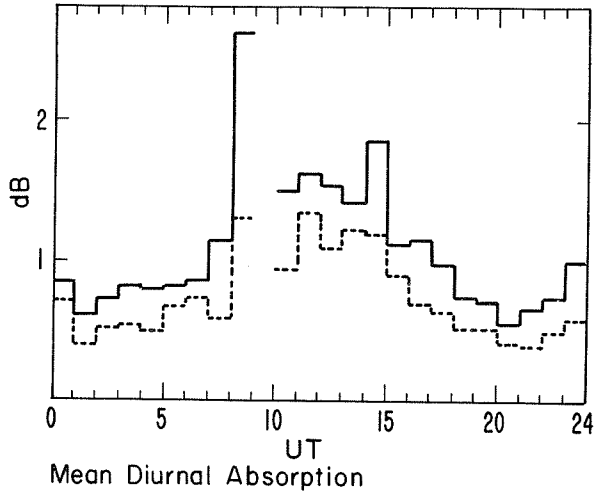

Mean Diurnal Absorption

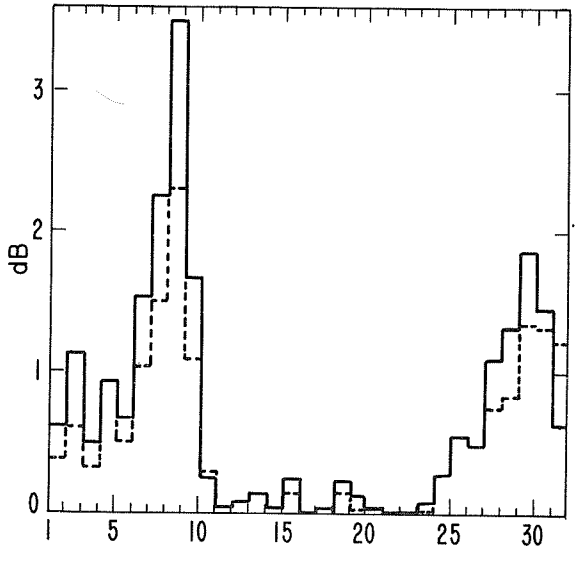

Day to Day Variation

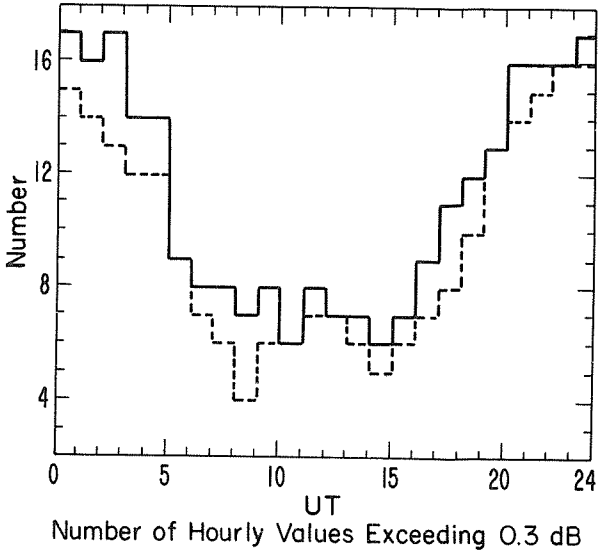

Number of Hourly Values Exceeding 0.3 dB

"Magnetic Storm Effects at Arecibo"

by

L. L. Cogger and G. J. Nelson
Arecibo Observatory, Arecibo, Puerto Rico

Introduction

Arecibo, Puerto Rico (N18.5° W66.8° geographic; N30° E2.4° geomagnetic) is a tropical location, yet because of its geomagnetic latitude can also be considered a midlatitude station. The effects of magnetic storms observed at Arecibo are different from those at both higher and lower latitudes. In this report we shall indicate some storm features evident in data collected during the period March 7-10, 1970.

The incoherent scatter radar facility was operated intermittently for various purposes, so some storm coverage was achieved. In addition, the Faraday rotation of the 137 MHz transmission from the ATS-3 satellite was monitored full time. Because the receiving direction is only 15 degrees from the geomagnetic field lines, the total content determined by this technique is quite closely related to the content in a magnetic tube of force. Clear skies allowed full photometer coverage of [OI] 5577A and [OI] 6300A throughout the nights of interest.

The Storm

Although routine ionospheric observations are undertaken at the Arecibo Observatory, many quiet period phenomena are understood only partially or not at all. Data have rarely been collected through a magnetic storm so our knowledge of the disturbed ionosphere is even more limited. In this section we shall confine our discussion to features which can safely be attributed to the disturbance.

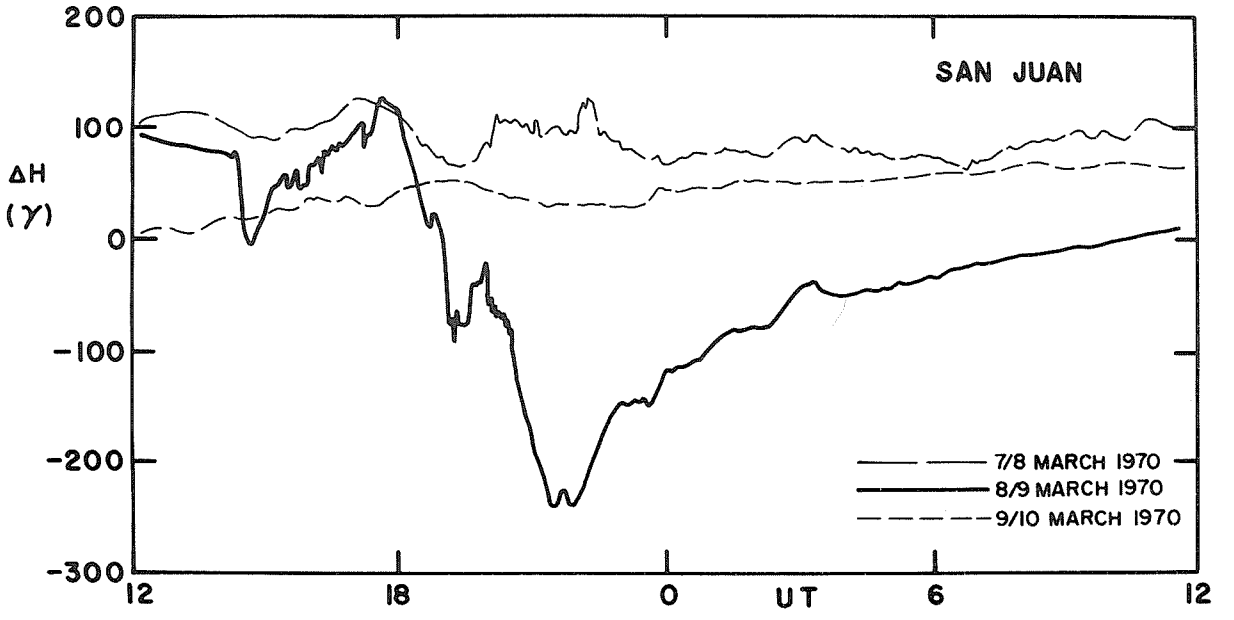

Fig. 1. Reproduction of magnetograms recorded at San Juan, Puerto Rico during the period March 7-10, 1970. Variations in the H-component are shown as a function of universal time (UT).

A reproduction of the H-component magnetogram traces taken at San Juan, P.R. (70 km from the Observatory) is presented in Figure 1 to serve as a time reference. Data from March 8/9 will be compared with that from the preceding and following days which were much quieter. The relevant observed parameters are shown in Figure 2. Times are UT for all the curves. Local solar time at Arecibo is UT - 4.46 hr.

Total Content. An obvious feature of the data is the large general enhancement in total electron content on March 8. This enhancement was sustained for about 12 hours through the daytime period, and was likely basically due to the increased height of the F layer (h_{max}) resulting in a reduced loss rate. The content did not vary smoothly, however, for there are several large peaks. In contradiction to what was stated above, the peak at 1800 UT occurred while the layer was falling, not rising.

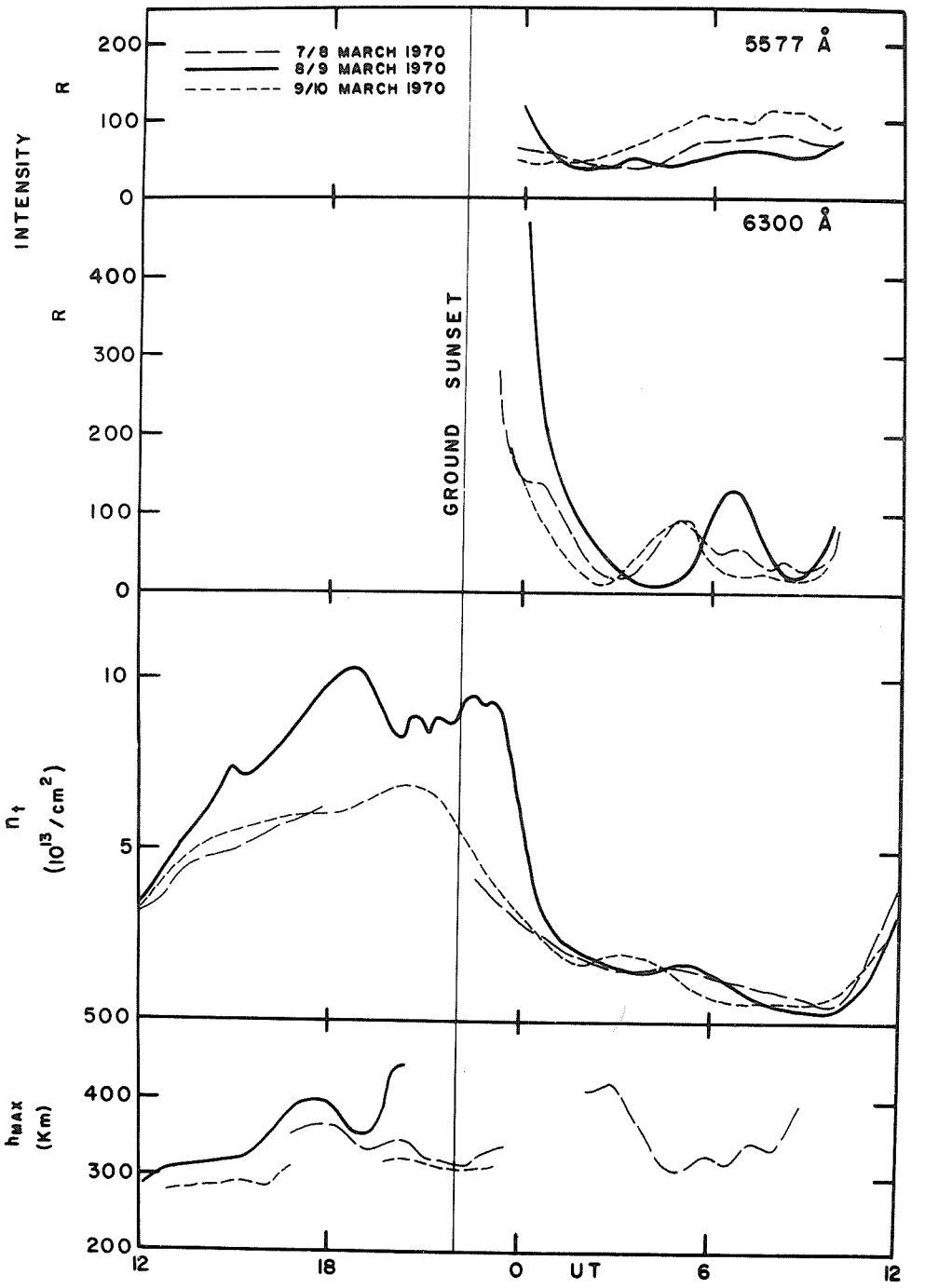

Fig. 2. Data obtained at Arecibo during the period of interest. The bottom figure gives h_{max}, the real height of the maximum electron density determined by the incoherent backscatter technique; the center figure shows the total electron content deduced from Faraday rotation measurements; and the top figure indicates the emission rates of the red and green lines of atomic oxygen in the night airglow.

When the layer was highest there was a valley in the content. Moreover, a second large peak appeared after sunset and at that time the content was about 5 x 10^{13} el/cm^2 above that for the other days. The radar was not operating during this period so no h_{max} data are available, but from other Arecibo data we have found that these evening enhancements are also accompanied by a lowering of the F layer [Nelson and Cogger, 1970]. Ionogram results from Wallops Island (N49.3° geomagnetic) do show a dramatic 300 km drop in the virtual height of the underside of the layer between 2230 and 2315 UT (Figure 3). If this event occurred over a large area simultaneously, it would coincide with the enhancement at Arecibo. This enhancement was followed by a rapid decrease in content, 5 x 10^{13} el/cm^2 in one hour compared with 5 x 10^{13} el/cm^2 in 4 hours on the other days. This decay began 2.5 hours later than on March 9/10.

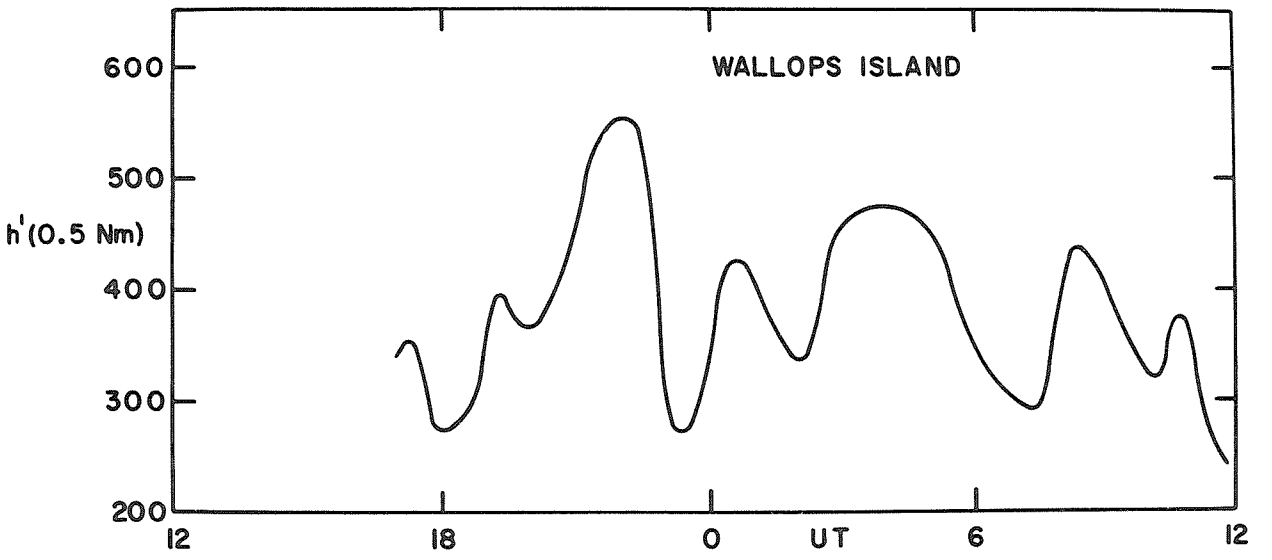

Fig. 3. The virtual height of the F layer above Wallops Island for March 8/9, 1970.

Height Variations of the F Layer. Altitude profiles of electron density distribution are available for times of backscatter observations. The height of the density maximum is shown for these times in Figure 2. The layer remained somewhat higher through the day on March 8 compared with other days. The marked rise of h_{max} to 450 km at 2030 UT must certainly be a storm effect. The layer is again high at 0600 UT, but this is usual behavior: h_{max} at Arecibo generally rises after sunset and stays high until about local midnight when it steadily drops to about 300 km in a manner similar to that shown for March 8/9.

Airglow Observations. Here again we do not want to confuse storm effects with typical nighttime behavior of the atomic oxygen lines (5577A and 6300A). The red line is enhanced for a period almost every night, usually near 0200 60WMT. This is a consequence of the F layer falling to a level where dissociative recombination of O_2^+ becomes more rapid. No additional excitation source is needed.

A large enhancement is evident in the figure and takes place on March 8/9 at the time corresponding to the rapid content decrease. The intensity, 400R ($\pm$ 25%) at 0015 UT is the highest yet obtained from over 200 nights of observation. At 2015 UT it is about 4 times that for March 9/10 which is similar to the ratio of the rates of ionization loss for these nights. There is a coincident enhancement of [OI] 5577A on March 8/9 as expected from the dissociative recombination mechanism.

F Region Temperatures. Ion and electron temperatures were not monitored over a sufficient period for the effects of the storm to be determined. At 2000 UT on March 7 and 8 the electron temperature at 277 km was 1920 and 2120°K respectively, and the ion temperature was 1280 and 1300°K so there were not marked differences in the diurnal maxima. It should be noted that although 2000 UT is about the usual time of the diurnal maximum at Arecibo [Rao, 1968], the main phase of the storm was not fully developed at this time (Figure 1) so there may have been heating after 2000 UT. The minimum F region nighttime temperature for March 7/8 was 1030°K at 0800 UT. The expected error in these measurements is $\pm$ 5%.

Discussion

An evening enhancement of ionization is characteristic of magnetic storm events at Arecibo. Data from 25 storms have shown that almost invariably this phenomenon is associated in time with the negative bay of the H-component, and the magnitude of the enhancement is a function of the amplitude of the negative phase. Exceptions to this behavior are confined to disturbed periods when the H-component varies smoothly; that is, when there is little fine structure evident. The source of the enhancement has not been determined. Several mechanisms have been discussed and discounted [Nelson and Cogger, 1970] including diffusion from the protonosphere, production by ionizing radiation, and north-south transport. The interpretation is made more difficult by the fact that the magnitude of these enhancements ($\sim 10^{13}$ el/cm^2) is the same or more than the content of a tube of force 1 cm^2 above Arecibo extending to the equatorial plane [Titheridge, 1968].

The fact that for both daytime and nighttime enhancements the layer falls in altitude while the ionization is increasing supports the suggestion made by Nelson and Cogger [1970] that a common mechanism may be responsibile for both events. This is quite different to the situation at higher latitudes reported by Evans [1970]. The enhancements he observes at Millstone Hill occur in the daytime

and are always accompanied by an increase in h_{max}. They are apparently caused by electric fields associated with the ring current which raise the F layer and thus reduce the loss rate. A general increase in h_{max} is observed at Arecibo (Figure 2) but it is probably not due to the ring current which is not expected to flow at latitudes as low as that of Arecibo (L = 1.4).

The airglow observations can be adequately interpreted without recourse to bombardment by energetic auroral particles. Although a small flux of incoming particles is possible, the intensities are not very different on the three nights, and the evening enhancement on March 8 can be explained by dissociative recombination of O_2^+.

Acknowledgements

The Faraday rotation observations were made with equipment lent by Dr. DaRosa of Stanford University. Ionograms and magnetograms were obtained from World Data Center A, Upper Atmosphere Geophysics. Arecibo Observatory is operated by Cornell University under contract to the National Science Foundation and with partial support from the Advanced Research Projects Agency.

REFERENCES

EVANS, J. V. 1970 Paper presented at the 1970 Spring URSI Meeting, Washington, D. C.

NELSON, G. J. and L. L. COGGER Enhancements in electron content at Arecibo during geomagnetic storms, submitted to Planet. Sp. Sci.

RAO, P. B. 1968 Electron concentrations and electron and ion temperatures in the F region for magnetically quiet and disturbed conditions, J. Geophys. Res., 73, 1661.

TITHERIDGE, J. E. 1968 Calculations of diurnal changes in the exosphere, J. Atmosph. Terr. Phys., 30, 1843.

9. AIRGLOW

"Optical Observations at the AFCRL Geopole Observatory Thule A.B., Greenland from 6-10 March 1970: Descriptive Overview"

by

S. M. Silverman and J. G. Moore
Air Force Cambridge Research Laboratories
L. G. Hanscom Field
Bedford, Massachusetts 01730

Introduction

Observations of the behavior of visual aurora and of optical emissions in regions near the geomagnetic pole have shown distinct differences from the behavior in the auroral zone and even from that in regions intermediate between auroral zone and geomagnetic pole. Discussions of the general auroral behavior may be found in Davis [1962], Lassen [1967, 1969] and Sandford [1967]. Sandford, in particular, described and defined the polar glow aurora associated with polar cap absorption events, in which the sequence of the intensities of the OI and N_2^+ emissions followed that of the PCA. The period from 6-10 March 1970 was one in which a small or moderate PCA occurred, and the optical emission data from a high latitude station such as Thule A.B. are thus of interest in connection with this.

The AFCRL Geopole Observatory at Thule A.B. carries out a number of diverse measurements of geophysical interest. We present here the optical observational results, concentrating on those from the scanning spectrometer and the four-barrel photometer. We compare these with some other geophysical measurements also made at Thule A.B. The emphasis here will be on the observations, though we will present also a preliminary essentially qualitative interpretation of the results. Figures illustrative of the results are included at the end. These are, for the most part, not explicitly referred to in the text.

Instrumentation

The scanning spectrometer is a one meter Fastie-Ebert model with a reciprocal linear dispersion of about 8 angstroms per mm over the spectral range of 3000 A to 7500 A. The grating is driven by a cam which gives a "triangular" wavelength scan whereby the wavelength increases linearly to a selected maximum value and then decreases linearly at the same rate to a selected minimum value. The process is then repeated. An up-down spectral scan is completed in a little over 10½ minutes. Slit widths are adjustable and are usually varied between 0.5 to 2.0 mm for the applications at Thule giving wavelength resolutions of 4 to 16 A. The instrument has been absolutely calibrated and line intensities in Rayleighs are easily obtained from chart deflections.

The four-barrel photometer contains four telescopes, interference filters, field stops and photomultiplier tubes. The objective lens has a 5.5 inch aperture and the field stops limit the field of view to approximately 4° circular. EMI 9502B type photomultipliers are used. The interference filters limit the photometer response as is shown in the following table:

Wavelength of peak response	Width at 50% response	Transmission at selected wavelengths
5290A	16 A	$T_{5290} = 53\%$
5567A	13.5 A	$T_{5577} = 9.5\%$
5887 A	19.8 A	$T_{5893} = 50\%$
6294 A	19.8 A	$T_{6300} = 49.9\%$

The absolute intensities of the three emission lines λ5577, 5893, 6300 A determined by the scanning spectrometer may also be used as a cross check on the absolute intensities provided by the photometers and an estimate of the continuum contamination can be made.

Scanning Spectrometer Results

During the period 6-10 March the nighttime period, defined as the period between astronomical twilights, ranged from a little over three hours on March 6 to zero on March 9 and 10. Hence,

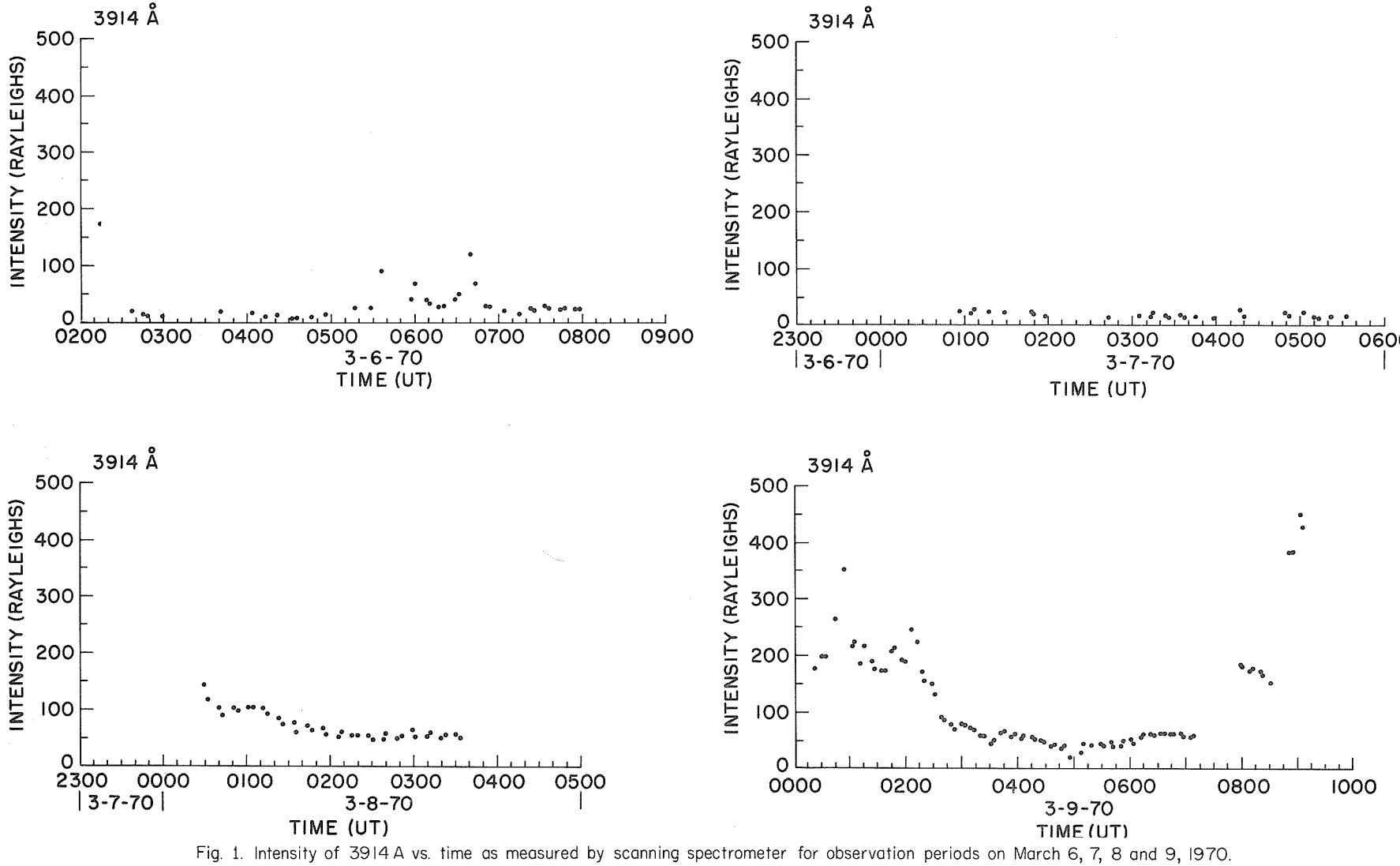

Fig. 1. Intensity of 3914 A vs. time as measured by scanning spectrometer for observation periods on March 6, 7, 8 and 9, 1970.

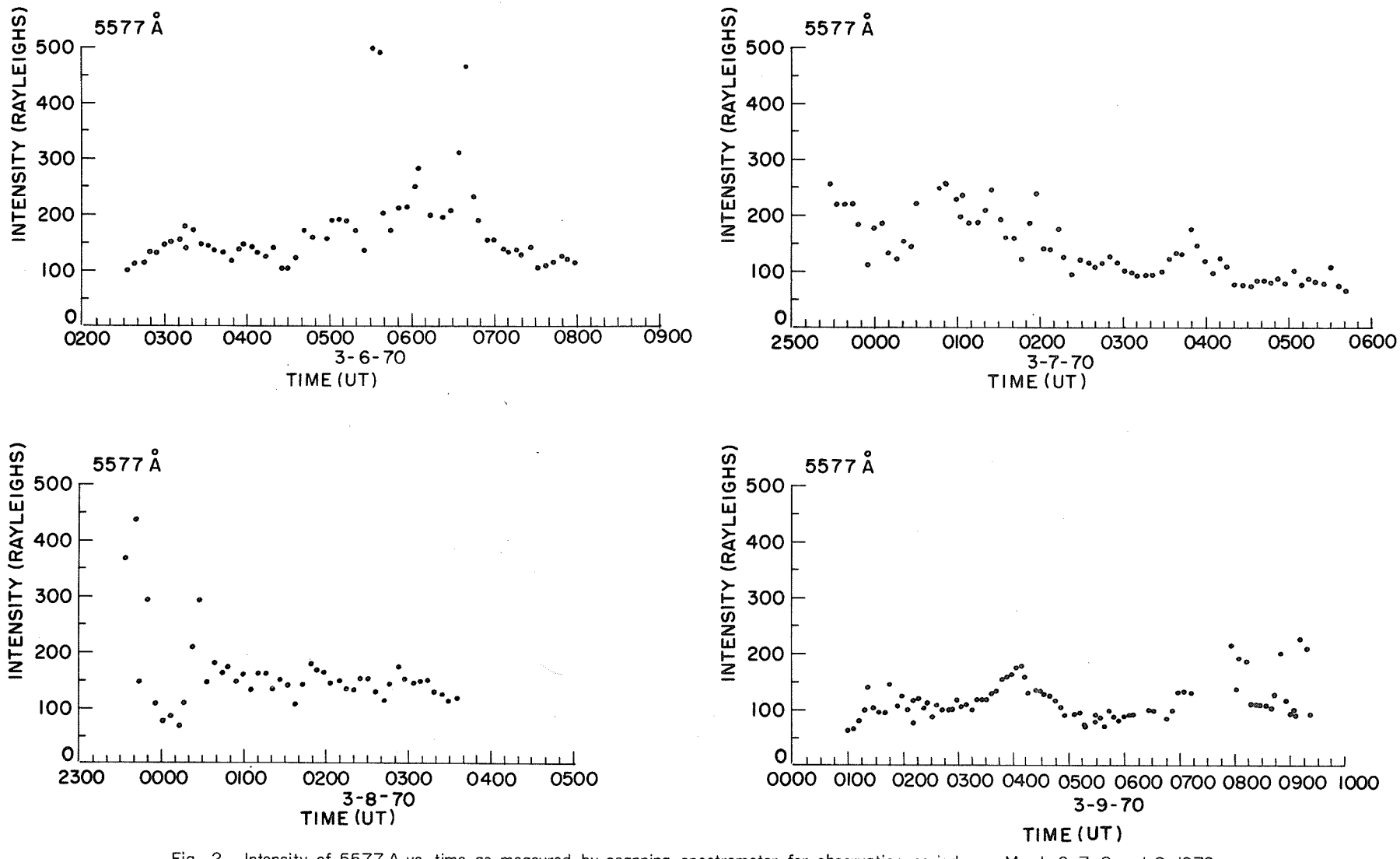

Fig. 2. Intensity of 5577 A vs. time as measured by scanning spectrometer for observation periods on March 6, 7, 8 and 9, 1970.

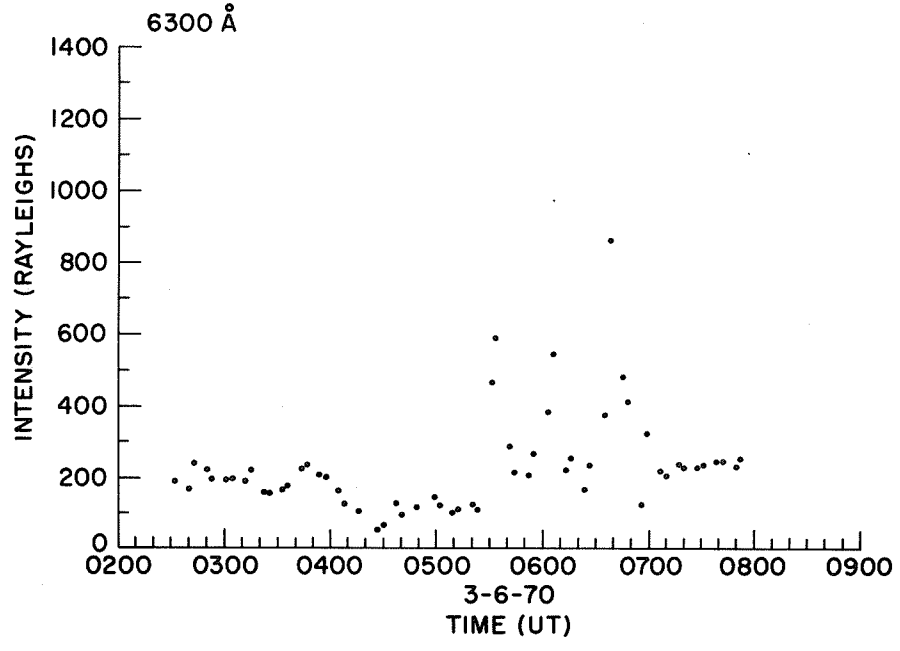

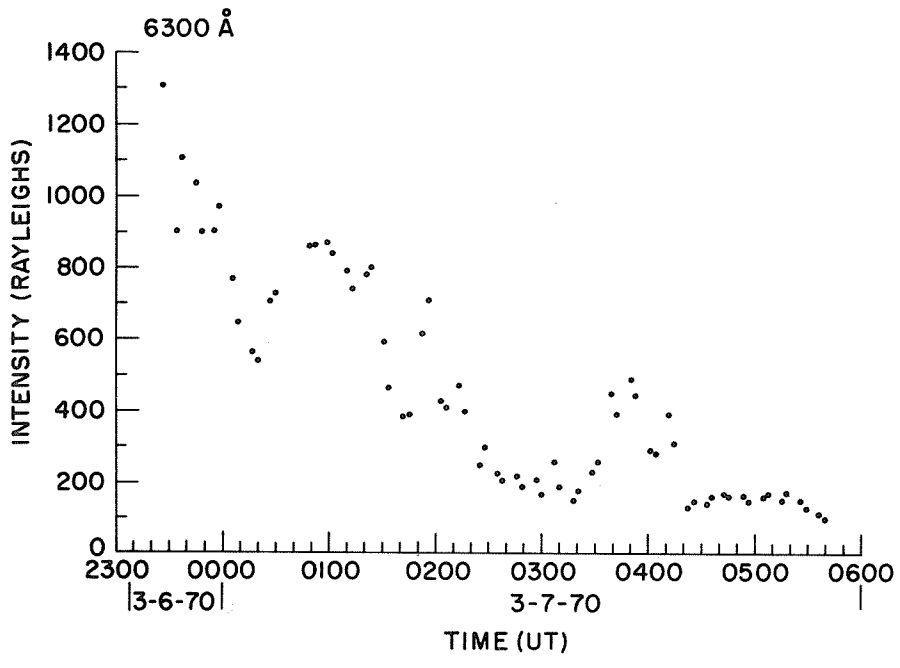

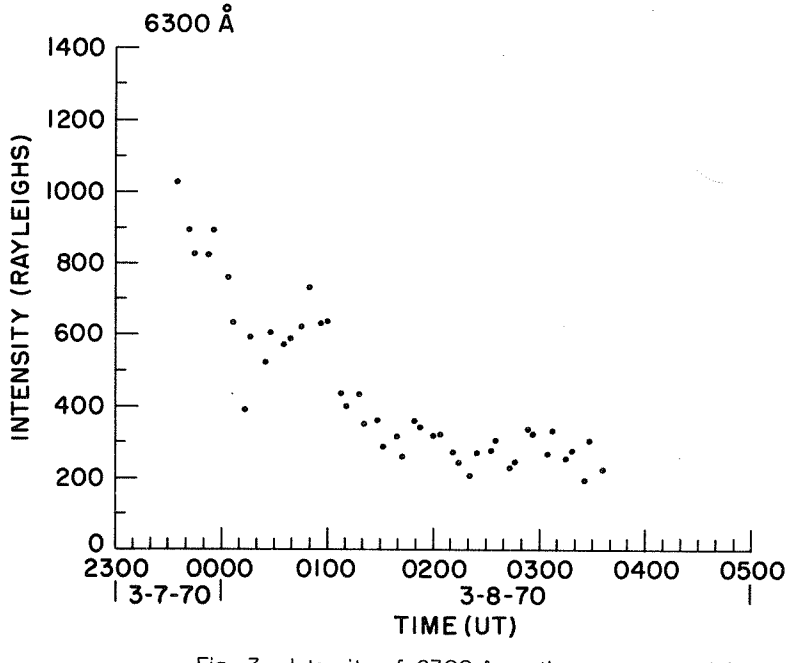

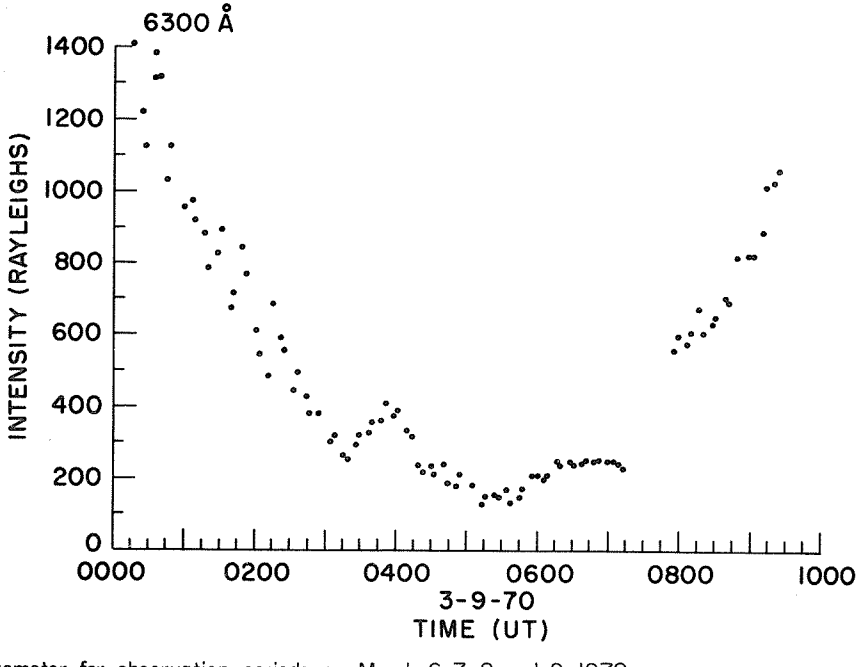

Fig. 3. Intensity of 6300 A vs. time as measured by scanning spectrometer for observation periods on March 6, 7, 8 and 9, 1970.

twilight effects and-or post-twilight decays are present in much of the data. The spectra were scaled, where possible, for the emissions at 3914 A, 4278 A, 5200 A, 5577 A, 5893 A, 6300 A and 6364 A. The resulting intensities for 3914 A, 5577 A and 6300 A are shown graphically in Figures 1-3. For convenience, we discuss these separately for the individual days. All times are UT.

March 6. Data were obtained from about 0230 to 0800 UT. No significant riometer absorption was present during this period though some had been present a few hours previously. Visual auroral activity was noted at about 0530 UT. The 6300 A emission (Figure 3) seems most sensitive to disturbances, showing sharp peaks in activity at about 0530, 0600 and 0640 UT. These peaks are also found in the 5577 A (Figure 2) emission and, though not as marked, in the 3914 A (Figure 1) emission. This latter indicates that there appears to have been some particle precipitation during these periods. A more general and much less intense disturbance earlier in the evening with peak about 0350 UT is not reflected in the N_2^+ emissions, nor is it obviously reflected in the 5577 A emission. The 5200 A emission, while fluctuating by a factor of 2-3 is not sufficiently out of the noise to allow for conclusions. The 5893 A emission remains fairly steady with an approximate average intensity of 60R in the early hours and 90R in the later hours.

March 6-7. Data were obtained from about 2330 to 0540 UT. Riometer data showed slight absorptions during this period not exceeding 0.2 dB. The solar depression angle varied from about 8° at the beginning of the period to about 19° at the end of the period. Twilight effects are evident in the 6300 A, 5893 A and 5200 A emissions. There appear to be a number of disturbance effects superimposed on the decay of the 6300 A emission throughout almost the entire period, and these are reflected in increased 5577 A emission at the same times. If we estimate background levels for the two emissions and consider only the increased intensity above this as being due to the disturbance, then the 5577 A increase can be approximately estimated by taking 0.2 of the increased 6300 A increase, this being the ratio of the states in the dissociative recombination reaction [for references see Silverman, 1970]. As pointed out by Pal [1968] however, preferential deactivation of the ^1D state will lead to a fraction of intensities which increases as the height of production decreases, and this could be used as an indication of the height changes during a disturbance. For four peaks during this time period the ratios of 5577 A intensity above the estimated background level to 6300 A intensity above the estimated background level are all close to 0.3, indicating that excitation is occurring below the normal F-region heights of production. The increase of intensity between 0150 and 0200 UT is of particular interest since it corresponds with the time of the maximum phase of what appears to be the largest flare in this period. The solar depression angle was about 15° at this time, corresponding to a shadow height of about 225 km, but the majority of the 6300 A emission is expected to be above this height. This suggests a flare connection with this increase, though it is difficult to accept the size of the increase if radiation above is involved because of the long path length. In addition, the presence of other intensity increases, noted earlier, shows that this interesting possibility must be treated with caution. The 5893 A emission, though fluctuating, remains relatively stable with average intensities ranging from about 90R in the early part to about 70R in the later part of the observations. The N_2^+ emission shows no increase at this time and this supports a radiation origin.

March 7-8. Data were obtained from about 2300 to 0330 UT. Riometer data show that a PCA had begun between 1025 and 1100 UT on March 7, reaching a maximum of 5.2 dB at about 1500 UT on the 8th. The optical observation period was thus during the maximum phase of the PCA. The solar depression angle varied from about 6° to almost 18°, and twilight effects are evident in both the 6300 A and 5893 A emissions. The 6300 A emission shows a well-defined increase peaking at about 0050 UT. The N_2^+ emission in the period from 0030 to about 0130 UT is about twice as high as later in the observation period. The 5200 A emission intensity is also higher during this period than later or during previous days. Thus, particle precipitation at about 0100 UT is indicated. The 5893 A emission intensity remains in the neighborhood of 60R following the twilight decay.

March 8-9. Data were obtained from about 2300 to about 0920 UT. Riometer data show that the PCA was continuing during this period, though the absorption was considerably less than on the preceding day, with a maximum of 0.4 dB. The solar depression angle varied from about 5° through a maximum of 18° to about 9° at the end of the observational period. Twilight effects are particularly evident in the 6300 A emission both at the beginning and the end of the observational period, and are also present for the 5893 A emission.

Disturbances are evident in the 6300 A emission at several times during the night, as, for example, from about 0320 to about 0420 UT. During this period, centered at about 0400 UT, the 5577 A and 3914 A emission intensities (Figures 1 and 2) are also enhanced. If we take the increased intensities above an estimated background level, then the 5577 A to 6300 A intensity ratio is of the order of 0.45, appreciably greater than that, 0.30, for the enhancements of 6-7 March. The presence of increased 3914 A emission, however, indicates that the additional 5577A emission comes from different mechanisms at different altitudes, one at high altitudes associated with the 6300 A emission, as on 6-7 March when the 3914 A emission intensity remained essentially constant, and one at low altitudes associated with the 3914 A emission. It is known that for auroras the ratio of 5577A to 3914 A is of the order of 2 but can vary between 1 and 3 depending on the position in space of the

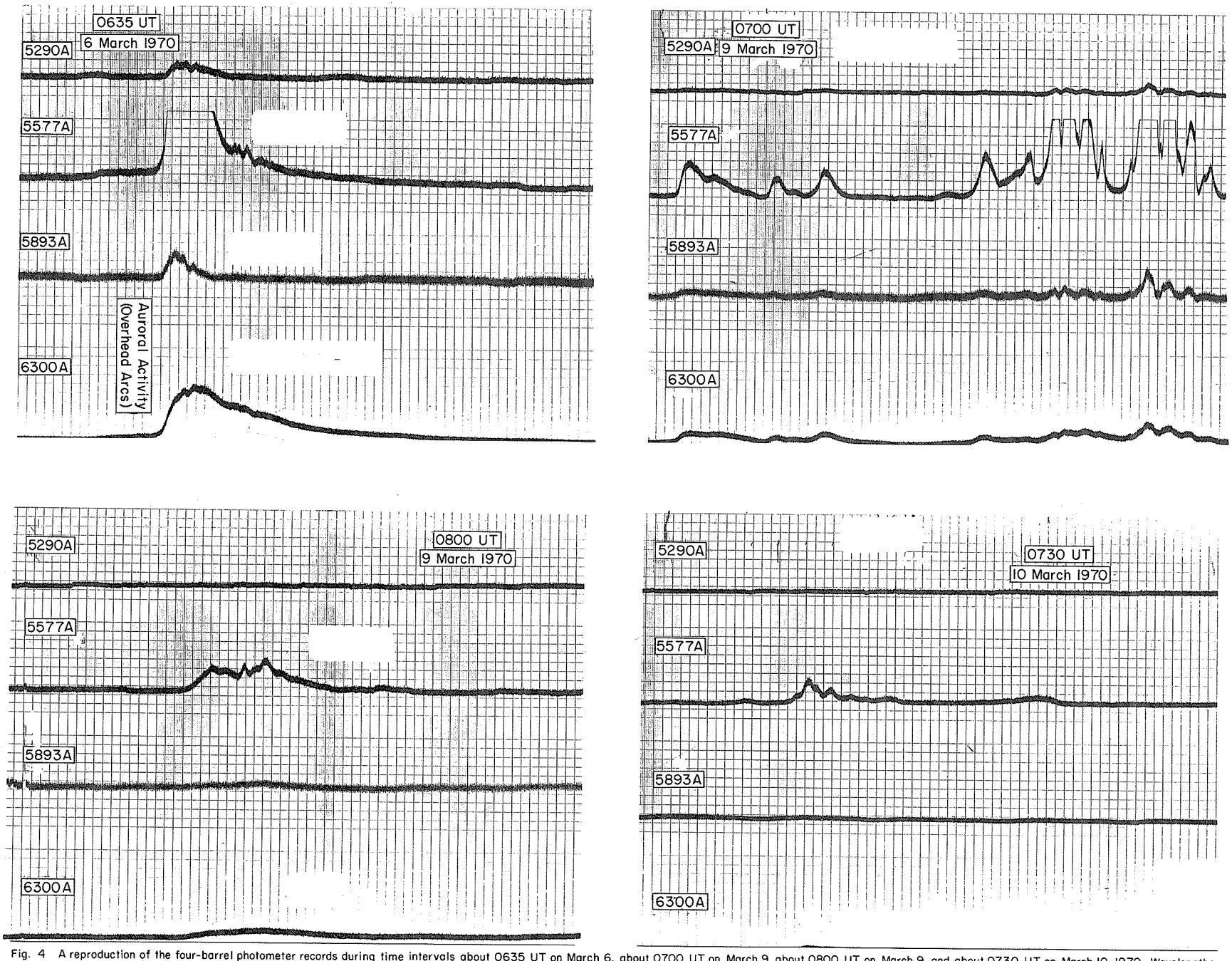

Fig. 4 A reproduction of the four-barrel photometer records during time intervals about 0635 UT on March 6, about 0700 UT on March 9, about 0800 UT on March 9, and about 0730 UT on March 10, 1970. Wavelengths for each channel are labelled. Each major chart division along the X-axis represents 20 seconds of time. Relative intensity is measured along the Y-axis in arbitrary units.

measurements [see the review by Monfils, 1968], and on the type of aurora [Sandford, 1967]. The Geopole all-sky camera shows an arc near the horizon in the southeast and a diffuse brightening over much of the sky at 0345 UT. By 0350 UT the arc had moved out of range of the camera. The diffuse brightening was still clearly evident until at least 0415 UT. Sandford [1967] has shown that for mantle aurora, statistically, the ratio of 5577 A to 3914 A emission intensities depends on magnetic time. For our case this ratio, from his figure, would be about 1. If we use this to estimate the low altitude contribution, then the ratio of the high altitude 5577 A intensity (obtained by difference from the total additional intensity) to the 6300 A intensity is 0.29, consistent with the ratios obtained on 6-7 March.

Intense overhead auroras were present later in the day, and the absence of data on the plots in the period around 0730 UT is due to saturation of the intensities resulting from the auroral activity. The spectrum shows well marked development of the N_2^+ bands and the Vegard-Kaplan bands of N_2.

Photometeric Results

The four-barrel photometer at the AFCRL Geopole Observatory had been installed to monitor changes of intensity rather than absolute intensities. Our discussion of the photometric results (Figure 4) is therefore in these terms, though some indication of the absolute values can be obtained by comparison with the results of the scanning spectrometer (Figure 5).

6 March. Enhanced emission of 5577 A and 6300 A occurred between 0110 and 0210 UT. The intensity variations during this period are similar to those which are associated with aurora at other times. The all-sky camera records from Thule (Qanaq) do not show aurora during this period, but these were twilight conditions, with solar depression angles ranging from 13° to 16°, so that the presence of faint aurora cannot definitely be ruled out. Auroral activity resulted in fluctuations on the photometer during the periods about 0530, 0600 and 0635 UT, the same times noted on the spectrometer records. The photometric records show fluctuations of intensity with periods in the range of about 5-20 seconds. At 0530 and 0600 UT there appear to be two trains about 4 minutes apart. Similar periodicities and behavior have been noted in the auroral zone on many occasions [see, for example, Campbell, 1970, and the references cited therein]. During these periods both the 5290 A and 5893 A filters showed a marked increase. It is not clear, however, whether these were increases in the continuum and line emission or were molecular bands within the range of the filters. The scanning spectrometer data do not show increases for the sodium emission during these periods, so that other excitations must be present. We have not yet examined our data carefully enough to determine what these are. A preliminary look indicates that these may be the 1st positive bands of N_2.

7 March. The increase in intensity in the period 0150-0200 UT concurrent with the major solar flare is also evident in the photometer records as a fairly steady increase in both 5577 A and 6300 A over this period. Smaller increases for a 1-2 minute period are also present at about 0212 and 0218 UT. Similar small and steady increases occur at about 0335 and 0339 UT, and at 0408 and 0412 UT. Fluctuating peaks of intensity in the 5577 A emission occur at about 0638 and 0643 UT with the intervals between fluctuations 20 seconds in the first and 50 seconds in the second case.

9 March. The most interesting part of these records is between 0700 and 0800 UT, a time of pronounced auroral activity as seen on the all-sky camera. The intensity variations of the 5577 A and 6300 A emissions are quite evident, with intervals between the fluctuations from 20 to 60 seconds. In the period around 0710 UT the 5290 A and 5893 A traces also show marked activity, which may be due to higher excitation resulting in the emission of molecular bands in the regions passed by the filter. Examination of the spectrometer records shows no sodium enhancement, so that the situation is probably similar to that on 6 March. Similar activity is shown in the 5577 A and 6300 A emissions in the period about 0750 UT.

10 March. Fluctuations in the 5577 A emission similar to those of the preceding day are present at about 0720 UT. Intervals between fluctuations are of the order of 20-40 seconds.

All-sky Camera

During the period 6-10 March 1970 the all-sky camera at Geopole operated only intermittently and, in a number of frames, with multiple exposures. As a result usable data are available only for 9 March, Figure 6. All-sky camera data from Thule (Qanaq), about 1° to the north of Geopole, are available for the entire period, and were furnished to us through the courtesy and kindness of Dr. K. Lassen, Danish Meteorological Institute. Our discussion will make use of both sets of data.

6 March. The period from 0520 to 0650 UT was characterized by three well defined periods of auroral activity. These coincided in time with the active periods noted in the spectrometric and photometric data.

7 March. No aurora was present.

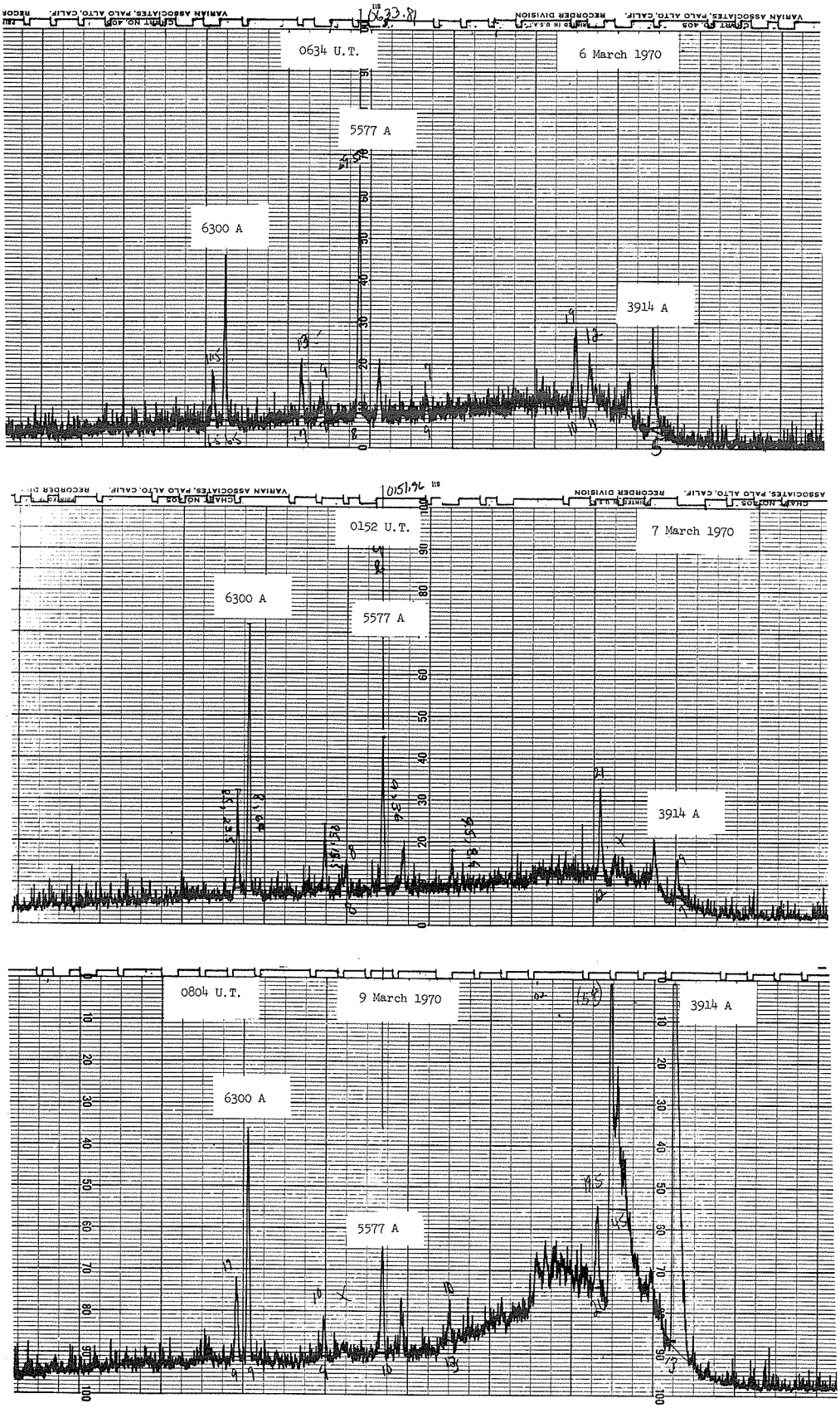

Fig. 5 A reproduction of the chart records of the scanning spectrometer for the time intervals centered at 0634 UT on March 6, at 0152 UT on March 7, and at 0804 UT on March 9, 1970. The spectral lines discussed in the text are labelled.

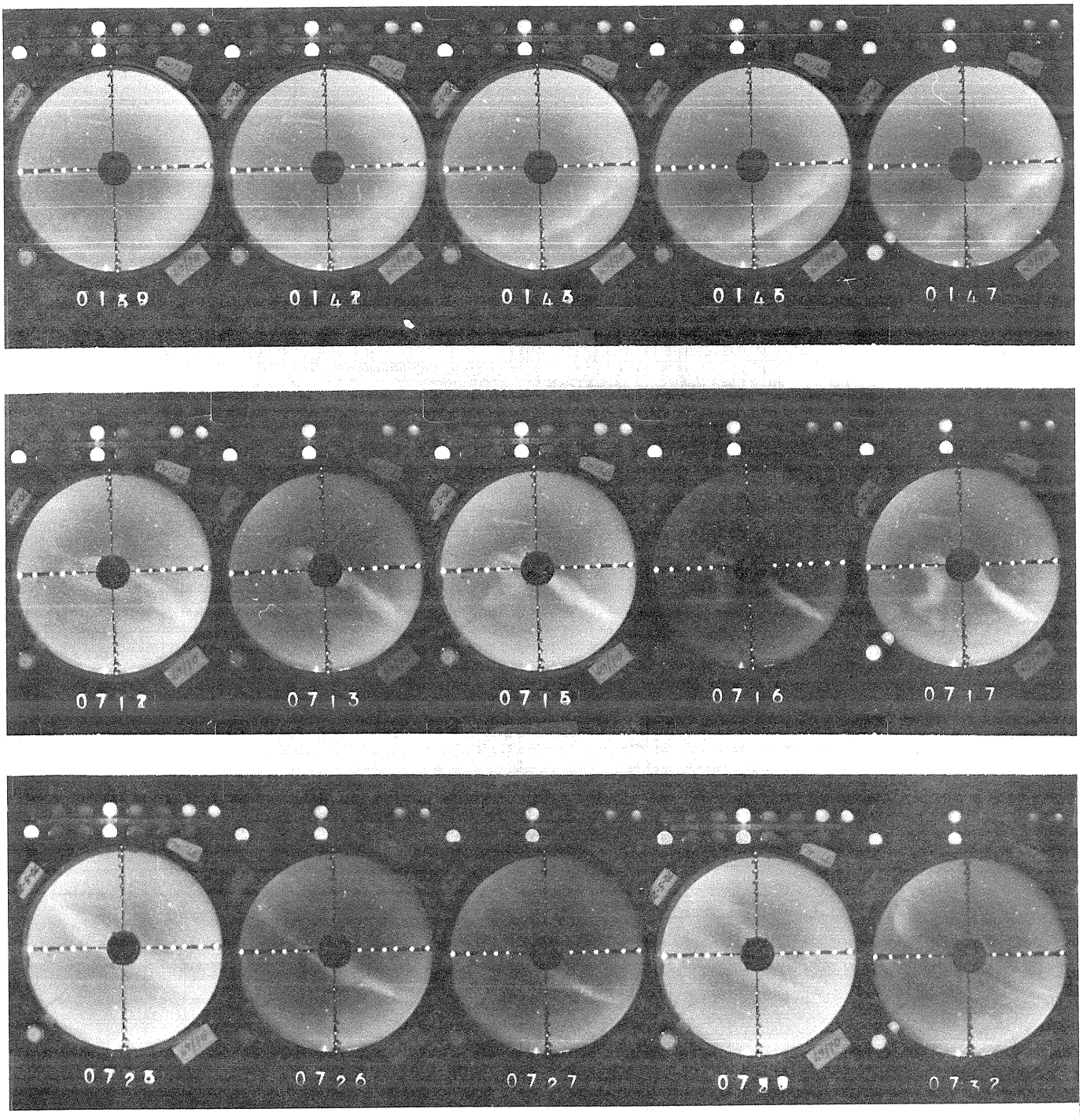

Fig. 6 A reproduction of the all-sky camera film taken during March 9, 1970 at Geopole. Time in UT is indicated on each frame. Multiple exposure due to faulty camera operation is identified by multiple digits, i.e., frame at 0147 UT is the only single frame registered. All others are double exposed. North is at the right of each frame while east is at the bottom.

8 March. Except for a faint, fleeting aurora at about 0200 UT no aurora was observed. The observing period ended at about 1200 UT, prior to the magnetic storm sudden commencement at 1417 UT.

9 March. This was the most active night with regard to auroral activity during the period 6-10 March, with auroras present several times during the night. Usable data from the all-sky camera at Geopole were obtained on this day, and these will be the basis of the following description. In general the arcs were aligned along the sun-earth azimuth, a behavior in accord with that typically found for the polar cap [see, for example, Davis, 1960, 1962; or for Thule specifically, Danielsen, 1969]. Marked auroral activity was present during the periods from about 0140 to 0150 UT; 0210 to 0220 UT; 0345 to 0355 UT; 0610 to 0620 UT; and through most of the period from 0645 UT until twilight effects became too strong at about 0810 UT.

During the period 0140 to 0150 UT an arc was present aligned from the NW to the SE and to the east of Geopole. A patchy aurora was present to the east of this arc in the northeast. At 0147 UT the arc definitely broke up. The zenith photometer records showed fluctuations in the period from 0145 to 0155 UT indicating the start of the breakup as somewhat earlier. An enhancement of the 3914 A N_2^+ emission also occurred at this time, indicating a connection of the breakup with particle precipitation. During the period from 0210 to 0220 UT, a faint arc was present in the zenith for the first two minutes, and a diffuse patch was present to the east which moved in a north to south direction during the period. The zenith photometer showed fluctuations of intensity from about 0206 to 0217 UT. The scanning spectrometer showed an enhancement of the 3914 A N_2^+ during the period 0200 to 0215 UT, indicating particle precipitation. At 0345 UT an arc was present near the horizon in the southeast quadrant and another, less well defined, parallel to this, closer to the station, and centered more to the north. The more prominent arc had moved out of the field of view by 0349 UT. A diffuse glow over much of the sky remained until at least 0355 UT. Enhancements of the major emissions are seen in the scanning spectrometer records for about an hour, with maxima at about 0400 UT. It is interesting to note that the 6300 A and 5577 A emissions do not peak at the same time. The 6300 A peak is at about 0350 UT with a lesser second peak at about 0400 UT, while the 5577 A peak is between 0402 and 0408 UT. The photometer records confirm this behavior. The 3914 A emission does not show any marked peaks at these times. At 0612 UT an arc becomes visible on the southern horizon a few degrees west of south. The arc moves to the north reaching an elevation angle of about 60° by 0619 UT and then breaks up about 0620 UT. A second arc is visible to the east. The 6300 A emission shows a noticeable but not very marked enhancement starting at about 0550 UT and continuing on until the intense auroral emission later in the evening. The photometer records do not show any strong enhancement. At 0645 UT an arc is visible in the southeastern quadrant near the horizon and this remains distinct until at least 0705 UT, with perhaps a slight movement to the southeast. At about 0658 UT a second arc becomes visible towards the southwest, aligned in a direction that would take it over or near the zenith if extended. This intensifies and moves across the zenith and towards the northeast horizon. By 0710 UT breakup has occurred with a suggestion of multiple arcs and with convolutions which are particularly marked in the southwestern half of the sky. This phase continues until at least 0720 UT. From 0730 UT until the end of observations multiple arcs, initially two and subsequently at least four, develop and extend across the zenith from the southwest to the northeast horizon. The auroral activity is reflected in strong intensity variations in both photometer and scanning spectrometer.

Discussion

The period preceding 6-10 March was one of much activity, both solar and magnetic [Solar-Geophysical Data, Sept. 1970; AFCRL Geophysics and Space Data Bulletin, 7 (No. 1), First Quarter 1970] so that the attribution of effects to specific causes is difficult. We note, however, an effect of the Polar Cap Absorption event, a possible effect of a solar flare, and the presence of luminosity fluctuations with time intervals similar to those previously observed in the auroral zone. We discuss these below.

A Polar Cap Absorption event began between 1025 and 1100 UT on March 7 [R. Cormier, private communication], presumably resulting from the class 2B or 3B flare which occurred at about 0140 UT on that date. The PCA was a moderate one, lasting at most two days with a maximum absorption of the order of 5 dB. A geomagnetic storm of unusual intensity and short duration began at 1417 UT on 8 March [Akasofu, private communication]. Because of the short duration of the PCA, the twilight conditions over much of the observational period, and the overall disturbed character of the period, it is not possible to compare spectral intensities with the course of the PCA for more than two or three points. The 6300 A emission intensity was used to eliminate short term disturbed periods (of the order of 1-2 hours or less) since the post-twilight decay served as a readily apparent base line. The intensities for the remaining times for which the solar depression angle was greater than 17° were then averaged for the 5577 A, 6300 A, 3914 A and 4278 A emissions. These are listed in Table 1 together with the times and the riometer absorptions for these periods. Some N_2^+ emission was present on 7 March following the flare but preceding the PCA onset. This, together with a barely noticeable riometer absorption, is indicative of some particle precipitation during this period. N_2^+ emission was definitely present during the PCA of 8-9 March, and the decline of intensity on the 9th is consistent with the much reduced riometer absorption on that date. The ratio of the two N_2^+ emissions

was at the low end of the normal range found in aurora, but the experimental values are not sufficiently reliable to distinguish between different modes of excitation, and the lowness of the ratio may indicate experimental error in scaling. The 5577 A and 6300 A intensities are higher on the 8th than on the days preceding or following, and this is also consistent with the anticipated correlation with the PCA. A quantitative estimate of the effect, however, cannot be made because of the disturbed character of the period preceding the PCA and the consequent difficulty of establishing a reference level of intensities. The intensities themselves are relatively low, indicating a low particle flux, consistent with the moderate character of the PCA shown by the riometer records. If we take the reference level for the N_2^+ as zero, then the intensities on the 8th and 9th, taken together with the riometer absorptions, indicate a strong softening of the energy spectrum from the 8th to the 9th [see, for example, Hultqvist, 1969, p. 79, for a discussion of the use of concurrent riometer and luminosity data as a measure of hardness].

Table 1

Emission Intensities 6-9 March 1970

Date	Time Period	Emission Intensities				Riometer Absorption
		5577	6300	3914	4278	
6	0300-0430	136	166	--	--	0
7	0420-0540	82	144	<10	<10	0.1-0.2
8	0300-0330	135	280	55	25	2.1-2.3
9	0415-0605	97	179	42	17	0.2-0.3

The largest solar flare during the period began at about 0140 UT on March 7, ended between 0300-0400 UT, and had its maximum phase at about 0150 UT. The 6300 A photometric record shows an increase beginning at about 0149 UT, a maximum at about 0150 UT, then a decrease for about 20 seconds followed by a slow increase to the maximum for the entire period at about 0155 UT, followed by a slow decrease with a return to the original level at about 0200 UT. The 5577 A intensity shows a similar behavior. The initial increase is of interest because it occurs at the same time as the maximum of the solar flare. The solar depression angle at this time was about 15°, corresponding to a shadow height of about 225 km. Allowance for screening by the long path length in the lower atmosphere might rule out a direct effect, depending on the screening height for the appropriate radiations. Another possible mechanism would involve the production of energetic photoelectrons at greater heights and their downward movement along the magnetic field lines. We have not investigated the various possibilities and point out here only the concurrence of the intensity increase with the solar flare maximum, and the possibility of their causal connection. Similar increases are also observed in the absence of flares, however, and caution must therefore be exercised in this attribution. A search for flare-connected increases of intensity would be of interest but we have not yet attempted this.

Luminosity fluctuations of the order of seconds to minutes were observed on a number of occasions. On some occasions, notably on 9 March, these are definitely associated with the presence of auroral activity. The appearance of the fluctuations is similar to published reports of irregular geomagnetic micropulsations. It seems likely to us that the luminosity fluctuations are due to fluctuations in the flux of low energy electrons, as would be true of the Pi micropulsations. The use of the same nomenclature for these luminosity fluctuations as is used for micropulsations, as suggested by Campbell [1970], appears to us to be useful. It would also seem worthwhile to determine whether they are or are not correlated with the micropulsations, and whether, if so, the origin is in the region of open or closed field lines. Heacock, Hessler and Olesen [1970] have proposed that periodically-structured Pc 1 micropulsations originate outside the polar cap and travel in an F-layer horizontal waveguide. They have also given examples to show that for polar substorms, at least, no persistent relationship is found between Thule (Qanaq) micropulsations and those in the auroral oval. They also find some types of micropulsations which originate mainly on polar cap field lines or in the polar ionosphere. We feel that the period 6-10 March 1970 would provide a good opportunity to separate the possible sources, whether from polar field lines or by ducted travel from the oval, and to compare these with the luminosity fluctuations.

Acknowledgments

We wish to thank Mr. Ray Cormier, Air Force Cambridge Research Laboratories for the provision of riometer absorptions; Dr. K. Lassen, Danish Meteorological Institute, for the use of all-sky

camera film from Thule (Qanaq); personnel of the Polar Atmospheric Processes Branch, AFCRL, for operation and maintenance of the optical equipment at Geopole; and personnel of Sea Farm, Inc. for reduction of intensities from the scanning spectrometer data.

REFERENCES

CAMPBELL, W. 1970 Rapid Auroral Luminosity Fluctuations and Geomagnetic Field Pulsations, J. Geophys. Res., 75, 6182-6208

DANIELSEN, C. 1969 Auroral Observations at Thule, Danish Meteorological Institute Geophysical Papers, March

DAVIS, T. N. 1962 The Morphology of the Auroral Displays of 1957-1958, J. Geophys. Res., 67, 75-110

DAVIS, T. N. 1960 The Morphology of the Polar Aurora, J. Geophys. Res., 65, 3497-3500

HEACOCK, R. R., V. P. HESSLER and J. K. OLESEN 1970 The 2-0.1 Hz Polar Cap Micropulsation Activity, J. Atm. Terr. Phys., 32, 129-138

HULTQVIST, B. 1969 Auroral and Polar Cap Absorption in Atmospheric Emissions, B. McCormac and A. Omholt, Eds., Van Nostrand Reinhold, pps. 73-90

LASSEN, K. 1967 Polar Cap Aurora in Aurora and Airglow, B. McCormac, Ed., Reinhold Publ. Co., pps. 453-464

LASSEN, K. 1969 Polar Cap Emissions in Atmospheric Emissions, B. McCormac and A. Omholt, Eds., Van Nostrand Reinhold, pps. 63-71

MONFILS, A 1968 Spectre Auroraux, Space Sci. Rev., 8, 804-845; see particularly pps. 832 ff

PAL, S. R. 1968 Studies of Night Airglow, Ph. D. Thesis, the Gujarat Univ., India

SANDFORD, B. 1967 High Latitude Night Sky Emissions in Aurora and Airglow, B. McCormac, Eds., Reinhold Publ. Co., pps. 443-452

SILVERMAN, S. 1970 Night Airglow Phenomenology, Space Science Reviews, in press

"Zenith Airglow Intensity at Dodaira Station, Tokyo Astronomical Observatory"

by

World Data Center-C2 for Airglow
Tokyo Astronomical Observatory
Mitaka, Tokyo, Japan

The zenith airglow intensities in Rayleigh for λ5577A and λ6300A are shown in the following figures for March 5, 6, 7 and 8, 1970 as observed at the Dodaira station (N36°00', E139°12') of the Tokyo Astronomical Observatory. These data were furnished by World Data Center-C2 for Airglow.

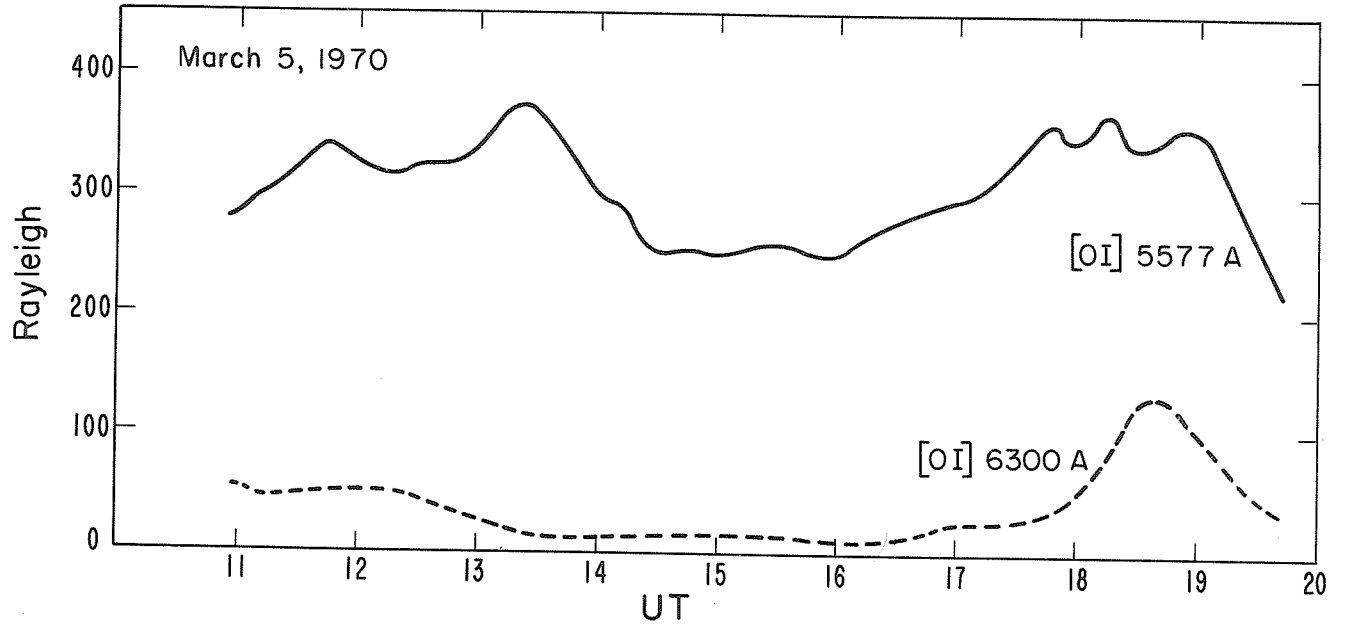

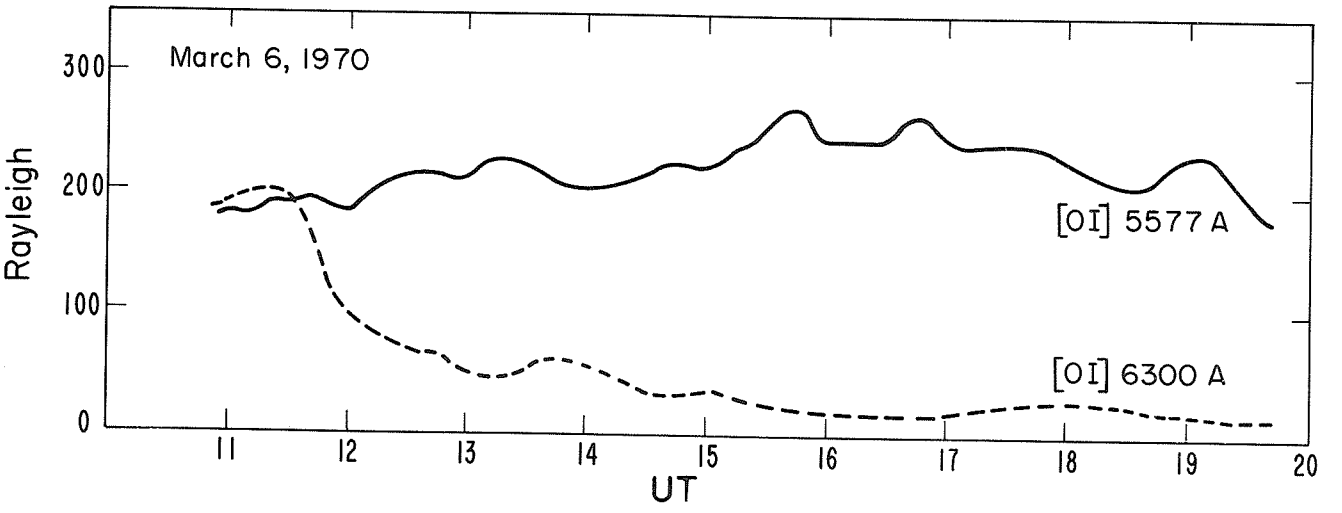

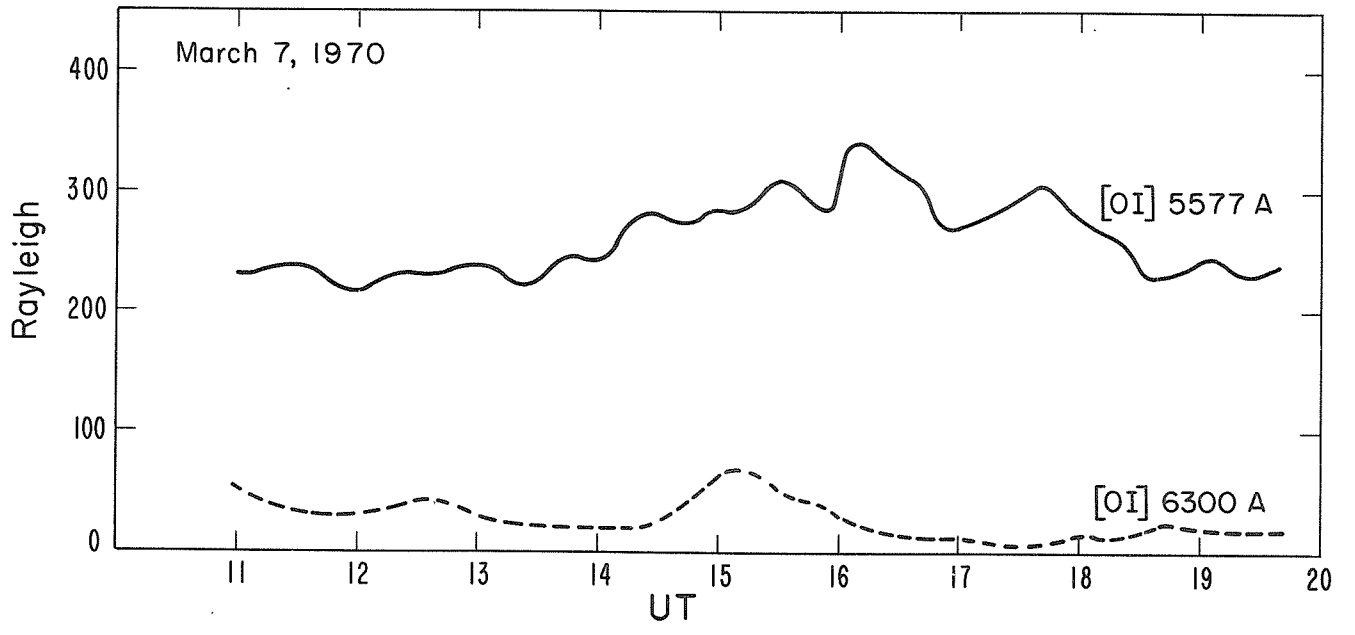
March 7, 1970
Rayleigh
400
300
200
100
0
[OI] 5577 A
[OI] 6300 A
11
12
13
14
15
16
17
18
19
20
UT

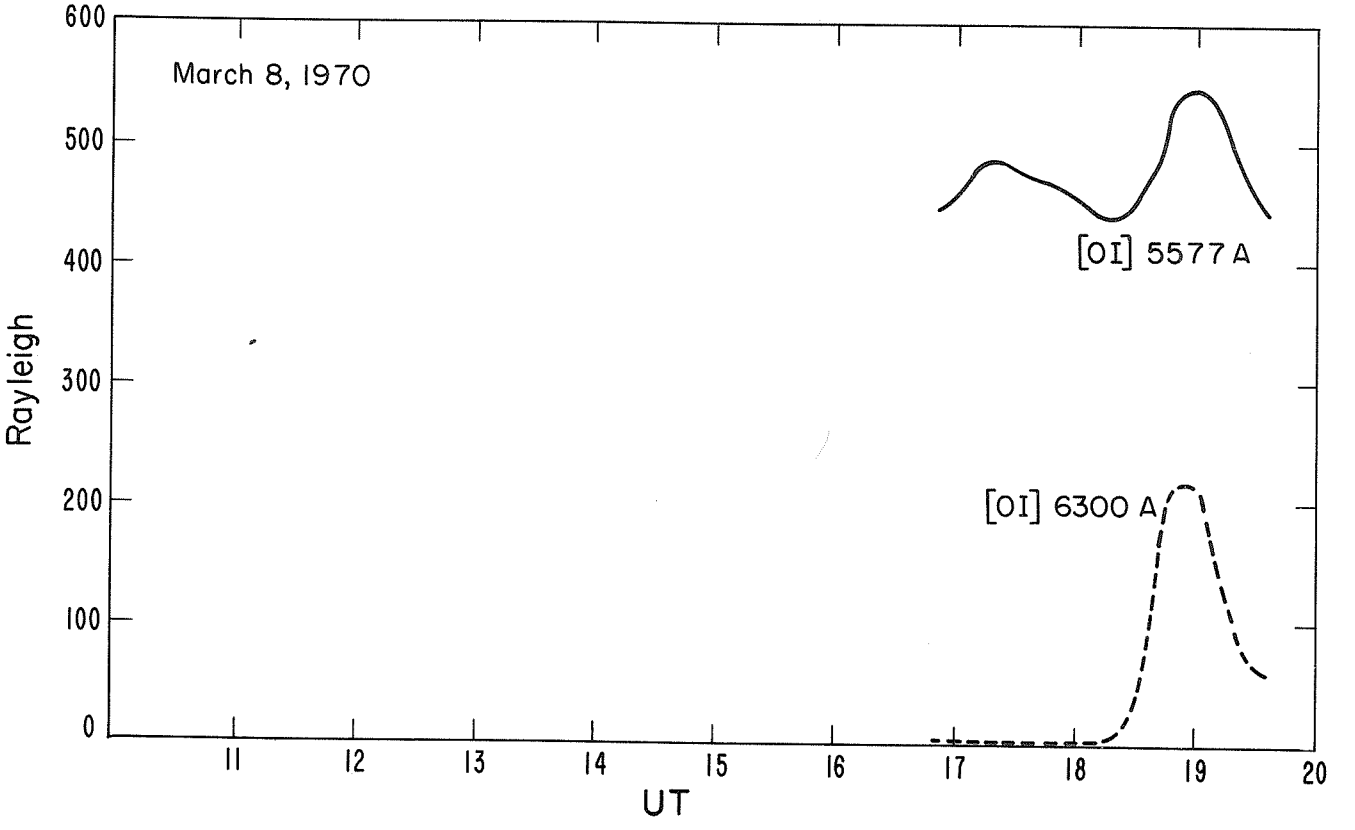
March 8, 1970
Rayleigh
600
500
400
300
200
100
0
[OI] 5577 A
[OI] 6300 A
11
12
13
14
15
16
17
18
19
20
UT

"Minor Emissions in the SAR Arc of March 8/9, 1970"

by

R. J. Hoch and L. L. Smith
Battelle Memorial Institute
Pacific Northwest Laboratories
Richland, Washington

and

K. C. Clark
Physics Department
University of Washington
Seattle, Washington

Stable Auroral Red (SAR) arcs have in recent years been monitored by Hoch and Clark [1970] from Rattlesnake Mountain at Richland, Washington, where the magnetic L coordinate at 400 km is L = 2.9. Although the red oxygen doublet at 6300, 6364A (1.96 ev excitation) is the prominent and often only spectral feature, the possibility of other auroral emissions carries diagnostic interest far out of proportion to relative intensity. In particular, one seeks arc-associated enhancements of atomic oxygen at 5577A (4.17eV), molecular nitrogen ions at 4278A (18.7 eV), atomic nitrogen at 5199, 5201A (2.37 eV), and, for reasons of anti-correlation, the atomic hydrogen Balmer Lines at 6563A and 4861A.

In normal mid-latitude auroras these emissions are routinely detected by use of meridian and image intensifier spectrographs and by scanning interference filter photometers, and all these techniques have recorded the major red emission in SAR arcs. An example of a SAR-arc spectrum in the magnetic meridian plane is shown in Figure 1, which is from the March 23/24, 1969 spectra obtained at Richland. The selective enhancement of the red doublet is seen in the overhead arc just south of zenith, and poleward the normal aurora is also evident. While the separation in latitude of the SAR arc and the polar aurora is well documented [Hoch and Clark, 1970; Ichikawa and Kim, 1969], there is usually some overlap of background emission into the region occupied by the SAR arc. This is the principal reason why observed intensities of weaker features often cannot with certainty be ascribed to the SAR-arc. Intense arcs provide the surest opportunities to do so, and all-sky photometric scans are especially valuable in revealing where arc-associated emission may occur.

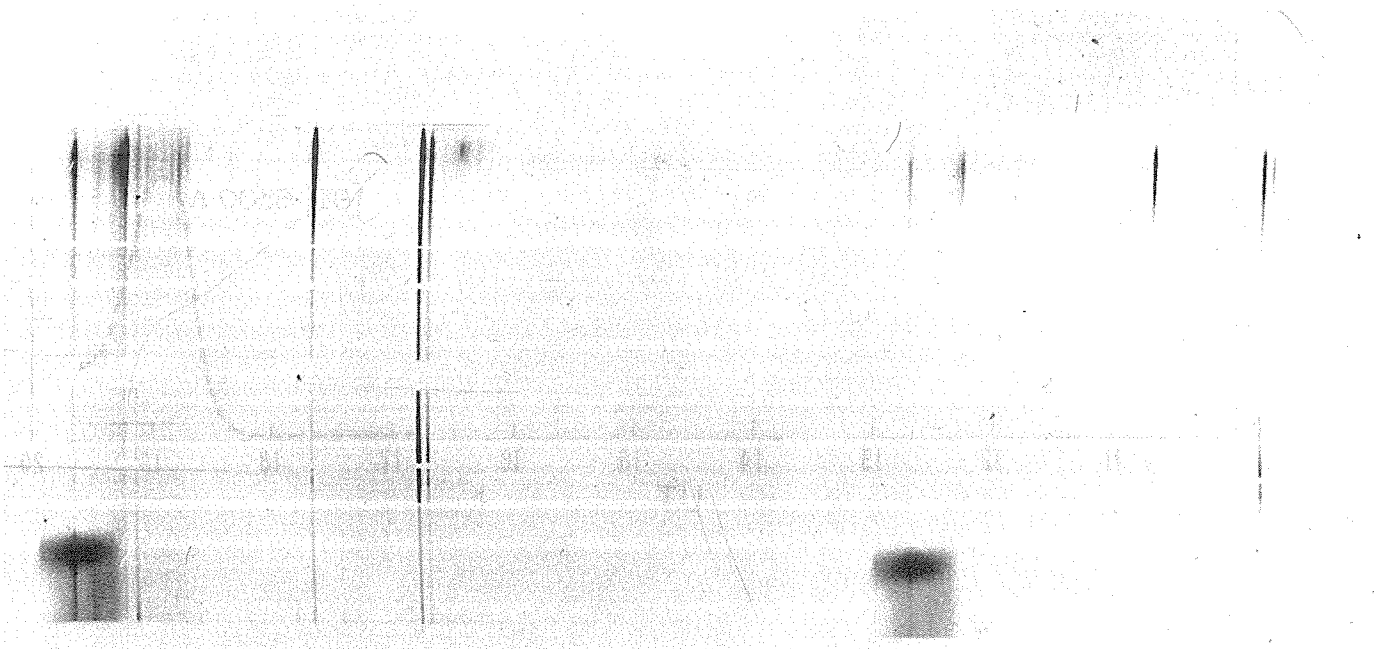

Fig. 1. Spectrum of SAR-arc in Richland magnetic meridian, 1953 PST - 23 March 1969. Exposure times 25 and 5 minutes. Red doublet is at right of visible spectrum; north horizon is at top. Disregard enhanced exposure patch at lower left.

Hydrogen arcs are known to be lower and more poleward than SAR-arcs, and triangulation spectral measurements from the 600 km Richland-Banff baseline [Clark et al., 1970] have demonstrated the separation. The weak forbidden atomic nitrogen doublet is very difficult to localize within a SAR-arc because of diffusion and low intensity; one report of it has been given by Carleton and Roach [1965]. Molecular nitrogen ions have also produced weak but identifiable emission, as will be reported here.

The red and green line intensities in oxygen, however, remain as principal data. The SAR-arc of March 8/9, 1970 yields good measurements of arc-localized increases above the broad background. This arc was quite intense following the end of astronomical twilight, reaching 3.5-4.0 kR at the observing times of 1950-1953 PST. Figure 2 illustrates photometric records of this arc made in almucantar sweeps. Absolute calibrations are obtained by use of carbon-14 standard and known star crossings. Final data include corrections for zodiacal, galactic, and background light, for atmospheric extinction, and for Van Rhijn brightening appropriate to a layer at 400 km.

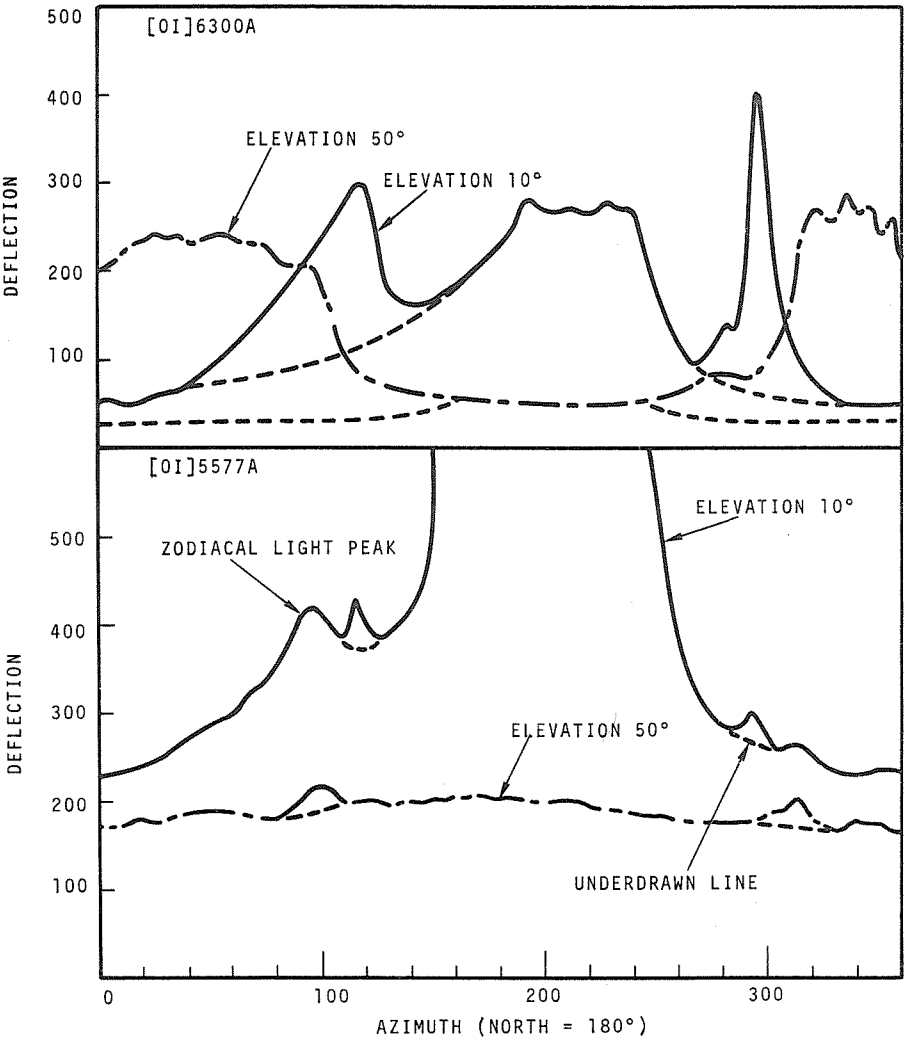

Fig. 2. Chart records of red and green SAR-arc emissions in 10° and 50° almucantar photometer sweeps. 1950 PST - 8 March 1970.

Table 1 tabulates the corrected intensities in the arc I_a at various elevation angles, the correction factors used for extinction and layer geometry, and the resulting ratio of red to green intensities. This ratio is seen to remain about constant at

$$\frac{I_a(6300)}{I_a(5577)} = 26 \pm 3$$

over the range of elevation angles for which arc measurements of the green line were valid. At other times $I_a(5577)$ was below sure detectability, while $I_a(6300)$ remained large.

Table 1

Table of corrected intensities in kR, extinction and geometry correction factors, and intensity ratios. 1950 PST - 8 March 1970.

Elevation angle	10°E	15°E	20°E	30°E	50°E	50°W	30°W	20°W	15°W	10°W
$I_a(5577)$	0.153	0.176	0.138	0.129	0.142	-	-	-	-	-
$I_a(6300)$	3.88	4.09	3.99	3.71	3.32	3.00	2.94	2.39	2.20	2.13
$\exp(\tau_\lambda m(z))$ λ=5577	2.48	1.87	1.61	1.39	1.24	1.24	1.39	1.61	1.87	2.48
λ=6300	1.75	1.46	1.34	1.22	1.14	1.14	1.22	1.34	1.46	1.75
h = 400 km V(z,h)	2.66	2.40	2.14	1.72	1.26	1.26	1.72	2.14	2.40	2.66
$\frac{I_a(6300)}{I_a(5577)}$	25	23	29	29	23	-	-	-	-	-

The occasional nature of the 5577A arc emission is to be emphasized. On the previous two nights of March 6/7 and 7/8 a SAR-arc was detected, being perhaps a single arc lasting the three nights and occurring in unision with the main phase of a single geomagnetic storm. On the first two nights $I_a(6300)$ was only a few hundred Rayleighs, and $I_a(5577)$, if present, was below limits of certainty with respect to airglow and polar aurora. The red-to-green ratio, which came as low as 26:1 on the third night, is to be compared with 80:1 reported by Barbier [1960] in an even brighter arc, with 10:1 and 4:1 reported by Schaeffer [1969] as lower limits with weak intensities, and with the comment of Roach [1970] that many attempts to record $I_a(5577)$ have failed to yield even 80:1 when the arc was bright enough to permit possible detection of both intensities. The extreme case of monochomatic excitation of 5577A at mid-latitudes is the purely green arc reported by Manring and Pettit [1957] over New Mexico; its production has remained quite puzzling.

On the night of March 8/9, 1970 there was also measured a very weak arc of purely 4278A (N_2+ 1st neg. bands) equatorward in elevation angle relative to the principal SAR arc. This is of interest because of its high (18.7 eV) excitation level. Corrections for background and geometry are difficult. The measured intensity $I_a(4278)$ = 5R is here reported. This is the measured intensity in a 25A band centered at 4278A. To deduce from this measurement the total emission in the first negative bands would require an estimate of the N_2+ion temperature. We believe this to be the first mid-latitude observation of the 4278A emission in a SAR arc.

We now consider what these data may mean in regard to the excitation processes in a SAR-arc. It is useful to interpret these data in terms of thermal electron energy distributions. However, it must be kept in mind that intensity measurements at only two or three wavelengths cannot establish any more than the gross characteristics of the actual distribution.

Relating the light output to an electron energy distribution requires straightforward consideration of atmospheric composition and the cross sections for excitation and quenching. The typical atmosphere near 400 km under conditions of high solar activity [CIRA (1965), mod. 9] is assumed, and the temperature of 1200°K which is used for neutral scale heights is that measured by Hays et al. [1969] for a SAR arc. Excitation cross sections are taken from the calculations of Smith, Henry, and Burke [1967]. Recent reviews of quenching collisions given by Hunten and McElroy [1966] and Peterson and Van Zandt [1969] lead to the conclusions that at 400 km deactivation is negligible for $O(^1S)$ (5577A) but amounts to about 37 percent for $O(^1D)$(6300,6364A). The latter figure is based upon a quenching rate constant of $\beta = 7.5 \times 10^{-11}$ cm^3 sec^{-1} and a density of $n(N_2) = 4.7 \times 10^7$ cm^{-3}. Allowance is made for temperature and density changes through the vertical extent of the typical SAR-arc.

It could be possible to account for the observed $I_a(6300)$ using hot ambient electrons at a temperature about 4000°K and a density somewhat above 10^5 cm^{-3}. Roble [1969] reached a similar conclusion. The stability of emission at 6300A suggests that the electron temperature and density do not fluctuate greatly. However, the rather sporadic occurrence of $I_a(5577)$ poses different requirements, which are not reasonably satisfied by readjusting a simple thermal distribution. As shown in Figure 3, the observed red-to-green ratio, if produced by a Maxwellian distribution, would require an electron temperature of about 9000°K. The disparity between these two temperatures is too large to be reconciled by accentuating thermal gradients in the arc or by decreasing the electron density, although there is occasion for some adjustment. It is more reasonable to postulate the occurrence of an appropriate high energy tail on the principal electron distribution.

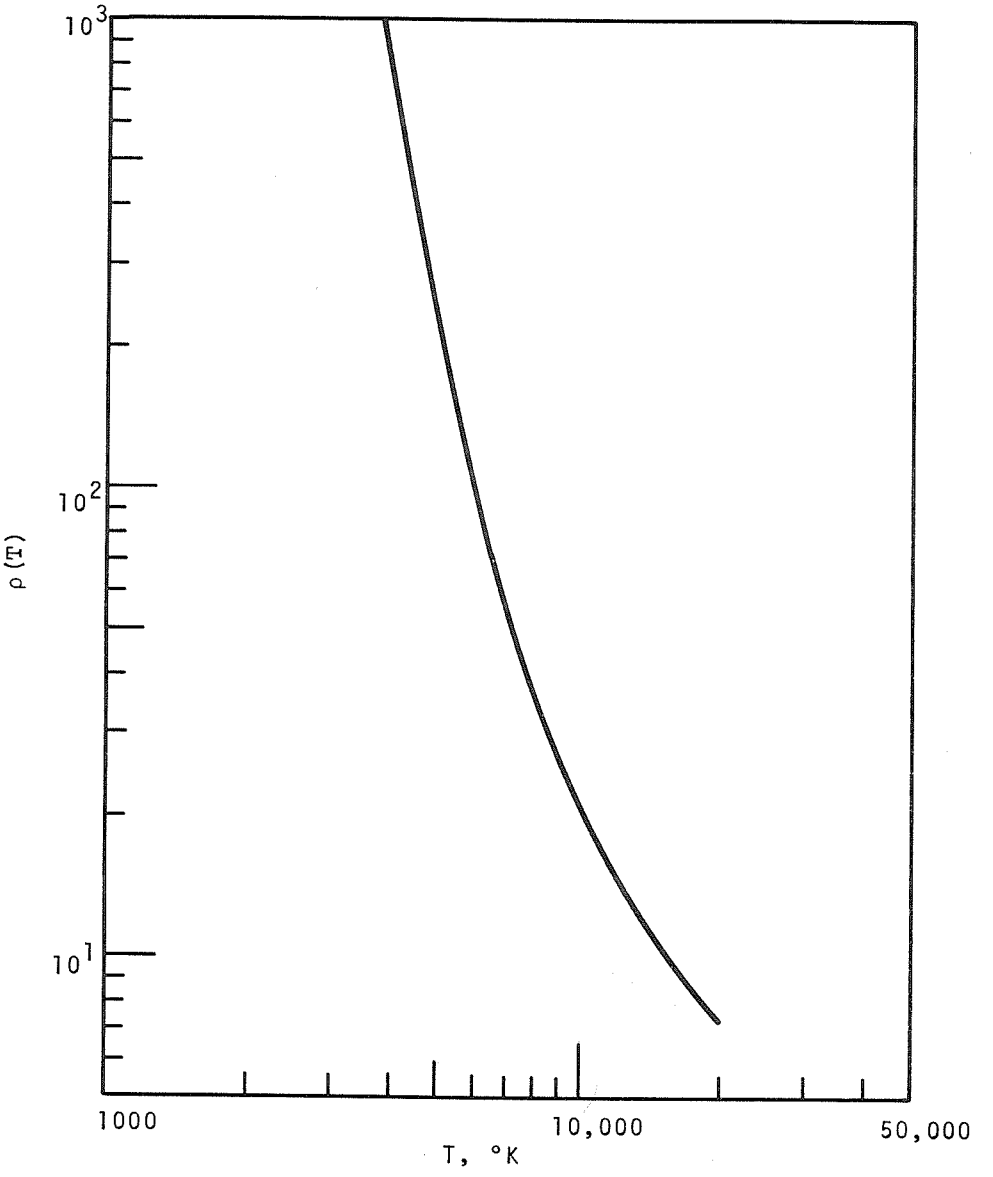

Fig. 3. Calculated red-to-green ratio including altitude dependence of volume emission rate.

To characterize this distribution, it is sufficient to use at 400 km an electron density of 1.3 x 10^5 cm^{-3} at a temperature of 4200°K and to replace the function above 2.0 eV by a second thermal distribution at 9000°K, preserving continuity at the junction. Only about 1 percent of the electrons are involved in the high energy tail, but the increase in population is adequate to provide the observed intensity. This combined distribution is illustrated in Figure 4 and is presented as a consistent, though not unique, description. The total content is satisfied by the cooler portion below 2.0 eV, while the minor but warmer fraction above this energy influences the intensity ratio critically through its temperature. Very valuable evidence concerning fluctuations postulated at the higher energies would be afforded by direct measurement of the flux of hot electrons, as might be made with incoherent radiofrequency backscatter techniques, if time and place could coincide. It is not the purpose of this report to speculate on the correct cause of the varying high energy component. Its production could easily be made a part of any injection model, while the location of the SAR-arc would remain stable at the latitude of the plasmapause.

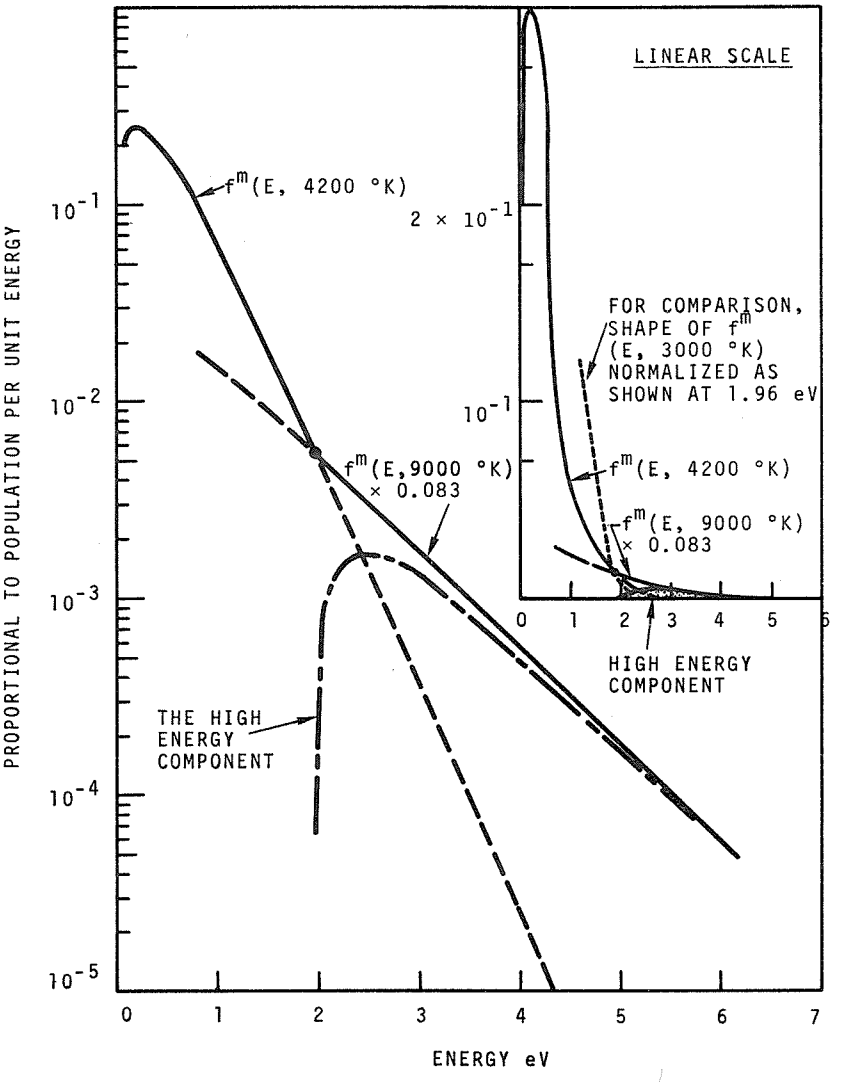

Fig. 4. Composite electron energy spectrum at 400 km consisting of Maxwellian distributions at 4200°K below 2.0 eV and at 9000°K above 2.0 eV.

Acknowledgement

These studies have been supported by the U.S. Atomic Energy Commission contract AT(45-1)-1830 and by the National Science Foundation grants GA-3914, 14406.

REFERENCES

BARBIER, D. 1960 L'arc auroral stable, Annales. Geophys., 16, 544.

CARLETON, N. P. and J. R. ROACH 1965 Spectrographic observations of a mid-latitude red auroral arc, J. Geophys. Res., 70, 1262.

CLARK, K. C., R. J. HOCH and L. L. SMITH 1970 Spectral data on SAR arcs, EOS Trans. Amer. Geophys. Union, 51, 791, SPA 50

1965 CIRA 1965 (Cospar International Reference Atmosphere), North-Holland Publishing Co., Amsterdam, 1965

HAYS, P. B., A. F. NAGY and R. G. ROBLE 1969 Interferometric measurements of 6300A Doppler temperature during a magnetic storm, J. Geophys. Res., 74, 4162.

HOCH, R. J., E. MAROVICH and K. C. CLARK	1968	Reappearance of a stable auroral red arc at mid-latitudes, J. Geophys. Res., 73, 4213.
HOCH, R. J. and K. C. CLARK	1970	Recent occurrences of stable auroral red arcs, J. Geophys. Res., 75, 2511.
HUNTEN, D. M. and M. B. MC ELROY	1966	Quenching of metastable states of atomic oxygen by molecular oxygen and nitrogen, Rev. Geophys., 4, 303.
ICHIKAWA, T. and J. S. KIM	1969	Observations of M arc at Moscow, Idaho, USA, J. Atmos. Terr. Phys., 31, 547.
MANRING, E. R. and H. B. PETTIT	1957	A study of the airglow emission at 5577, 5890 and 6300A with a photometer of high spectral purity, The Threshold of Space, Pergamon Press, 58-64.
PETERSON, V. L. and T. E. VAN ZANDT	1969	$O(^1D)$ quenching in ionospheric F-region, Planet. Space Sci., 17, 1725.
ROACH, F. E.	1969 1970	Personal communication. Personal communication.
ROBLE, R. G.	1969	A theoretical and experimental study of the stable mid-latitude red arc (SAR-arc), Ph.D. thesis, University of Michigan, Ann Arbor, Michigan.
SCHAEFFER, R. C.	1969	Personal communication.
SMITH, K., R.J.W. HENRY and P. G. BURKE	1967	Calculation on the scattering of electrons by atomic systems with configurations 2_p^q, Phys. Rev., 157.

"Airglow Variations, Mid-Latitude Red Arc around March 8, 1970"

by

J. Christophe and G. Weill
Institut d'Astrophysique
98bis Boulevard d'Arago
75 - Paris 14° - France

This report presents some of the data obtained by the French network of airglow stations on March 8, 1970, along the Meridian sector of Europe and Africa. The stations used here and corresponding radiations observed are as follows:

Table 1

Station	Country	Latitude	Longitude	Colors observed							
				7250	6300	6100	5893	5577	5200	4278	3670
Haute Provence	France	N43.9°	E 5.7°	x	x	x	x	x	x	x	x
Sde Boker *	Israel	N30.9°	E34.8°	x	x	x	x	x	x		
Adi-Ugri **	Ethiopia	N14.9°	E38.8°	x	x	x	x	x	x		
Zeekoegat	South Africa	S33.1°	E22.5°	x	x		x	x	x		x

* Operated in cooperation by the Department of Environmental Sciences, University of Tel Aviv, Ramat-Aviv, Israel.

** Operated in cooperation with Geophysical Observatory, Hailé Sélassié I University, Addis Ababa, Ethiopia.

Data from a number of other stations (Indian Ocean, Antarctica) are not yet available. In the period March 6-10, the weather was favorable on March 6, 7 and 8, as shown in Table 2.

Table 2

Station	Mar 6	Mar 7	Mar 8	Mar 9	Mar 10
Haute Provence	1	3	2	2	3
Sde Boker	1	2	2	3	3
Adi-Ugri	1	1	2	3	3
Zeekoegat	1	1	1	1	1

1 = good
2 = partly good
3 = bad

The bulk of the data presented here come from 9 lines of observations; their intersections with the emission layers at two assumed altitudes are summarized in Table 3.

This period was marked by the occurrence of exceptional events in the night-sky emission at all stations during the night March 7 to 8. These events included the brightest mid-latitude aurora seen at Haute-Provence since July 8, 1958, a broad and intense arc of emission at mid-northern latitude, and a considerable airglow enhancement of 6300 Å radiation over a wide range of middle and low latitudes. These events are unmistakably connected to the development of the geomagnetic storm.

Table 3

Station	Zenithal Distance	Azimuth	Line	Coordinates at 100 km		Coordinates at 300 km	
Haute - Provence	75°	North	1	N46.91°	E5.72°	N51.61°	E5.72°
	46°	North	2	N44.83°	E5.72°	N46.53°	E5.72°
	75°	South	3	N40.93°	E5.72°	N36.23°	E5.72°
Sde Boker	75°	North	4	N33.91°	E34.83°	N38.60°	E34.83°
	75°	South	5	N27.92°	E34.83°	N23.22°	E34.83°
Adi-Ugri	75°	North	6	N17.87°	E38.82°	N22.57°	E38.82°
	75°	South	7	N11.81°	E38.82°	N7.19°	E38.82°
Zeekoegat	75°	North	8	S30.12°	E22.50°	S25.41°	E22.50°
	75°	South	9	S36.08°	E22.50°	S40.79°	E22.50°

Mid-Latitude Aurora

Observations started at Zeekoegat, in the geomagnetically conjugate area of Haute-Provence, at 1807 UT (Astronomical twilight at 1823 UT.) Auroral activity began to develop, in line 9 (see Table 3) at about 1900 UT, reached a peak of 7000 rayleighs (slant) for the red lines 6300 about 2045 UT, and decreased quasi-exponentially with a time constant of about 90 minutes until 2400 UT.

At Haute-Provence, clouds interfered with measurements along lines 1 and 3 until 2100 UT; the aurora was then observed to decrease monotonically on line 1 until 2400 UT. Slant intensities on line 1 were as in Table 4.

March 8, 1970 - Slant intensities of the mid-latitude aurora about 2100 UT (line 1).

Table 4

Radiation	6300 (OI)	5577	4278
Time	2053 UT	2057 UT	2109 UT
Intensity	26,120	1720	670

The cloud situation was better along line 2 and measurements started about astronomical twilight at 2005 UT. The auroral maximum occurred at 2052 ± 2 min UT, and was marked by a considerable emission of N_2^+ 1st negative, observed in the near UV. The corresponding enhancement was 100 R in 5577 radiation and 400 R in 6300 Å, (Figure 1). Line 2 at 2052 UT crossed the earth shadow at 1050 km, latitude 51.5° North. The great N_2^+ enhancement was likely to originate in the sunlit region of the aurora. It was reported from the same station (Nguyen Huu Doan, 1970) that this aurora was visible with the naked eye in the North - North-East from 2045 till 2130 UT as vertical red rays with draperies. The aurora was visible, at its maximum, up to an elevation of 40°.

At 2100 UT, the 6300 intensity along lines 1 and 2 started increasing again to reach its major peak of 1900 R at 2130 UT. This peak was not noticeable on any of the other radiations, nor could it be detected in any radiation in the conjugate area (lines 8 and 9) or at the stations of lower latitude. The scanning photometers at Haute-Provence detected no latitude maximum in the range 36° to 52° N in the early part of the night, and the 2130 UT maximum of red line intensities, despite its spectral purity resembling that of a Mid-latitude Red Arc, cannot be identified with such a phenomenon, but rather with a mid-latitude red aurora.

Mid-Latitude Red Arc ?

From 2230 UT March 8 until 0330UT March 9 the 6300 intensity was enhanced along line 3. The enhancement peaked at 600 R about 24 hours. It was clear from the scanning photometer records that the enhancement had an elongated arc-like structure. The arc was centered on latitude 40° N and had a width at half intensity of 600 km, assuming a 300 km altitude. It was separated by a marked

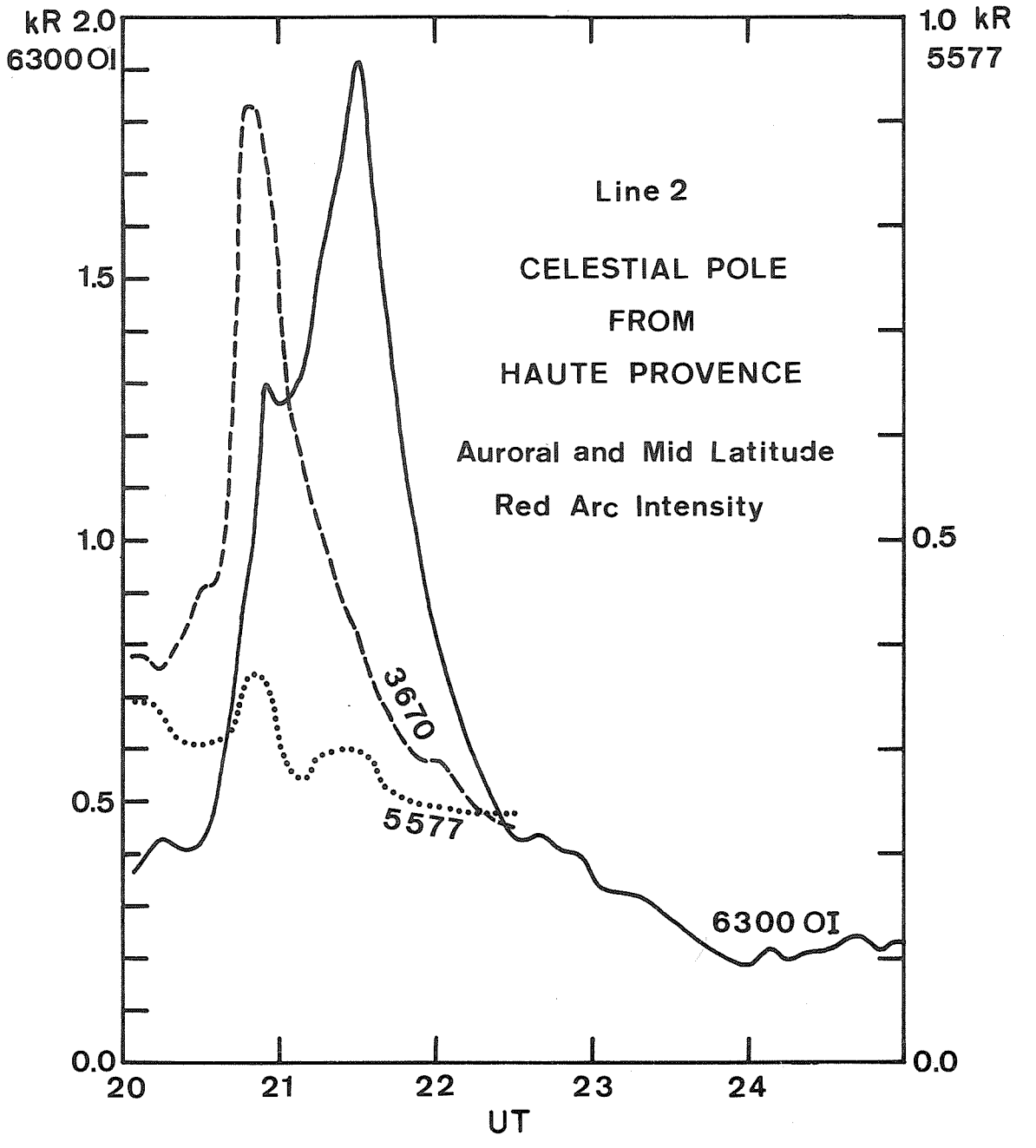

Fig. 1. Mid-latitude aurora March 8, 1970

trough from the poleward's auroral enhancement which subsided all night but was then about its minimum. The latitude-time map in Figure 2a was derived from the scanning photometer.

A concommitant enhancement of about 10 Rayleighs occurred for the NI doublet 5198 - 5200 Å, together with a 100 Rayleighs enhancement of the OI Green line. On the basis of these spectral characteristics, we would attribute to an effect of ionization drift to lower altitudes and subsequent faster recombinations. Unfortunately, the ionospheric data for this period and region are badly spoiled by spread F and cannot be analysed quantitatively.

A notable fact is that neither at the time of the arc maximum, nor at any other time throughout the night, could any arc-like structure be detected in the conjugate region of the Southern Hemisphere, (Figure 2b).

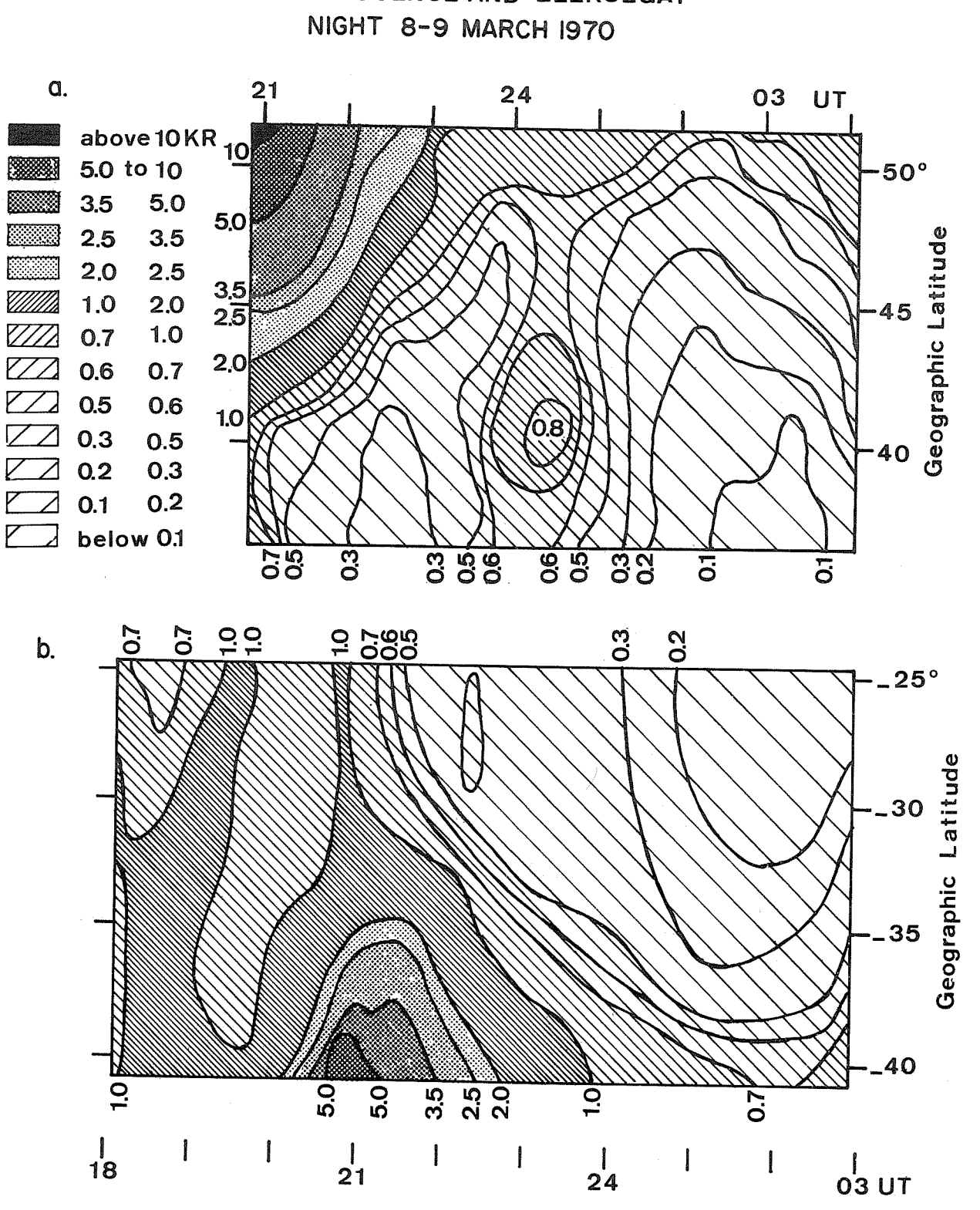

Fig. 2. (a) Latitude-time map within hemisphere derived from scanning photometer March 8-9, 1970
(b) Latitude-time map conjugate region of southern hemisphere.

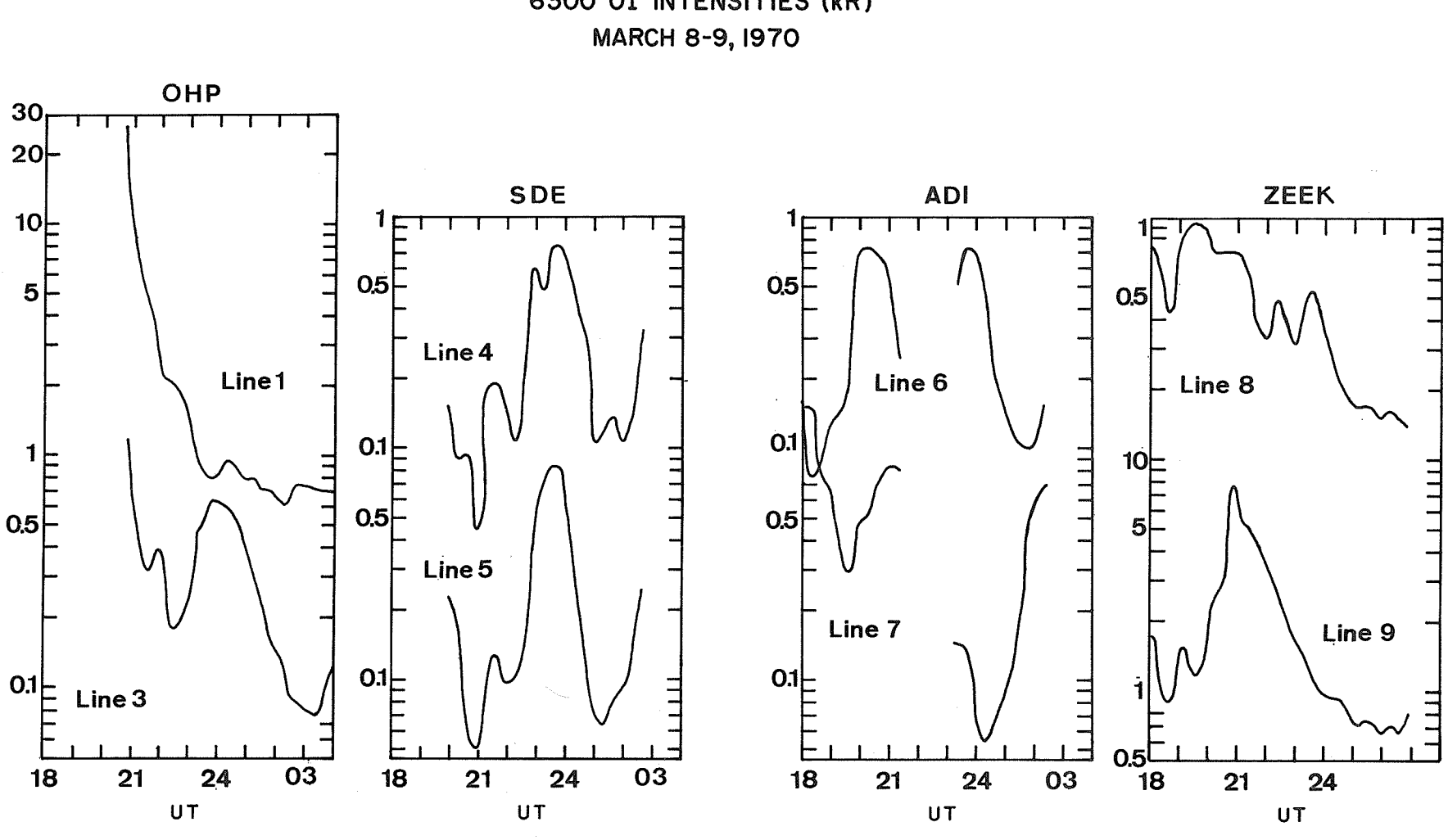

Fig. 3. 6300 OI intensities versus time for 8 of the 9 lines.

Low-Latitude Airglow Enhancement

At all stations, a marked relative maximum was recorded about 2337 UT ± 10 min, at least in some directions. This can clearly be seen in Figure 3, where 6300 OI intensities are plotted versus time for eight of the 9 lines. The enhancement appears to be controlled by Universal Time rather than local time. It was also detected on the green OI line and on the 5198-5200 NI doublet and the relative intensities of these emissions were not noticeably different from those observed in inter-tropical arcs. We believe that radiative recombination of O_2^+ is responsible for the enhancements. To account for it, a considerable amount of ionization must have been drifting into the atmosphere over a considerable range of latitudes. The latitude profiles of 6300 Å intensity are given for the four stations in Figure 4, for the night under study and for the reference night of March 6 to 7, about 2335 UT.

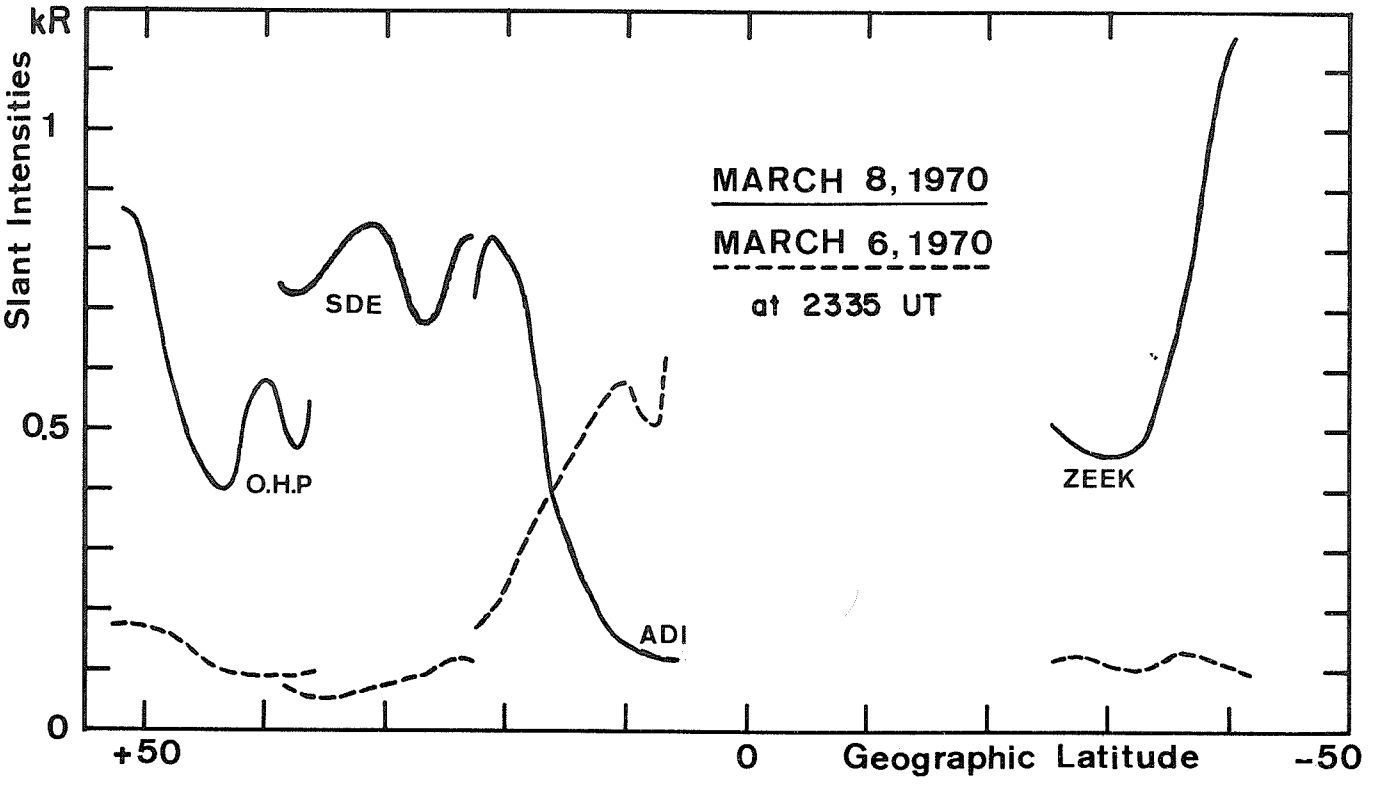

Fig. 4. Latitude profiles of 6300 Å intensity for the four stations for March 8 compared to March 6, 1970.

10. AURORA

"Polar Aurora Observation at Mt. Lomnicky Stit"

by

M. Rybansky
Astronomical Institute of the Slovak Academy of Sciences
Skalnate Pleso, Czechoslovakia

The polar aurora have been observed at Mt. Lomnicky Stit on March 8, 1970. There is a corona station at the peak of the mount (geographic coordinates λ = E 20° 18'15", ϕ = N49° 11'46") but unfortunately, it is not equipped to carry out such kind of observations. Therefore, it is possible to describe a visual observation only.

Geomagnetic latitude of the Mt. Lomnicky Stit is about 48° N and polar aurora of such outstanding intensity can be observed here only once per about ten years. At about 1900 UT the green aurora was seen on the north physical horizon, the astronomical twilight ended at 1845 UT. This picture did not change up to 2040 UT. At this time suddenly bright and red rays appeared. They were perpendicular to the horizon and climbed up to 50° above it. Time duration of a single ray was about two minutes. Illumination caused by the aurora was comparable with the illumination caused by the half-moon disk. The aurora faded out at about 2100 UT. Perhaps for half an hour the north horizon was still weakly shining.

The aurora have been probably caused by a strong flare which occurred in McMath region 10614 on March 7, 1970 at 0140 UT at S12 E10. Then the time interval between the flare and appearance of the polar aurora is 43 hours.

The picture below was taken at 2050 UT with exposure time of 20 seconds, diaphragm 1:2.8 on ORWO-NP 27 film. Except for polar aurora the stars up to 4th magnitude are visible. On the left side α, β and η Cas, on the right side α and η Cep. The villages on the foreground are situated at the boundary between Czechoslovakia and Poland.

Fig. 1. Polar aurora photographed from Mt. Lomnicky Stit on March 8, 1970, 2050 UT.

"Middle-Latitude Aurora of March 8-9, 1970 at Zvenigorod"

by

V. G. Sobolev, A. A. Kozlova, E. P. Kropotkina,
L. V. Simakova, Yu. L. Truttse, N. N. Shefov,
and O. T. Yurchenko
Institute of the Physics of the Atmosphere
USSR Academy of Sciences, Moscow

On the night of March 8-9, 1970, a strong aurora of III IBC was observed at the Zvenigorod Geophysical Observatory, the Institute of the Physics of the Atmosphere, USSR Academy of Sciences (ϕ = N55.7°, λ = E2^{h}27^m). During the same period a geomagnetic storm with sudden commencement occurred at 1715 MDT (Moscow Decree Time) (1415 UT) on March 8, 1970. According to the data of the Krasnaya Pakhra Magnetic Station which is the closest to the Zvenigorod Geophysical Observatory the storm maximum (K = 9) was observed within the interval of 2100 to 2400 MDT (1800 to 2100 UT).

Conditions for observations of the aurora were favorable. Although in the evening the western horizon was covered by light clouds, by night the sky became absolutely clear. The average coefficient of transparency in the range of 5000 to 6000 Å was 0.7. The observational conditions on the previous and next nights were approximately the same as on the night of the aurora.

Observation of the aurora emission in the range of 3200 to 7000 Å was conducted by patrol spectrographs SP-48 and SP-49 [Gerasimova and Yakovleva, 1956; Galperin et al., 1957] which recorded the visible and ultraviolet protions of the spectrum, respectively. The spectrographs were directed northwards at the angle of 30° to the horizon. One of the spectrographs had an all-sky camera which permitted the registration of the radiation intensity distribution along the meridian within the range of 5700 to 7000 Å. The emission within the range of 10400 to 11200 Å was recorded by the spectrograph SP-50 with the image converter FKT-1 [Shefov, 1961]. Observations by spectrographs were carried out from 1915 to 0624 MDT (1615 to 0324 UT). The time of individual exposures is listed in Table 1. The intensity of oxygen emission at 6300 Å at the zenith was recorded by an electrophotometer with an interference filter. Measurements were conducted each 5 min from 2058 to 0611 MDT (1758 to 0311 UT) with two 30-min breaks at about 2200 and 0000 MDT (1900 and 2100 UT). From 2230 to 0500 MDT the shapes of the aurora were photographed with the aid of the Stoffregen all-sky camera at a frequency of one frame per minute. In addition, emission at 6300 Å was also observed by the Fabry-Perot interferometer [Truttse and Yurchenko, 1970a,b] which made it possible to obtain estimates of the Doppler temperature at the height of this emission. The measurements were performed in the northward direction at the angle of 30° to the horizon.

Table 1

Emission intensities (kiloRayleighs)

λ,Å	Atom or molecule	Transition	Multiplet	March 7-8		March 8-9				March 9-10
				MDT 2031-0457 UT 1731-0157	MDT 1900-2037 UT 1600-1737	MDT 2037-2259 UT 1737-1959	MDT 2259-0033 UT 1959-2133	MDT 0033-0457 UT 2133-0157	MDT 0457-0624 UT 0157-0324	MDT 2034-0455 UT 1734-0155
3884	N_2^+	1NG(1,1)				0.47	3.8	0.32		
3914	N_2^+	1NG(0,0)			9.6	9.3	57	8.5	2.2	
3978	N_2	VK(1,12)					1.6	0.76		
3998	N_2	2PG(1,4)				0.39	3.8	0.45		
4026	NII	$3^1P°-4^1G$	40				0.44			
4035	NII	$3^3F°-4^3G$	39				0.46	0.06		
4041	NII	$3^3F°-4^3G$	39							
4043	NII	$3F°-4^3G$	39			0.02	2.8	0.64		
4057	NII	$3^3F°-4^3G$	39							
4059	N_2	2PG(0,3)					1.9	0.15		

Table 1 (continued)

Emission intensities (kiloRayleighs)

λ,Å	Atom or molecule	Transition	Multiplet	March 7-8		March 8-9				March 9-10
				MDT 2031-0457 UT 1731-0157	MDT 1900-2037 UT 1600-1737	MDT 2037-2259 UT 1737-1959	MDT 2259-0033 UT 1959-2133	MDT 0033-0457 UT 2133-0157	MDT 0457-0624 UT 0157-0324	MDT 2034-0455 UT 1734-0155
4070	OII	$3^4D^0-3^4F$	10							
4072	OII	$3^4D^0-3^4F$	10							
4072	N_2	VK(2,13)								
4076	OII	$3^4D^0-3^4F$	10			0.52	8.6	1		
4079	OII	$3^4D^0-3^4F$	10							
4092	OII	$3^4D^0-3^4F$	10							
4095	N_2	2PG(4,8)								
4112	OII	$3^4P^0-3^2F$	21				0.35	0.07		
4120	OII	$3^4P^0-3^4D$	20							
4121	OII	$3^4P^0-3^4P$	19				0.3	0.04		
4151	NI	$3^4P-4^4S^0$	6							
4167	N_2^+	1NG(3,4)								
4169	OII	$3^4P^0-3^4P$	19							
4172	NII	$3^1D^0-4^3F$	43			0.56	4	0.63		
4176	NII	$3^1D^0-4^1F$	42							
4185	OII	$3^2F^0-3^2G$	36							
4190	OII	$3^2F^0-3^2G$	36							
4199	N_2^+	1NG(2,3)				0.3	2.4	0.27		
4236	N_2^+	1NG(1,2)			0.25	1.1	5.5	0.8		
4242	NII	$3^3D^0-4^1F$	47							
4242	NII	$3^3D^0-4^3F$	48		0.18	0.17	0.6	0.15		
4278	N_2^+	1NG(0,1)			0.48	1.9	9.2	1.4		
4317	OII	$3^4P-3^4P^0$	2							
4320	OII	$3^4P-3^4P^0$	2			0.06	0.45	0.06		
4320	N_2	VK(1,13)								
4337	OII	$3^4P-3^4P^0$	2							
4340	HI	Hγ	1							
4344	N_2	2PG(0,4)				0.23	1.6	0.16		
4346	OII	$3^4P-3^4P^0$	2							
4347	OII	$3^2D-3^2P^o$	16							
4349	OII	$3^4P-3^4P^0$	2							
4351	OII	$3^2D-3^2P^0$	16							
4368	OI	$3^3S^0-4^3P$	5							
4369	OII	$3^2D^0-3^2D$	26			0.28	1.3	0.2		
4378	OII	3^2D-4^2F								
4379	NIII?	$4^2F^0-5^2G$	17			0.08	0.35	0.04		
4415	OII	$3^2P-3^2D^0$	5							
4417	OII	$3^2P-3^2D^0$	5			0.09	0.85	0.1		

Table 1 (continued)

Emission intensities (kiloRayleighs)

λ,Å	Atom or molecule	Transition	Multiplet	March 7-8		March 8-9				March 9-10
				MDT 2031-0457 UT 1731-0157	MDT 1900-2037 UT 1600-1737	MDT 2037-2259 UT 1737-1959	MDT 2259-0033 UT 1959-2133	MDT 0033-0457 UT 2133-0157	MDT 0457-0624 UT 0157-0324	MDT 2034-0455 UT 1734-0155
4425	N_2	VK(2,14)								
4430	NII	3^3P-4^3D				0.3	2.3	0.33		
4440	NII	3^3P-4^3D								
4452	OII	$3^2P-3^2D^0$	5							
4460	NII	$3^3D-3^3P^0$	21							
4466	NII	$3^3D-3^3P^0$	21			0.22	1.5	0.26		
4467	N_2^+	1NG(6,8)								
4478	NII	$3^3D-3^3P^0$	21			0.04	0.12	0.02		
4486	N_2^+	1NG(5,7)								
4486	NII	$3^3D-3^3P^0$	21							
4488	NII	$3^3D-3^3P^0$	21			0.11	0.46	0.04		
4508	NII	$3^3D-3^3P^0$	21							
4516	N_2	1NG(4,6)				0.08	0.34	0.09		
4534	N_2	VK(3,15)				0.17	1.4	0.22		
4554	N_2^+	1NG(3,5)				0.54	1.9	0.29		
4574	N_2	2PG(1,6)								
4591	OII	$3^2D-3^2F^0$	15							
4596	OII	$3^2D-3^2F^0$	15							
4600	N_2^+	1NG(2,4)				0.43	0.24	0.3		
4601	NII	$3^3P^0-3^3P$	5							
4607	NII	$3^3P^0-3^3P$	5							
4621	NII	$3^3P^0-3^3P$	5							
4631	NII	$3^3P^0-3^3P$	5			0.12	0.4	0.08		
4639	OII	$3^4P-3^4D^0$	1							
4642	OII	$3^4P-3^4D^0$	1			0.11	0.8	0.19		
4649	OII	$3^4P-3^4D^0$	1							
4651	OII	$3^4P-3^4D^0$	1			0.24	1.7	0.44		
4652	N_2^+	1NG(1,3)				0.36	2.8	0.29		
4662	OII	$3^4P-3^4D^0$	1			0.05	0.38	0.08		
4676	OII	$3^4P-3^4D^0$	1			0.04	0.29	0.09		
4709	N_2^+	1NG(0,2)				0.5	6.2	0.66		
4857	OII	3^4S-3^4D					0.24			
4861	HI	H_β	1				0.25			
4891	OII	$3^4S^0-3^4P$	28							
4895	NII	$2^3D^0-3^1P$	1				0.12			
5003	NII	$3^3P^0-3^3S$	4							
5005	NII	$3^3D-3^3F^0$	19				2.3	0.5		

Table 1 (continued)

Emission intensities (kiloRayleighs)

λ,Å	Atom or molecule	Transition	Multiplet	March 7-8		March 8-9				March 9-10
				MDT 2031-0457 UT 1731-0157	MDT 1900-2037 UT 1600-1737	MDT 2037-2259 UT 1737-1959	MDT 2259-0033 UT 1959-2133	MDT 0033-0457 UT 2133-0157	MDT 0457-0624 UT 0157-0324	MDT 2034-0455 UT 1734-0155
5200	$[NI]_{21}$	$2^4S^0-2^2D^0$			0.83	0.76	1.2	0.4		
5577	$[OI]_{32}$	2^1D-2^1S		0.25	11	12	55	9		0.3
5632	O_2^+	1NG(1,0)					8			
5667	NII	$3^3P^0-3^3D$	3				0.5			
5680	NII	$3^3P^0-3^3D$	3				0.84			
6300	$[OI]_{21}$	2^3P-2^1D		0.19	7.5	4.5	20	3.5	2	0.11
6364	$[OI]_{21}$	2^3P-2^1D		0.08	2.2	2	6	1.2	0.53	0.04
6455	OI	$3^5P-3^5S^0$	9				0.05			
6468	N_2	1PG(8,5)					0.84			
6482	NII	$3^1P^0-3^1P$	8							
6484	NI	$3^4D^0-4^4F$	21				0.29	0.05		
6544	N_2	1PG(7,4)					2.2			
6563	HI	Hα	1				0.6			
6624	N_2	1PG(6,3)					2.7			
6671	N_2	1PG(12,10)					1.5			
6705	N_2	1PG(5,2)					4	0.3		
6764	N_2	1PG(11,9)					1			
6789	N_2	1PG(4,1)					3	0.3		
10828	OH	(5,2)						9	9.8	
10830	HeI	2^3S-2^3P	1						1.3	
11036	N_2^+	M(0,0)						4.5		

Visually the picture of the aurora was as follows. About 2045 MDT on March 8 (1745 UT) a homogeneous pulsing arc of rather small width flared up. By 2150 MDT (1850 UT) ray forms appeared. At 2150 MDT (1850 UT) the rays twined upward reaching the zenith. By 2155 MDT (1855 UT) the rays faded but the homogeneous arc remained, varying by width and brightness. Until 2330 MDT (2030 UT) sometimes rays and even columns of low brightness flared up. At 2330 MDT (2030 UT) the glow intensity in the columns and their extent sharply increased. From 2340 MDT (2040 UT) to 2355 MDT (2055 UT) the emission was very intense, directed to the south from the zenith and stable. A corona was observed, columns in the west and east were red, the glow in the north was green. After 0000 MDT (2100 UT) a diffuse glow remained in the north. It continued pulsating without changing appreciably its size and brightness. By 0400 MDT (0100 UT) the emission faded.

Spectral data obtained show that the aurora was typical, low-latitude with the predominance of radiation in emission at 6300 Å. The intensities of other emissions especially $1PGN_2$, $2PGN_2$ and VK N_2 bands and also the Meinel system N_2^+ are low and reached maximum values apparently only during the periods of sharp increases of the aurora. The intensity of continuum reached 10 R/Å near 6400 Å during the second auroral flare.

The behavior of the hydroxyl emission did not differ from the earlier obtained variations on the basis of the data of observations during the IGY [Shefov, 1969].

The intensities of recorded emissions (in kiloRayleighs) are listed in Table 1. As evident from electrophotometric measurements and pictures taken by all-sky camera the most intense periods of the

aurora were much lower than photographic exposures during spectral observations. This undoubtedly led to some underestimating of the intensities listed in Table 1 since during the calculation of the absolute values of the latter it was supposed that the intensity of the glow during the whole exposure was constant. Visual, electrophotometric and all-sky observations show that during exposures from 2033 to 2259 MDT (1733 to 1959 UT) and from 2259 to 0030 MDT (1959 to 2130 UT) there were considerable short-term increases of the intensity. For the emission at 6300 Å at the zenith they were approximately by 50 and 20 times, respectively. The maximum recorded intensity of red emission at the zenith was 17 kR (2138 MDT or 1838 UT), 20 kR (2342 MDT or 2042 UT), 16 kR (0611 MDT or 0311 UT) (See Figure 1).

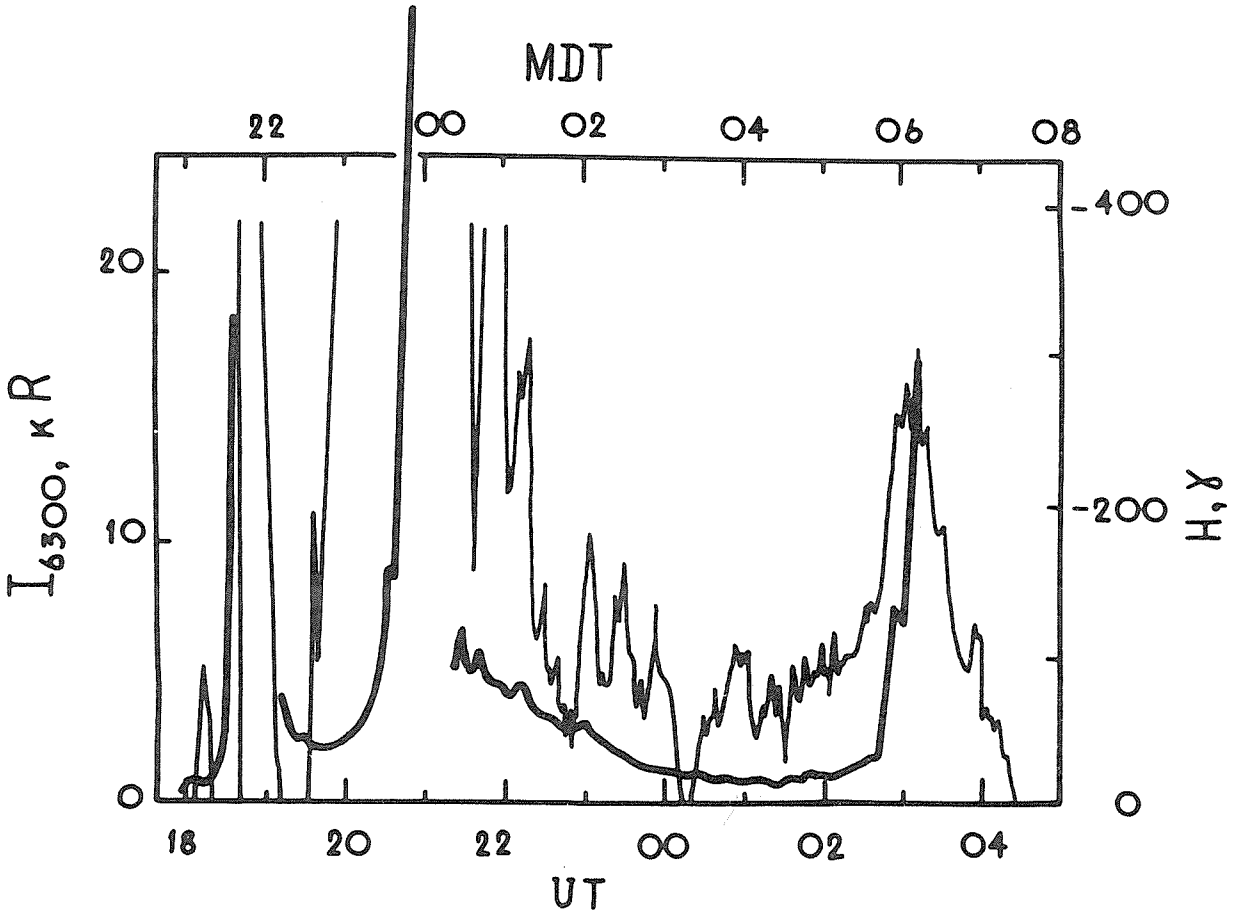

Fig. 1. Variations of the red emission intensity (thick line) and the H-component of the geomagnetic field according to Voeikovo (thin line).

According to the data of the all-sky camera (which recorded only the second flare) the integral intensity of the glow reached a maximum value at 2351 MDT (2051 UT) (See Figure 2). Isophote maps of some frames where this flare is photographed are given in Figure 3. As evident, at the moment of the flare maximum the increase of the intensity in the circumterrestrial region reached 10 times.

During the night of the aurora three flares of the intensity of the emission at 6300 Å at about 2150 MDT (1850 UT), 2351 MDT (2051 UT) and 0610 MDT (0310 UT) were recorded. The approximate duration of the first two flares was about 30 min. Apparently the southern boundary of the aurora at the moments of the maximum was 30 to 35° of geomagnetic latitude.

The measured latitudinal distribution of the red emission is in good agreement with the earlier detected [Truttse, 1968] latitudinal dependence of the intensity of this emission during geomagnetic disturbances obtained on the basis of observations during the IGY.

The intensity of red emission at local midnight on the night of March 7-8 was about 60 Rayleighs and on the night of March 9-10 about 200 Rayleighs. During the night the variations nearly did not differ from typical nocturnal variations.

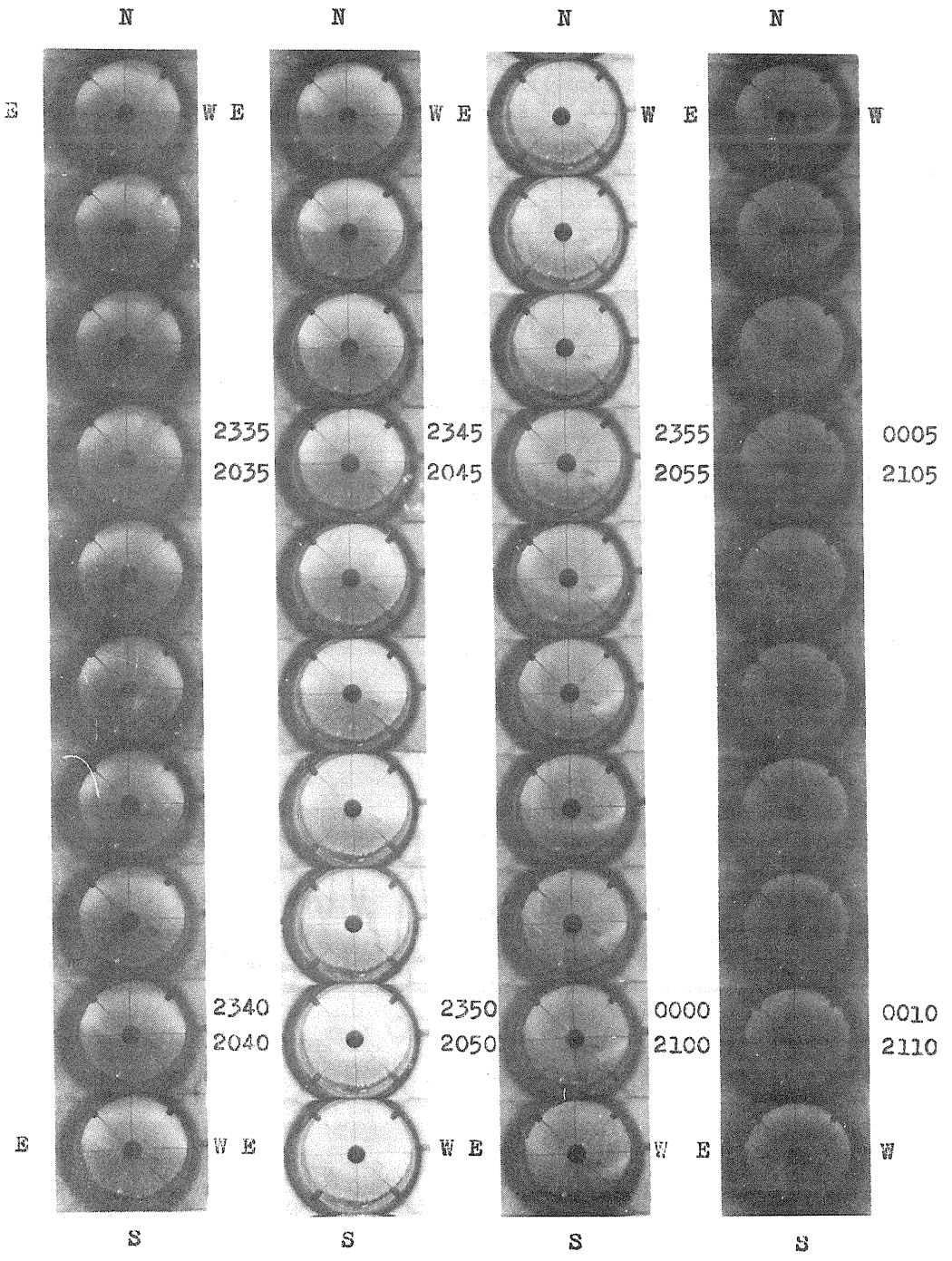

Fig. 2. All-sky camera photographs of the aurora from 2330 to 0010 MDT (2030 - 2110 UT).

The intensities of the nightglow emission for the night preceding the aurora and for the next night are listed in Table 1.

Three estimates of the Doppler temperature of the emission at 6300 Å were obtained which show that during the aurora the temperature was 2000°K. As mentioned earlier [Truttse and Yurchenko, 1970a,b], the increase of the Doppler temperature is greater than that which is predicted according to the Jacchia model [1964]. Since measurements were conducted northward at a zenithal distance of 60°, the temperature value obtained refers to the geomagnetic latitude of about 56° (assuming that the height of the red emission is about 400 km).

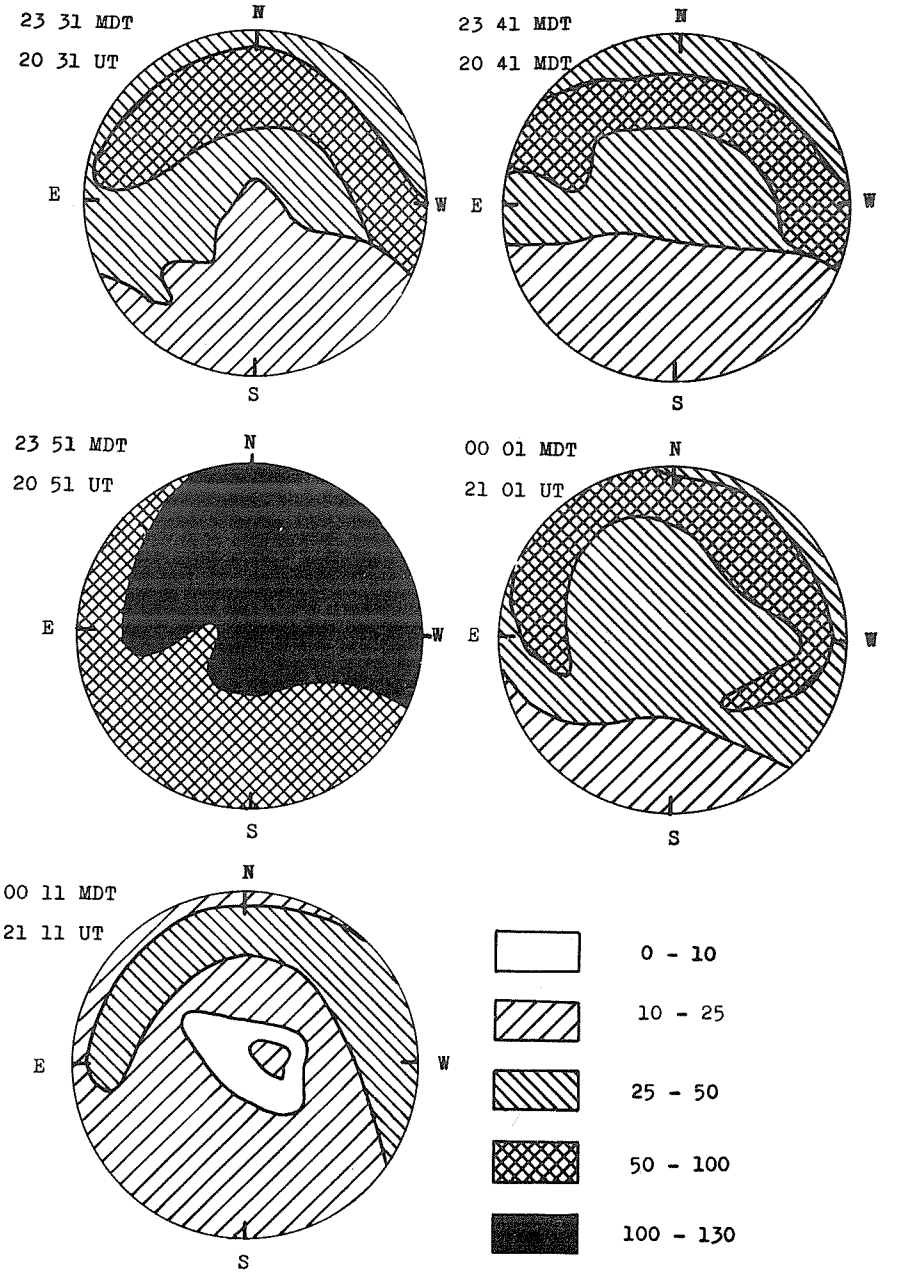

Fig. 3. Isophote maps of the integrated light of aurora for some frames. Intensities are normalized to the zenithal intensity (it is 100) for the 2351 MDT (2051 UT).

REFERENCES

JACCHIA, L. G. 1964 Smithsonian Astrophys. Obs., Special Rep., No. 170

GALPERIN, G. I., A. V. MIRONOV and N. N. SHEFOV 1957 Spectrographs to be used for investigations of atmospheric emission during the IGY of 1957-1958, Mém. Soc. Roy. Sci., Liège, 18, No. 1, 68-69

GERASIMOVA, N. G. and A. V. YAKOVLEVA 1956 A set of spectrographs with the diffractive grating. Instruments and techniques of experiments, USSR, No. 1, 83-86

SHEFOV, N. N. 1961 Observations of the OH emission in Zvenigorod spectral, electrophotometric and radar researches of aurorae and airglow, No. 5, USSR Acad. Sci., 18-24

SHEFOV, N. N. 1969 Hydroxyl emission of the upper atmosphere. 1. Behaviour during a solar cycle, seasons and geomagnetic disturbances. Planet. Space Sci., 17, No. 5, 797-813.

TRUTTSE, Yu. L. 1968 Upper atmosphere during geomagnetic disturbances. I. Some regular features of low-latitude auroral emissions. Planet. Space Sci., 16, No. 8, 981-992.

TRUTTSE, Yu. L. and O. T. YURCHENKO 1970a Temperature of the upper atmosphere from the 6300 Å emission data. Astron. Circular, USSR Acad. Sci., No. 571, 5-6.

TRUTTSE, Yu. L. and O. T. YURCHENKO 1970b Temperature of the upper atmosphere. Planet. Space Sci., 18

"Visual Auroral Observations in Canada, February - March, 1970"

by

Peter M. Millman
National Research Council of Canada, Ottawa

Visual auroral observing in Canada has been carried out on a systematic basis from a network of stations during the 14 years from July 1957 to June 1971. The nature of the program has been described briefly by Millman [1968].

During 1970 regular hourly reports were received from some 44 meteorological stations, and less-regular observations from a number of other locations manned by volunteers in Canada and northern U.S.A. Because of the interest in the active period during the first half of March, 1970, the visual observations made in the interval February 24 to March 20, 1970, have been examined in some detail.

Normally, reports where local cloud cover was greater than 8/10 are discarded. During the 25-day period indicated above the average number of stations reporting each day in the interval 0000-1200 UT was 26, and the corresponding average number of reports received was 130. From these the greatest northern and southern extents of visual aurora were determined in geomagnetic latitude over the general area between geographic longitudes 60°W and 140°W. This covers primarily geomagnetic longitude zones G and H with small portions of zones F and A on the borders [See Annals of the IGY, XVI, 154].

The results have been plotted in the upper portion of Figure 1. In the lower part of the figure is plotted the percentage of reports received each day that indicated aurora of some type.

It will be noted that the percentage aurora peaks strongly on March 8 with a secondary peak on March 1. The southern extents for these two dates are 56° and 59°, respectively, the two lowest minima during the period studied. The greatest northern extent near March 8 is G.M. lat. 79°, showing a slight tendency for the auroral zone to expand both north and south, at the time of a major disturbance. The drop in auroral activity after the disturbance, from March 8 to March 11, is very striking.

REFERENCES

MILLMAN, P. M. 1968 The Canadian visual auroral program, Annales de Geophysique, 24, 513-516

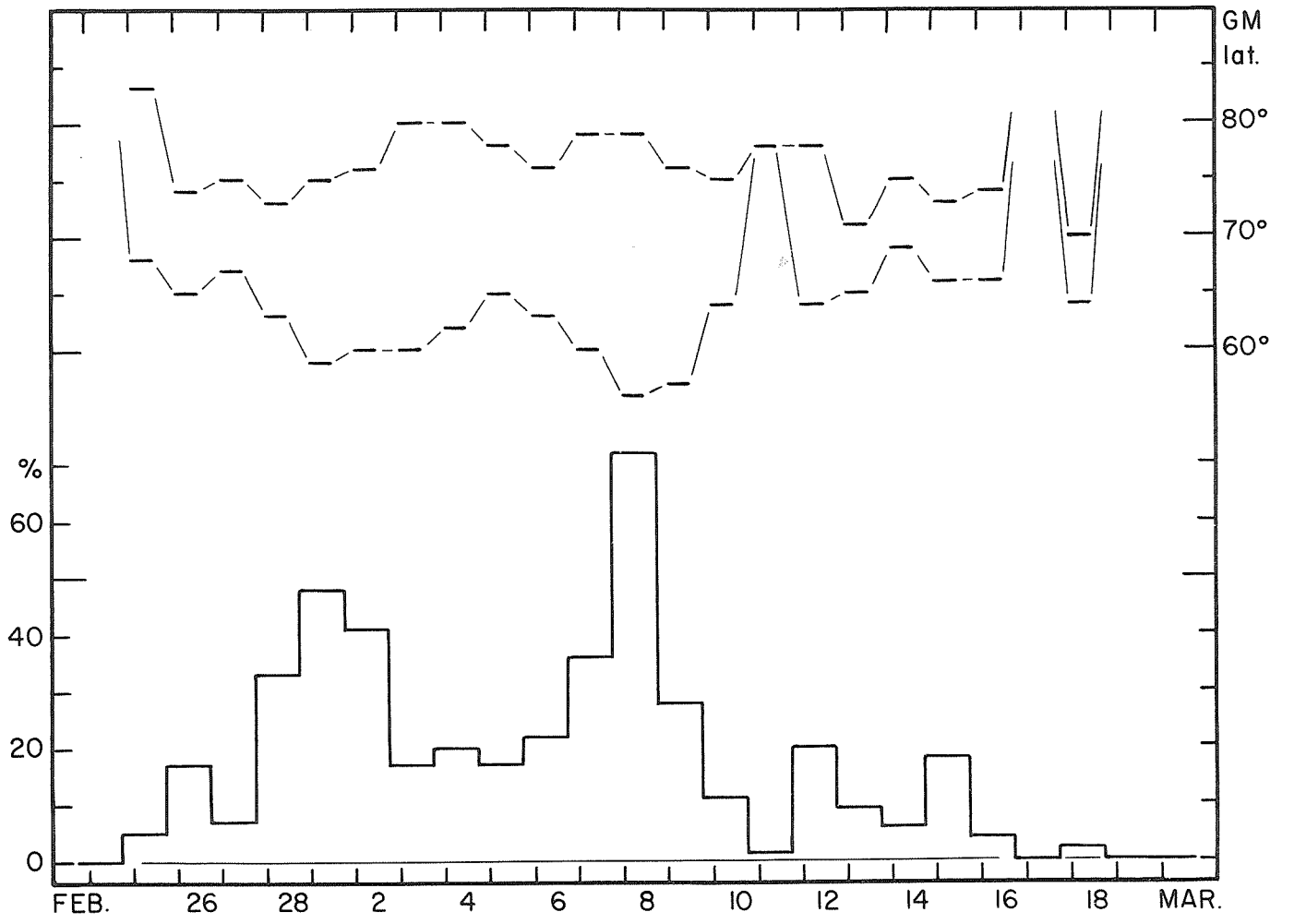

Fig. 1. A plot of auroral activity for 25 days in the February - March period 1970.
Below: The percentage of visual reports received each day which contained observations of some type of aurora.
Above: The greatest southern and northern extent for visually observed aurora seen in sectors G and H and plotted in coordinates of geomagnetic latitude. Dates plotted are UT. Dates and observations analyzed here were all made in the period 0000-1200 UT.

"Auroral Infrasonic Wave Activity at College, Alaska During the March 8, 1970 Magnetic Storm"

by

Charles R. Wilson
Geophysical Institute
University of Alaska
College, Alaska 99701

Continuous observations of infrasonic waves associated with auroral substorm activity are made at College, Alaska with a four microphone array. The horizontal trace velocity V_h, the azimuth of arrival ϕ , and the wave form are determined for each infrasonic wave packet [Cook, 1962]. The morphological characteristics of auroral infrasonic wave substorms have been described in a series of papers based on five years of observations at College, Alaska, [Wilson 1969a, 1969b, 1969c, 1970].

During the great magnetic storm of March 7-8, 1970 there was a high infrasonic noise level at College due to local winds, however, large amplitude auroral infrasonic waves were observed above the noise on both days. The signals are listed below in Table 1 giving the horizontal trace velocity (V_h = C sec α where C is the local speed of sound and α is the angle between the wave normal and the horizontal), the azimuth ϕ from which the signal has come, the amplitude of the signal in dynes/cm^2 and the UT time of arrival of the signal (LT = UT-10 hrs at College).

Table 1

Auroral Infrasonic Waves

7 March 1970

U.T.	V_h(m/sec)	ϕ	Amplitude (dynes/cm^2)
1809	795	324°	2.5
1856	640	303°	2.7
1917	625	302°	1.9
1952	435	315°	1.9

8 March 1970

U.T.	V_h(m/sec)	ϕ	Amplitude (dynes/cm^2)
0616	620	56°	4.5
1257	375	359°	5.2
1428	510	8°	4.6
1452	575	341°	3.4
1507	340	303°	3.5
1526	530	352°	4.3
1531	475	345°	5.5
1557	580	357°	5.2
1604	520	311°	5.5
1618	450	338°	5.3

The typical relationship [Wilson, 1969a] of the onset of infrasonic wave activity to the development of the DP currents during a magnetic substorm is illustrated in Figure 1 by the substorm at 1420 UT on 8 March 1970. The times of arrival are shown by arrows on the insensitive H College magnetogram for the auroral infrasonic waves listed in Table 1. A very sharp negative pressure pulse was received at College at 1428 UT just 8 minutes after the sudden onset of a very strong negative bay in H. This auroral infrasonic signal, as shown in Figure 2, was traveling toward the south with a high trace velocity characteristic of a pressure wave from a source at ionospheric heights. The 30 MHz riometer at College measured a sudden onset of "F" type auroral absorption of greater than 20 dB beginning at 1418 UT. The riometers at Fort Yukon and Inuvik to the north of College on the magnetic meridian showed sudden absorption onsets at 1422 and 1423 UT, respectively,

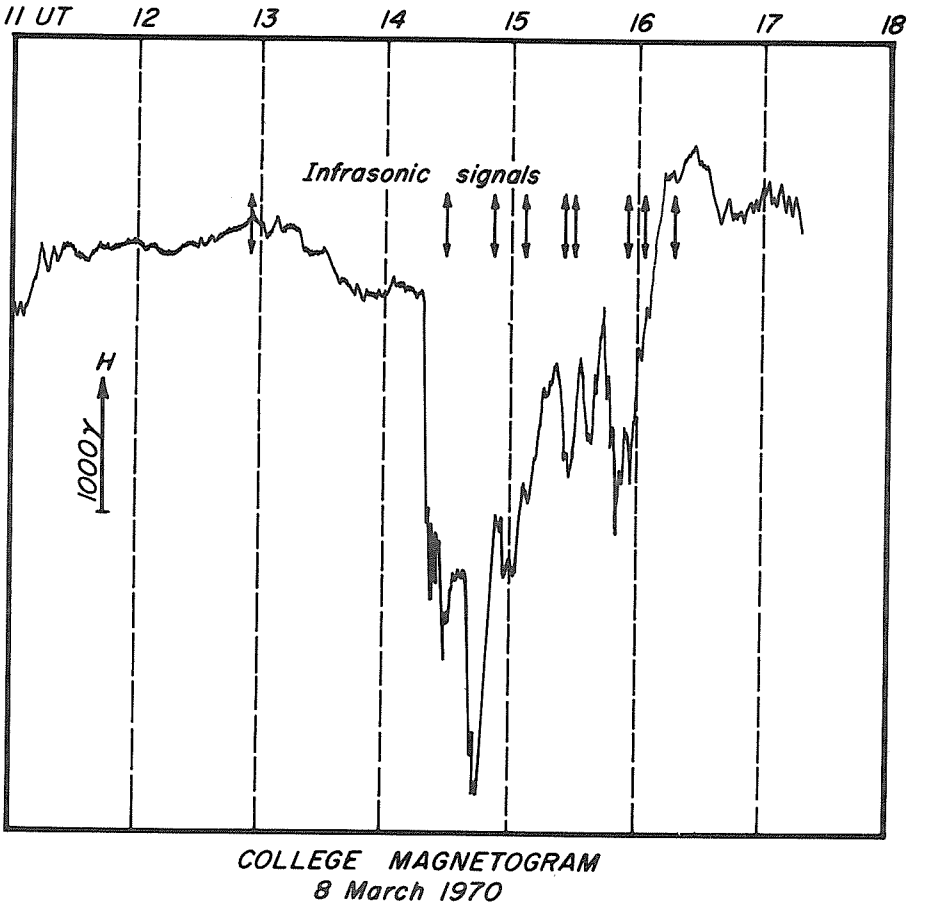

Fig. 1. College insensitive H magnetogram with the arrival times of auroral infrasonic waves shown by arrows for 8 March 1970

indicating that the auroral disturbance was expanding poleward over College with a speed of about 2.4 km/sec. Thus, the infrasonic signal at 1428 UT was radiated in the direction opposite to that of the motion of the region of auroral electron precipitation. A negative pulse and a somewhat longer acoustic delay time of 10 minutes are characteristic of this kind of source.

The other signals shown in Figure 1, beginning at 1452 UT, are of the type associated with the supersonic motion of auroral electrojets as described by Wilson [1969b]. Thus, the signal at 1452 UT from 341° can be associated with the zenith crossing at 1444 UT of a supersonic auroral electrojet as indicated by the sharp negative bay in H, the eastward change in D and the minus to plus change in Z.

The auroral infrasonic signals in the bottom half of Figure 2 were scaled at 1526 and 1530 UT as listed in Table 1. There were, however, coherent pressure waves throughout the period shown from 1523 to 1536 UT. This is characteristic of very intense auroral infrasonic substorms during the later part of the disturbance.

The earlier signal at 0616 UT on 8 March from 56° was probably associated with a westward traveling surge over eastern Canada [Wilson, 1969c]. The late morning signals on 7 March are also related to supersonic auroral electrojet motions as shown by analysis of the College magnetograms.

Overcast sky prevented good all-sky camera coverage of the 8 March substorm at 1418 UT, however, the infrasonic records can be used in conjunction with the College magnetograms to show that supersonic auroral electrojet motions from NW to SE were taking place during this intense polar substorm. This is typical of auroral substorm activity in the early morning local time sector.

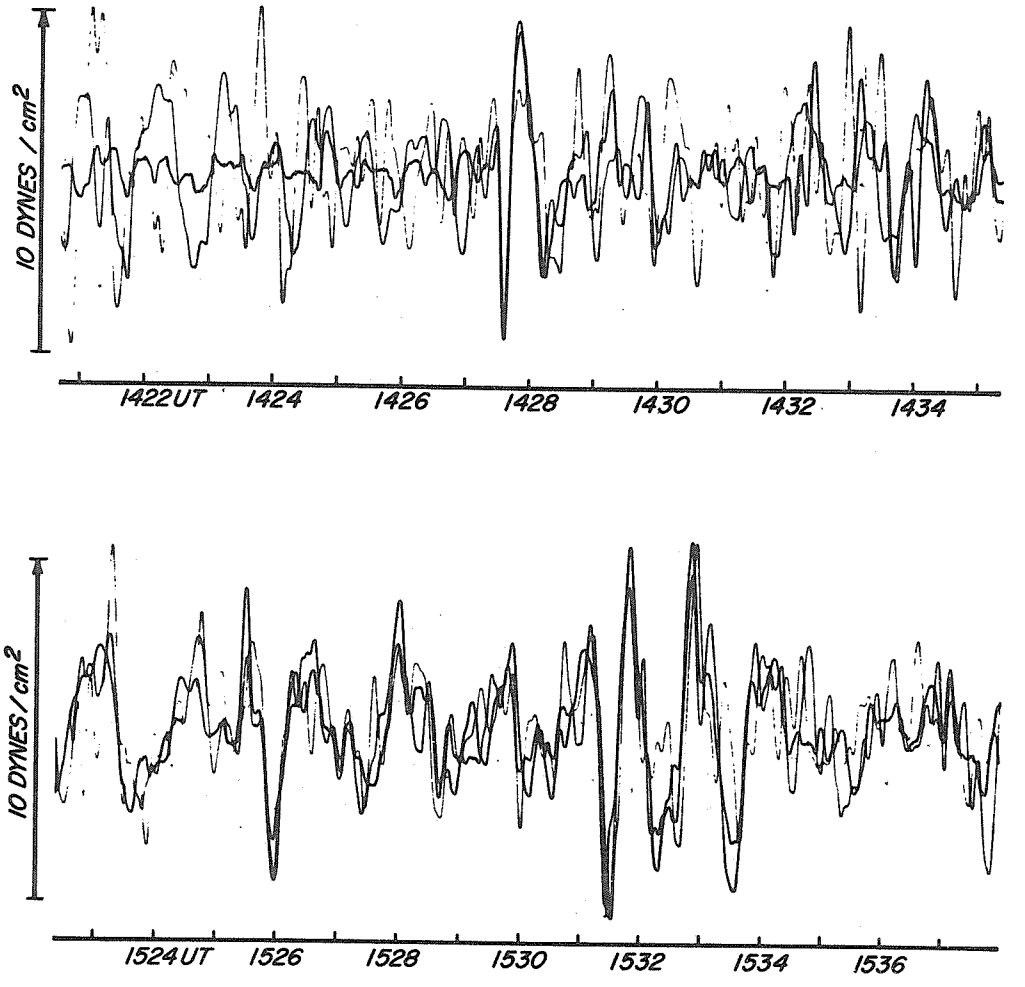

Fig. 2. Superposed infrasonic microphone traces that have been time shifted to show coherent auroral infrasonic waves. Positive pressure is upward.

Acknowledgements

This work has been supported by the Advanced Research Projects Agency, in cooperation with the U.S. Department of Commerce, NOAA, Geoacoustics Group.

REFERENCES

COOK R. K. 1962 Strange sounds in the atmosphere, Sound, 1, 25

WILSON, CHARLES R. 1969a Auroral infrasonic waves, J. Geophys. Res., 74, 1812-1836

WILSON, CHARLES R. 1969b Infrasonic waves from moving auroral electrojets, Planet. and Space Sci., 17, 1107-1120

WILSON, CHARLES R. 1969c Two-station auroral infrasonic wave observations, Planet. and Space Sci., 17, 1817-1845

WILSON, CHARLES R. 1970 Auroral infrasonic and ionospheric absorption substorms, J. Atmos. Terrest. Phys., 74, 4511-4522

USCOMM-NOAA-ASHEVILLE-4-23-71--1100

Upper Atmosphere Geophysics Report UAG-1
"IQSY Night Airglow Data" by L. L. Smith, F. E. Roach and J. M. McKennan of Aeronomy Laboratory, ESSA Research Laboratories, July 1968, single copy price $1.75. [Catalog No. C52.16/2:1]

Upper Atmosphere Geophysics Report UAG-2
"A Reevaluation of Solar Flares, 1964-1966" by Helen W. Dodson and E. Ruth Hedeman of McMath-Hulbert Observatory, The University of Michigan, August 1968, single copy price 30 cents. [Catalog No. C52.16/2:2]

Upper Atmosphere Geophysics Report UAG-3
"Observations of Jupiter's Sporadic Radio Emission in the Range 7.6-41 MHz, 6 July 1966 through 8 September 1968" by James W. Warwick and George A. Dulk, Department of Astro-Geophysics, University of Colorado, October 1968, single copy price 30 cents. [Catalog No. C52.16/2:3]

Upper Atmosphere Geophysics Report UAG-4
"Abbreviated Calendar Record 1966-1967" by J. Virginia Lincoln, Hope I. Leighton and Dorothy K. Kropp of Aeronomy and Space Data Center, Space Disturbances Laboratory, ESSA Research Laboratories, January 1969, single copy price $1.25. [Catalog No. C52.16/2:4]

Upper Atmosphere Geophysics Report UAG-5
"Data on Solar Event of May 23, 1967 and its Geophysical Effects" compiled by J. Virginia Lincoln, World Data Center A, Upper Atmosphere Geophysics, ESSA, February 1969, single copy price 65 cents. [Catalog No. C52.16/2:5]

Upper Atmosphere Geophysics Report UAG-6
"International Geophysical Calendars 1957-1969" by A. H. Shapley and J. Virginia Lincoln, ESSA Research Laboratories, March 1969, single copy price 30 cents. [Catalog No. C52.16/2:6]

Upper Atmosphere Geophysics Report UAG-7
"Observations of the Solar Electron Corona: February 1964 - January 1968" by Richard T. Hansen, High Altitude Observatory, Boulder, Colorado and Kamuela, Hawaii, October 1969, single copy price 15 cents. [Catalog No. C52.16/2:7]

Upper Atmosphere Geophysics Report UAG-8, Parts 1 and 2
"Data on Solar-Geophysical Activity October 24 - November 6, 1968" compiled by J. Virginia Lincoln, World Data Center A, Upper Atmosphere Geophysics, ESSA, March 1970, single copy price $1.75. Part 1 [Catalog No. C52.16/2:8/1], Part 2 [Catalog No. C52.16/2:8/2]

Upper Atmosphere Geophysics Report UAG-9
"Data on Cosmic Ray Event of November 18, 1968 and Associated Phenomena" compiled by J. Virginia Lincoln, World Data Center A, Upper Atmosphere Geophysics, ESSA, April 1970, single copy price 55 cents. [Catalog No. C52.16/2:9]

Upper Atmosphere Geophysics Report UAG-10
"Atlas of Ionograms" edited by A. H. Shapley, ESSA Research Laboratories, May 1970, single copy price $1.50. [Catalog No. C52.16/2:10]

Upper Atmosphere Geophysics Report UAG-11
"Catalogue of Data on Solar-Terrestrial Physics", compiled by J. Virginia Lincoln and H. Patricia Smith, World Data Center A, Upper Atmosphere Geophysics, ESSA, June 1970, single copy price $1.50. [Catalog No. C52.16/2:11]